MULTI-SCALE EVACUATION MODELS TO SUPPORT EMERGENCY AND DISASTER RESPONSE

by

Fardad Haghpanah

A dissertation submitted to Johns Hopkins University in conformity with the requirements for the degree of Doctor of Philosophy

Baltimore, Maryland

July 2020

Abstract

Evacuation is a short-term measure to mitigate human injuries and losses by temporarily relocation of exposed population before, during, or after disasters. With the increasing growth of population and cities, buildings and urban areas are over-populated which brings about safety issues when there is a need for emergency evacuation. In disaster studies, simulation is widely used to explore how natural hazards might evolve in the future, and how societies might respond to these events. Accordingly, evacuation simulation is a potentially helpful tool for emergency responders and policy makers to evaluate the required time for evacuation and the estimated number and distribution of casualties under a disaster scenario.

The healthcare system is an essential subsystem of communities which ensures the health and well-being of their residents. Hence, the resilience of the healthcare system plays an essential role in the resilience of the whole community. In disasters, patient mobility is a major challenge for healthcare systems to overcome. This is where the scientific society enters with modeling and simulation techniques to help decision-makers. Hospital evacuation simulation considering patients with different mobility characteristics, needs, and interactions, demands a microscopic modeling approach, like Agent-Based Modeling (ABM). However, as the system increases in size, the models become highly complex and intractable. Large-scale complex ABMs can be reduced by reformulating the micro-scale model of agents by a meso-scale model of population densities and partial differential equations, or a macro-scale model of population stocks and ordinary differential equations. However, reducing the size and fidelity of microscopic models to meso- or macro-scale models implies certain drawbacks.

This dissertation contributes to the improvement of large-scale agent-based evacuation simulation and multi-scale hospital evacuation models. For large-scale agent-based models, application of bug navigation algorithms, popular in the field of robotics, is evaluated to improve the efficiency of such models. A candidate bug algorithm is proposed based on a performance evaluation framework, and its applicability and practicability are demonstrated by a real-world example. For hospital evacuation simulation, crowd evacuation considering people with different physical and mobility characteristics is modeled on three different scales: microscopic (ABM), mesoscopic (fluid dynamics model), and macroscopic (system dynamics model). Similar to the well-known Predator-Prey model, the results of this study show the extent to which macroscopic and mesoscopic models can produce global behaviors emerging from agents' interactions in ABMs. To evaluate the performance of these multi-scale models, the evacuation of the emergency department at Johns Hopkins University is simulated, and the outputs and performance of the models are compared in terms of implementation complexity, required input data, provided output data, and computation time.

It is concluded that the microscopic agent-based model is recommended to hospital emergency planners for long-term use such as evaluating different emergency scenarios and effectiveness of different evacuation plans. On the other hand, the macroscopic system dynamics model is best to be used as a simple tool (like an app) for rapid situation assessment and decision making in case of imminent events. The fluid dynamics model is found to be suitable only for studying crowd dynamics in medium to high densities, but it does not offer any competency as an evacuation simulation tool.

Adviser: Dr. Benjamin W. Schafer

Readers: Dr. Takeru Igusa and Dr. Kimia Ghobadi

Acknowledgement

The journey to obtain a PhD is like a never-ridden roller coaster—full of surprising ups and downs. For some people, it is five years of challenges to conduct a high quality research, and for some others, it is much more, such that the research challenges can be over-shadowed by other bumps and obstacles along the way. Maybe a global pandemic is the best way to frame and conclude a bumpy journey: lots of uncertainties growing exponentially, things getting out of control, and you managing a crisis to mitigate losses. Yes! I am talking figuratively about the PhD journey, and yes, I am talking literally about COVID-19. Finishing a PhD degree and writing a dissertation on disasters during a global pandemic, while ironic, is strange and certainly overwhelming. However, all those obstacles have made me stronger. This may sound like a cliché, but how else you would be able to stay calm and behave rationally when all your family, friends, and you, yourself, are at risk of a serious and unknown virus that has interrupted life everywhere and taken away your job offers, and you know it may take at least a few years for the economy to recover. I feel stronger and am a better person today amidst all these struggles, and if you have managed to stay calm and lucid, and protected and helped yourself and others during these difficult times, or any other difficulties you may have gone through, then the highest kudos to you.

I would like to thank Dr. Benjamin W. Schafer for guiding me through my PhD. I remember all those times that we brainstormed together to find a research path that would make both of us happy. I learned how to break down a research problem into pieces and solve one piece at a time, and I learned how to set a research objective and try to achieve that, without losing focus and deviating from the main path. I sincerely appreciate his support

during this global pandemic, as well. I also would like to thank Dr. Judith Mitrani-Reiser, my first advisor. I came to Hopkins because of her interesting works, but unfortunately, I only had the chance to work with her for a short time. I am certain that she did all she could to help me continue my PhD at Hopkins, and I appreciate her support.

There were no memories if your friends were not there to make them, so I would like to thank all my Hopkins friends, specially Hamid Foroughi and Gary Lin. They have been great friends for me and helped me with my research and job search. My email inbox is full of messages sent by Hamid and Gary about open positions, interesting conferences, and articles. Thanks to all my Hopkins friends that shared this journey with me and tolerated my weirdness: Abdullah Mahmoud, Andreia Alvares, Astrid Fischer, Caitlin Jacques, Chu Ding, Dave Fratamico, Farshid Alambeigi, Guanbo Bian, Joel John, Julia Carroll, Kevin Sam, Megan Boston, Reza Behrou, Teodora Adzharova, Victoria Ding, Yinan Liu, Zhidong Zhang, and many others.

Last but certainly not least, I would like to thank my family for always supporting me, loving me, and trusting me. It is not easy not seeing my family for a few years and knowing that I probably will not get to see them for another few years just because of some political conflicts, but no politician or physical distance can break a family bond.

Contents

List of Tables

List of Figures

This page is intentionally left blank.

Chapter 1

Introduction

1.1. Disaster Risk Management

Natural disasters are the result of interactions between three main systems: (1) the physical environment which includes the sources of hazards, (2) the social environment which includes people and societies, and (3) the built environment which includes buildings, roads, bridges, and other structural systems. In the traditional approach to disaster management, professionals from different disciplines separately addressed their own contribution. Hazards were studied by earth and atmospheric scientists, performance of buildings and infrastructures under extreme loads was analyzed by structural engineers, and emergency management challenges, such as preparation, response, and, recovery, were handled by social scientists and emergency management professionals. Significant efforts have been taken in the last two decades to integrate these disciplines to build mutual understanding among professionals involved in managing disasters and take more effective and progressive actions [1].

In general, natural disasters are different from technological disasters and health pandemics in terms of the nature of the events, their impact on societies, and prevention and response strategies. However, all disasters are similar in causing human and economic losses. Recent events, such as the 2005 Hurricane Katrina, the 2012 Hurricane Sandy, and the current COVID-19 global pandemic, have proven that our built environment is yet vulnerable to disasters, specifically, the critical infrastructures on which the operation and economy of

societies depend. Modern societies and the life of their residents are highly dependent on the operation of infrastructures and essential services. Any disruptions to the normal performance of these critical nodes can have negative impacts on the economy of the society and welfare of the residents. Such natural events along with the emerging issues of climate change have increased the awareness on the importance of critical infrastructure resilience and the shift from direct protection measures towards a more adaptive approach. The resilience concept better allows for the consideration of unexpected events. In any event, one of the main factors that can lead to catastrophic consequences is that the intensity of the event is larger than what was considered in the design of the infrastructures or the protection systems. This implies a lack of agreement between current design criteria and the potential impact of natural hazards considering their future patterns [2]. The outcome of this shift are national and regional critical infrastructure protection and resilience strategies and programs [3].

Resilience generally refers to the ability of a system to recover from shock, insult, or disturbance, and the quality or state of being flexible, and it is used rather differently in different fields [4]. In the disaster management domain, resilience is generally defined as *"the capacity of a system, community or society potentially exposed to hazards to adapt, by resisting or changing in order to reach and maintain an acceptable level of functioning and structure."* [5] Although protection measures, such as physical protection of infrastructures, structural retrofitting, and cyber protection of information systems are extremely important and necessary in making infrastructures and communities more resistance against disasters, it is impossible to reach a zero-risk level where the systems are protected against all types of disruptions even with severe intensities. Therefore, due to the fact that preventive and protective efforts are not completely reliable, or otherwise costs would be unsustainable, a focus is made on enhancing resilience to cope with inevitable events. Considering the high costs of developing reliable preventive and

protective measures, resilience-based approaches have become more advantageous by reducing the protection expenses for certain risk scenarios and improving the response and recovery capabilities [6,7].

In the context of disaster risk management, there are two main types of risk mitigation measures: structural measures and non-structural measures. In the following sections, we will review different types of measures that are taken to reduce risks due to natural hazards and technological accidents.

1.1.1. Structural Measures

Structural risk mitigative measures are actions taken to modify the physical environment or the built environment aiming at reducing the intensity or frequency of hazards, the extent of exposed population, or the vulnerability of the built environment. The structural measures can be divided into two categories:

- long-term measures, such as structural retrofitting for seismic or flood hazards, hazard protection structures (e.g. levees or avalanche defense walls), and permanent relocation, and
- short-term measures, such as lava flow diversion, sandbag walls, or evacuation.

There has been a specific attention to structural measures aimed at mitigating the intensity or frequency of hazards in the past two decades; however, failure to take a holistic perspective in disaster risk mitigation has led to adverse effects on the overall level of risk. One example is the construction of levees to protect shoreline communities against floods, which then leads to further urban developments around the flood prone areas due to the unrealistic perception of safety by the private sector and lack of proper urban planning strategies by the public sector. The levees can increase flood risk at the downstream or increase

tsunami risk which put at risk the increasing exposed population due to urban development. This cycle leads to more catastrophic floods [8].

Structural measures aimed at mitigating the vulnerability of buildings is one of the most common long-term measures. Seismic retrofitting of existing buildings using different techniques such as interior or exterior bracing, column retrofitting, or base isolation are examples of such measures. Regarding flood risk, elevating buildings in floodplain areas has been the common practice in many European countries. An important issue to consider when designing retrofitting measures is possible adverse effects of these measures on the vulnerability of the buildings to other hazards. As an example, elevating due to floods can have adverse effects on the seismic resistance of buildings and will increase the total risk profile. In the disaster literature, this is referred to by taking a multi-hazard or an all-hazard approach in risk mitigation [8].

1.1.2. Non-Structural Measures

Non-structural risk mitigative measures refer to social, economic, and managerial activities aiming at making communities more adaptive and resilient to disruptive events. Similar to structural measure, non-structural measures can be divided into two categories:

- long-term measures, such as preparedness programs, education and training programs to raise risk and climate change awareness, land use planning, etc.
- short-term measures, such as post-disaster building usability checks and emergency, evacuation, business continuity plans, etc.

The significant impact of planning on the capability of communities in absorbing, adapting, and recovering from emergencies and disasters is evident. Planning modifies the physical characteristics of the environment and the social and economic characteristics of the

communities for longer periods than the life cycle of individual buildings or infrastructures. Consequently, as an effective sustainable plan (urban use plan, emergency plan, business continuity plan, or recovery plan) can significantly reduce the extent of damages and losses to a community, lack of planning or poor planning can create or exacerbate risks [8].

Education and preparedness programs can have a significant impact on the preparedness and resilience of communities. Education programs help people gain a realistic perception about risks to which they are exposed and learn about actions they need to take before and after disasters; for example, storing food and necessary items, securing furniture, developing home emergency plans or kits, or switching off utility supplies such as gas to prevent leak or explosions [9,10]. Responders also need education and training. Lack of coordination among different responding teams (public authorities, police, firefighters, red cross, etc.), lack of information regarding available resources and channels to have access to resources, and most importantly, the evident gap between the actions perceived by authorities and residents' expectations are examples for issues that can be addressed through responders' training [11,12].

1.2. Crowd Mobility and Evacuation

Evacuation is a critical short-term structural measure to mitigate human injuries and losses by temporarily relocation of exposed population before, during, or after disasters. The increasing population growth and urban development have led to over-populated buildings and open areas, which creates safety issues when there is a need for emergency evacuation. For example, in 2017, during hurricane Irma, about 6.5 million people were evacuated from the southern states in the US just before the hurricane, including about 2000 patients from 35 hospitals. Evacuation is a complex socio-physical process due to the large number of people,

their personal characteristics and behaviors, their interactions, external factors such as buildings or urban geometries, and the uncertainties and pressure of an extreme event. The dynamics of evacuation processes should be investigated from physical, physiological, psychological, and social perspectives [13]. The dynamics of evacuations vary depending on the event and the evacuation environment. For example, in case of hurricanes or tsunamis, evacuation might be ordered a few days before the event, while in case of fire emergencies, the evacuation takes place when the fire is already ignited. In addition, the evacuation process for an office building is different than that of a hospital or large-scale evacuations.

1.2.1. Large-Scale Evacuation

Evacuation of urban areas is often an effective action when the potential impact and consequent damages and losses of a disaster are expected to be significant and beyond the resistance capacity of the area. One of the earliest cases considering large-scale evacuation as an emergency response policy was in early 1980's when the Federal Emergency Management Agency (FEMA) was assigned to develop a civil defense policy for a mass relocation in the event of a nuclear attack [14,15]. A few examples of recent mass evacuations are listed in Table 1-1.

Large-scale evacuations are complicated processes with different challenges to face. From an operational perspective, the large number of people evacuating on foot along with the vehicular traffic can lead to significant congestions which are of great concern to transportation agencies. For example, the investigation of the 9/11 disaster in New York City and Washington D.C. showed that a large number of evacuees headed toward the mass transit stations to escape the city, which caused unpredicted congestions in many parts of the city [15].

Table 1-1. A few examples of recent mass evacuations

Event	Date	Location	Population
Hurricane Irma	September 2017	Southern USA	6.5 million
Hurricane Matthew	October 2016	Southern USA	2.5 million
Typhoon Hagupit	December 2014	Philippines	1 million
Cyclone Phailin	October 2013	India	1 million
Flash Flood	June 2013	India	1 million
Fukushima Daiichi Nuclear Disaster	March 2011	Japan	200,000
Sichuan Earthquake	May 2008	China	200,000
Wildfire	October 2007	California, USA	900,000

The interactions of evacuees with the built environment is also different in mass evacuations. The streets and sidewalks may be blocked by debris from damaged buildings or safety barriers placed by emergency responders, which creates unfamiliar detours for evacuees. Another challenge is evacuees' attitude regarding following evacuations instructions. During the 2005 Hurricane Katrina, 25% of the residents of the New Orleans metropolitan area did not evacuate their homes despite numerous efforts to inform the residents about the necessity of evacuation. Half of those that did not evacuate, thought it was safer to stay at home, while other factors were unrealistic perception of danger, religious faith, lack of trust to authorities, financial difficulties, lack of a private vehicle, and community or personal attachment [16]. Other operational challenges are collaboration and cooperation of the responding agencies, unfamiliarity of tourists and commuters with routes and landmark facilities used in evacuation messages, and information sharing to the public [15]. From a scientific perspective, a number of specific characteristics have been identified in crowd dynamics studies for large-scale evacuations [17], including vaulted distribution of pedestrians at bottlenecks, layering in

opposite pedestrian flows, zonation in cross pedestrian flows, and formation of shockwaves (or pressure waves) in high-density population of evacuees.

Recent natural disasters have proven that our built environment is yet vulnerable to disasters and even when buildings are compliant with building codes, significant damage and consequent human and financial losses can occur [18]. Given the incapacity of buildings and lifelines to resist extreme loads and the increasing frequency and intensity of natural disasters due to climate change, the frequency of mass evacuations has been increased, as well. In this regard, there is a need for systemic analysis of large-scale pedestrian evacuation in big cities to better understand how evacuees respond to evacuation instructions and behave under different scenarios.

1.2.2. Building Evacuation

Evacuation of a building can be triggered by two types of events: (1) local events that only affect a single or a small number of buildings, for example a fire emergency, active shootings, or hazmat spills, and (2) regional events that affect urban areas, for example hurricanes, earthquakes, large-scale chemical leakages. In most cases, the occupants of the buildings have to evacuate immediately and leave the building premises. Building evacuation is mainly a challenge in mid- and high-rise buildings in which the evacuees have to use the stairs to descend and reach the main egress.

Building evacuation can be classified based on the time of the event: pre-event evacuation, peri-event evacuation, and post-event evacuation. Pre-event evacuation refers to a situation in which the occupants have to evacuate a building due to an imminent hazard, for example, evacuation due to a forthcoming tsunami, flood, or landslide. In a pre-event evacuation, the physical space (i.e. the building) is not yet impacted by the event; therefore,

the evacuees can take pre-defined evacuation routes, or main corridors and stairs, to leave the building. Peri-event evacuation denotes a situation in which the evacuation has to be done during the development of a hazardous event, for example, a fire emergency or chemical spills in laboratories. The specific challenge in these situations is that as the occupants try to leave the building, the event is developing and can cause unpredictable problems. For example, in case of a fire emergency, the smoke or flames may block corridors or stairs, which force the evacuees to change their routes. This can be a significant barrier for occupants that are not familiar with the building. Post-event evacuation implies a situation where the event has already happened, and the occupants of a building need to evacuate due to possible collapse of the building or other exacerbating factors, for example, evacuation after a strong earthquake. Similar to peri-event evacuation, post-event evacuation implies routing in an unknown environment. Certain parts of a building may be damaged due to an earthquake, which makes the evacuation process difficult and dangerous. In all types of building evacuations, the main challenge is minimizing the occupants' evacuation time considering their mobility and health characteristics and the physical characteristics of the buildings and exit routes.

The history of building evacuation goes back to the late 1800's when a few cases of fires in theaters led to the death of several hundred people. These events made the engineering community rethink building safety and emergency exits [13,19,20]. However, recent incidents show that there is still need for improvement on building emergency exit. According to the US National Fire Protection Association (NFPA), between 2009 to 2013, an average of 14,500 fires were reported in high-rise buildings in the United States with an average of 40 civilian deaths, 520 civilian injuries, and $154 million in direct property loss per year [21]. This shows that although current building codes establish the minimum requirements for the safe design

of buildings, to further ensure the safety of the occupants, there is still a need to consider additional life safety features regarding emergency exits. In this regard, certain questions have been raised by engineers and emergency professionals, such as "What egress components are recommended to evacuate a high-rise building? Are elevators suitable for evacuation purposes? What design measures or procedures should be employed to improve egress efficiency?" [22].

1.2.3. Evacuees with Disabilities

Evacuation is a socio-physical process in which humans interact with each other and with the built environment under extreme conditions. The diverse mobility characteristics and needs of evacuees, specially evacuees with disabilities, can make the evacuation process more complicated. The Americans with Disabilities Act of 1990 (ADA) defines the term 'disability' as: "with respect to an individual, a physical or mental impairment that substantially limits one or more of the major life activities of such individual; a record of such an impairment; or being regarded as having such an impairment" [23 p. 7]. However, ADA does not define different types of disabilities. Individuals with temporary or permanent disabilities are classified based on different criteria by professional health organizations [24–26].

Evacuation of individuals with disabilities is the main challenge of hospital evacuations. Every year, many hospitals are forced to evacuate their patients due to natural disasters or man-made incident [27–29]. In the United States, due to the recent devastating hurricanes, many hospitals had to partially or completely evacuate their patients. In 2005 Hurricane Rita, the University of Texas Medical Branch Hospital evacuated 427 patients in about 12 hours [30]. During the 2005 Hurricane Katrina, about 1500 patients were evacuated from the Tulane's Teaching Hospital [31], and about 111 pediatric tertiary care patients were evacuated in 12 hours [32] and 121 neonates from New Orleans in 3 days [33]. Most recently,

in Hurricane Irma 35 hospitals evacuated 1900 patients in 2017 [34]. In 2017 Hurricane Harvey, 1500 patients were evacuated from 45 hospitals [35]. Between 2000 to 2017, there were 154 reported hospital evacuations in the United States, of which 71% were due to natural disasters, 16% man-made threats, and 13% incidents such as fires and chemical fumes. According to the data, 30% of the evacuations lasted for more than 24 hours. Compared to 1971-1999, there has been an increase in the man-made and incident events [36,37].

Evacuation of patients with different mobility disabilities, specially patients in intensive care units (ICUs), is a complicated process that needs planning, training, careful monitoring of the situation, and efficient decision-making and execution. ICU patients are especially vulnerable during evacuation because they are medically fragile and need additional considerations during evacuations due to their critical conditions. For example, depending on the health problems, different patients in ICU sections need different equipment such as oxygen, ventilator, continuous IV therapy, or isolation kits, and the procedure to find a receiving hospital is complicated and subject to hospital patient transfer policies and insurance policies. Evacuation of ICU patients has been a major challenge recently in the United States. In 2011, during Hurricane Irene, the New York University Langone Medical Center evacuated 19 neonates from the Neonatal ICU. The Neonatal ICU was forced again to evacuate during the 2012 Hurricane Sandy in which 21 neonates were evacuated due to power outage [38]. These events have triggered hospitals to conduct ICU evacuation drills [39–41]. In addition, hospitals have been mandated, or highly recommended, to have transport and transfer protocols for emergency situations, specifically for critically ill patients [42,43].

Hospital evacuation, in general, poses certain challenges. Unlike building evacuation and city evacuation, patients in a unit of a hospital are mainly evacuated based on a prioritization system. The criteria to set patient priorities depend on the nature of the

emergency, health status of the patients, characteristics of the exit routes, length of evacuation, and available resources (human resources, equipment, and transportation means). Transferring patients to other hospitals or health institutions requires a significant level of coordination and adherence to protocols set by both the sending hospital and the receiving institution.

1.3. Modeling Techniques for Socio-Physical Systems

There are different methods to model socio-physical processes and systems, such as emergency evacuations, in which humans interact with each other and with the built or natural environment. These methods can be classified into three main groups: microscopic, macroscopic, and mesoscopic modeling. Microscopic modeling is a bottom-up approach where complicated global behaviors of a system are assumed to be predicted by modeling the fundamental elements of the system and defining their behavior during interactions with other elements and environment [44]. Agent-based modeling (ABM) and cellular automata are two examples of such methods. The advantage of microscopic modeling is that by defining the behaviors and rules on a microscopic level, diverse and unexpected macroscopic or mass responses can be observed which are not exhibited by single elements. Microscopic models such as ABM have been used in different subject areas, such as game theory [45,46], social sciences [47,48], economics [49,50], urban planning [51,52], and public health [53,54]. In the context of evacuation simulation, elements or agents of the system are typically (but not exclusively) the evacuees.

Macroscopic modeling is a top-down approach to study the behaviors of complex systems. The first step in developing macroscopic models is to identify the internal components of the system and external systems that can have impacts on the behavior of the system. This is an interdisciplinary process where experts try to identify and find causal

linkages between these components. System dynamics modeling (SDM) and regression analysis are two examples of macroscopic models. Macroscopic modeling has seen significant applications in many disciplines, such as engineering, social sciences, public health, supply chain management, etc. [55–58]. In evacuation simulation, the whole population to be evacuated may be considered as one entity on a macroscopic level.

The third class of simulation methods is mesoscopic modeling which is developed to fill the gap between microscopic models that describe the behavior of individuals and macroscopic models that represent a system by its aggregated components. The objective of mesoscopic modeling is to efficiently study the behaviors of systems and their underlying interactions that are not easy to describe on the micro or macro levels [59,60]. In such models, the laws that define the behavior of a system are simplified, and the nuances are eliminated. Examples of mesoscopic modeling methods are the fluid dynamics and lattice-gas models. These types of models are commonly used in the study of fluids, gases, and traffic or crowd dynamics [59,61,62]. In traffic and crowd simulation, vehicles and pedestrians are modeled as a continuum flow.

In general, macroscopic and mesoscopic models tend to ignore social behaviors of individuals in decision-making processes while microscopic models possess the advantage of having the capability of implementing unique behaviors and interactions of heterogeneous individuals by which diverse and unexpected macroscopic responses can be observed. However, microscopic models are difficult to implement due to complexities in defining exhaustive rules for human behaviors and decision-making processes.

1.4. Motivation

In a disaster, public and healthcare officials must decide whether to evacuate patients or shelter in place. Evacuation is costly, disruptive, and risky for fragile patients. Furthermore, hospitals are an essential component of societies, especially during disasters when they provide triage capability for injuries; therefore, hospital operators and emergency responders prefer not to shut down hospital operations and evacuate. On the other hand, sheltering in place may expose patients and hospital staff to major safety risks as the event (e.g. a hurricane) intensifies. To make this complicated decision and perform an efficient evacuation (mass or single facility evacuation), emergency teams and decision makers need to evaluate current policies and available resources. To evaluate the efficiency of emergency policies and plans, emergency teams need training and drills; however, training and drill programs can be costly and disruptive. A mass evacuation drill requires the cooperation and coordination of the residents, police, firefighters, and all involved parties for a significant time. It may disrupt the daily routine of the commercial sector and be a financial burden on the public and private sector. Hospital evacuation drills are also costly and disruptive [63–65]. They interrupt the complex healthcare schedules and requires the participation of the core personnel of the hospital. Due to the limitations of evacuation drills, they cannot be conducted frequently to simulate different emergency scenarios. Other limitations of hospital evacuation drills are short shelf life, lack of design focus, danger, and poor reliability [65]. This is where modeling and simulation come to support emergency management. Evacuation simulation is a helpful tool that can support emergency planers and decision makers by providing an estimation of intermediate and final evacuation times. Emergency planners and decision makers use these estimations to develop emergency plans or evaluate the efficiency of current plans in terms of

available resources and level of utilization. These tools can be used to run what-if scenarios to further evaluate the response performance under different likely or unlikely conditions.

Evacuation is a spatiotemporal process in which the state of the process varies through space and time. For spatiotemporal models with multiple types of interacting elements, we can reduce the complexity of models by reformulating the micro-scale model of agents with a meso-scale model of population densities and partial differential equations, or a macro-scale model of population stocks and ordinary differential equations (see Figure 1-1).

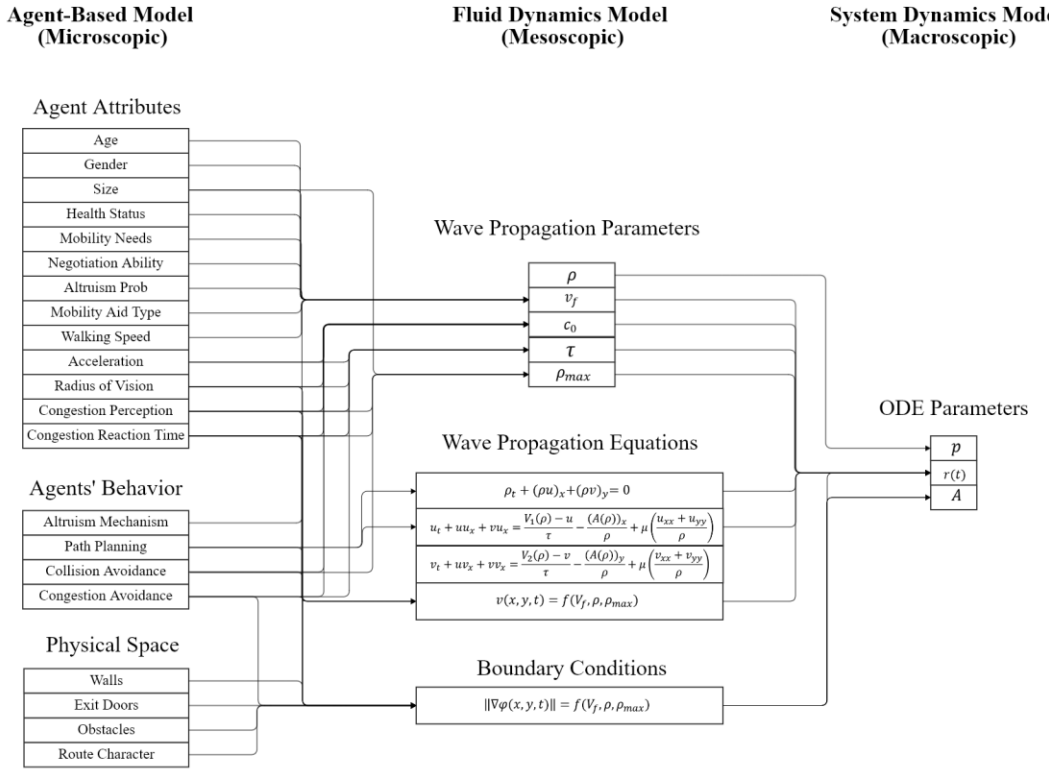

Figure 1-1. How a micro-scale evacuation model reduces to a meso-scale and a macro-scale model.

While model reduction lessens model complexity, it compromises the ability to predict emergent system-level behaviors that cannot be predicted by simply studying the agent-level behaviors. Therefore, depending on what is expected from an evacuation model, the right tool

can be a sophisticated microscopic model or a simple macro model. Accordingly, the goal of this research effort is to study the extent to which macroscopic and mesoscopic evacuation models can produce results emerging from evacuees' interactions in ABM considering crowds with different mobility characteristics and needs, as in hospital evacuation. In this study crowd dynamics considering people with different physical and mobility characteristics is modeled on three different scales: microscopic (ABM), mesoscopic (FDM), and macroscopic (SDM). The results of this study provide a spectrum of models for emergency decision makers to evaluate evacuation policies, and insight for modelers about expected behavior of evacuation models on different scales.

1.5. Summary of Dissertation Contents

In Chapter 2, the efficiency of large-scale agent-based evacuation modeling is improved by using the bug navigation algorithms. A performance evaluation framework is introduced to compare the relative performance of bug algorithms. To demonstrate applicability, a large-scale agent-based pedestrian evacuation model is developed, with the candidate bug algorithm implemented in the model, to simulate the evacuation of the city of Iquique in Chile. The results are compared with those from another study and with data from an evacuation drill that was conducted in 2013 in the city. In Chapter 3, an agent-based evacuation model is developed for non-ICU patients. Patient evacuees are classified using a patient classification system developed based on patients' mobility characteristics and needs. In addition, three simple benchmark test cases are introduced for which the results from the ABM is analyzed. In Chapter 4, to address the diversity limitation of FDMs, the Payne-Whitham fluid dynamics model is extended by introducing multiple waves to represent different types of evacuees (patients). The extent of improvements in the application of FDMs

for heterogenous crowds is investigated by comparing the results of the original and improved models with those from the ABM for the benchmark test cases. In Chapter 5, to further improve the capabilities of macroscopic hospital evacuation models, a state-of-the-art SDM is developed to model the evacuation of patients with different mobility characteristics by reducing the ABM using regression analysis. In Chapter 6, to demonstrate the applicability of the evacuation models developed in Chapters 3, 4, and 5, the evacuation of the Emergency Department of the Johns Hopkins Hospital is simulated and the models are compared in terms of modeling complexity, required input data, and provided output data. In Chapter 7, a summary of major contributions, research limitations, and future research paths are presented to conclude the dissertation.

Chapter 2

Efficient Large-Scale Agent-Based Evacuation Modeling Using Bug Navigation Algorithms

2.1. Introduction

In disaster studies, simulation is widely used to explore how natural hazards might evolve in the future, and how societies might respond to these events. In many disasters, evacuation of buildings or urban areas is an important step towards ensuring public safety. Accordingly, evacuation simulation is a potentially helpful tool for emergency responders and policy makers to evaluate the required time for evacuation and the estimated number and distribution of casualties under a disaster scenario.

Evacuation simulation can be classified into two main families: macroscopic models and microscopic models. Macroscopic models consider crowds as a whole, e.g. fluid-dynamic models, whereas microscopic models predict the crowd dynamics by considering individual behaviors and interactions. Microscopic models can be discrete like Cellular Automata (CA) or continuous, such as social force models and Agent-Based Models (ABMs) [66]. Each of these modeling approaches has specific advantages and disadvantages. Macroscopic models fail to incorporate social behaviors of individuals in decision-making processes, and they are suitable only for environments where obstacles have rather simple shapes [67]. Macroscopic fluid-dynamic models are difficult to implement due to the highly complicated and nonlinear differential equations and the various hypotheses required for setting up the equations [66].

Although microscopic models can incorporate individual's behaviors, they are not free of deficiencies. Social force models, for example, do not properly address different and uncertain behaviors of individuals under pressure. CA models perform well for low to medium size crowds, but for highly crowded scenarios, the results can be unrealistic [68]. The advantage of ABM is that by defining the behaviors and rules on the microscopic level (i.e. the agents), diverse and unexpected macroscopic or mass responses can be observed [44]. Although ABMs are computationally more expensive and can be difficult to implement due to the complexities in defining exhaustive rules, they possess the advantage of having the capability of implementing unique behaviors of heterogeneous individuals — an important feature which is not properly addressed in other models. In the context of evacuation simulation for urban areas, as the model increases in size, the computation cost increases significantly. For such large-scale simulations, computation time can go up to tens of hours. This can particularly be problematic in imminent or unforeseen events where there is a need to evaluate different scenarios for rapid decision making.

To address the computation burden of large-scale evacuation simulations, we need to focus on the trade-off between accuracy and computational efficiency, and try to answer the question: can we simplify some components of the agent-based model such that accuracy will not be decreased greatly while computation speed is increased significantly? This study suggests using the bug navigation algorithms for the navigation of pedestrians. Bug algorithms are a family of robot navigation algorithms popular in robotics. Current literature on agent-based evacuation modeling of urban areas have not focused on the computation time of simulations. Furthermore, to the best of our knowledge, this is the first study on the application of bug navigation algorithms for evacuation simulation; therefore, in the following

paragraphs, we will look at current approaches in agent-based evacuation simulation, the bug navigation algorithms, and how they differ from other path planning algorithms.

2.2. Literature Review

There have been numerous studies on simulating evacuations using ABM in which each individual is modeled as an agent. For example, Helbing et al. [69] combined two modeling approaches and developed an agent-based pedestrian behavior model using a force model (including socio-psychological and physical forces) to simulate panic and jamming mechanisms in crowd evacuations. Pan et al. [70] developed a multi-agent based framework where agents have three different navigation behaviors: locomotion (walk, run, stop, turn and side-shift), steering (seek, follow, and collision avoidance), and social (competitive, queuing, and herding). When an agent is blocked by a crowd, it may choose randomly among the stopping (i.e. avoiding collision), turning (i.e. attempting a different path), or moving backward (i.e. maintaining its personal space) motions. Per collision avoidance, the rules are simple and intuitive; if an agent identifies an obstacle both in front and on one side of itself, then it steers toward the opposite side. As another example, when two agents see a head-to-head situation in a corridor, they steer to the sides to avoid running into each other. For queuing, agents share information with each other to determine their positions in the queue. Those closer to the destination (or intermediate target) get higher priority in the queue.

Shi et al. [71] used the *environment driving factor* for the navigation of agents, which is similar to the Artificial Potential Fields method. The driving factors help agents navigate through exits, danger zones, and crowds by assigning different positive or negative values to each grid in the environment based on the proximity to these elements. In the discrete-space building evacuation model developed by Y. Lin et al. [72], an exit cell is predefined for each

cell in the environment, and the shortest path to the exit cell is computed. To account for collision avoidance, each cell can be occupied by only one agent. The tsunami evacuation model developed by Mas et al. [73] uses the Anguelov variant of the A* (A star) algorithm [74], on grid spaces. To avoid collision, the predictive collision avoidance method [75] is used. A maximum capacity is also established for each grid space to be used for pedestrians and vehicles. Therefore, if an agent wants to enter a saturated grid, it must wait for another agent to leave the grid and make extra room. Mordvintsev et al. [76] developed an agent-based city evacuation model coupled with dynamic flood simulation. The flooded area propagates dynamically as the pedestrians move towards the safe zone using global path planning. The global path map updates each 30 seconds as the flood propagates over the city. The Artificial Potential Fields method is used for pedestrian navigation. To avoid collision with obstacles and other agents, the Optimal Reciprocal Collision Avoidance (ORCA) method [77] has been used.

Di Mauro et al. [78] developed a hybrid model to focus on the interactions between vehicles and pedestrians. In this model, the vehicle-pedestrian interaction could occur at any place across and along the streets. Both pedestrians and vehicles can use the width of the street, where the capacity for both vehicles and pedestrians is modeled as a variable depending on the relative ratio between the number of pedestrians and vehicles. Werberich et al. [79] developed an agent-based model to study pedestrian crossing behaviors. In this regard, two main crossing behaviors were defined: pedestrians cross the streets at intersections or predefined crossing points; or pedestrians cross the streets at any location if a gap acceptance criterion is met. In the evacuation model developed by Liu et al. [67], each agent navigates in space by identifying the feasible region around itself. The feasible region is defined as the reachable space not blocked by obstacles or other agents in a circle within the agent's stride

length. The agent moves to a point inside the feasible region that is closest to the destination using waypoint graphs and convex polygons of passable spaces. Poulos et al. [80] used a set of disjoint polygons and vertices to represent obstacles and exit points inside a building. The shortest path is calculated from each vertex using the Dijkstra's Algorithm. The shortest path is the path going through those vertices of obstacles with internal angle of less than 180 degrees. The collision avoidance is implemented using the ORCA principle where each agent adjusts its velocity, preferably as little as possible, to avoid collisions with obstacles or other agents.

To identify fast and reliable bug navigation algorithms for large-scale city evacuation modeling, a performance evaluation framework is developed. The framework consists of a set of typical obstacles that can be challenging for navigation algorithms to process, and a set of performance indices. A selection of algorithms from the bug family is evaluated using this framework, and their relative performance is compared. The rest of the paper is structured as follows: in Section 2, the details of the performance evaluation framework is elaborated. Section 3 presents the results of evaluation of selected bug algorithms using the framework. In Section 4, we will study the performance of each bug algorithm and discuss what the results of the evaluation imply. To demonstrate the applicability of the bug navigation algorithms, an agent-based pedestrian evacuation model is developed in NetLogo [81] with the candidate bug algorithm implemented for the navigation of agents. The model is used to simulate the evacuation of the city of Iquique in Chile. In Section 5, the results are compared with those from another study and with data from an evacuation drill that was conducted in 2013 in the city.

2.3. Performance Evaluation Framework

In general, pedestrian movements are different from vehicle movements. Vehicles have to follow lane boundaries and switch lanes when under certain conditions. However, pedestrian movements are subjected to more randomness and are within more complex boundary conditions. There are different techniques to implement pedestrian movements, such as the shortest path algorithms, potential field theory, and navigation algorithms. These techniques have relative advantages and disadvantages when the size of the model (i.e. number of agents, size of the physical environment, and sizes, numbers, and shapes of the obstacles) is large, as in city evacuation simulation. Those using shortest path algorithms, such as the Dijkstra's Algorithm, can generate globally optimal paths, but they incorporate this unrealistic assumption that evacuees have perfect knowledge about the environment, obstructed roads, and the status of the event. Moreover, they need preprocessing of the simulation environment to develop origin-destination paths for all nodes in the model [82]. These models can be computationally expensive for large-scale city evacuation modeling specifically when accounting for damage conditions, where there could be obstacles with complex shapes and numerous vertices, or when the model incorporates dynamic features of an event, such as flood propagation or possible collapse of buildings during evacuation, where the origin-destination paths should be updated at every time step. On the other hand, bug algorithms do not need any preprocessing or global information of the environment and can be potentially fast, however, they may not present realistic crowd movements [83].

A performance evaluation framework is developed to judge the bug algorithms. The framework is called the COPE (Convergence, Optimality, Precision, and Efficiency) performance evaluation framework and consists of three main components: (1) a set of benchmark obstacles which have been shown to be challenging in navigation simulations

based on the literature and modeling experience; (2) the performance evaluation metrics; and (3) the navigation algorithms to be evaluated. It should be emphasized that this framework provides a relative performance index, i.e. adding new or removing algorithms will change the results.

2.3.1. Benchmark Obstacles

The candidate bug algorithm for an agent-based large-scale evacuation model should be capable of navigating evacuees through obstacles with any shapes and sizes. To find such an algorithm, a set of benchmark obstacles can be identified which are challenging for the algorithms to process. The obstacle-set should contain different objects depending on the specification of the built environment and the graphical specifications of the modeling platform, e.g. whether obstacles have smooth boundaries or are in the form of pixels.

For this study, five typical challenging obstacles are identified (see Figure 2-1): a long L-shaped obstacle, a U-shaped obstacle (with the target inside or outside of the obstacle), an obstacle with a pixelated edge, a T-shaped corridor, and a closed box obstacle.

2.3.2. Performance Evaluation Metrics

The COPE performance evaluation metrics consist of four indices taking values from 0 to 1: (1) convergence, (2) optimality in terms of length of generated paths, (3) precision in flagging trapped agents, and (4) efficiency in terms of computation speed. For each navigation algorithm and each obstacle, *convergence* is evaluated by the ratio of the number of converged (i.e. successful) simulations to the total number of simulations. Failure to converge refers to cases where an agent is stuck in an infinite loop and cannot reach its destination. *Optimality* is evaluated by normalizing the length of the generated path with respect to the length of the

optimal path. Regarding *precision*, some algorithms define specific criteria to identify trapped agents, but these criteria may fail to (or incorrectly) flag agents as trapped. *Precision* is evaluated by the ratio of number of falsely flagged (false positive) and falsely not-flagged (false negative) agents to total number of agents. *Efficiency* is evaluated by normalizing the computation time it takes for an algorithm to finish the simulation with respect to the fastest algorithm.

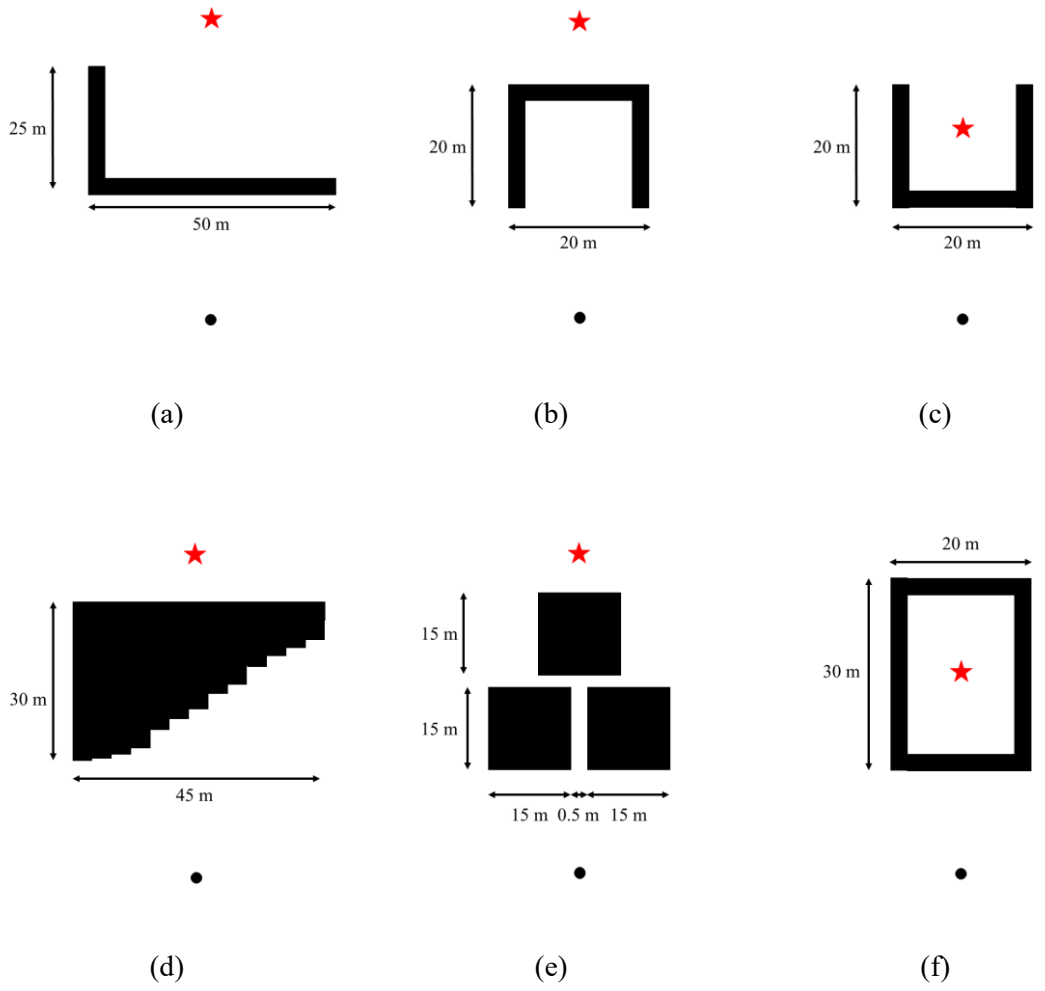

Figure 2-1. Benchmark obstacle: (a) long L-shaped obstacle, (b) U-shaped obstacle with target outside, (c) U-shaped obstacle with target inside, (d) obstacle with pixelated edge, (e) T-shaped corridor, and (f) closed box obstacle. Legend: black circle: agent (diameter = 50 cm); red star: target; black blocks: obstacles.

The COPE indices for each algorithm-obstacle pair can be calculated using Equations (2-2) to (2-5). The average values of COPE indices are then taken over the set of obstacles for each algorithm, as in Equations (2-6) to (2-9). The total performance index for each algorithm can be obtained using Equation (2-1) providing an index from 0 to 1.

$$I_i = \frac{\omega_c C_i + \omega_o O_i + \omega_p P_i + \omega_e E_i}{\omega_c + \omega_o + \omega_p + \omega_e} \tag{2-1}$$

$$C_{ij} = \frac{S_{ij}}{N_{ij}} \tag{2-2}$$

$$O_{ij} = \frac{\min_{i \in alg}(L_{ij})}{L_{ij}} \tag{2-3}$$

$$P_{ij} = 1 - \frac{F_{ij}}{N_{ij}} \tag{2-4}$$

$$E_{ij} = \frac{\min_{i \in alg}(T_{ij})}{T_{ij}} \tag{2-5}$$

$$C_i = \frac{1}{n}\sum_{j=1}^{n} C_{ij} \tag{2-6}$$

$$O_i = \frac{1}{n}\sum_{j=1}^{n} O_{ij} \tag{2-7}$$

$$P_i = \frac{1}{n}\sum_{j=1}^{n} P_{ij} \tag{2-8}$$

$$E_i = \frac{1}{n}\sum_{j=1}^{n} E_{ij} \tag{2-9}$$

where for algorithm i and obstacle j, S_{ij} is the total number of converged runs, N_{ij} is the total number of runs, L_{ij} is the length of the generated path, F_{ij} is the total number of agents falsely flagged or not flagged as trapped, T_{ij} is the computation time, n is the number of obstacles,

and ω_c, ω_o, ω_p, and ω_e are weights for convergence, optimality, precision, and efficiency, respectively. These weights must be positive. Since we need fast navigation algorithms that primarily can navigate obstacles with different shapes, convergence and efficiency have bigger weights than other indices. Therefore, the following weights are recommended: $\omega_c = 3$, $\omega_o = 1$, $\omega_p = 1$, and $\omega_e = 3$.

A higher COPE Index implies a relatively better performance. It is noteworthy to highlight that the COPE performance index is not an absolute index, i.e. adding a new algorithm would require a re-evaluation of all other algorithms, and this may change their performance indices. This is due to the fact that optimality and efficiency indices are evaluated based on the most optimal and the most efficient algorithms in the set. If the new algorithm that is added to the set turns out to be faster or more optimal than the previous algorithms, the optimality and efficiency of all other algorithms need to be re-evaluated based on the new algorithm.

2.3.3. Navigation Algorithms

The bug algorithm family is a family of robot navigation algorithms that gives logical solutions when no global information of the environment is available. All these algorithms make three assumptions: (1) the robot is a point object which means it has no physical size; (2) the robot has a perfect localization which means it has perfect information of its location relative to a predefined origin at any time; and (3) it has precise sensors [84]. These algorithms use range sensors and/or tactile sensors to identify obstacles and find a way to pass through and reach the destination. Some of these algorithms can do better than others for a given environmental setting, but may perform weaker for other different settings [83,85]. Since evacuees take locally optimal paths when passing obstacles [86,87], algorithms that perform

logically for the most different environmental settings have the highest potential to be used for the navigation of agents in city evacuation simulations.

The navigation algorithms considered for this study are: Bug1 and Bug2 [84], DistBug [88], KBug [89], and TangentBug [90]. Among these algorithms, Bug1 and Bug2 identify obstacles when the agent hits one, TangentBug identifies obstacles using a radius of vision, and DistBug and KBug use a combination of both. Figure 2-2 illustrates general schema of how these navigation algorithms work for a simple square-shape obstacle. A short description of these algorithms is provided here; for more details, please refer to the references. According to Bug1, the agent moves toward the target along a straight line. When it hits an obstacle (hit point), it randomly turns right or left and follows the obstacle boundary to find the closest point on the boundary to the target (leave point). Upon returning to the hot point, the agent selects the shortest direction (left or right) to move along the obstacle boundary and reach the leave point. As per Bug2, the agent draws a straight line from its initial location to the target (m-line) and follows this line. When an obstacle is reached, it randomly turns right or left and follows the obstacle boundary until it meets the m-line again. If the meeting point is closer to the target than the hit point, the agent leaves the obstacle and follows the m-line; if it is farther, the agent continues following the obstacle boundary, and if it returns to the hit point, the agent or the target will be considered to be trapped. DistBug is similar to Bug2 except for using the m-line while following the obstacle boundary, the agent checks if the target is visible or a leaving condition is met at each step. The DistBug algorithm comes with three optional extensions that can improve its performance. Here, *DB**** denotes the DistBug algorithm with different combinations of its extensions. For example, DB13 refers to the DistBug algorithm with the first and third extensions included. Extension 1 controls the direction of the agent when it hits an obstacle. Extension 2 reverses the following direction of the agent at

most once when the current heading drives the agent away from the target. Extension 3 bounds the searching area along the obstacle boundary by virtual obstacles centered at the target with specific radii. KBug uses a local sensor to find obstacles from a certain distance (radius of vision). When the agent finds an obstacle, it evaluates the farthest points to the left and right on the obstacle boundary and selects the one which is closest to itself. The agent leaves the obstacle boundary when it does not identify any obstacle between itself and the target. TangentBug uses the local tangent graph (LTG) method to find the locally optimal path. The LTG includes all the free space and the portions of the boundaries of obstacles that lie in the visible area. The agent constructs the LTG at each time step and selects the node that is closest to the target.

Depending on the features and capabilities of the simulation platform, these algorithms may perform relatively different, and they may result in different performance indices, particularly regarding computational efficiency. In this regard, since NetLogo provides a pixel- or patch-based environment, the round-edge obstacles and those having inclined edges with respect to the main horizontal and vertical axes will have pixelated edges. Having obstacles with many vertices affects the performance of some of the bug algorithms.

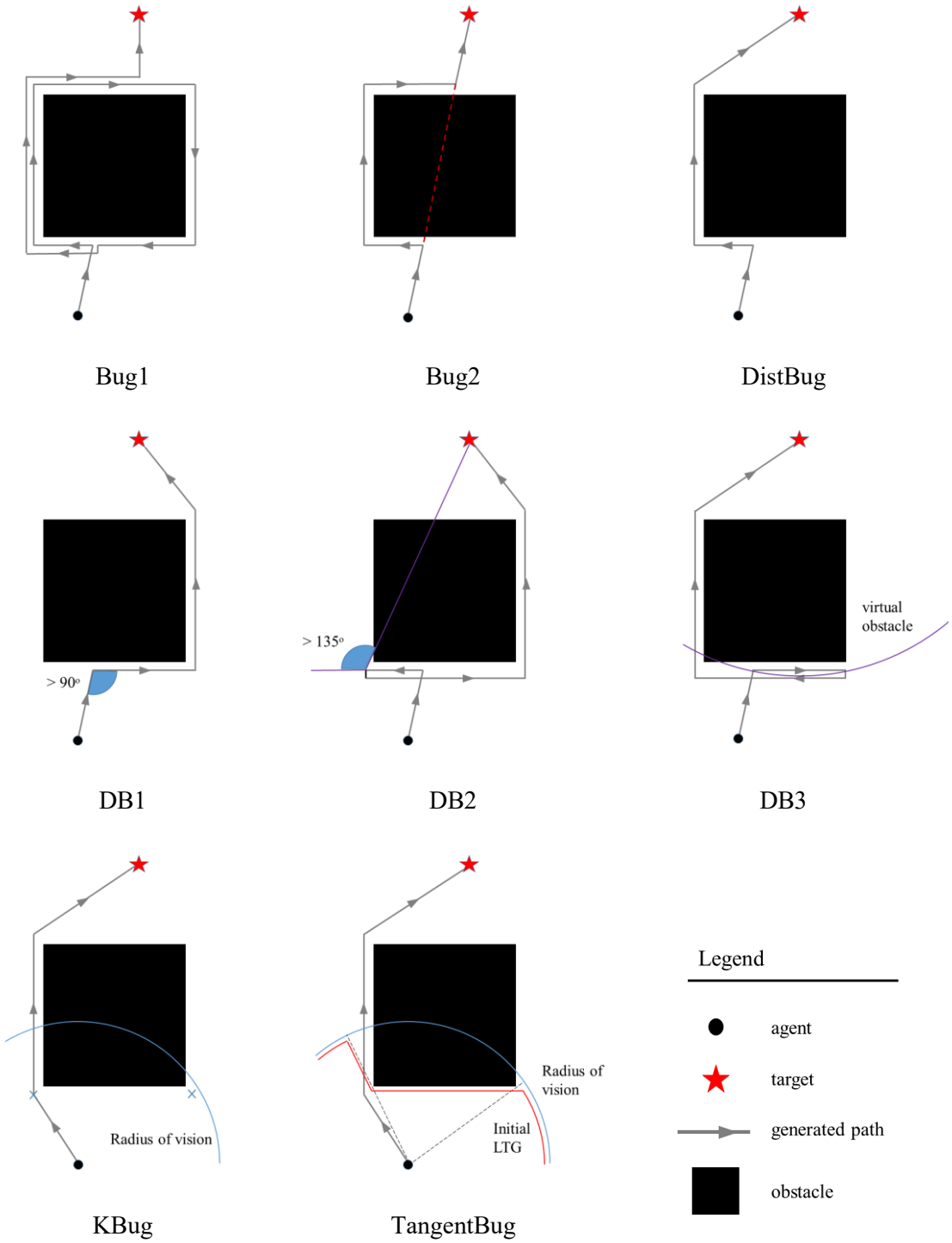

Figure 2-2. Generated paths by different algorithms.

2.4. Evaluation of Navigation Algorithms

For each algorithm-obstacle pair, 1000 simulations are conducted to account for possible initial positions and initial local directions of agents. In each simulation, a target is placed on one side of the obstacle with an agent on the other side, as shown in Figure 2-1. The simulations are implemented in NetLogo using a computer with an Intel Zeon E3-1505M v5 @ 2.8 GHz processor and a 32GB memory.

2.4.1. Results

The results of the simulations are presented in Figures 2-3 to 2-8 in the form of graphical traces. According to the results, one can see that algorithms like Bug1 and Bug2, which only use tactile sensors to detect obstacles, generate less optimal, hence less realistic, paths when compared with algorithms that use range or hybrid sensors. In addition, the paths generated by KBug and TangentBug algorithms are significantly different than other algorithms. This is due to the fact that these algorithms use range sensors to detect obstacles; therefore, the agents start moving away from the obstacles before reaching them. However, KBug and TangentBug use different algorithms to avoid obstacles, which leads to different behaviors. Furthermore, the behavior of algorithms is not consistent for different obstacles. For example, KBug seems to be successful in generating the most optimal and realistic paths for the L-shape, T-shape, and the pixelated obstacle; however, the results for other obstacles are not as satisfactory. Regarding the TangentBug algorithms, although theoretically it should provide the most optimal paths, the results show a great deal of issues in optimality and convergence. To better visualize the results of the simulations, we need to study the algorithms based on the indices of the COPE framework.

The results of the performance evaluation are presented in Figures 2-9 to 2-11. Figures 2-9 and 2-10 show how each of the navigation algorithms performed for each obstacle and in total, respectively. In terms, of convergence, except for KBug and TangentBug, all other algorithms converged for all the obstacles. DB23 and DB123 have generated the most optimal paths, while Bug1's solutions are the least optimal. As for precision, most DB algorithms performed well in identifying trapped agents; however, when extensions 2 and 3 are both included, the algorithm's capability in correctly identifying trapped agents is affected. Regarding efficiency, TangentBug is the slowest one, while all other algorithms have comparable computation speeds.

Figure 2-11 shows the final performance indices for all the algorithms. All DB algorithms have similar total performance, while the total performance of DB1 is slightly better than the rest at 96%, and therefore it is the best candidate among this selection of algorithms. DB1 converges for all the benchmark obstacles, provides rather locally optimal paths among the selected algorithms, can correctly identify trapped agents, except for the case of the obstacle with pixelated edges where its precision index is 0.97, and it is the most efficient algorithm in terms of computation time.

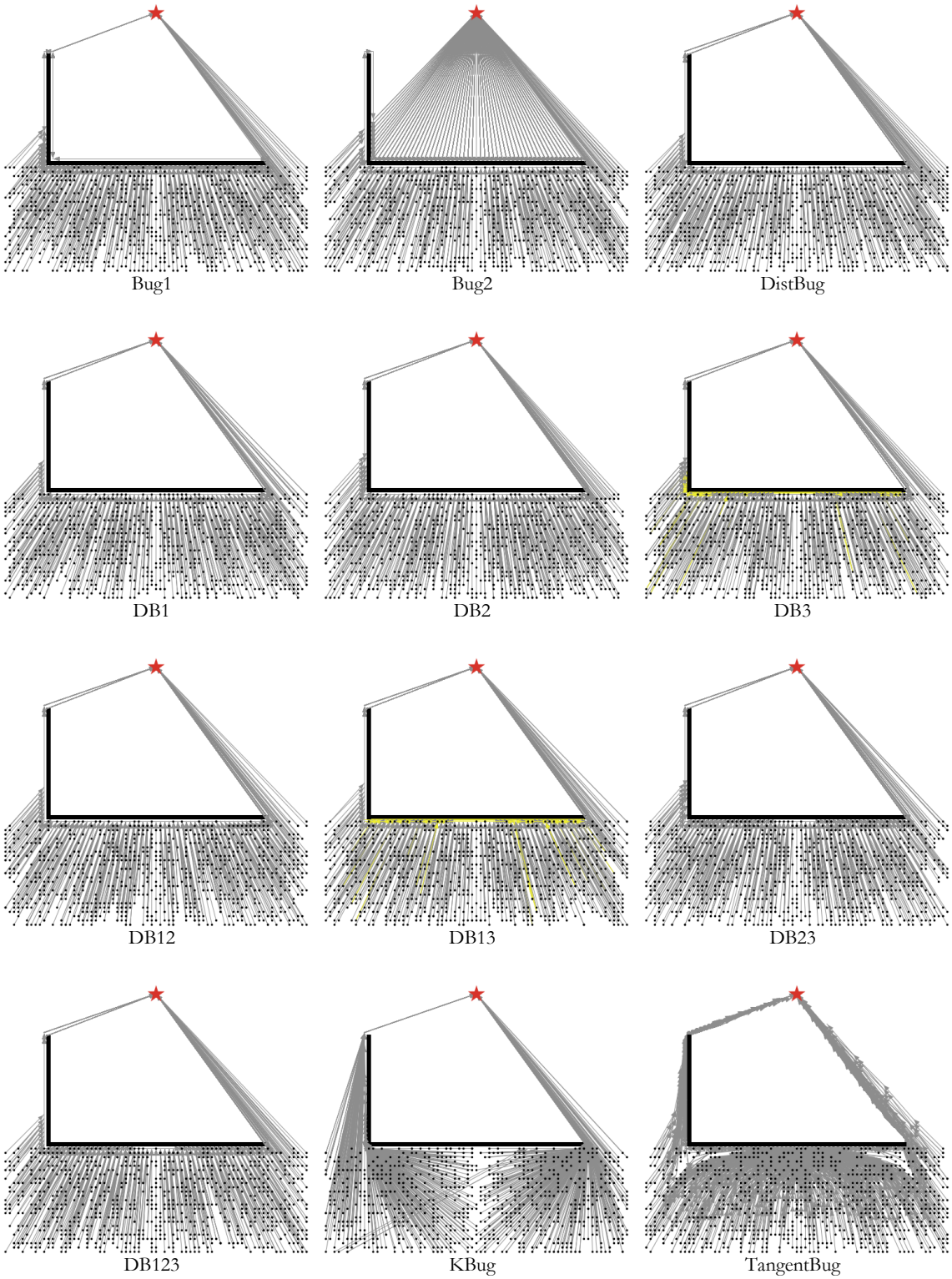

Figure 2-3. Results for the L-shaped obstacle. Legend: red star: target; black circles: initial positions of agents; grey lines: converged simulations; yellow lines: false-flagged simulations.

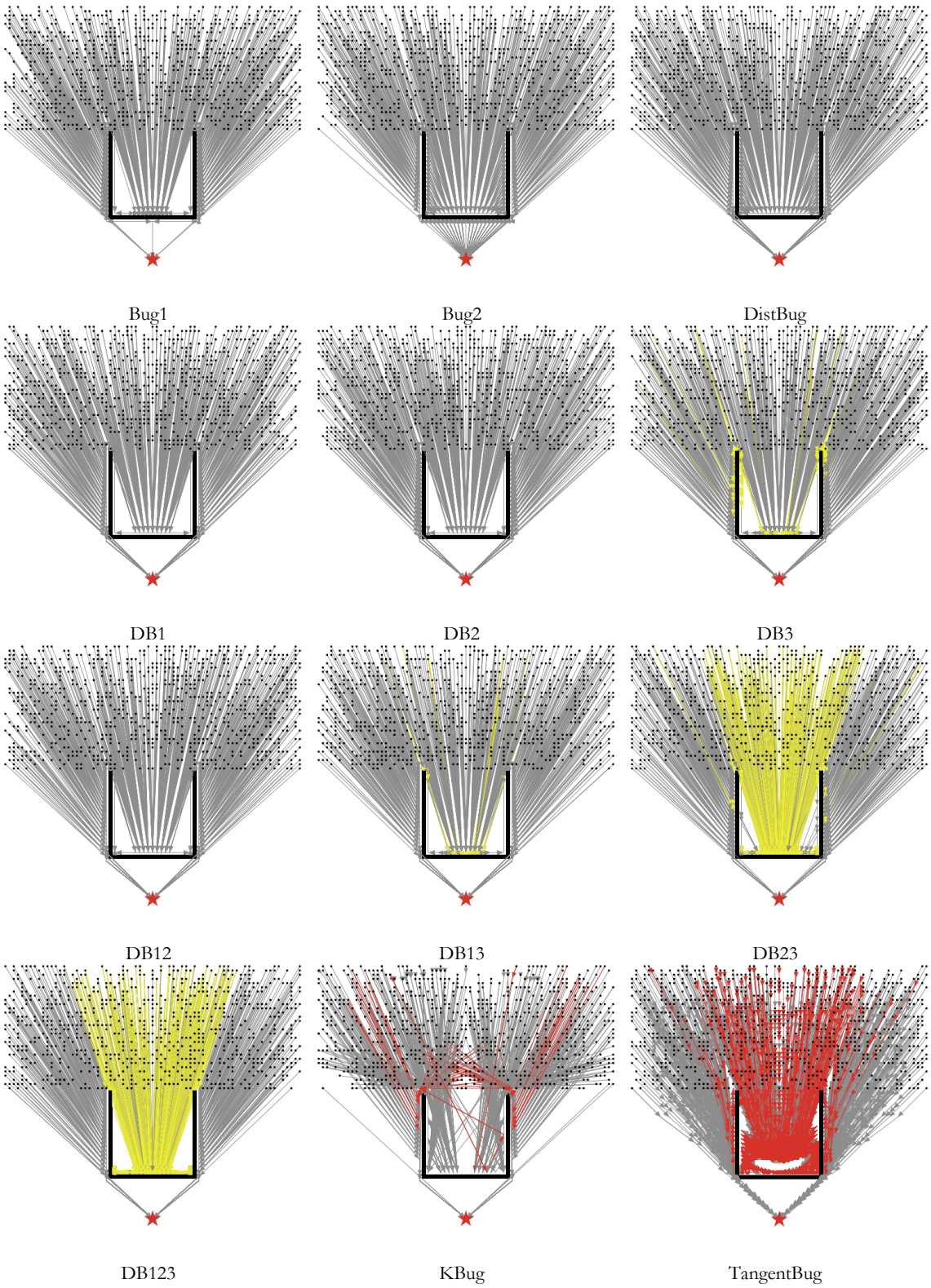

Figure 2-4. Results for the U-shaped obstacle. Legend: red star: target; black circles: initial positions of agents; grey lines: converged simulations; red lines: non-converged simulations; yellow lines: false-flagged simulations.

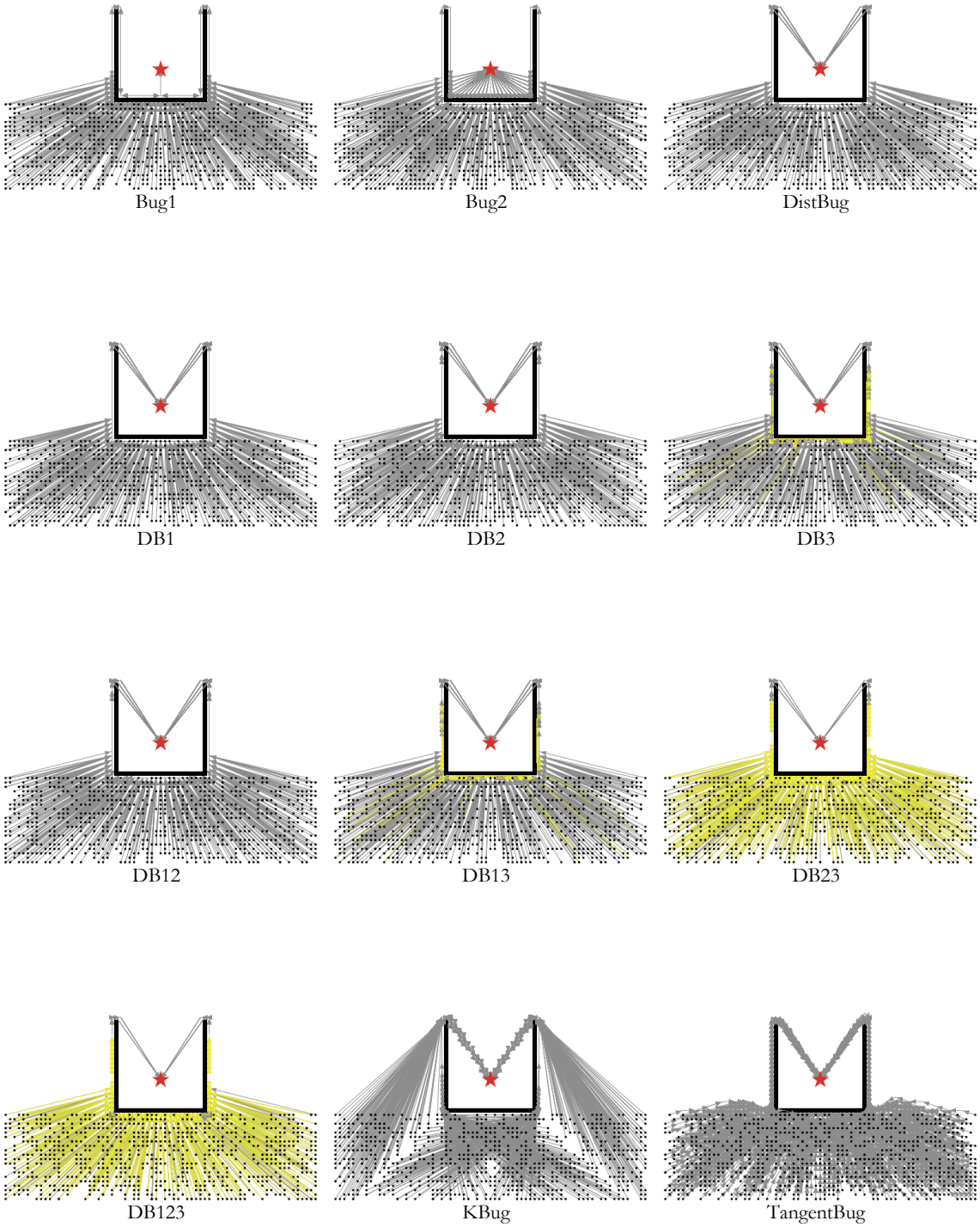

Figure 2-5. Results for the U-shaped obstacle with target inside. Legend: red star: target; black circles: initial positions of agents; grey lines: converged simulations; yellow lines: false-flagged simulations.

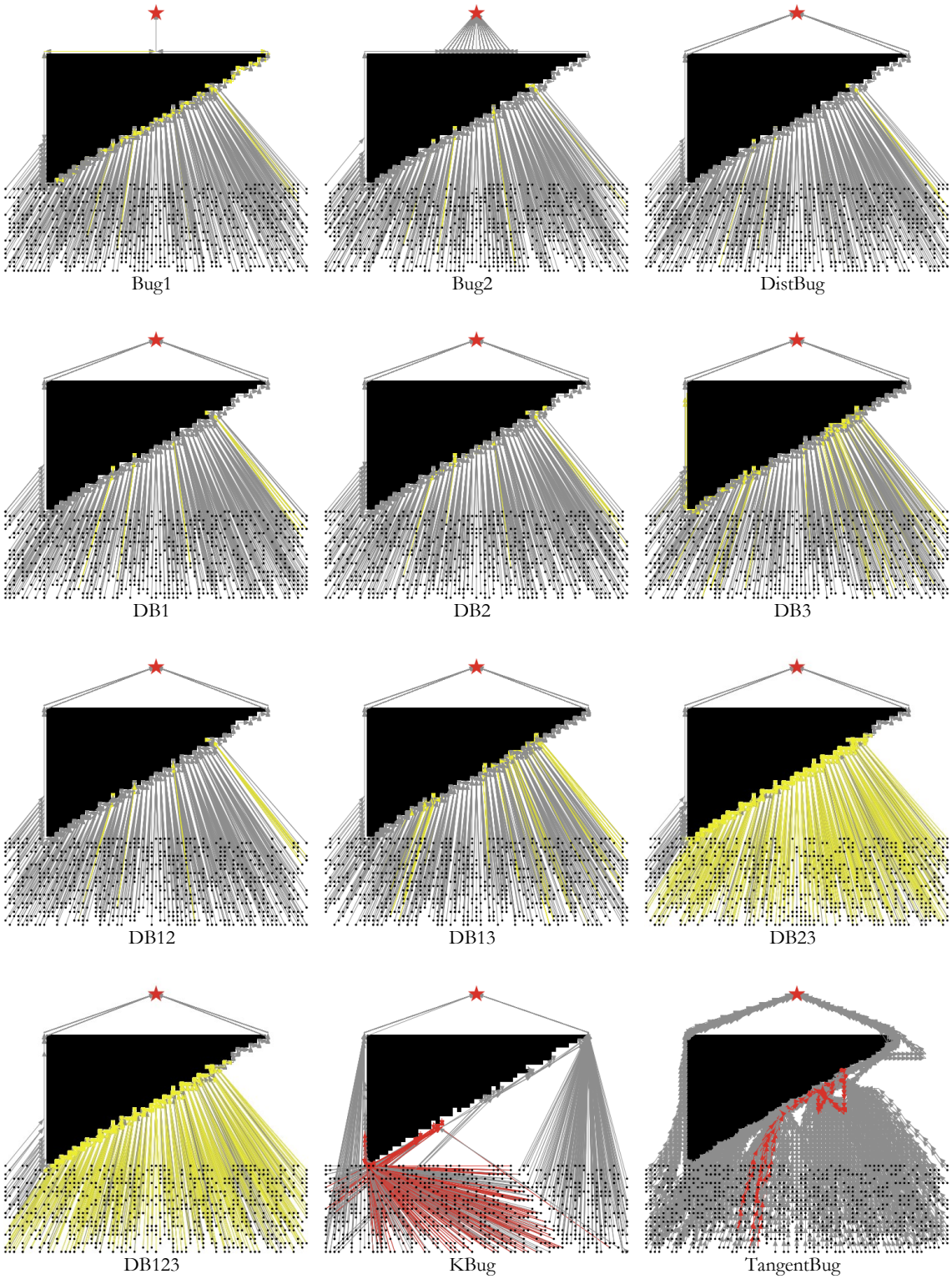

Figure 2-6. Results for the pixelated obstacle. Legend: red star: target; black circles: initial positions of agents; grey lines: converged simulations; red lines: non-converged simulations; yellow lines: false-flagged simulations.

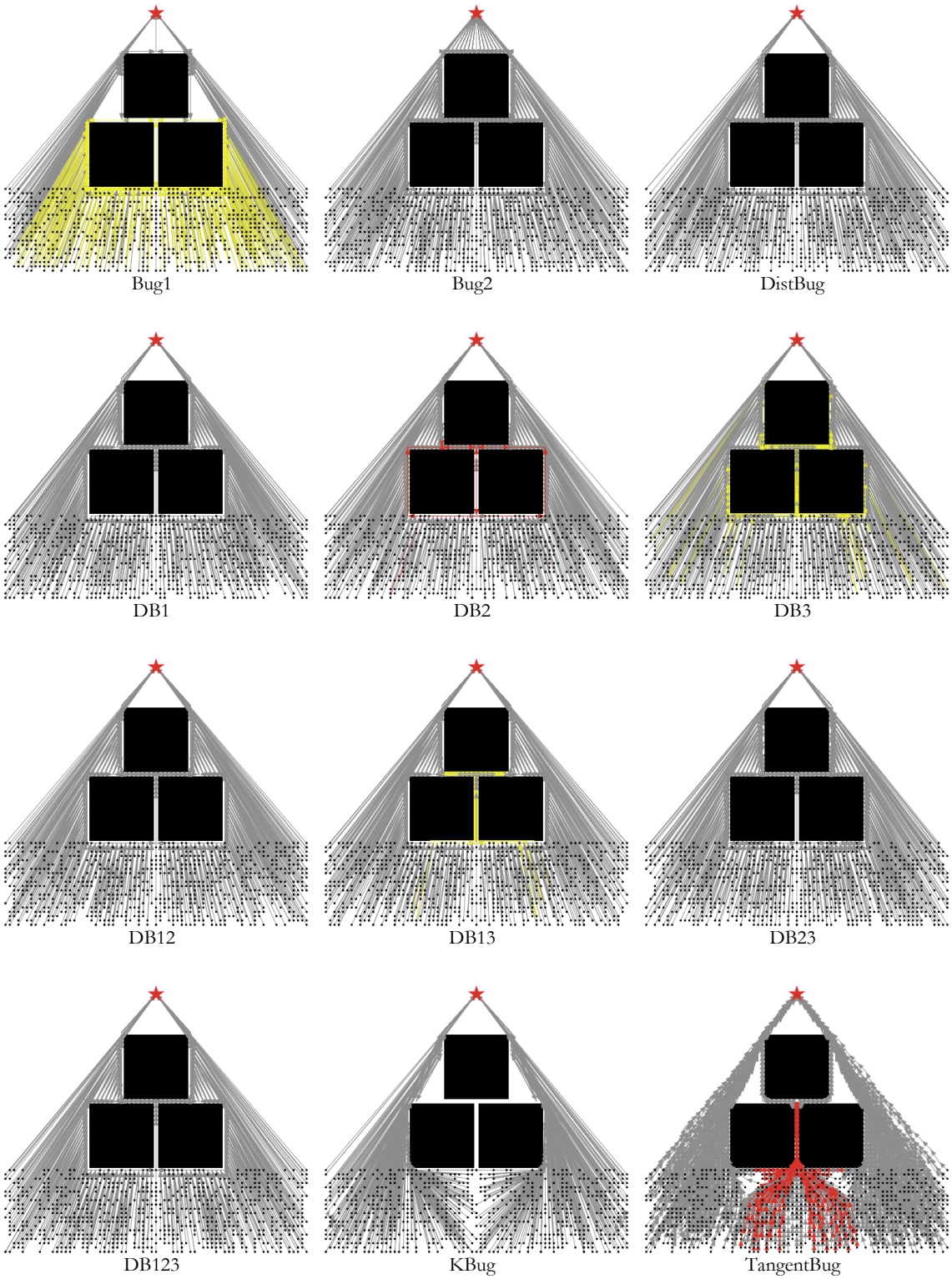

Figure 2-7. Results for the T-shaped corridor. Legend: red star: target; black circles: initial positions of agents; grey lines: converged simulations; red lines: non-converged simulations; yellow lines: false-flagged simulations.

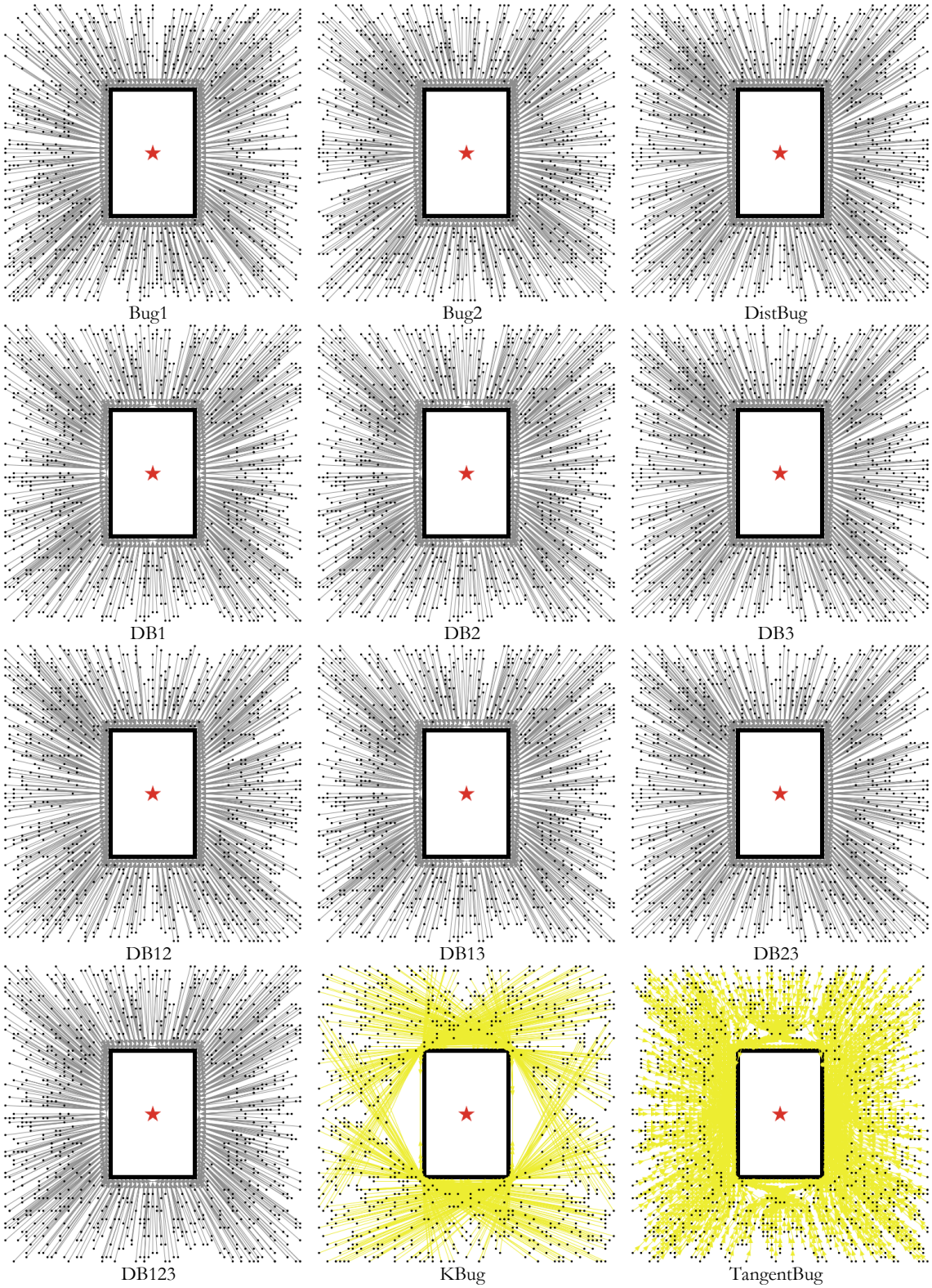

Figure 2-8. Results for the closed box obstacle. Legend: red star: target; black circles: initial positions of agents; grey lines: converged simulations; yellow lines: false-flagged simulations.

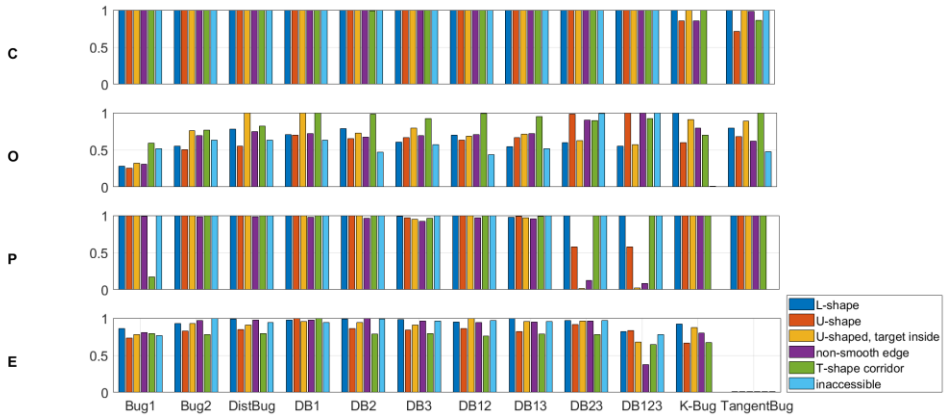

Figure 2-9. COPE indices grouped by algorithms

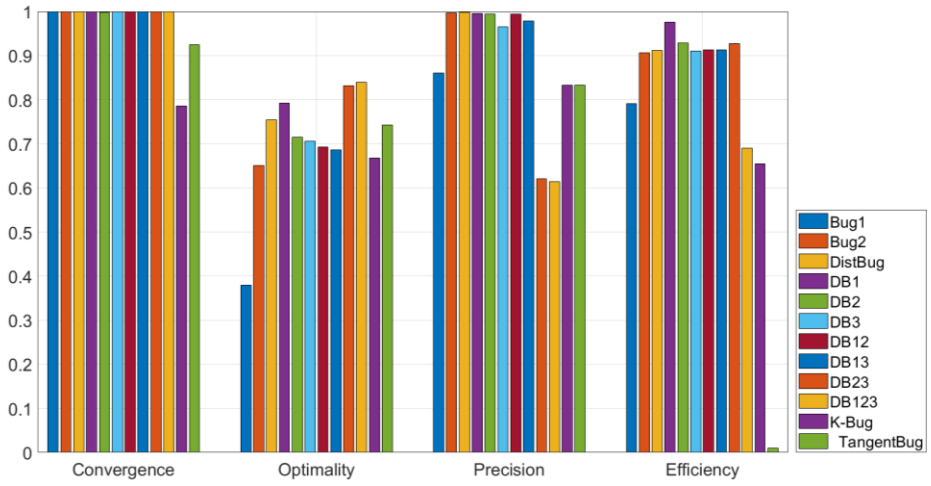

Figure 2-10. Average values of COPE indices for the algorithms

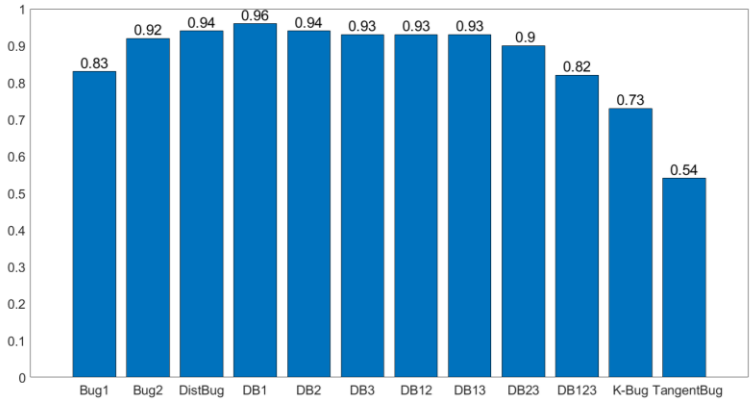

Figure 2-11. COPE index of algorithms

2.4.2. Discussion

In the following section, we will explore the results of the simulations, and explain why some of the algorithms fail to perform for certain obstacles.

Bug1 Algorithm: According to the Bug1 algorithm, when an agent reaches the leave point on the boundary of an obstacle, if it identifies another obstacle in front, it will consider itself as trapped. In environments such as the T-shaped corridor or wide obstacles with pixelated edges where the space between obstacles' corners is small (one patch in the context of this study), this will lead to false-flagging agents as trapped. Figure 2-12 shows an example in which the red cross is where the agent is falsely flagged as trapped.

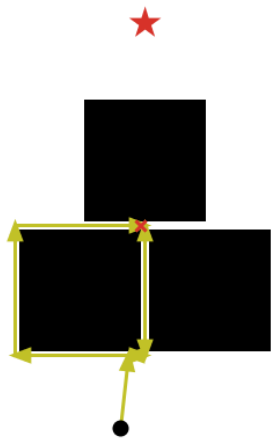

Figure 2-12. Bug1 - false flagging error

Bug2 Algorithm: According to the Bug2 algorithm, when an agent is following the boundary of an obstacle, if it returns to the hit point, it considers itself as being trapped. This can be problematic where obstacles have pixelated edges (see Figure 2-13). In general, aside from this error, the algorithm is simple, fast, works well for obstacles with any shapes, and generates shorter paths than Bug1, except for maze-like obstacles where the agent might get into cycles leading to longer paths [84].

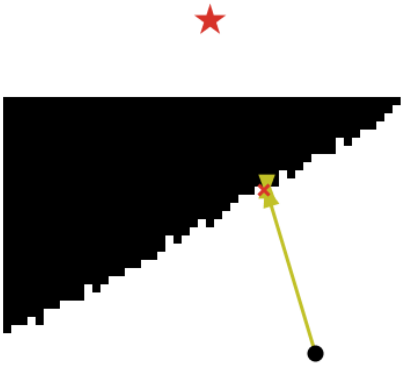

Figure 2-13. Bug2 - false flagging error

KBug Algorithm: The KBug algorithm does not converge for obstacles with numerous vertices. Agents get stuck along the vertices and are not able to find a path to pass the obstacle (see Figure 2-14). This is an acknowledged issue in the robot navigation literature; it is intuitive and recognized that obstacles with numerous vertices are difficult for algorithms to process, particularly for those using a range sensor [91]. In general, KBug does not perform well when obstacles or vertices of a single obstacle are close to each other, it does not provide any criteria to identify trapped agents, and it is relatively slow due to continuous screening of the environment; however, it can generate rather optimal paths for different obstacles when there is no convergence issue.

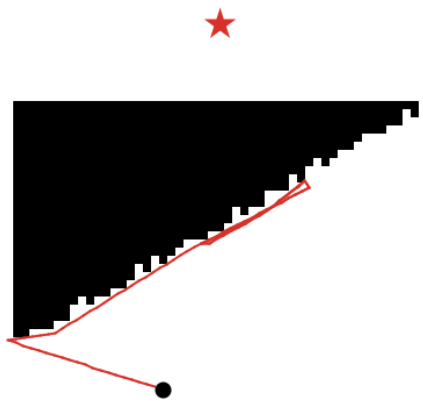

Figure 2-14. KBug - failure to converge

DistBug Algorithm: DistBug is developed based on Bug2 with improved leave conditions; therefore, it generates more optimal paths if the visual radius is large enough. However, since it is basically the Bug2 algorithm, it has Bug2's error in falsely identifying trapped agents. Moreover, the optional Extension-2 and Extension-3 lead to unnecessary change of direction when an agent is following the obstacle boundary, which causes the agent to be flagged as trapped when reaching a relatively wide obstacle with respect to its visual

radius (see Figure 2-15). In addition, generated paths are not optimal (i.e. realistic) due to the change of direction while following the obstacle boundary due to the Extension-2 and Extension-3 rules. These extensions to DistBug work well only if the size of the obstacle is relatively small with respect to the agent's visual radius. In general, excluding Extension-2 and Extension-3 rules, DistBug generates fairly optimal paths, and is relatively more efficient to compare with Bug1, Bug2, and KBug algorithms.

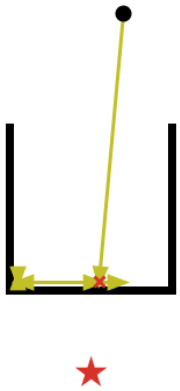

Figure 2-15. DistBug - false flagging error

TangentBug Algorithm: TangentBug can generate paths that approach the globally optimal paths when the environment is simple, and the agent's visual radius is relatively large with respect to the size of the obstacles [90]. Theoretically, it can handle obstacles with any shapes while generating optimal paths; however, it is not efficient for pedestrian navigation in which obstacles can be large with respect to the agent's visual radius; unlike in robot navigation, where obstacles are not wide relative to the robot's visual radius. This does not necessarily lead to failure to converge, but it makes agents show unrealistic behavior when navigating a wide obstacle with respect to the agent's visual radius (see Figure 2-16). A solution is to set the visual radius of the agents to a large number, but this might be unrealistic depending on the scale of obstacles, health or age status of individuals, and the maximum

visible distance (e.g. in case of evacuation involving fire and smoke), and it will make the algorithm more expensive. Another challenge in the implementation of TangentBug is building the Local Tangent Graph (LTG) for obstacles with complex and non-convex shapes and for narrow pathways. Failure to build the perfect LTG leads to failure in finding the optimal path. It also leads to convergence issues and false-flagging agents as trapped. In theory, the LTG should be continuous, but in practice, the implementation of the LTG can be challenging. This can lead to errors in identifying nodes [92]. The most prominent disadvantage of this algorithm is its computational cost. The algorithm takes much more time (of an order of 1000 to 10,000 in this study) than other algorithms to finish a simulation. This is a huge drawback in the use of TangentBug for large-scale city evacuation simulation.

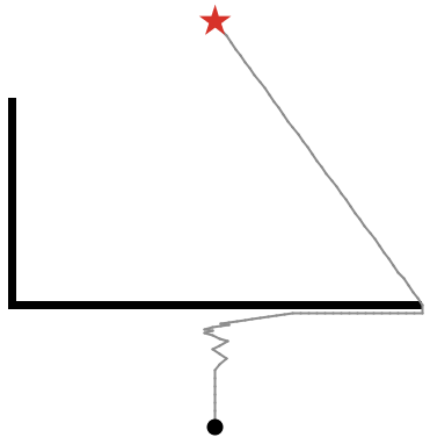

Figure 2-16. TangentBug - unrealistic behavior

2.5. Application: Evacuation of Iquique, Chile

To demonstrate applicability of the DB1 algorithm, a large-scale agent-based evacuation model is developed to simulate the evacuation of the city of Iquique, Chile. To evaluate the performance of the model and gain insight into the relative advantages and disadvantages of using bug navigation algorithms, the results and performance of the model

are compared with those from another study conducted by a team of scientists from the Chilean National Research Center for Integrated Natural Disaster Management and Pontificia Universidad Católica de Chile. The outputs of these two models are also compared with available data from a drill performed in Iquique in 2013. Global results of the drill are presented in the report of the National Office of Emergency of the Ministry of Interior and Security [93]. However, in order to evaluate the models, detailed time measures taken by the National Research Center for Integrated Natural Disaster Management (CIGIDEN) were used.

2.5.1. Input data

The coastal city of Iquique is in north Chile (20°13'S, 70°09'W) with a population of 180,000 people. The city is located in a subduction zone and is constantly affected by several earthquakes. The most recent event was the M_W 8.2 earthquake in 2014, which was followed by a tsunami that reached the coastline just 19 minutes after the ground motion ended [94]. Even though the entire city has to be evacuated in case of an emergency, this study focuses only on the downtown and historic zone of the city. In case of a tsunami, the National Office of Emergency of the Ministry of Interior and Security (ONEMI) has established that people have to evacuate to zones with an elevation of 30 m.a.s.l. [95]. The mean length from the shoreline and the border line of the security zone is about 2 km. Figure 2-17 shows the city, evacuation zone, evacuation routes, and the population distribution over the evacuation zone.

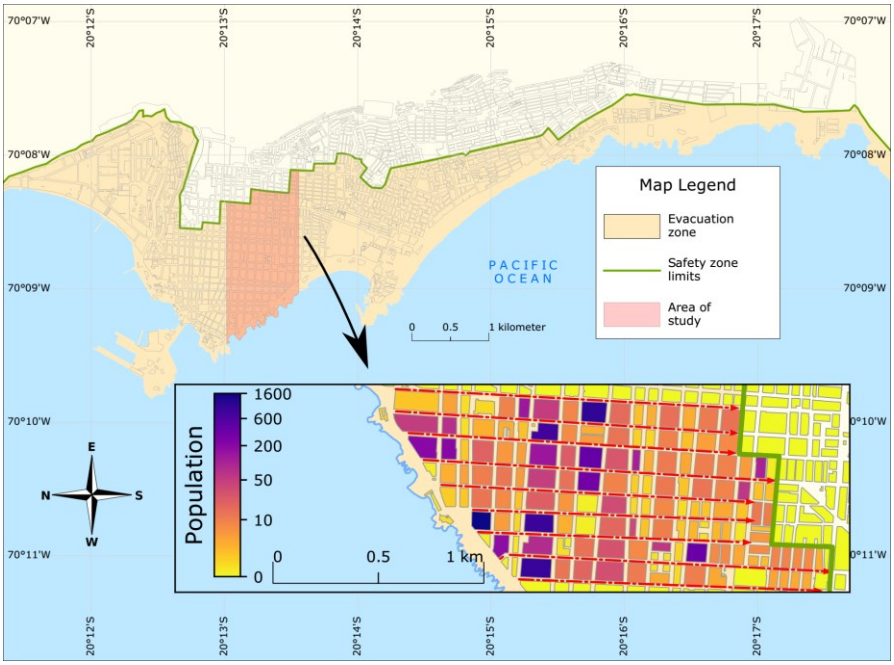

Figure 2-17: Map of Iquique showing the evacuation zone, evacuation routes, and population distribution.

The input data for the simulation is obtained from a team of scientists from the Chilean National Research Center for Integrated Natural Disaster Management and Pontificia Universidad Católica de Chile based on a previous study on the evacuation of Iquique [96]. In this study, the distribution of the population over the city was calculated using an origin-destination survey from 2012 for a morning scenario [97]. An estimated of 34,000 people are placed in the study area. According to exposure studies, 13,000 people are considered to be on streets (pedestrians) and 21,000 inside buildings with the number of occupants in each building known. The specifications of the buildings, such as building function and number of floors, are also provided. The time it takes for occupants of the buildings to evacuate onto the streets (vertical evacuation) is estimated for different types of buildings with different number of floors according to Poulos [80].

To estimate the number of vehicles, the motorization rate of the city was used. Iquique has a density of 23.7 vehicles per urban hectare, the highest density in Chile, yielding a total of 4,890 cars on the streets. Vehicles are separated into two categories: parked cars and moving cars. Considering that there is about 50 km-lane in the area of interest and using an average density of 40 veh/km-lane, which is a typical value for networks that are not congested, a total of 2,000 moving vehicles and 2,890 parked vehicles are considered. Vehicles are randomly distributed along the streets.

2.5.2. Evacuation models

The evacuation of Iquique is simulated by an agent-based evacuation model (Model A) which uses DB1 for the navigation of pedestrians. The results of the simulation will be compared with those from another study (Model B) conducted by a team of scientists from the Chilean National Research Center for Integrated Natural Disaster Management and Pontificia Universidad Católica de Chile. The specifications of these models are elaborated in the following subsections.

2.5.2.1. ABM with the robot navigation algorithm (Model A)

The agent-based evacuation model is developed in NetLogo. The core purpose of this model is to provide a user-friendly and fast evacuation simulation tool to support rapid decision making in the face of disasters. The model consists of two interactive modules: a pedestrian navigation module and a vehicle navigation module. Pedestrians avoid collision based on maximum population density. For this study, each pedestrian is considered to occupy a 50 cm by 50 cm area. To simplify the model, other human behaviors such as herding and information sharing are not implemented. The vehicle navigation module uses a simplified car following algorithm to handle car agents. A simplified vehicle navigation algorithm is

implemented to address the computation time advantage of the model. Acceleration and deceleration of vehicles are neglected; therefore, vehicles drive with a constant speed, and stop abruptly if needed. Two types of interactions are considered between pedestrians and vehicles: (1) Pedestrians use sidewalks along the streets while the main interaction between cars and pedestrians takes place at intersections. At those intersections with traffic light, both vehicles and pedestrians follow the traffic light considering just green and red phases. At intersections without traffic light, pedestrians have the right to cross the streets and vehicles stop for pedestrians to pass; (2) Pedestrians use the whole width of streets and interact with vehicles while walking. Similar to intersections without traffic light, pedestrians can walk on streets and vehicles shall stop for pedestrians to pass. Furthermore, pedestrians have the ability to use personal vehicles and share rides with each other.

The model uses GIS shapefiles as input data. Building blocks' and road network's shapefiles are imported containing information such as number of people, number of buildings, types of buildings in each building block, and the characteristics of roads including number of lanes, direction (one-way or two-way), and road type. Upon loading the transportation network, the Floyd-Warshall algorithm is used to find shortest paths between all pairs of nodes. If the road network changes (due to damages or propagation of the hazard), the Dijkstra algorithm is used to calculate new paths for vehicles running into blocked roads. Residents come out of the buildings (vertical evacuation) based on a constant rates calculated according to Castro et al. [96]. Walking speed of pedestrians is considered to follow a normal distribution with a mean of 1.34 m/s and standard deviation of 0.21 m/s [98]. The Length of vehicles varies from 4 m to 6 m, and they move at the speed limit which is 55 kmph (35mph) on local roads and 90 kmph (55 mph) on highways.

2.5.2.2. ABM with path planning and collision avoidance algorithm (Model B)

Similar to Model A, this model uses an agent-based approach to represent people and vehicles. The model is based on the work of Castro et al. [96], where each agent follows a route to a pre-defined objective using a collision avoidance algorithm. The selection of the evacuation route for each agent is obtained using the Dijkstra's algorithm, where it is assumed that agents know the entire distribution of the geometrical obstacles and the location of all exits. The movement of the agents is modeled using the Optimal Reciprocal Collision Avoidance principle (ORCA) developed by Van Den Berg et al. [77]. Each agent is represented as a circle while obstacles are considered with polygonal shapes. The collision avoidance algorithm performs an optimization problem where each agent tries to move to a preferred position considering all the other possible positions that other agents can have, preventing two or more agents to use the same physical space at the same time. This process is repeated at each time step of the simulation allowing one to capture, in a natural way, the congestion when several agents move close to each other. In addition to the physical interaction between agents, the model also considers the change of the pre-movement time when an agent walks nearby to another agent who still has not started to evacuate. This consideration is made to avoid congestion due to people standing on the doors or stairs when evacuating. Characteristics such as herding and information sharing were neglected in this approach.

During the evacuation simulation, there are three parameters to set for each agent: the radius, maximum speed of movement, and the pre-movement time. As the collision avoidance algorithm is limited to circular shapes, both pedestrians and vehicles are assumed to have representative radii. In the case of pedestrian, agents have a radius of 0.225 m, while for vehicles the radius is 1.015 m. The latter value was selected based on the width of regular vehicles. The maximum walking speed, which is the preferred speed of each agent when there

is no congestion, is sampled from a Weibull distribution for each agent. The shape and scale parameters used for pedestrians are $k = 10.14$ and $\lambda = 1.41\ m/s$, respectively. For vehicles, the Weibull's parameters are $k = 40$ and $\lambda = 15.5\ m/s$. Therefore, the mean values of the maximum speed for pedestrian and vehicles are 1.34 m/s and 55 km/h, respectively.

The effect of the slope is also considered for the agent's movement. Pedestrians' walking speed is affected by a reduction coefficient (ϕ) based on the formula given by Tobler [99] shown in Equation (2-10). This coefficient reduces the maximum speed of the agents according to the angle of street (θ). Vehicles do not have a reduction in their maximum speed.

$$\phi = \exp\left(-3.5\left(\left|\tan(\theta) + 0.05\right| - 0.05\right)\right) \tag{2-10}$$

2.5.2.3. Major differences

The main difference between Model A and Model B is in agent navigation. For pedestrians, Model A uses the DB1 bug navigation algorithm for path planning and maximum density for collision avoidance which are simple methods, while Model B uses the Dijkstra's algorithm for path planning and ORCA for collision avoidance which greatly adds to the calculations at each time step, for each of thousands of agents. As a result, Model A is simpler and faster than Model B but may not be as accurate. To evaluate what this means for the performance of these models in simulation of city evacuation in terms of accuracy and computation time, the results of the two models are compared with available drill data.

2.5.3. Results

For each model, the evacuation simulation of Iquique is repeated 50 times to account for the variability in the model. This case study can be used as a benchmark for the computational time of the model. The results of the simulations are shown in Figures 2-18 to 2-20 and Table 2-1.

Table 2-1. Summary of results for total evacuation of the city

	Drill (min)	**Model A (min)**	**Model B (min)**	**Model A relative error**	**Model B relative error**
Time to 25% evacuation	6.0	6.2	8.6	4%	43%
Time to 50% evacuation	12.0	12.2	14.3	2%	19%
Time to 75% evacuation	18.5	17.4	19.0	-6%	3%
Time to 95% evacuation	29	25.3	23.6	-13%	-19%
Time to total evacuation	46.5	69.4	39.5	49%	-15%
Computation time	-	10	2200	-	-

Figure 2-18 shows the total evacuation curve obtained from the drill and Models A and B. Both models provide acceptable results when compared to the drill data. Model A is more accurate than Model B until the 75% of evacuation ($variance_A^{75\%} = 0.6, variance_B^{75\%} = 4.5$) while for the final 25% of evacuation, Model A underestimates the arrival time and overestimates the final evacuation time by 50% ($variance_A^{100\%} = 39.3, variance_B^{100\%} = 7.0$). The reason for the overestimation lies in the optimality of DB1. Most classical bug algorithms, including DistBug, make the agents follow the boundaries of obstacles. This can lead to longer paths for agents that face many obstacles on their route. Upon further investigation of the results, 110 pedestrians (0.33% of total population) were found to cause this overestimation, which were located on the west side of the city with more obstacles (buildings) to navigate, and with slow walking speeds (0.9 – 1.0 m/s).

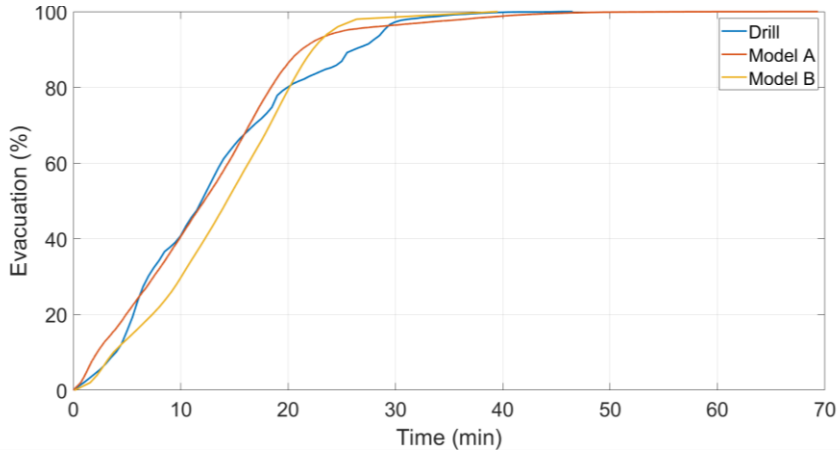

Figure 2-18: Total evacuation curves from the drill, Model A, and Model B

Figures 2-19 and 2-20 show the evacuation curves for those residents that arrived in the safe zones from two of the evacuation routes (Street 1 and Street 2) during the city evacuation. For Street 1, both models overestimate the arrival times. Model A shows more accurate results to compare with Model B; however, as explained above, it substantially overestimates the final arrival time. Regarding Street 2, Model B shows to be relatively more successful in capturing the evolution of arrivals while Model A underestimates the arrival times.

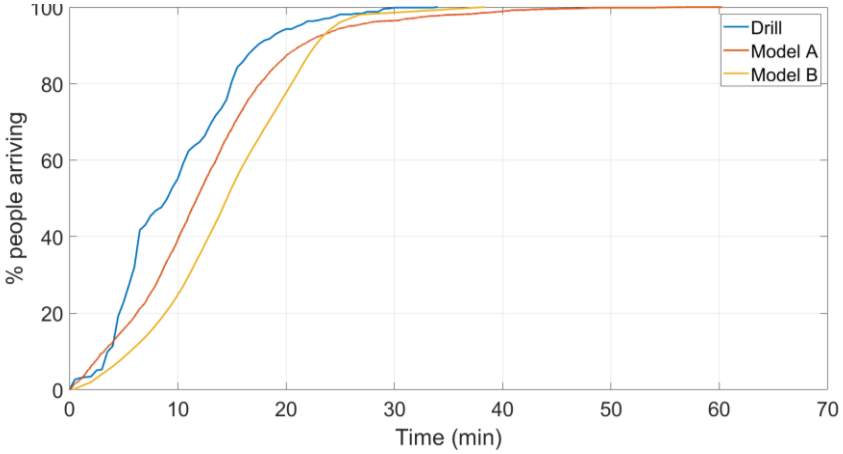

Figure 2-19: Evacuation curve showing percentage of people arriving in safe zone from Street 1.

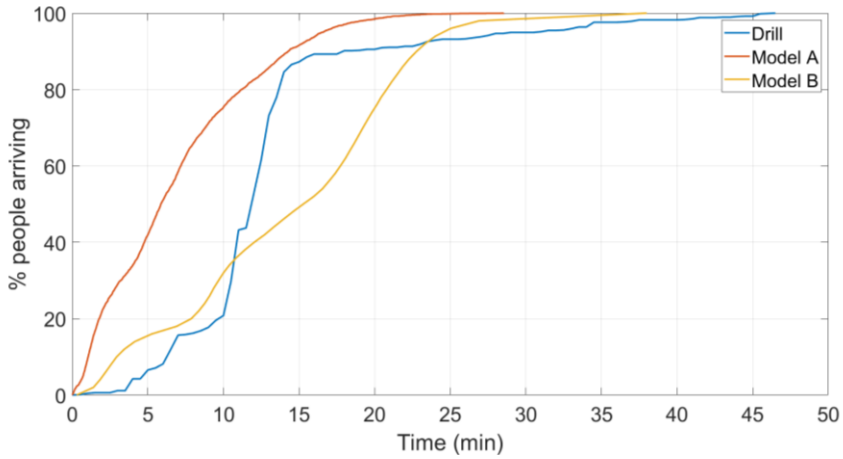

Figure 2-20: Evacuation curve showing percentage of people arriving in safe zone from Street 2.

After comparison of Model A and Model B, it is important to compare them in terms of computation time. The simulations are conducted on a computer with an Intel Zeon E3-1505M v5 @ 2.8 GHz processor and a 32GB memory. On average, it takes 10 minutes for Model A to run one simulation while for Model B, the computation time is 36 hours. Although these models are programmed in different languages (Model A in NetLogo and Model B in Python), and different machines are used to run these models, the difference in computation times is substantial enough to reach to the conclusion that Model A is a faster evacuation simulation tool. This difference can be explained due to the large number of nodes and obstacles that Model B uses for the calculation of the optimal route at every time step for each agent, while in Model A, each agent only analyzes its neighborhood.

In summary, Model A which uses DB1 can produce acceptable results for evacuation time of up to 95% of the evacuating population, but the final evacuation time obtained from the model is overestimated. Moreover, Model A can simulate the evacuation of a city on the

microscopic level in a short time which is a major benefit for situations in which there is a need for rapid decision making.

2.6. Conclusions

Computational models are powerful tools that can help emergency responders and decision-makers evaluate different scenarios, interventions, or policies. Simulation of large-scale evacuations are challenging; from one hand, macroscopic models can only provide limited information on the global evolution of the evacuation, on the other hand, microscopic models are computationally expensive. This study tries to address this challenge by developing a high-speed large-scale agent-based evacuation model. A set of classical bug navigation algorithms is selected, and their performance is evaluated in terms of convergence, optimality, precision, and efficiency. To demonstrate applicability, a large-scale agent-based pedestrian evacuation model is developed, with the candidate bug algorithm implemented in the model, to simulate the evacuation of the city of Iquique in Chile. The results are compared with those from another study and with data from an evacuation drill that was conducted in 2013 in the city. The results show that the model can perform relatively acceptable in terms of accuracy while the computation time is reduced significantly.

The COPE performance evaluation index can be further improved by defining benchmarks for optimality and efficiency so that the COPE framework will provide absolute performance indices. Furthermore, other bug algorithms should be evaluated to identify a more competent candidate algorithm for large-scale agent-based evacuation models. It is also necessary to study how other type of agent-based evacuation models (e.g. models based on social forces or potential field theory) perform to compare with bug navigation algorithms.

Chapter 3

Hospital Evacuation: Microscopic Agent-Based Modeling

3.1. Introduction

Researchers and decision makers have long been using traditional statistical methods such as regression analysis to develop predictive models for social, physical, and socio-physical systems. Although these modeling methods can be useful, they have specific disadvantages. Statistical models are developed based on available data of the system; this implies that if data is not available for a specific initial conditions or system boundary conditions, there will be no model. Furthermore, regression models use system-level data to explain the behavior of a system or networks of systems. Therefore, the heterogeneous behaviors of the elements of the systems are neglected. When it comes to complex systems, the inter-element interactions and the unique behaviors of elements lead to unpredictable nonlinear system-level emergent behaviors. In addition, top-down models, such as regression models, cannot explain why a system behaves differently under different conditions or over spatial or time domains. In short, the intrinsic diversity of the system is left unexplained. Consequently, there have been an increasing interest in using bottom-up methods, such as agent-based models (ABMs), to study socio-physical systems [100].

Agent-Based Modeling is a bottom-up modeling approach where complicated global behaviors of a system can be simulated by modeling the fundamental elements (agents) of the system and defining their behavior during interactions with other agents or the environment [44]. Each agent interacts with other agents and the environment based on a set of decision rules while accounting for underlying uncertainties. The advantage of agent-based modeling is that by defining the behaviors and rules on a microscopic level (i.e. the agent level), diverse and unexpected macroscopic or mass responses can be observed which are not exhibited by single agents. ABMs have been used in different subject areas, such as game theory [45,46], social sciences [47,48], economics [49,50], urban planning [51,52], and public health [53,54].

3.1.1. The Schelling Model

To better understand the capabilities of ABMs, we will demonstrate the development of the Schelling model of segregation [101]. The Schelling model is one of the earliest ABMs and was developed to study residential segregation of ethnic groups in urban areas. The model was introduced by Thomas Schelling, an American economist and the 2005 Noble Prize winner in Economic Sciences along with Robert Aumann for *"having enhanced our understanding of conflict and cooperation through game-theory analysis"* [102]. The model shows how personal preferences and perception of difference can lead to collective segregation. In this model, each agent represents a household and occupies one cell within a rectangular space. The rectangular space represents a virtual city. Each cell can be occupied by one agent only. Agents are grouped by their ethnicity into two groups (let's say blue and red). Each agent evaluates its *happiness* by comparing the fraction of its neighbors which belong to its ethnic group (f) with a predefined tolerance threshold (F). If the threshold is not met (i.e. $f < F$), the agent relocates to another empty cell where the ethnic fraction is at least F (i.e. $f \geq F$). A higher threshold value implies

a lower tolerance to the presence of neighbors from another ethnic group in the neighborhood. For each agent, the neighbors are the 8 surrounding agents. The mathematical form of the agents' decision rule is shown in Equations 3-1) and (3-2).

$$f(P_i) < F \rightarrow (x_i = \hat{x}_i | f(\hat{x}_i) \geq F) \quad 3\text{-}1)$$

$$f(P_i) = \frac{\dim\,(N_{p_i}^*)}{\dim\,(N_{P_i})} \quad (3\text{-}2)$$

where for agent P_i, x_i is its current position, $\hat{x}_i$ is the candidate new position, $N_{p_i}^*$ is the array of neighbors which belong to the same ethnic group, and N_{P_i} is the array of all the neighbors.

Two cases will be evaluated: (1) case 1: $F = 25\%$, and (2) case 2: $F = 75\%$. The space is a 50-cell by 50-cell square which is initially occupied by the two groups of agents over 90% of the available cells.

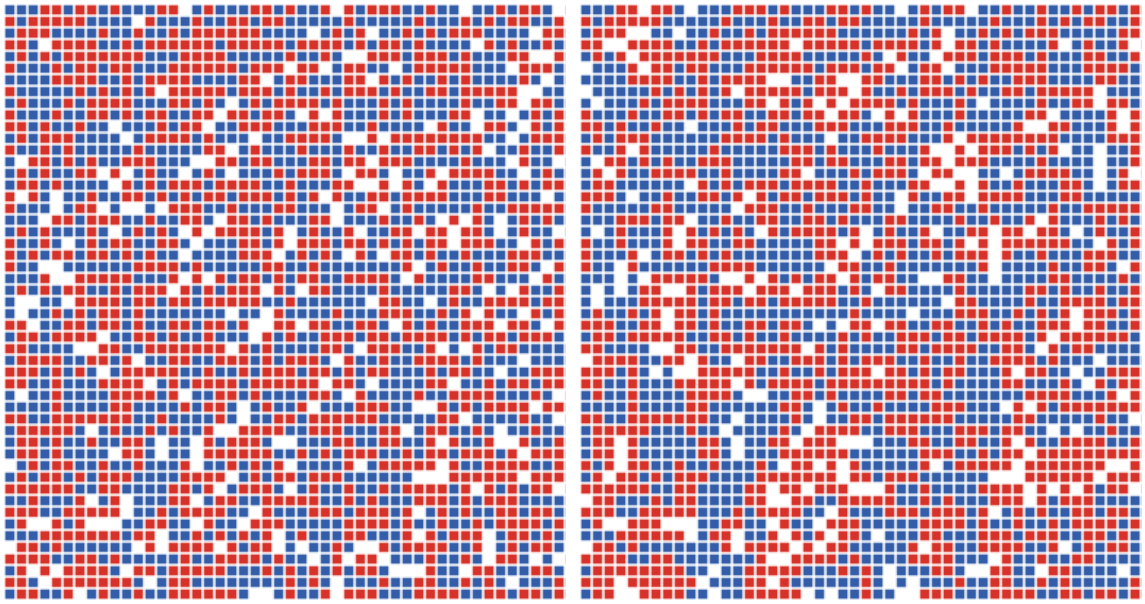

(a) (b)

Figure 3-1. The Schelling Model with F = 25%: (a) initial condition, (b) final condition.

The results for case 1 (F = 25%) is shown in Figure 3-1. Initially, 6% of the household are not happy with their neighbors. The model shows the city reaches a stable condition after 9 time-steps. Each time-step is the time it takes for the households to evaluate their neighborhood and relocate. After 9 time-steps, there are no unhappy households, and on average, 57% of neighbors of each agent are from the agent's group.

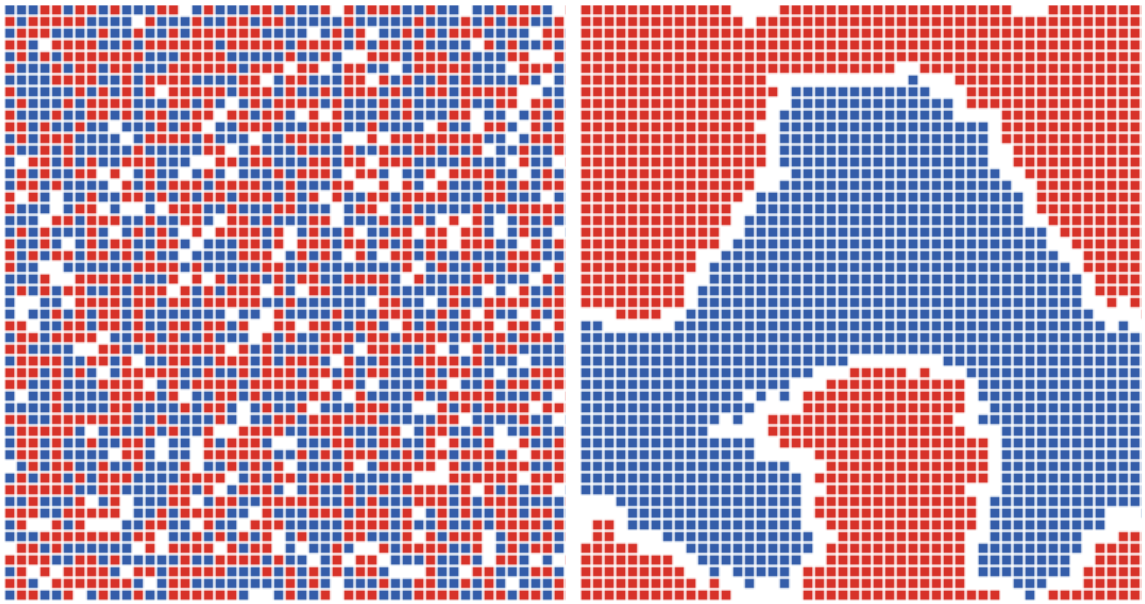

(a) (b)

Figure 3-2. The Schelling Model with F = 75%: (a) initial condition, (b) final condition.

Figure 3-2 shows the results for case 2 (F = 75%). Initially, 90% of the household are not happy with their neighbors. The model shows the city reaches a stable condition after 340 time-steps. At the stable condition, there are no unhappy households, and on average, 99.9% of neighbors of each agent are from the agent's group. As one can see, when the residents have a higher threshold regarding preference towards their ethnic groups, a clear residential segregation pattern evolves through time in the city, while with a lower threshold, no segregation is observed, and the random initial pattern remains with minor changes. Schelling

model shows that when considering this simple decision rule, noticeable segregation patterns start to emerge for threshold values of bigger than 1/3 [103].

3.1.2. Microscopic Evacuation Simulation

As discussed before in Chapter 1, evacuation is a socio-physical process in which humans interact with each other and with the built environment under extreme conditions. When it comes to hospital evacuation, the unique mobility characteristics and needs of patients make the evacuation process more complicated. The interactions between the patient evacuees and the hospital staff, the built environment (hospital building), and among patients themselves can lead to evacuation patterns which are not easy to predict. Consequently, agent-based modeling can be a useful tool to study the evacuation process in hospitals. In the next section, we will review the literature on the application of agent-based modeling in the simulation of hospital evacuation and explore different patient classification systems recommended by researchers and health professionals.

3.2. Literature Review

ABMs have been used in a vast variety of applications in engineering and social sciences, specifically as a supporting tool for decision making. In the context of evacuation, agent-based modeling is used to simulate evacuation of buildings, terminals, stadiums, etc. [67,104,105]. Although such studies consider heterogeneous populations, they do not consider evacuees with special mobility needs and characteristics. In this regard, there are few studies that have considered the heterogeneous behavior of patients and evacuees with disabilities and its effect on the evacuation process.

Those studies that have focused on agent-based hospital evacuation modeling are limited in number. Christensen and Sasaki [106] developed an ABM (called BUMMPEE) for hospital evacuation which represents the diversity and prevalence of disabilities among the evacuees. To represent the diversity of disabilities, six criteria are identified as the mobility parameters of agents: walking speed, physical size, ability to traverse, perception, psychological profile, and assistance needs. Based on these criteria, patients are classified into seven groups: motorized wheelchair users, non-motorized wheelchair users, the visually impaired, the hearing impaired, the stamina impaired, individuals without disabilities familiar with the environment, and individuals without a physical or sensory disability but less familiar with the environment. Moreover, four environmental characteristics are identified that can significantly affect the behavior of evacuees with disabilities: type of exit, route character, obstacles, and planned systems (e.g. safety requirement). The BUMMPEE model is used in other studies for the simulation of the evacuation of airports, stadiums, and high-rise buildings considering evacuees with disabilities [107–109]. In another study [65], patients are categorized into 4 groups: immobile patients who could not be moved from their beds, immobile patients who could be moved from their beds but only with considerable difficulty and an associated delay, immobile patients who could be moved with relative ease given the assistance of one or more members of staff, and mobile patients able to move on their own with some staff directions. Although the literature on the application of agent-based modeling in evacuation simulation of hospitals is limited, there is a great body of work dedicated to the mobility characteristics of different groups of evacuees characterized by parameters such age, gender, health status, type of mobility impairment, etc. [110,111].

Bish et al. [112] used an optimization model to develop an efficient evacuation plan for a hospital considering different types of patients. In this study, patients are classified into

9 groups: Intensive Care with ventilator (ICv), Intensive Care (IC), Neonatal Intensive Care with ventilator (NICv), Neonatal Intensive Care (NIC), Pediatric Intensive Care with ventilator (PICv), Pediatric Intensive Care (PIC), Other Bed-Bound (OBB), Ambulatory Oxygen-Dependent (AOD), and Other Ambulatory (OA). Furthermore, nursing teams are classified into two groups: teams with ventilator training and regular teams; ambulances into three groups: Critical Care Transport (CCT), Advance Life Support (ALS), and Basic Life Support (BLS); and beds into four groups: ICU, NICU, PICU, and regular beds.

To broaden our knowledge on patient disabilities, it is important to review the best practices and recommended classification systems for patients based on disabilities. These classification systems are developed by professional health organizations with the aim of providing a complete portfolio of patients or people with disabilities. The Americans with Disabilities Act of 1990 (ADA) defines the term 'disability' as: "with respect to an individual, a physical or mental impairment that substantially limits one or more of the major life activities of such individual; a record of such an impairment; or being regarded as having such an impairment" [23 p. 7]. However, ADA does not define the types of disabilities in any context.

The World Health Organization (WHO) published the International Classification of Functioning, Disability and Health (ICF) in 2001 [24]. ICF does not consider people as the units of classification, i.e. ICF does not classify people, rather it describes the condition of each person within an array of health or health-related domains. The result is a 4-level classification system with hundreds of classes which are assigned with unique codes. For example, b7302.3 indicates severe impairment of power of muscles of one side of body. Another source for patient classification is the study entitled "Guidelines for Evacuation of Individuals with Disabilities during Disasters" published by the American Medical Response and Department of Health and Human Services [25]. Although this guideline does not provide

a patient classification, it offers a useful source of information in the form of recommendations that can be used to classify patients. For example, it lists the following patients as those who need an ambulance: ventilator dependent patients, patients requiring continuous IV therapy, oxygen dependent individuals, individuals in need of a constant power source for suction pumps or any other bio-medical equipment usage, pregnant women experiencing contractions those in the eighth month of gestation or beyond, and so on.

With a different perspective, Harvard School of Public Health [26] categorizes patients based on evacuation priority into 4 general groups: patients who are in immediate danger, ambulatory patients, patients on general care units who require some transport assistance, patients on intensive care units.

The studies reviewed above have approached the challenges involved in the evacuation of people with disabilities by classifying evacuees based on their disabilities and required equipment. However, considering all types of ICU and non-ICU patients with different mobility needs require a thorough investigation on patients' needs, required level of care for each class of patients, priorities in patient evacuation, and many more factors and processes. For example, depending on the health problems, different patients in ICU sections need different equipment such as oxygen, ventilator, continuous IV therapy, or isolation kits, and the procedure to find a receiving hospital is complicated and subject hospital patient transfer policies and insurance policies. The mobility characteristics and needs of non-ICU patients are less diverse, hence mainly agent-based evacuation simulation software packages consider ambulatory patients and those non-ambulatory patients which need primary equipment such as wheelchairs or non-ICU beds. These software packages (e.g. building EXODUS) consider people with disabilities by modifying their walking speed, size, and ability to traverse different

paths (e.g. ramps and stairs). A complete review of these software packages and their features is conducted by the National Institute of Standard and Technology [113].

In this study, we will develop an agent-based evacuation model for non-ICU patients. In this regard, a patient classification system is developed based on mobility characteristics and needs. For path planning and collision avoidance, we will use the common algorithms from the literature: the Dijkstra's algorithm for finding shortest paths, and the Karamouzas' algorithm for collision avoidance.

3.3. The Agent-Based Model

3.3.1. Patient Classification

The first step in developing an agent-based model is to define what an agent represents in the model. In the context of evacuation modeling, each agent represents an individual; however, different individuals have different behavior in the model. Mainly, there are two type of agents: patients and staff. While patients and staff have the mutual purpose of reaching to safe zone, staff help patients, hence they move back and forth between the evacuation zone and the safe zone. Furthermore, patients have different class codes because they behave differently in the case of an evacuation. In this study, for patient classification, and in general, for developing an agent-based hospital evacuation model, a series of meetings were held to benefit from the experiences, expertise, and perspectives of healthcare professionals and experts within the Johns Hopkins University and Health System. These meetings were aimed at understanding the challenges and barriers in successful hospital evacuation, how modeling and simulation can help the healthcare systems to fill these gaps, and what the potential limitations and challenges in the modeling process can be. The details of the discussions are

presented in Appendix A. in what follows, the key notes and findings from these meeting are briefly listed:

Prioritization, procedure, patient needs

- The evacuation procedure completely depends on the scenario. Evacuation due to a heatwave is completely different than a fire scenario.
- The patient needs for evacuation depend on many factors: nature of the event, nature of patients' health issue, their acuity level, length of evacuation, means of transportation, etc.
- Evacuation prioritization depends on the nature of the event, e.g. the time and the imminence of the event can change the priorities. In addition, the operational policies of hospitals may change depending on the event. Therefore, a question to be addressed is: is the main problem the loss of functionality? or is it patient safety?
- There is no specific framework for pre-prioritization of ICU patients for evacuation.
- Patient prioritization for evacuation takes place on the spot by the physician in charge of an ICU based on his/her assessment on the statuses of patients.
- Regarding patient transfer, hospitals keep patients within their networks for different reasons, such as financial interests, insurance limitations, or pre-established agreements. This can lead to either longer evacuation delays due to limited receiving hospitals or shorter delays due to pre-defined agreements.
- During mass evacuations, the receiving hospitals set up a separate triage for transferred non-ICU patients to minimize the disruption of regular emergency department patient flow.

- There are a few state-level ICU bed database and patient transfer systems (e.g. NY, MD, and TX); however, these databases are not much practical, that is why hospitals still make phone calls to find ICU beds during evacuations.

ICU patients

- The specific needs of ICU patients are different on a case-by-case basis. This can bring too much complexity if the patients are categorized just based on the units in which they are hospitalized (i.e. ICU, NICU, PICU, etc.).
- On the other hand, for the classification of ICU patients, it may not be a good and practical approach to go deeper than ICU, NICU, PICU, etc. The problem will be too complex and with no data, there is in fact no advantage from a practical point of view.
- As for ICU patients, the problem is too broad, and it needs to be broken further down, so a case-by-case approach is preferred. We need to focus on one specific type of patient because the evacuation and transfer process for each patient is different and depending on the scenario and how ill the patient is, the process can significantly vary. Modeling all patients together would not be the best and most practical approach.
- There are different Levels of Care identified for ICU patients. These can be the criteria for classification of ICU patients and their required equipment.

Modeling

- There is a need for fast and reliable models to be used in real-time decision-making processes.
- Focusing on specific patients (e.g. transplant patients) can be more practical and useful and will lead to something that actually hospitals and emergency managers are willing to use.

- Although a lot of studies are being done and many models and tools are developed, hospitals and emergency teams mainly do not use these tools. There is a need for a more practical approach.
- Hospitals would be more interested in a model for one specific type of patient and for a specific scenario. There is an essential need for a more practical approach by bringing physicians and hospital staff into the modeling process.
- Regarding agent-based modeling, agent interaction exists among ambulatory patients and between ambulatory patients and hospital staff when they voluntarily help those having trouble walking. Moreover, agent-based modeling can help track the patients and find main reasons for evacuation delays. As these are the main advantages of using agent-based modeling for hospital evacuation, we should have a specific focus on these factors: (1) altruism and staff support; (2) agent tracking.
- Total evacuation time per se is not interesting, rather the required resources as a function of available time for safe evacuation is a more interesting and useful path for a modeling study.

Data

- There is almost no available data on hospital evacuation. Certain hospitals and health systems (specifically in southern states) that have prior evacuation experiences possess data on their evacuation procedures, however, these data are completely inaccessible to research societies.

Other

- There are many other complications based on the prior experiences, e.g. sometimes there is a need for mental health units due to special situation of mental health patients; or in hurricane Sandy, a hospital was faced with many issues to evacuate patients under

the criminal justice system. The situation was exacerbated as none of the patients could speak English.

The main outcome from these meetings is the identification of two major challenges in modeling hospital evacuation: (1) Considering ICU patients brings a lot of complexities into the modeling process. To properly tackle this issue, we need to separate ICU patients as they need more in-depth considerations. (2) There is no hospital evacuation data available (for research purposes). Although there may be some limited sources of data available or expected to be available through negotiations, unanimously, the aforementioned experts think the possibility to have access to a useful database within a reasonable time (one or two years) to be used in this study is significantly low. Therefore, this study is based on the limited available data on patient evacuation in the literature.

For the classification of patients, two perspectives are considered: (1) different characteristics and mobility needs of patients, and (2) available data on mobility characteristics and needs. As discussed before, patients have diverse attributes, need different equipment, and their attributes and needs also depend on the type of route (e.g. plain floor, ramps, stair, etc.) Although there exist thorough patient classification systems (as discussed in Section 3.2.), many of these groups of patients share similar mobility needs or characteristics. In addition, available data on mobility characteristics of patients (or people with disabilities) does not cover all types of patients. Consequently, a patient classification system is developed, based on available data, to be used as the basis for agent classification in the ABM (Figure 3-3).

According to the patient classification system, patients are classified into 5 groups: (1) visually impaired, (2) hearing impaired, (3) mobility impaired, (4) mentally impaired, and (5) non-disabled. Mobility impaired patients are further classified into 5 sub-groups: wheelchair users, motorized wheelchair users, stamina impaired (including crutch and walker users), high

acuity bed bound, and low acuity bed bound patients. Non-disabled patients are also divided into 2 groups: elderly or children, and adults.

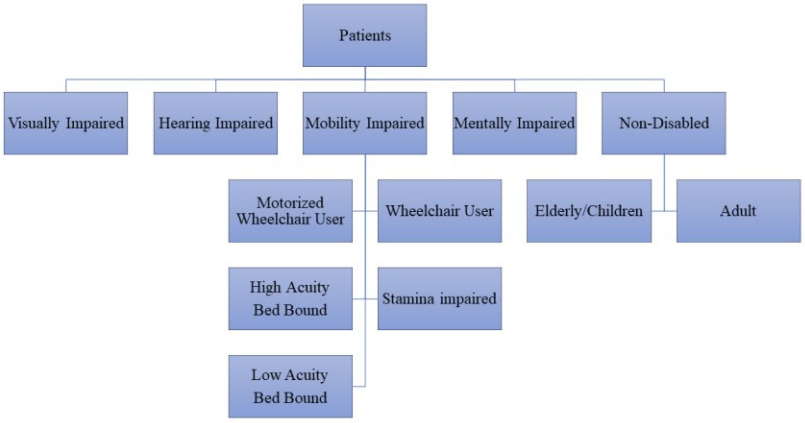

Figure 3-3. Patient Classification System

The mobility attributes of the staff agents and patient agents are listed in Table 3-1 and Table 3-2, respectively.

Table 3-1. Mobility attributes of staff agents

Attributes	**Description**	**Data Type**
status	status of the agent regarding patient evacuation assistance: 1 = idle 2 = moving toward a patient 3 = helping 4 = self-evacuation	categorical
assigned patients	a list containing the IDs of the patients the agent has helped or is helping	array of integers
free speed	free flow walking speed in [m/s]	floating point number
speed	current speed in [m/s]	floating point number
size	body size (diameter) in [m]	floating point number

Table 3-2. Mobility attributes of patient agents

Attributes	Description	Data Type
class	1 = visually impaired 2 = hearing impaired 3 = wheelchair user 4 = motorized wheelchair user 5 = stamina impaired 6 = high acuity bed bound 7 = low acuity bed bound 8 = mentally impaired 9 = elderly or children (non-disabled) 10 = adult (non-disabled)	categorical
assistance	assistance need: 1 = no 2 = preferred 3 = yes	categorical
assistance type	type of needed assistance: 1 = not needed 2 = general 3 = special	categorical
assistance number	number of needed assistants	integer
assigned assistant	id of the staff/patient helping the agent	integer
status	status of the agent regarding patient evacuation assistance: 1 = idle 2 = waiting to get help 3 = helped 4 = helping another patient 5 = self-evacuation	categorical
free speed	free flow walking speed in [m/s]	floating point number
speed	current speed in [m/s]	floating point number
size	body size (diameter) in [m]	floating point number

In Table 3-1, *status* refers to the current activity of the staff agents. In the model, each staff agent is doing one the following tasks: staying idle (before the evacuation or during the evacuation when the staff agent is waiting for task assignment), moving toward a patient to help, helping a patient move toward exit doors, or evacuating the hospital without a patient. The *assigned patients* attribute is a list containing the ID of all the patients that the staff agent has helped or is already helping to move toward exit doors. This list can be used in the post-processing phase to track patients and staff and find barriers or unnecessary delays in the evacuation process. The free speed and size of the staff agents are listed in Table 3-3. The current speed of all agents is calculated according to the collision avoidance algorithm explained in Section 3.3.3.

In Table 3-2, *class* refers to the class of each patient agent determined based on the patient classification system shown in Figure 3-3. The *assistance* attribute indicates whether the patient agent needs help for evacuation. Those patient agents that need help (assistance = 3) cannot move without help and are the top priority in receiving help from staff agents. Those that prefer help (assistance = 2) can move slowly without help but move faster when being assisted. The *assistance level* attribute indicates whether the patient needs assistance that can be provided by anyone (staff or other patients) or they need special assistance that can only be provided by the hospital staff. The *assistance number* attribute determines the number of assisting agents that the patient agent needs for evacuation. For simplicity, it is considered that all number of needed assistants provide the same type of assistance (general or special). Similar to staff agents, *status* refers to the current activity of the patient agent. The free speed and size of the patient agents are listed in Table 3-3 [110,111].

Table 3-3. Free moving speed and size of the agents

Agent Class	Free Speed on Floors [m/s]		Free Speed on Ramps [m/s]		Free Speed on Stairs [m/s]		Size [m]
	Assisted	Not Assisted	Assisted	Not Assisted	Assisted	Not Assisted	
Staff	-	1.4	-	0.9	-	0.7	0.5
Visually impaired	0.69	0	0.61	0	0.61	0	0.5
Hearing impaired	1.25	0	0.9	0	0.7	0	0.5
Wheelchair user	1.25	0.69	0.89	0.5	0.89	0	0.8
Motorized wheelchair user	-	0.89	0.89	0.7	0.89	0	0.8
Stamina impaired	0.78	0.57	0.49	0.36	0.69	0.33	0.5
Bed bound	0.89	0	0.67	0	0.67	0	1×2*
Mentally impaired	1.25	0	0.7	0	0.7	0	0.5
Elderly/Children (non-disabled)	-	1.05	-	0.7	-	0.6	0.5
Adult (non-disabled)	-	1.25	-	0.9	-	0.7	0.5

* Bed bound patients occupy a 1 m by 2 m rectangle, which can also be modeled by two attached circular agents, each with a diameter of 1 m.

In developing the patient classification system, the mobility needs are also considered. Patient mobility needs for each class of patients are listed in Table 3-4.

Table 3-4. Mobility needs of agents

Agent Class	Assistance Need	Assistance Type	# Assistants
Visually impaired	Yes	General	1
Hearing impaired	Preferred	General	1
Wheelchair user	Yes	General	1
Motorized wheelchair user	No	Not needed	0
Stamina impaired	Preferred	General	1
High acuity bed bound	Yes	Special	2
Low acuity bed bound	Yes	Special	1
Mentally impaired	Yes	General	1
Elderly/Children (non-disabled)	Preferred	General	1
Adult (non-disabled)	No	Not needed	0

3.3.2. Path Planning Algorithm

The movement engine of every agent-based evacuation model consists of two components: path planning and collision avoidance. In this section, we will explain the path planning algorithm used in the ABM. The premise of agent path planning is based on the fact that evacuees take locally optimal path when passing through obstacles, rooms, and corridors to reach their destination [86,87]. Consequently, the path planning problem in agent-based evacuation models are mainly resolved using shortest path algorithms. In this regard, the environment is represented with a graph in which the nodes represent the obstacles' vertices, bottlenecks, and all entrance and exit doors.

In graph theory, the shortest path problem is defined as finding the minimum weighted distance between two nodes in a graph. Several algorithms have been developed to solve the

shortest path problem, among which, the followings are the most efficient ones: Dijkstra's algorithm [114] that finds the shortest path from a source node to all other nodes in a graph; Floyd–Warshall algorithm [115,116] that solves all pairs shortest paths with positive and negative link weights; Bellman–Ford [117,118] algorithm which is similar to the Dijkstra's algorithm but with both positive and negative link weights; and the A* algorithm [119] which is a heuristic algorithm for single pair shortest path. In this study, the Dijkstra's algorithm is used for path planning. For demonstration purposes, the algorithm is used to find the shortest path in a simple environment.

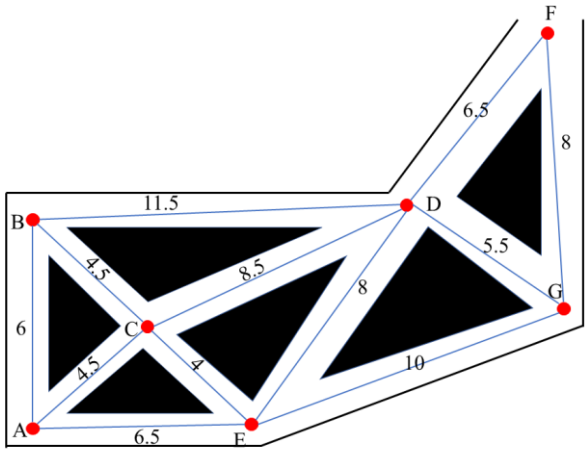

Figure 3-4. A node network on a simple environment

Figure 3-4 shows a part of a building with a node network constructed to find the shortest path from node A to node F. The numbers on the links show the distance between nodes in meters. The Dijkstra's algorithm starts by assigning a large number (let's say infinity) to nodes. These numbers show the distance from the origin (node A) to the corresponding node. We will update these numbers as moving forward. The Dijkstra's algorithm records the visited notes in an array. The array is initially empty (visited = {}).

Step 1: the first node to visit is the origin, node A. The visited nodes array updates to visited = {A}. The distance from node A to node A is zero, which is smaller than infinity, so we update the distance to node A to zero, and the shortest path from node A to node A is through node A (duhh!). We will update the distance values for the unvisited neighbor nodes of the last node in the visited nodes array, which is node A. the unvisited neighbor nodes to node A are nodes B, C, and E, and the distance from A to these nodes are 6, 4.5, and 6.5, respectively, which are all smaller than the current distances (infinity), so we update the shortest distance and the node to get to nodes B, C, and E. Figure 3-5 shows the graph after step 1. The white circles are the unvisited circles, the red circles represent the visited circles, and the values above each node shows the shortest distance to that node and the node to get there.

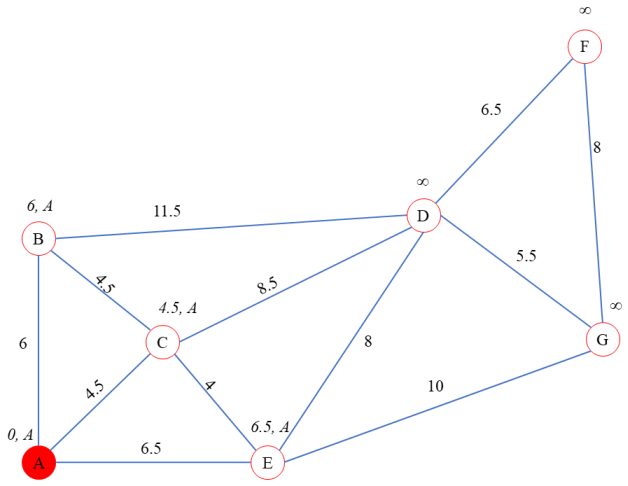

Figure 3-5. Dijkstra's algorithm example (step 1)

Step 2: the next node to visit is the unvisited node with the lowest calculated distance, which is node C. The visited nodes array updates to {A, C}. Similar to step 1, we will update the distance values for the unvisited neighbor nodes of the last node in the visited nodes array, which is node C. the unvisited neighbor nodes are B, D, and E. The total distance to get to B

through C is 9 (4.5 + 4.5) which is larger than the current distance to get to B (which is 6 and through A), so we do not update node B. The total distance to get to D through C is 13 (4.5 + 8.5) which is smaller than the current distance to get to B (which is infinity), so we do update node B. The total distance to get to E through C is 8.5 (4.5 + 4) which is larger than the current distance to get to B (which is 6.5 and through A), so we do not update node B. Figure 3-6 shows the updated graph after step 2.

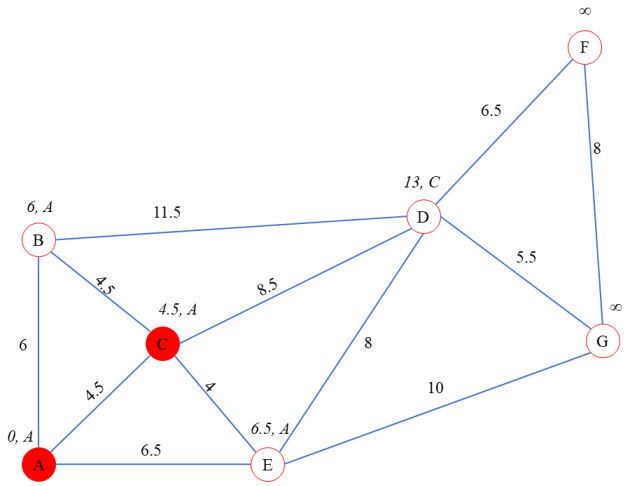

Figure 3-6. Dijkstra's algorithm example (step 2)

Step 3: the next node to visit is node B (visited nodes = {A, C, B}). The only unvisited neighbor node to node B is node D. The total distance to get to D through B is 17.5 (6 + 11.5) which is larger than the current distance to get to D (which is 13 and through C), so we do not update node D. Figure 3-7 shows the updated graph after step 3.

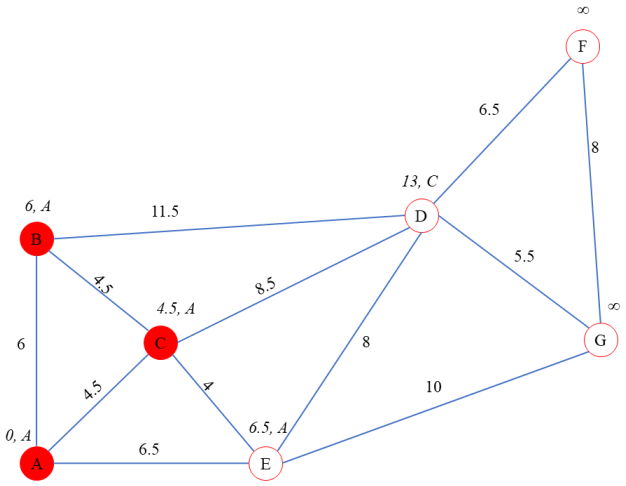

Figure 3-7. Dijkstra's algorithm example (step 3)

Step 4: the next node to visit is node E (visited nodes = {A, C, B, E}). The unvisited neighbor nodes to node E are D and G. The total distance to get to D through E is 14.5 (6.5 + 8) which is larger than the current distance to get to D (which is 13 and through C), so we do not update node D. The total distance to get to G through E is 16.5 (6.5 + 10) which is smaller than the current distance to get to G (which is infinity), so we update node D. The updated graph after step 4 is shown in Figure 3-8.

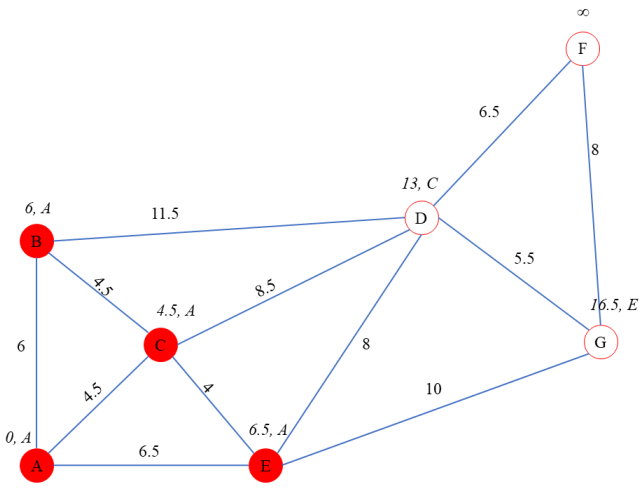

Figure 3-8. Dijkstra's algorithm example (step 4)

Step 5: the next node to visit is node D (visited nodes = {A, C, B, E, D}). The unvisited neighbor nodes to node D are F and G. The total distance to get to F through D is 19.5 (13 + 6.5) which is larger than the current distance to get to F (which is infinity), so we update node F. The total distance to get to G through D is 18.5 (13 + 5.5) which is larger than the current distance to get to G (which is 16.5 and through E), so we do not update node G. The updated graph after step 5 is shown in Figure 3-9.

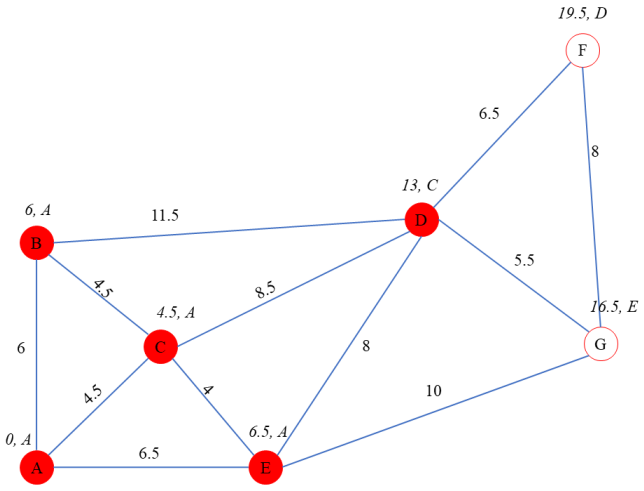

Figure 3-9. Dijkstra's algorithm example (step 5)

Step 6: the next node to visit is node G (visited nodes = {A, C, B, E, D, G}). The only unvisited neighbor node is node F. The total distance to get to F through G is 24.5 (16.5 + 8) which is larger than the current distance to get to F (which is 19.5 and through D), so we do not update node F. Since there is only the destination node (node F) left, the last node to visit is F and the algorithm stops. The Final graph is shown in X, which indicates that the shortest distance from A to F is 19.5 and the path is {A, C, D, F}.

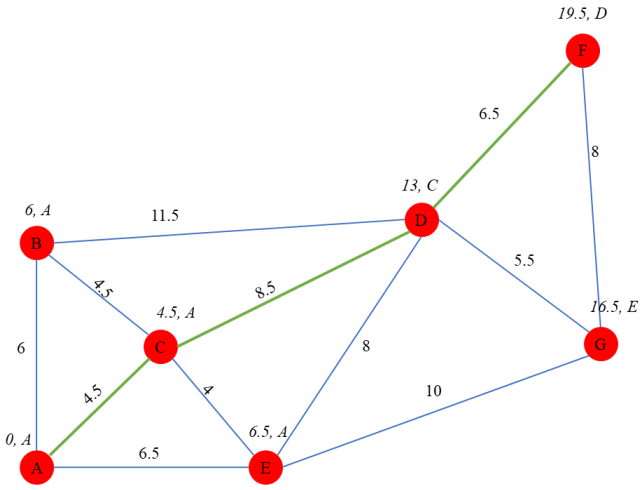

Figure 3-10. Dijkstra's algorithm example: final graph with the shortest path shown in green.

The pseudocode for the Dijkstra's algorithm is shown below

Box 3-1

```
function Dijkstra(graph, source):
        create vertex set Q
        for each vertex v in graph:
                dist[v] ← infinity
                prev[v] ← undefined
                add v to Q
        dist[source] ← 0
        while Q is not empty:
                u ← vertex in Q with min dist[u]
                remove u from Q
                for each neighbor v of u:
                        alt ← dist[u] + length(u, v)
                        if alt < dist[v]:
                                dist[v] ← alt
                                prev[v] ← u
        return dist[ ], prev[ ]
```

Using the Dijkstra's algorithm implies that the patient agents in the model have complete knowledge about the routes in the hospital. This is an unrealistic assumption; however, the evacuation paths in hospitals are pre-determined and shown with marks and signs, moreover, the hospital staff and those patients that know the best exit routes will help

other patients and direct them to the exit doors. This behavior is implemented in the model through information sharing which is explained in Section 3.3.4.

3.3.3. Collision Avoidance Algorithm

The path planning algorithm determines how an agent should go from its current position to the safe zone; however, the agent will have to navigate its way among other agents and any obstacles (e.g. dynamic obstacles) which were not considered in the path planning algorithm. The agent navigation is controlled by the collision avoidance algorithms.

The collision avoidance behavior at the local level is essential to give a realistic behavior to moving agents so that the ABM can produce emergent crowd behaviors which are observed in evacuations [17,75,120,121]. A number of collision avoidance algorithms have been developed which use different approaches with different complexity levels and performance measures. Mainly, these algorithms are based on the social force method, such as the agent-based social force model developed by Helbing and Molnar [122], or collision prediction, such as the Optimal Reciprocal Collision Avoidance (ORCA) algorithm developed by Van Den Berg et al. [123]. One drawback of social force models is the lack of anticipation and prediction, specifically in dense populations, which leads to unrealistic behaviors. The prediction-based algorithms extrapolate the trajectories of agents and use them to determine collisions in the near future [75]. In this study, the predictive collision avoidance model developed by Karamouzas et al. [75] is used.

In what follows, the Karamouzas' algorithm is explained. Suppose there are n agents $P_i, i = 1{:}\,n,$ in a virtual environment, each moving towards its destination. For simplicity, it is assumed that the agents move on a flat plane and are modeled as a disc with radius r_i. At time t, the agent P_i is at position $x_i(t)$, has an orientation $\theta_i(t)$ and moves with velocity $v_i(t)$.

Each agent also has a maximum or desirable speed u_i^{max} such that $\|v_i(t)\| \leq u_i^{max}$. At each time step, the agent P_i prefers to move towards its destination with its maximum speed. The maximum speed is gained gradually within a certain time τ. The force that drives the agent towards its goal is defined as:

$$F_g = \frac{1}{\tau}\left(u_i^{max} n_{gi} - v\right), \tag{3-3}$$

where $n_{gi} = \frac{g_i - x_i}{\|g_i - x_i\|}$ is the unit vector towards the agent's goal, and v is the agent's current velocity.

The agent has to avoid collision with the obstacles and walls, as well. let W denote the set of walls in the environment. From each wall $w \in W$ a repulsive force is exerted on the agent. This force can be calculated as:

$$F_w = \begin{cases} n_w \dfrac{d_s + r_i + d_{iw}}{(d_{iw} - r_i)\hat{}\kappa}, & if\ d_{iw} - r_i < d_s \\ 0 & otherwise, \end{cases} \tag{3-4}$$

where n_w is the normal vector of the wall, d_s is the safe distance from the wall, d_{iw} is the shortest distance of the agent from the wall, and the constant κ indicates the intensity of the repulsive potential.

Each agent prefers to keep a certain distance ρ_i from other agents as its personal space. This personal space is modeled as a disc centered at the position of the agent (x_i) with a radius of $\rho_i > r_i$. The agent P_i identifies a collision when another agent P_j enters its personal space at some time t_c:

$$\exists\ t_c \geq 0 \mid d_{ij} \leq \rho_i + r_j \tag{3-5}$$

where $d_{ij} = \|x_i - x_j\|$ is the center to center distance between the two agents.

Each agent resolves potential collisions within an anticipation time t_α by adjusting its trajectory. This adjusting behavior is modeled by applying an evasive force F_e from each colliding agent. To calculate F_e, first we need to identify agents that will collide with agent P_i some time before the anticipation time ($t_c^{ij} \leq t_\alpha^i$). To achieve this, we calculate the desired velocity of agent P_i by applying the goal force and the wall forces on the agent:

$$v_i^{des} = v_i + \left(\sum F_w + F_g\right) m_i \Delta t, \tag{3-6}$$

where m_i is the mass of agent P_i, and Δt is the time step. It is assumed that all agents have a unit mass.

Based on the calculated desired velocity, we calculate the future position of agent P_i as in X if it does not adjust its trajectory to avoid collision with other agents.

$$\tilde{x}_i = x_i + t v_i^{des} \tag{3-7}$$

Similarly, we calculate the future position of agents which are within the field of view of agent P_i. Since agent P_i does not know the desired velocity of other agents, we use their current velocities for the calculations, i.e.:

$$\tilde{x}_j = x_j + t v_j \tag{3-8}$$

We can now determine if agent P_i will collide with any agent within its field of view. According to Equation (3-5), a collision occurs when an agent enters the personal space of another agent. This condition can be evaluated using Equation (3-9).

$$\left\|\tilde{x}_j - \tilde{x}_i\right\| = \rho_i + r_j \tag{3-9}$$

Solving Equation (3-9) for t, we can estimate future collision time t_c^{ij}. If the equation yields no solutions or a single solution, then no collision will occur, but if it yields two solution (t_1 and t_2), we can have three cases:

(1) $t_1, t_2 \leq 0$: this implies a past collision and can be ignored.

(2) $t_1 < 0 < t_2$ or $t_2 < 0 < t_1$: this implies an imminent collision, i.e. $t_c^{ij} = 0$, so we add agent P_j to the colliding list of P_i.

(3) $t_1, t_2 > 0$: this implies that a collision will occur at time $t_c^{ij} = \min(t_1, t_2)$. If $t_c^{ij} \leq t_\alpha$, then agent P_j will be added to the colliding list of P_i.

After evaluating all the agents in the field of vision for collision, we sort the list in order of increasing time and keep the first N agents. This increases computational speed and also provides a realistic behavior reflecting natural human behavior.

The next step is to calculate an evasive force F_e^{ij} so that agent P_i can smoothly avoid each agent P_j in the list of colliding agents. The direction of the force is given by the unit vector $n_{ij} = \frac{\tilde{x}_i - \tilde{x}_j}{\|\tilde{x}_i - \tilde{x}_j\|}$ pointing from $\tilde{x}_j$ to $\tilde{x}_i$, where $\tilde{x}_i$ and $\tilde{x}_j$ are calculated using Equations (3-7) and (3-8) for $t = t_c^{ij}$. The magnitude of the force F_e^{ij} can be calculated by a piecewise function shown in Figure 3-11a in which $D = \|\tilde{x}_i - x_i\| + \|\tilde{x}_i - \tilde{x}_j\| - r_i - r_j$, which denotes the sum of distance between current position of P_i and its future position and the distance between P_i and P_j at the time of collision (see Figure 3-11b). the piecewise function is defined as follows:

$$f(D) = \begin{cases} \frac{\alpha}{D}\beta & D \leq D_{min} \\ \beta & D_{min} < D \leq D_{mid} \\ \frac{D_{max} - D}{D_{max} - D_{mid}}\beta & D_{mid} < D \leq D_{max} \end{cases} \quad (3\text{-}10)$$

in which α and β are the parameters of the function.

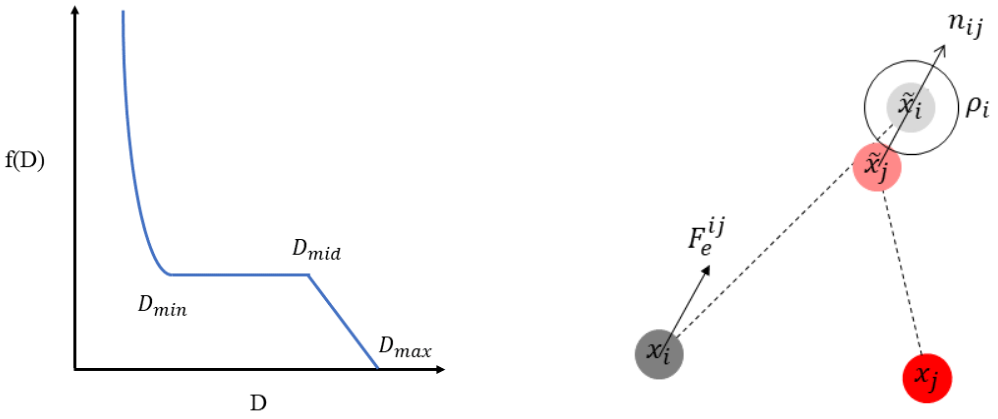

(a) (b)

Figure 3-11. (a) the collision avoidance function, (b) the collision avoidance force.

After calculating all the F_e^{ij} forces, we can calculate the total evasive force as follows:

$$F_e = \sum_{j=1}^{5} \omega_{ij} F_{ij}, \tag{3-11}$$

in which ω_{ij} is the weighting factor which gives higher priorities to the most imminent collisions.

The last step is to update the velocity and position of agent $\mathrm{P_i}$ according to Equation (3-12) and Equation (3-13), respectively.

$$v_i^{des} = v_i + \left(\sum F_w + F_g + F_e\right) m_i \Delta t \tag{3-12}$$

$$x_i^{new} = x_i + v_i^{des} \Delta t \tag{3-13}$$

The parameters of the Karamouzas' collision avoidance algorithm should be calibrated for evacuation dynamics. The calibration and validation procedures are explained in Section 3.3.5.

3.3.4. Social Behavior Model

An advantage of ABMs is that by defining behavioral rules on the agent level emergent mass behaviors can be observed which are not easy to predict if only isolated agents are studied. The information sharing and social behavior model used in this study are adopted from a previous study conducted at Johns Hopkins University by Liu et al. [67]. As discussed before, the Dijkstra's algorithm assumes that all the occupants have knowledge about evacuation paths. Although this assumption is not realistic, those occupants that do not have such a knowledge can gain information from other agents based on the information sharing and social behavior model. This implies that the unfamiliar agents will eventually gain information and follow the optimal routes but with delays and possible sub-optimal behaviors resulting from interacting with other agents. Those patient agents who are familiar with the building will follow the optimal paths generated by the Dijkstra's algorithm to go from their initial position to the safe zone. The unfamiliar patient agents will evaluate other agents in their field of view and adopt the destination of the plurality. If no other agent is found or agents within their field of view do not have the information about evacuation routes, the agents will locate a temporary destination based on a set of rules until more information is available. These rules are as follows:

(1) If an agent is in a room or corridor, it will set their destination to the closest door, or if there are exit signs, the agent will follow the direction shown by the sign. If there is no door or sign, the agent will move randomly.
(2) If an agent is in a corridor, it will prioritize staircases over doors.
(3) Agent will prioritize external exits over stairs and doors.
(4) If an agent is on stairs, it will descend until reaching the first floor and proceed to exit the staircase.

(5) Agents hold information about the room and corridors that they have visited and avoid those location upon returning.

Certain social behaviors, such as grouping, herding, rescuing, and information sharing, have been observed and described in evacuation studies [69,124–128]. Agents who share a specific attribute engage in grouping behavior, for example, agents who are familiar with the environment or patients from the same agent class. When a patient who can engage in grouping and is not a member of a group encounters another patient, who is also capable of grouping, it may join the group or form a new group with other agents based on the probability function shown in Equations (3-14) and (3-15).

$$P\left[grouping_{ij}\right] = \begin{cases} (1-\omega)f(d) + \omega\left(1 - \dfrac{\left|b_i - b_j\right|}{B}\right) & \left|b_i - b_j\right| \le B \\ (1-\omega)f(d) & \left|b_i - b_j\right| > B \end{cases} \tag{3-14}$$

$$f(d) = \begin{cases} 1 & d \le s \\ \exp\left(\dfrac{s-d}{s}\right) & d > s \end{cases} \tag{3-15}$$

where $\omega \in \{0, 1\}$ is the importance of social interaction, b_i and b_j are the home-base identifiers of agents i and j, respectively, B is a user-defined constant which denotes the maximum difference between two agents for which they are still willing to group together, d is the distance between two agents, and s is the maximum distance agent i can walk in one time step. Agents can switch groups if they find another group with which they share a stronger social bond.

Herding behavior is mainly observed among evacuees unfamiliar with the environment. The rules associated with herding behavior are explained before.

Rescuing and information sharing introduce altruism into the model. In the model, each agent is assigned an altruism probability (P_i^{alt}) which follows a normal distribution for

patient agents, $P^{alt} \sim N(0.8, 0.05)$ and is set to 1 for staff agents. Regarding rescuing, if an agent, who does not need assistance for mobility and is not helping other agents, encounters another agent in its field of view who needs general assistance, based on its altruism probability will decide to approach the agent and assist in moving. When an agent is helping another patient agent, their moving speed will be set to the assistance mode according to Table 3-3. When in rescuing mode, an agent can still engage in grouping or herding. For information sharing, agents assist other agents by sharing their information about the evacuation routes, location of safe zones, and impassable waypoints.

3.3.5. Calibration and Validation

The collision avoidance algorithm presented in Section 3.3.3. uses a set of parameters that controls the evacuation behavior of evacuees in terms of willingness to get close to each other (a.k.a. aggressiveness). The extent to which people are willing to walk close to each other depends on the size of their personal space and their collision prediction horizon, i.e. how far before a collision with another individual is predicted, a person will adjust its speed and trajectory. These attributes vary depending on the situation. A big group of people who are walking in an airport terminal hold a larger personal space than a group of people evacuating the same airport terminal. Therefore, the parameters of the collision avoidance algorithm should be calibrated for an evacuation situation. In this regard, two evacuation experiments are considered in which different evacuation scenarios in terms of room size, exit width, population, and mobility characteristics are studied.

In the first study [129], the evacuation of walkers (pedestrians) and crawlers from a corridor with an exit door is investigated by experiment. The experiment is repeated for

different exit widths (0.4-1.6 m) and different number of evacuees (5 to 60) and the results are represented by evacuation time and flow rate plots. Figure 3-12 shows the experimental setup.

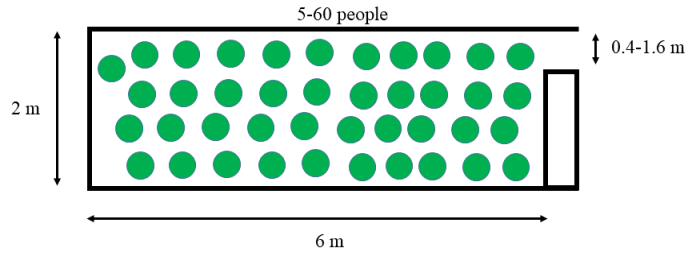

Figure 3-12. Schematic illustration of the evacuation experiment by Nagai et al. [129]

In the second study [130], the evacuation of walkers from a room-corridor environment is investigated for different number of evacuees (20, 40, and 60) and corridor widths (0.8-1.2 m). This experiment provided useful insights into the effect of bottlenecks on the flow of pedestrians. The experimental setup for this study is shown in Figure 3-13.

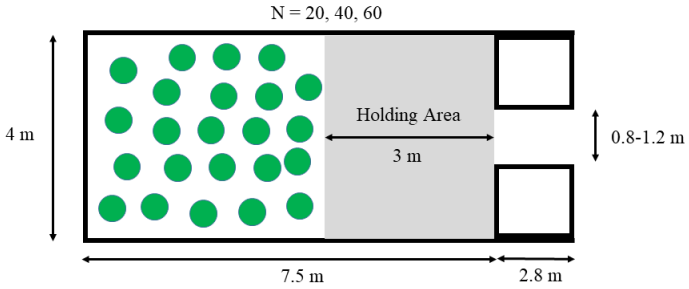

Figure 3-13. Schematic illustration of the evacuation experiment by Seyfried et al. [130]

The parameters of the collision avoidance algorithm are calibrated by simulating the experiments conducted in these two studies and considering the values originally recommended by Karamouzas et al. [75]. The calibrated values are listed in Table 3-5.

Table 3-5. Calibrated parameters of the collision avoidance algorithm

Parameter	Calibrated Value	Parameter	Calibrated Value
τ	0.5 sec	α	0.5
d_s	0.1 m	β	2
κ	3	d_{min}	0.5 m
ρ	0.2 m	d_{mid}	3 m
t_α	2 sec	d_{max}	4 m
N	3		

See Equations (3-3) to (3-13) for where the parameters are used. Figure 3-14 and Figure 3-15 show the results of the calibrated ABM compared with results from the evacuation experiments mentioned above. In this figure, the number of evacuees left in the room in each simulation is plotted with a time step of 0.1 s, hence the darker pixels show the more frequent number of evacuees at each time step over 100 simulations.

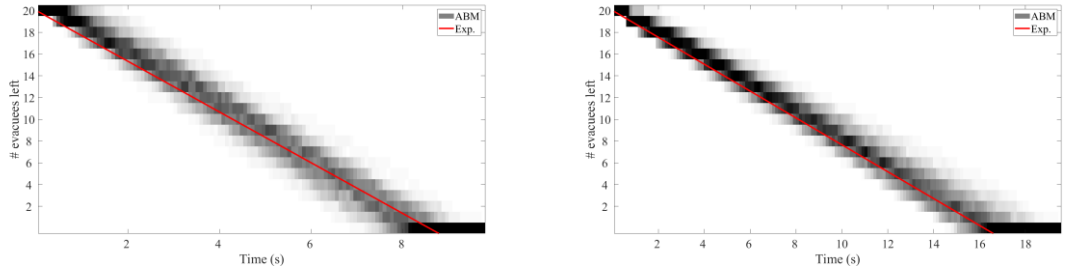

Figure 3-14. Comparing outputs from the ABM and the experiments from [129]: (a) 20 walking evacuees, exit width = 1.2 m, (b) 20 crawling evacuees, exit width = 1.2 m.

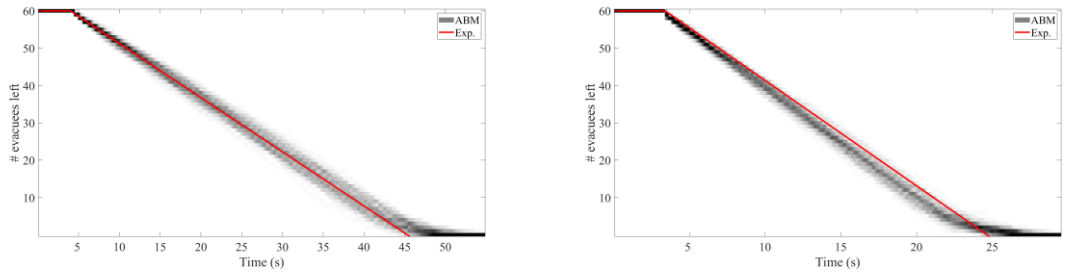

Figure 3-15. Comparing outputs from the ABM and the experiments from [130]: (a) 60 evacuees, exit width = 0.8 m, (b) 60 evacuees, exit width = 1.2 m.

Now that the mobility engine (collision avoidance algorithm) of the model is calibrated, we can obtain the flow characteristics of the ABM. The fundamental diagrams, i.e. speed-density and flow-density, are the most important quantitative characteristics of any flowing system (gases, fluids, pedestrian crowds, or traffic systems). These diagrams describe how the speed, v, and flow, $f = \rho v$, changes as a function of density, ρ. These diagrams are used in empirical and modeling studies on crowd dynamics as a validation technique [13,129–134].

To obtain the speed-density relation from the ABM, a steady-state condition should be simulated. For this, an open-end wide corridor is simulated with the number of occupants incrementally increasing and uniformly distributed over the corridor. Each simulation is repeated 100 times. In each simulation the average speed of occupants in the middle half section of the corridor is calculated over a certain time period. The occupants on the two sides of the middle half section are not considered to exclude the effect of boundaries. The size of the agents varies between 0.4 m to 1 m and their free flow speed ranges from 0.5 to 2 m/s. Figure 3-16 shows an illustration of the steady-state simulation using the ABM.

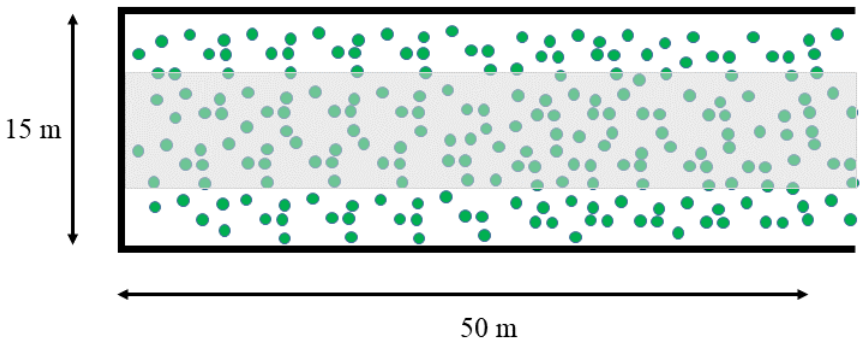

Figure 3-16. Simulation of the steady-state condition for the crowd flow

There are a certain number of models proposed by researchers for the speed-density relationship of crowd and vehicle flows. The Greenshields' model [135] considers a linear relationship between traffic speed and density:

$$v(\rho) = v_f \left(1 - \frac{\rho}{\rho_m}\right) \tag{3-16}$$

where v_f is the free flow speed, and ρ_m is the maximum density.

The modified Drake's model [132,136], a.k.a Northwestern University model, considers an exponential relationship between density and speed as follows:

$$v(\rho) = v_f exp\left(-7.5\left(\frac{\rho}{\rho_m}\right)^2\right) \tag{3-17}$$

The Underwood model [137], similar to Drake's model, uses an exponential function as shown in Equation (3-18).

$$v(\rho) = v_f exp\left(-\frac{\rho}{\rho_m}\right) \tag{3-18}$$

The speed-density and flow-density relationships obtained from the ABM are shown in Figure 3-17. Comparing the flow characteristics obtained from the ABM with those from the literature, it is clear that the characteristics of the flow that the ABM generates agree with

the modified Drake's model shown in Equation (3-17). Later, we will use the Drake's equation in the fluid dynamics model.

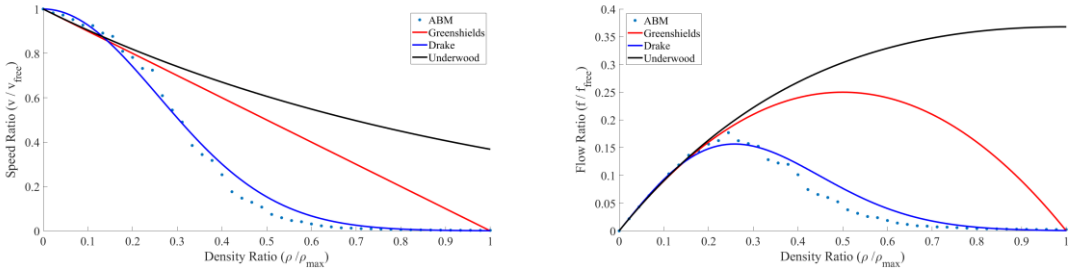

Figure 3-17. Fundamental flow diagrams of the ABM: Left: speed-density; Right: flow-density.

3.4. Benchmark Test Cases

In this section, three benchmark test cases are introduced to study the outputs of the ABM. These test cases will be used in Chapters 4 and 5 to compare the outputs of the fluid dynamics model and the system dynamics model with those from the ABM. These test cases are intended to approximate a simple environment, from which we can anticipate the exit patterns. The first test case is a single room, which is the simplest environment. The second test case is a two-room environment with different types of evacuees in each room. The third test case is a corridor with two rooms opening into the corridor. The simulation of each test case is repeated 100 times in which each agent is randomly positioned in their assigned location.

3.4.1. Single Room Test Case

The single room setup is shown in Figure 3-18. The room has a rectangular shape with a length of 4 m and a width of 8 m. The exit door is on the right side of the room with a width

of 1 m. There are 20 non-disabled adult patients in the room with body size of 0.5 m and free walking speed of 1.25 m/s according to Table 3-3.

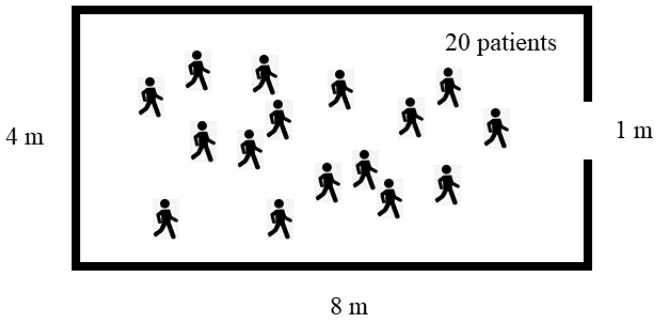

Figure 3-18. The single room test case

The results of the evacuation of the single-room test case modeled with the ABM for 100 simulations are shown in Figure 3-19 as a heat map. In this figure, the number of evacuees left in the room in each simulation is plotted with a time step of 0.1 s, hence the darker pixels show the more frequent number of evacuees at each time step over 100 simulations. The results show that the dominant exit dynamics is linear resulting in a final evacuation time of 12 to 18 seconds.

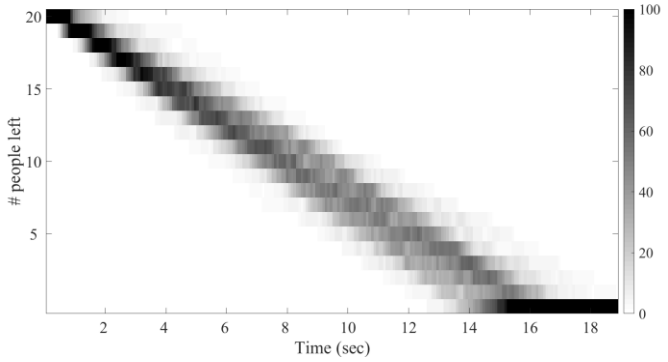

Figure 3-19. Single room test case: evacuation results from the ABM

To better analyze the variations in the outputs of the ABM, the statistics for the partial evacuation times at different evacuation percentiles are obtained (Figure 3-20). Table 3-6 lists the statistical measures at 25%, 50%, 75%, 90%, and 100% of the evacuation process. As shown in Figure 3-20a in blue, the average exit pattern is linear with an average final time of 15.3 seconds. The values of standard deviation show that as the evacuation process continues in time, the variability increases. The values of skewness and kurtosis show that the variability over 100 evacuation simulations for a simple single-room environment is symmetric and follows a normal distribution. Skewness and kurtosis can explain the variations in evacuation times and imply the existence of less probable extreme cases.

Table 3-6. Single room test case: statistical measures at different evacuation percentiles

Evacuation Percentile	Mean [s]	Standard Deviation [s]	Skewness	Kurtosis
25%	4.0	0.7	0.7	3.7
50%	7.9	1.0	0.1	2.4
75%	11.6	1.1	0.3	3.1
90%	13.9	1.2	0.1	2.9
100%	15.3	1.2	0.1	3.1

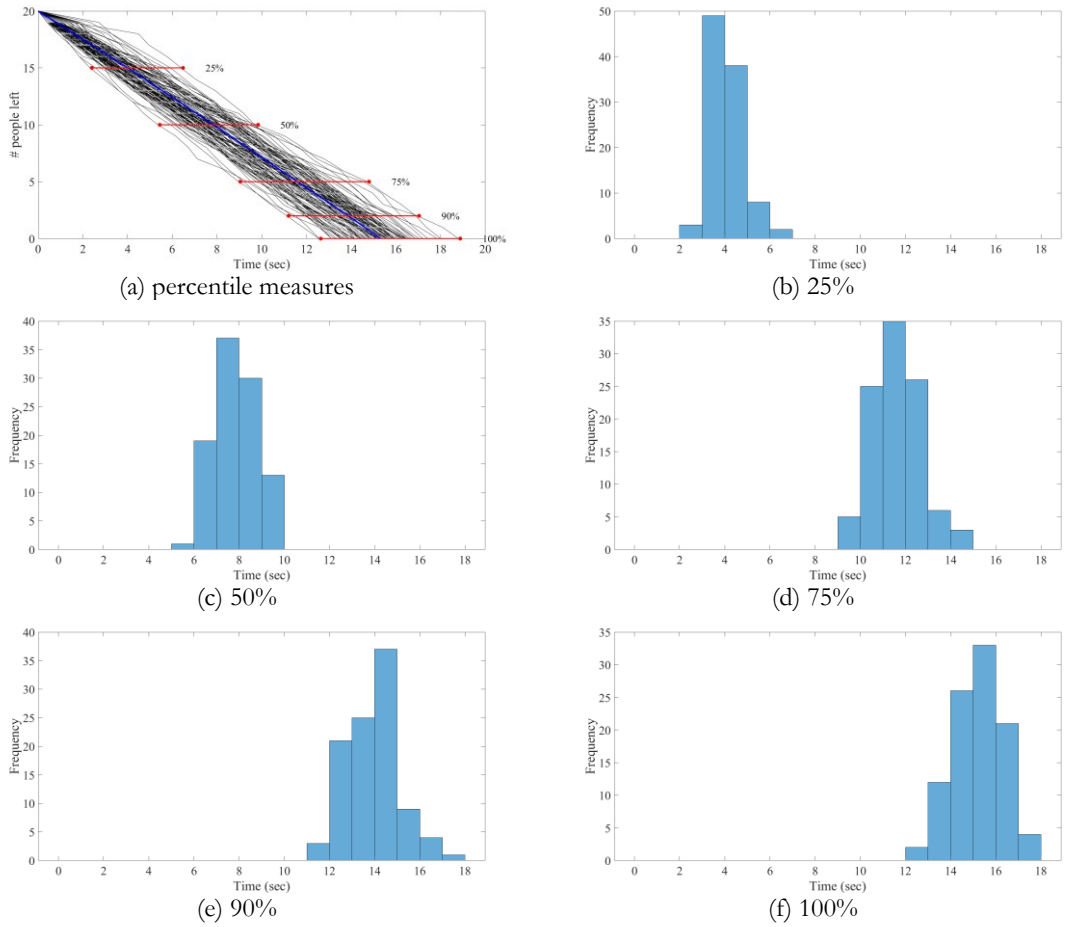

(a) percentile measures (b) 25%

(c) 50% (d) 75%

(e) 90% (f) 100%

Figure 3-20. Single room test case: partial evacuation times at different evacuation percentiles

3.4.2. Two-Room Test Case

The two-room setup is shown in Figure 3-21. Room 1 is a 4-m by 6-m rectangular room with a 1.6-m wide door, and Room 2 is a 6-m by 6-m square room with a 1.6-m wide door. There are 40 patients is Room 1, 30 with stamina impairment and 10 non-disabled adults, and 20 patients in Room 2, from which 5 patients are stamina impaired. According to Table 3-3, the body size of all the patients is 0.5 m, the free walking speed of stamina impaired patients is 0.57 m/s, and the free walking speed of non-disabled adults is 1.25 m/s.

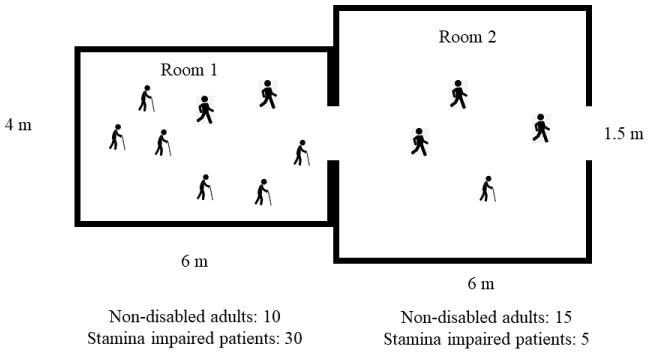

Figure 3-21. The two-room test case

The results of the evacuation of the two-room test case simulated with the ABM for 100 simulations are shown in Figure 3-22 to Figure 3-24 as heat maps for Room 1, Room 2, and total evacuation, respectively. The results show that the dominant exit dynamics in Room 1 is linear resulting in a final evacuation time of about 30 seconds. However, in a certain number of simulations (5% of all), a secondary pattern can be observed in which the evacuation rate is lower resulting in a total exit time of about 40 seconds. Further investigations revealed that this pattern occurs in cases in which initially there is significant number of stamina impaired patients near the door. In these cases, the high local density of slow walking occupant near the exit door hinders the evacuation flow.

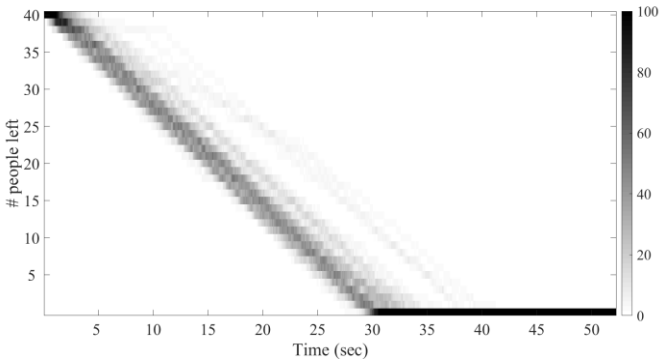

Figure 3-22. Two-room test case: evacuation results from the ABM for Room 1.

The evacuation dynamics in Room 2 is more complicated as the inflow from Room 1 affects the exit rate from Room 2. As it is clear from Figure 3-23, initially the exit dynamics are linear implying that the difference between inflow from Room 1 into Room 2 and the outflow from Room 2 is almost constant. However, after 10 seconds, the number of occupants in Room 2 stays constant as the large number of patients with stamina impairment (slow walkers) entering Room 2 is almost the same as the number of patients exiting Room 2. After another 20 seconds, this wave of slow walkers starts to exit Room 2 with a linear pattern. According to the results, the majority of the simulations show a final exit time of 40 to 45 seconds, but in a few numbers of simulations (5%), the delay due to the slow walking patients is slightly longer such that the final exit time can be extended to 50 seconds.

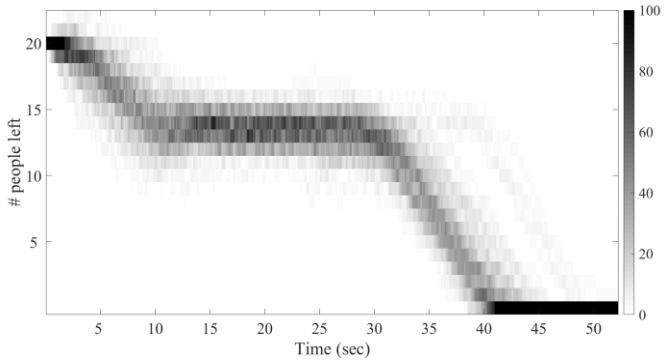

Figure 3-23. Two-room test case: evacuation results from the ABM for Room 2.

From Figure 3-24, the total exit pattern is approximately a piecewise linear curve in which the total exit rate drops after about 10 seconds. This drop is due to the arrival of the evacuees from Room 1. The total evacuation time is mainly between 40 to 45 seconds with an average of 41.9 seconds. As explained above, there is a secondary evacuation pattern in 5% of the simulations in which the final evacuation time is extended to 48 to 53 seconds.

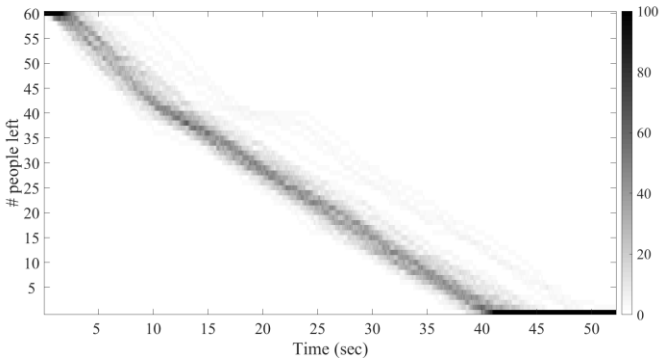

Figure 3-24. Two-room test case: total evacuation results from the ABM

To better analyze the variations in the outputs of the ABM, the statistics for the partial evacuation times at different evacuation percentiles are obtained (Figure 3-25). Table 3-7 lists the statistical measures at 25%, 50%, 75%, 90%, and 100% of the evacuation process. As shown in Figure 3-25a in blue, the average exit pattern can be approximated by a piece-wise linear curve with an average final time of 41.9 seconds. The values of standard deviation show that as the evacuation process continues in time, the variability increases. The values of skewness and kurtosis show that the variability over 100 evacuation simulations for a two-room environment is heavily right-skewed with a longer tail and a stronger peak than a normal distribution, which implies that more of the variance is the result of infrequent extreme deviations.

Table 3-7. Two-room test case: statistical measures at different evacuation percentiles

Evacuation Percentile	Mean [s]	Standard Deviation [s]	Skewness	Kurtosis
25%	9.0	1.8	1.4	5.9
50%	19.3	2.3	2.2	9.3
75%	30.1	2.5	1.9	7.7
90%	36.8	2.5	1.5	6.0
100%	41.9	2.5	1.5	6.2

As the ABM provides results on an agent level, we can analyze the results for each type of patients, as well. The results are shown in Figure 3-26 and Figure 3-27 as heat maps for stamina impaired and non-disabled adult patients, respectively. According to Figure 3-26, the exit dynamics for stamina impaired patients is initially slow as there are only a few of these patients close to the exit door in Room 2. However, as the large number of stamina patients arrives from Room 1, the exit rate increases after 15 seconds and reaches a constant state (linear exit dynamics). The results also show a secondary evacuation pattern for stamina impaired patients which is similar to the main pattern but with lower initial exit rates. As highlighted before, 5% of the simulations show a slower evacuation process that can extend the total evacuation time and the evacuation time for stamina impaired patients by about 10 seconds.

The evacuation dynamics for non-disabled adult patients is different than that for the stamina impaired patients. As it is clear from Figure 3-27, after an initial high exit rate, the rate decreases after about 10 seconds. The initial high exit rate is because of low density of patients close to the exit door in Room 2, however, the walking speed of those 10 non-disabled patients who are initially in Room 1 is significantly affected by the presence of slow walkers (stamina

impaired patients), which results in a lower exit rate. As mentioned before, in 5% of the simulations a secondary evacuation pattern can be observed in which there is a delay in the beginning of the evacuation due to a concentration of stamina impaired patients close to the exit door which causes a congestion.

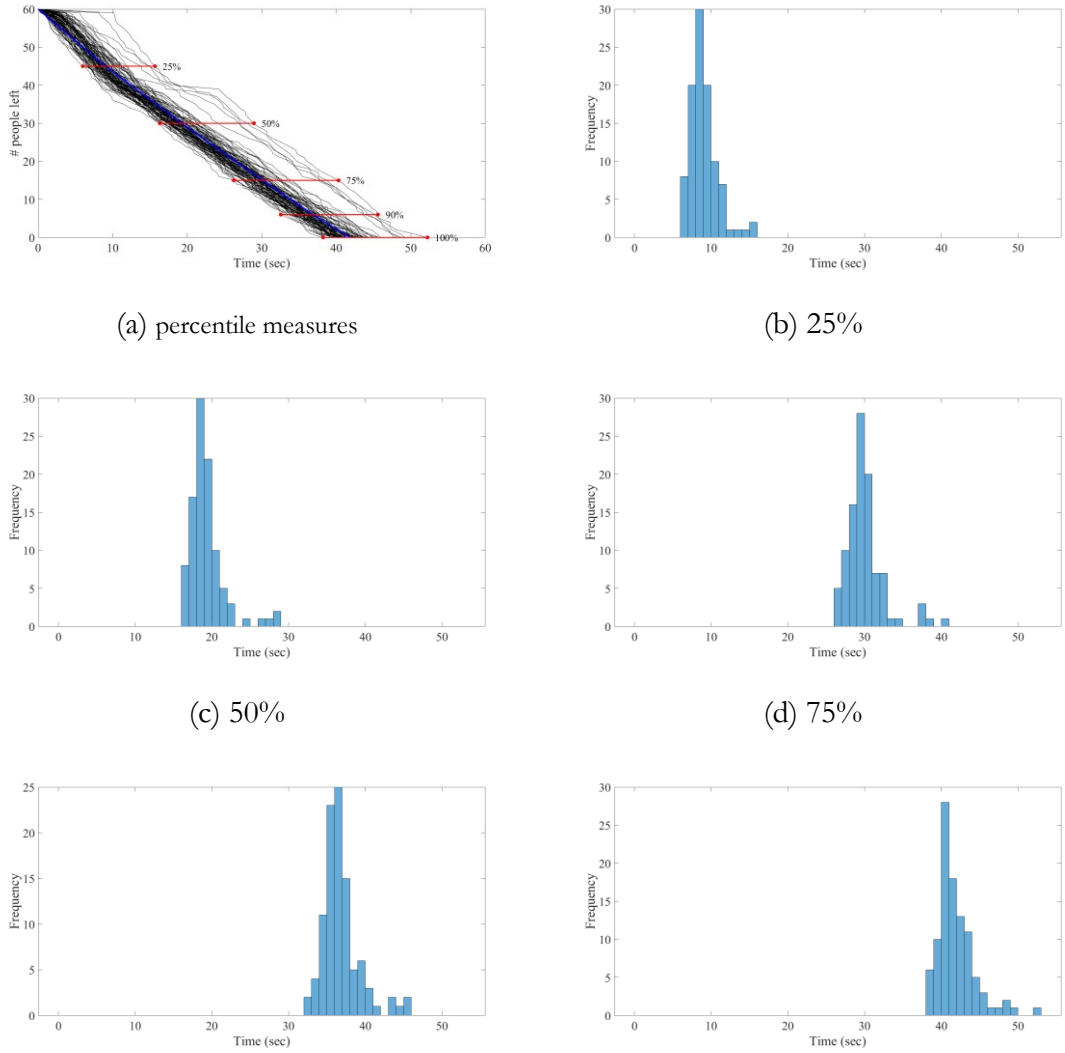

(a) percentile measures

(b) 25%

(c) 50%

(d) 75%

(e) 90%

(f) 100%

Figure 3-25. Evacuation percentiles for the two-room test case

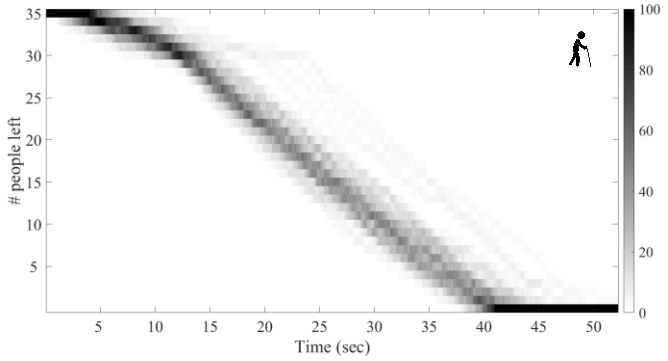

Figure 3-26. Two-room test case: evacuation results from the ABM for stamina impaired patients

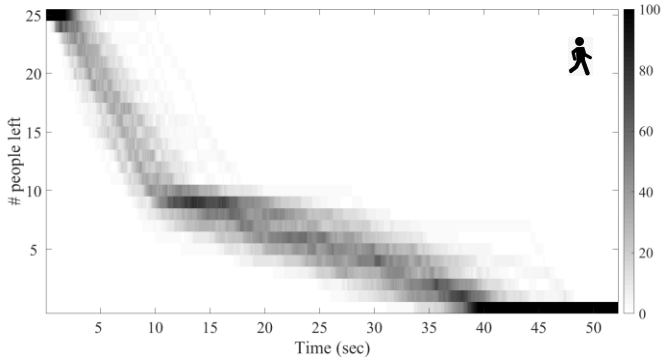

Figure 3-27. Two-room test case: evacuation results from the ABM for non-disabled adult patients

3.4.3. Two-Room-Corridor Test Case

The two-room-corridor setup is shown in Figure 3-28. Room 1 and Room 2 are 4-m by 4-m square rooms with 1.2-m wide doors. There are 5 wheelchair users in Room 1 and 10 visitors in Room 2. According to Table 3-3, the body size of wheelchair users is 0.8 m and their free moving speed is 0.69 m/s. For visitors, body size is 0.5 m and free walking speed is

1.4 m /s. The rooms open to a 14-m by 3-m corridor with a 1.2-m wide exit door on its right end.

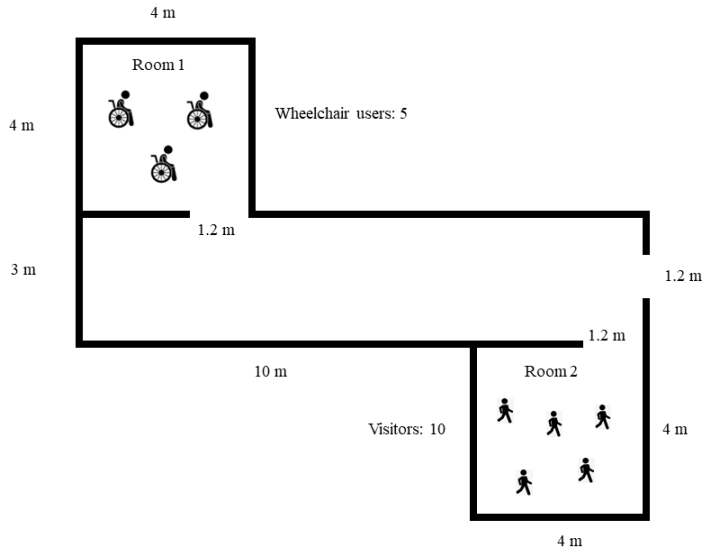

Figure 3-28. The two-room-corridor test case

The results of the evacuation of the two-room-corridor test case simulated with the ABM for 100 simulations are shown in Figure 3-29 to Figure 3-32 as heat maps for Room 1, Room 2, corridor, and total evacuation, respectively. The results show that the dominant exit dynamics in Room 1 is linear resulting in an evacuation time of 8 to 22 seconds with an average of 13.3 seconds. For Room 2, the results show a linear exit behavior with an evacuation time of 8 to 13 seconds with an average of 10.5 seconds. However, in a small number of simulations (4% of all), a secondary pattern can be observed in which the exit rate is lower resulting in a total exit time of 16 to 23 seconds. This pattern occurs in cases in which a temporary congestion is formed at Room 2's door when 4 or 5 evacuees reach the door simultaneously and try to exit.

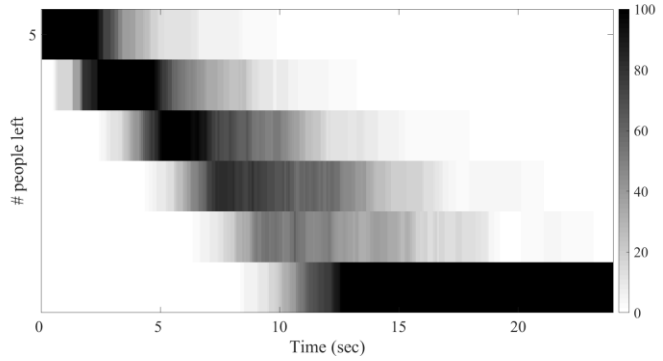

Figure 3-29. Two-room-corridor test case: evacuation results from the ABM for Room 1.

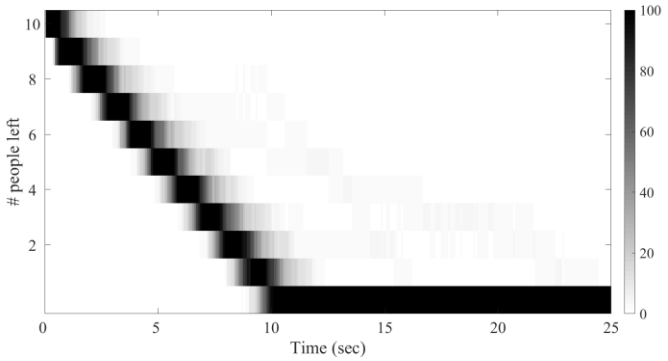

Figure 3-30. Two-room-corridor test case: evacuation results from the ABM for Room 2.

The evacuation dynamics in the corridor are more complicated as the inflows from Rooms 1 and 2 affect the exit rate from the corridor. From Figure 3-31, initially the number of evacuees in the corridor increases linearly due to the linear inflow from the rooms. After 5 to 10 seconds, as evacuees enter the corridor, those from Room 2 (which is closer to the corridor's exit door) start to exit the corridor, which makes the number of evacuees in the corridor fluctuate. Following the fluctuation, the number of evacuees stays constant at 5, which denotes the delay time between the last visitor and the first wheelchair user exiting the corridor. The last part is the evacuation of wheelchair users with a linear exit dynamic resulting in a total evacuation time of 26 to 40 seconds with an average of 31.3 seconds.

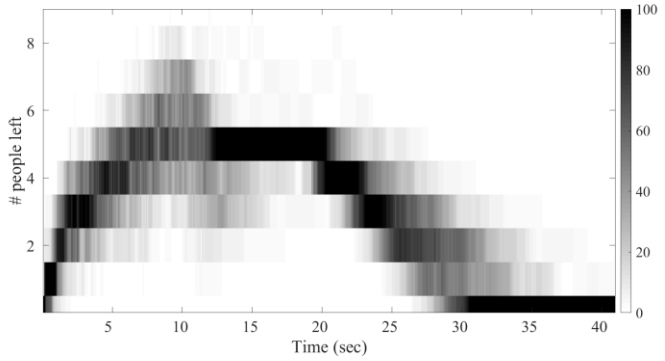

Figure 3-31. Two-room-corridor test case: evacuation results from the ABM for the corridor.

The total evacuation takes a piecewise linear pattern as shown in Figure 3-32. The initial part is a linear exit corresponding to the evacuees from Room 2, followed by a 10-second delay from $t = 10\ s$ to $t = 20\ s$ which is the time it takes between the last person from Room 2 and the first person from Room 1 to exit the corridor. The third linear part corresponds to the exit of evacuees from Room 1 when they reach the corridor's exit door. As explained above, there is a secondary exit pattern in 4% of the simulations in which the congestion in Room 2 changes the dynamics of the evacuation.

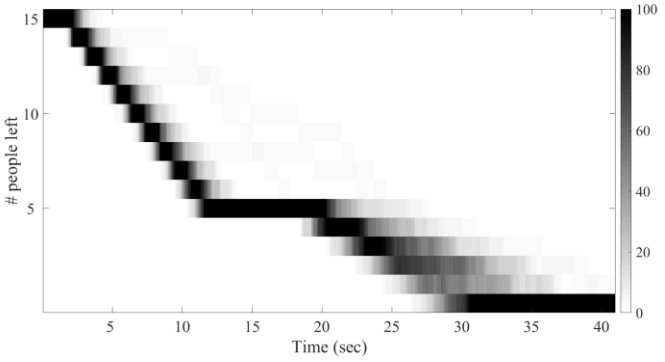

Figure 3-32. Two-room-corridor test case: total evacuation results from the ABM

To better analyze the variations in the outputs of the ABM, the statistics for the partial evacuation times at different evacuation percentiles are obtained (Figure 3-33). Table 3-8 lists

the statistical measures at 25%, 50%, 75%, 90%, and 100% of the evacuation process. The values of standard deviation show that as the evacuation process continues in time, the variability increases. The values of skewness and kurtosis show that over 100 evacuation simulations, in the first 50% of the evacuation, the variability in evacuation time is heavily right-skewed with a longer tail and a stronger peak than a normal distribution; however, in the second 50%, the variability in evacuation time is only moderately right-skewed with similar peaks to a normal distribution, which implies that the variance is mostly due to frequent modestly sized deviation rather than infrequent extreme deviations as in case of the first half of the evacuation.

Table 3-8. Two-room-corridor test case: statistical measures at different evacuation percentiles

Evacuation Percentile	Mean [s]	Standard Deviation [s]	Skewness	Kurtosis
25%	5.7	1.0	5.9	49.3
50%	8.8	1.4	4.8	29.7
75%	20.8	1.5	0.6	3.0
90%	26.5	2.2	0.6	3.4
100%	31.3	2.8	0.6	3.1

As the ABM provides results on an agent level, we can analyze the results for each type of patients, as well. The results are shown in Figure 3-34 and Figure 3-35 as heat maps for visitors and wheelchair users, respectively. The results for the evacuation of visitors correspond to those of Room 2 (with the time it takes to walk from Room 2's door to the corridor's exit door) as the room is only occupied by visitors, and the flow of visitors is not affected by the flow of wheelchair users. The evacuation time of visitors varies from 10 to 14

seconds with a secondary evacuation pattern (as explained before) resulting in evacuation times of 17 to 28 seconds and an overall average of 12.1 seconds.

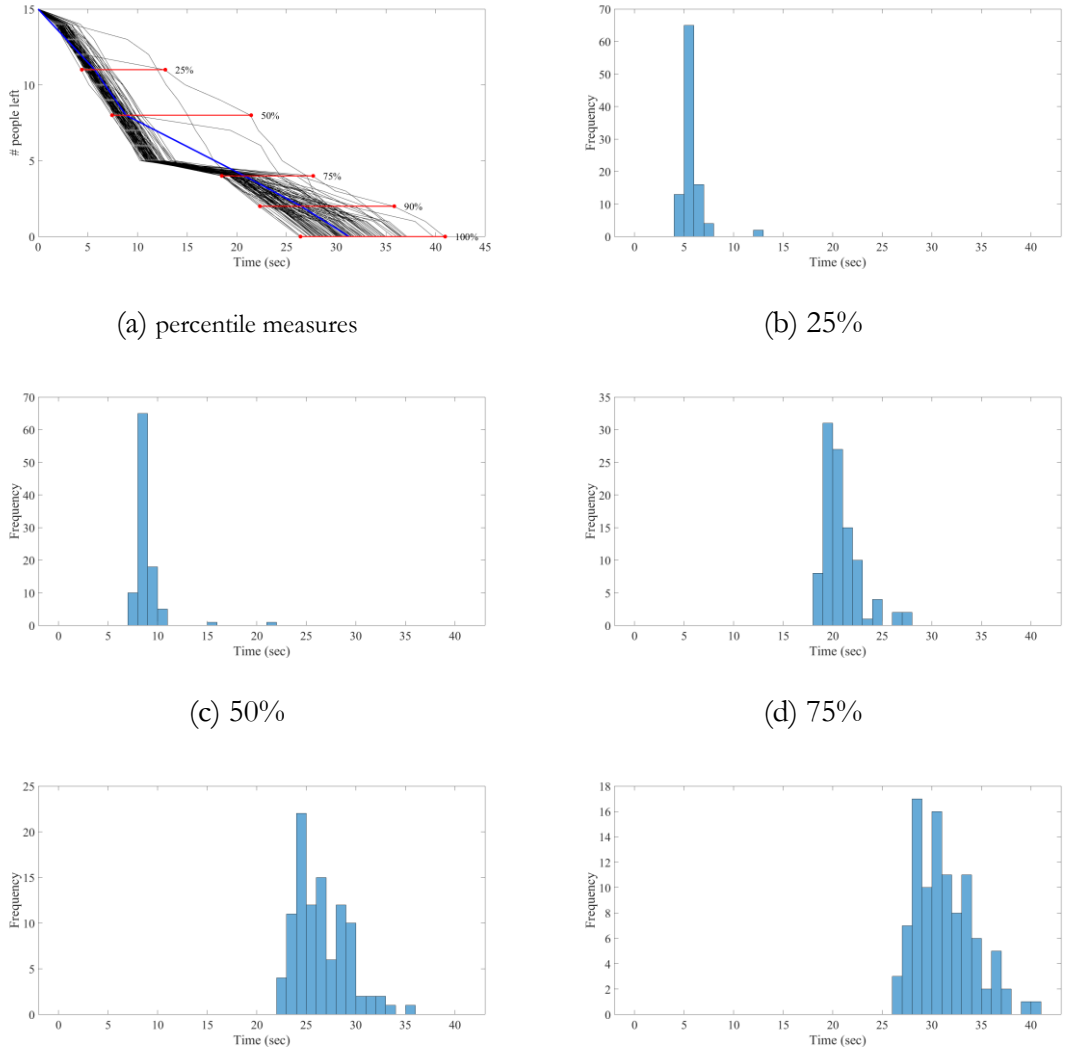

(a) percentile measures

(b) 25%

(c) 50%

(d) 75%

(e) 90%

(f) 100%

Figure 3-33. Two-room-corridor test case: partial evacuation times at different evacuation percentiles

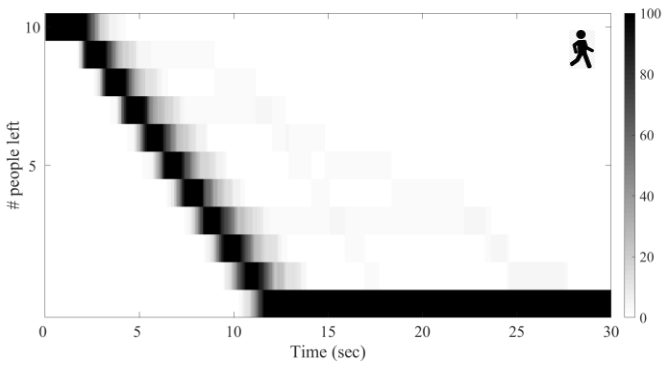

Figure 3-34. Two-room-corridor test case: evacuation results from the ABM for visitors

For wheelchair users, there is a delay of about 20 seconds for the first evacuees to exit the corridor. As the flow of wheelchair users reaches the exit door, they exit the corridor with a linear dynamic resulting in a final evacuation time of 26 to 40 seconds with an average of 31.3 seconds.

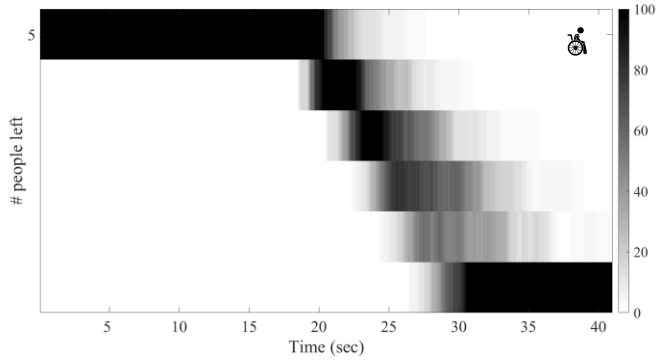

Figure 3-35. Two-room-corridor test case: evacuation results from the ABM for wheelchair users

3.5. Discussion

An advantage of computational models such as ABMs over statistical models such regression models is that the behavior of a system (a socio-physical system) can be studied under different initial or boundary conditions without the need for historical data. In agent-based modeling, by defining individual-level behaviors, we can predict different possible mass responses which may not be initially expected.

In the context of crowd mobility, when the characteristics of the environment are simple and the population is homogeneous, as in the single room test case, the evacuation dynamics are simple and easy to predict. The results of the simulation with the ABM for the single room test case show that the variations in the evacuation time are reasonable and agree with the empirical studies. However, in cases with a heterogenous population, the evacuation process can take different paths according to initial conditions. The results from the two-room test case show that in 5% of the simulations a longer evacuation time can be observed depending on the initial position of those group of patients with mobility impairment. These longer possible evacuation times are also implied by the high values of skewness and kurtosis for the total evacuation time. A similar phenomenon is also observed in the two-room-corridor test case where 4% of the simulations show a secondary exit pattern resulting in a longer evacuation time. A concentration of mobility impaired evacuees at bottlenecks or close to the exit doors can cause a congestion which hinders the evacuation process. According to the results, for a simple two-room or two-room-corridor environment with rather wide exits (1.2-1.5 m), a concentration of only 5 patients with mobility impairment close to the exit door can increase the total evacuation time by 25%. These possible local congestions in a bigger environment (an entire hospital) with hundreds of patients can cause significant delays in the evacuation process which are critical to anticipate when planning for emergency evacuations.

An advantage of agent-based modeling is that possible emergent mass behaviors, even if they are less probable to happen, can be predicted. The two-room and the two-room-corridor test cases are examples of such less probable situations, in which over 100 simulations, there were 5 situations that resulted 25% longer evacuation times. In the context of hospital evacuation, this implies that emergency planners can have statistical estimations for total and partial evacuation times for different types of patients, which can help plan for worst case scenarios.

3.6. Conclusions

The interaction among humans and the human-environment interaction make evacuation a complex socio-physical process. This process is more complex when studying hospital evacuation due to diverse mobility characteristics and needs of the patients as evacuees. The micro-level behaviors and decision-making in the process of hospital evacuation lead to diverse macro-level evacuation patterns and crowd dynamics which are not easy to predict. Furthermore, evacuation process depends on initial and boundary conditions, such diverse possible scenarios in terms of number and distribution of different types of patients in a hospital, unique physical features of hospitals, available resources (staff and equipment), and imminence and intensity of disruptive events. Given the scarcity of data on the factors affecting patient evacuation, modeling and simulation can plays an important role in disaster preparedness and response by providing emergency managers and decision makers with useful insights about evacuation process under different scenarios. Considering the bottom-up nature of the hospital evacuation process, microscopic methods such as agent-based models (ABMs) are mainly used to simulate the evacuation of patients and mobility impaired individuals.

In this study, an agent-based patient evacuation model is developed. A patient classification framework is developed based on mobility characteristics and needs of evacuees. Certain path planning, collision avoidance, and decision-making algorithms are adopted from the literature. The model is calibrated and validated based on empirical evacuation studies and established crowd flow characteristics in the literature. The model is then used on three benchmark test cases to study different evacuation dynamics. These benchmark test cases will be used in Chapters 4 and 5 to compare the results from the fluid dynamics and system dynamics models with those from the ABM.

The agent-based hospital evacuation models, such as the one developed in this study, can be used by hospital emergency managers and response teams to estimate the required time for the partial or complete evacuation of a hospital due to imminent events such fire emergencies or hazmat spill incidents. The ABM can predict which group or groups of patients will take the most time for evacuation, hence hindering the evacuation process. The model can also inform us about the reasons for evacuation delays, e.g. is it because the large number of patients evacuating makes congestion, or there is a need for more resources such as wheelchairs or hospital staff. Furthermore, hospital emergency teams can use these models to evaluate different intervention scenarios in terms of effectiveness.

Certainly, there is much left to improve on agent-based hospital evacuation models. There are many different types of patients or individuals with disabilities that need to be considered in models. For ICU patients — an important group of patients which were excluded in this study — the patient transfer process is different and much complicated. Including this group of patients in models implies the need for a database of available ICU beds in other hospitals. In addition, other factors such as insurance policies and inter- or intra-hospital agreements should be considered. Moreover, the need for specific equipment, such

as oxygen tanks and ventilators, for the evacuation of certain patients is not considered. The availability of these equipment can affect the evacuation process by introducing extra delay times. This is very critical as mainly patients in more critical conditions are in need of such equipment, and extra delay in the evacuation of these critically ill patients can impose serious risks to their lives if the complete evacuation of all patients is required in a short time.

Chapter 4

Hospital Evacuation: Mesoscopic Fluid Dynamics Modeling

4.1. Introduction

The flow of human crowds has increasingly become an interesting topic among researchers as cities are growing and population density of urban areas is increasing. The interest in studying crowd dynamics gained momentum in the 1990's when it was perceived that our knowledge of flow of human crowds was inadequate [138,139]. Another reason for the increasing interest in the study of crowd dynamics was safety and security. Researchers tried to model how crowds behave in different situations, such as at transport terminals, sport events, holy sites, political demonstrations, and fire escapes [140–144].

One approach to model crowd motion is microscopic modeling like age-based models (ABMs) as explored in Chapter 3. In micro-models, individuals are modeled as discrete entities with unique characteristics and behaviors. Another approach is to consider the crowd as a whole, which is especially applicable for large crowds. In these mesoscopic models, instead of modeling every individual, crowds are modeled as waves. From a sociological perspective, unorchestrated crowds are rational and shown to follow scientific rules of behavior [145]. Large crowds move in a similar manner as fluids; therefore, concepts of fluid dynamics can be adopted to formulate the flow of crowds. In this regard, fluid dynamics models (FDMs) have

been developed to describe crowd behaviors by teams of experts from crowd dynamics, fluid dynamics, and behavioral sciences. These models, which use nonlinear partial differential equations (PDEs), are mappable even in unsteady states and can provide analytical solutions for the dynamics of crowd motions [146].

Based on the fundamental laws of fluids, we can develop the equations of motion for crowds. The first fundamental law of fluids is the conservation of mass. Consider a generic infinitesimal 2D section of a fluid as shown in Figure 4-1.

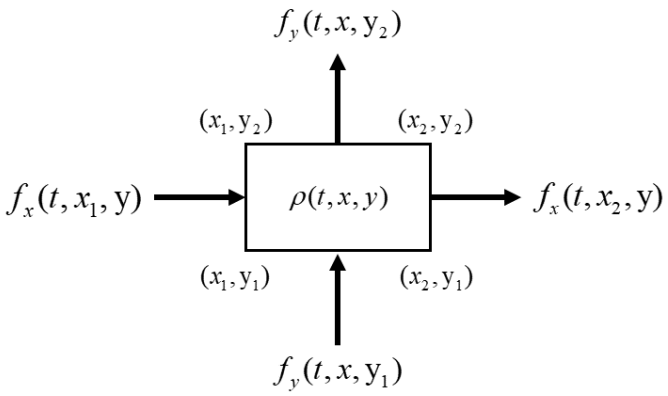

Figure 4-1. Conservation of mass

Here, f is flow which is the product of density and speed of flow as shown in Equations 4-1) and (4-2):

$$f_x(t, x, y) = \rho(t, x, y)u(t, x, y) \quad (4\text{-}1)$$

$$f_y(t, x, y) = \rho(t, x, y)v(t, x, y) \quad (4\text{-}2)$$

where $\rho(t, x, v)$ is fluid density, $u(t, x, y)$ is the fluid speed in the x-direction, $f_x(t, x, y)$ is the flow in the x-direction, $v(t, x, y)$ is the fluid speed in the y-direction, and $f_y(t, x, y)$ is the flow in the y-direction at time t and location (x, y).

The mass in the section from (x_1, y_1) to (x_2, y_2) at any time t is given by:

$$M_{t,x_1,y_1}^{t,x_2,y_2} = \int_{y_1}^{y_2} \int_{x_1}^{x_2} \rho(t,x,y)dxdy. \tag{4-3}$$

The total mass entering the section from $x = x_1$ from time t_1 to t_2 is:

$$M_{t_1,x_1,y_1}^{t_2,x_1,y_2} = \int_{y_1}^{y_2} \int_{t_1}^{t_2} \rho(t,x_1,y)u(t,x_1,y)dtdy, \tag{4-4}$$

and the total mass leaving the section from $x = x_2$ from time t_1 to t_2 is:

$$M_{t_1,x_2,y_1}^{t_2,x_2,y_2} = \int_{y_1}^{y_2} \int_{t_1}^{t_2} \rho(t,x_2,y)u(t,x_2,y)dtdy. \tag{4-5}$$

Similarly, we can calculate the total mass entering and leaving the section on the y-direction as shown in Equations (4-6) and (4-7).

$$M_{t_1,x_1,y_1}^{t_2,x_2,y_1} = \int_{x_1}^{x_2} \int_{t_1}^{t_2} \rho(t,x,y_1)v(t,x,y_1)dtdx \tag{4-6}$$

$$M_{t_1,x_1,y_2}^{t_2,x_2,y_2} = \int_{x_1}^{x_2} \int_{t_1}^{t_2} \rho(t,x,y_2)v(t,x,y_2)dtdx \tag{4-7}$$

According to the mass conservation law, the change in mass in any section of a fluid is equal to the difference of mass inflow and outflow from the boundaries of the section. This can be expressed in the first integral form as follows:

$$\int_{y_1}^{y_2} \int_{x_1}^{x_2} \rho(t_2,x,y)dxdy - \int_{y_1}^{y_2} \int_{x_1}^{x_2} \rho(t_1,x,y)dxdy$$

$$= \int_{y_1}^{y_2} \int_{t_1}^{t_2} \rho(t,x_1,y)u(t,x_1,y)dtdy - \int_{y_1}^{y_2} \int_{t_1}^{t_2} \rho(t,x_2,y)u(t,x_2,y)dtdy$$

$$+ \int_{x_1}^{x_2} \int_{t_1}^{t_2} \rho(t,x,y_1)v(t,x,y_1)dtdx - \int_{x_1}^{x_2} \int_{t_1}^{t_2} \rho(t,x,y_2)v(t,x,y_2)dtdx \tag{4-8}$$

Alternatively, we can rewrite this expression in the second integral form as:

$$\int_{y_1}^{y_2}\int_{x_1}^{x_2}\left[\int_{t_1}^{t_2}\frac{\partial}{\partial t}\rho(t,x,y)dt\right]dxdy$$

$$=\int_{y_1}^{y_2}\int_{t_1}^{t_2}\left[\int_{x_1}^{x_2}\frac{\partial}{\partial x}\rho(t,x,y)u(t,x,y)dx\right]dtdy$$

$$+\int_{x_1}^{x_2}\int_{t_1}^{t_2}\left[\int_{y_1}^{y_2}\frac{\partial}{\partial y}\rho(t,x,y)v(t,x,y)dy\right]dtdx \qquad (4\text{-}9)$$

As the upper and lower bounds of the integral are the same, Equation (4-9) can be combined into Equation (4-10).

$$\int_{y_1}^{y_2}\int_{x_1}^{x_2}\int_{t_1}^{t_2}\left[\frac{\partial}{\partial t}\rho(t,x,y)+\frac{\partial}{\partial x}\rho(t,x,y)u(t,x,y)+\frac{\partial}{\partial y}\rho(t,x,y)v(t,x,y)\right]dtdxdy=0 \qquad (4\text{-}10)$$

Equation (4-10) must be satisfied for all intervals of time, x, and y, therefore, the integral term should take the following form:

$$\frac{\partial}{\partial t}\rho(t,x,y)+\frac{\partial}{\partial x}\rho(t,x,y)u(t,x,y)+\frac{\partial}{\partial y}\rho(t,x,y)v(t,x,y)=0 \qquad (4\text{-}11)$$

Equation (4-11) is called the mass conservation law.

In the development of the FDMs, the following hypotheses are considered about the nature of pedestrian motion, proposed by Hughes [146]:

Hypothesis 1: the walking speed of pedestrians is determined by the mobility characteristics of the pedestrians, the physical characteristics of the ground on which they walk, and the local density of the surrounding pedestrians. Therefore, for a single type of pedestrian, the velocity components can be obtained as follows:

$$u=f(\rho)\hat{\phi}_x\ ,\quad v=f(\rho)\hat{\phi}_y, \qquad (4\text{-}12)$$

where $f(\rho)$ is the speed as a function of density, and $\hat{\phi}_x$ and $\hat{\phi}_y$ are the direction cosines of the trajectory. There are a certain number of models proposed by researchers for the speed-

density relationship of crowd and vehicle flows. The Greenshields' model [135] considers a linear relationship between traffic speed and density:

$$f(\rho) = v_f\left(1 - \frac{\rho}{\rho_m}\right) \tag{4-13}$$

where v_f is the free flow speed, and ρ_m is the maximum density.

The modified Drake's model [132,136], a.k.a Northwestern University model, considers an exponential relationship between density and speed as follows:

$$f(\rho) = v_f exp\left(-7.5\left(\frac{\rho}{\rho_m}\right)^2\right) \tag{4-14}$$

The Underwood model [137], similar to Drake's model, uses an exponential function as shown in Equation (3-18).

$$f(\rho) = v_f exp\left(-\frac{\rho}{\rho_m}\right) \tag{4-15}$$

Hypothesis 2: pedestrians share the same sense of task (potential); i.e. any two pedestrians at different locations with the same potential will have no interest in exchanging places. As there is no advantage in moving along a line of constant potential, the direction of motion of pedestrians is perpendicular to the potential field, i.e.:

$$\hat{\phi}_x = \frac{-\frac{\partial \phi}{\partial x}}{\sqrt{\left(\frac{\partial \phi}{\partial x}\right)^2 + \left(\frac{\partial \phi}{\partial y}\right)^2}} \quad , \quad \hat{\phi}_y = \frac{-\frac{\partial \phi}{\partial y}}{\sqrt{\left(\frac{\partial \phi}{\partial x}\right)^2 + \left(\frac{\partial \phi}{\partial y}\right)^2}}, \tag{4-16}$$

in which $\phi(x, y)$ is the potential field at (x, y).

Hypothesis 3: pedestrians follow the optimal path to their destination while trying to avoid high density locations. To incorporate the effect of local density into the calculations for the direction of motion, the distance between potential levels must be proportional to pedestrian density, as shown in Equation (4-17).

$$\frac{1}{\sqrt{\left(\frac{\partial \phi}{\partial x}\right)^2 + \left(\frac{\partial \phi}{\partial y}\right)^2}} = g(\rho)\sqrt{u^2 + v^2} \tag{4-17}$$

where $g(\rho)$ is the discomfort factor for pedestrians.

Combining Equations (4-11), (4-12), (4-16), and(4-17) gives the governing equation of motion for pedestrians based on the mass conservation law:

$$\frac{\partial \rho}{\partial t} - \frac{\partial}{\partial x}\rho f^2(\rho)g(\rho)\frac{\partial \phi}{\partial x} - \frac{\partial}{\partial y}\rho f^2(\rho)g(\rho)\frac{\partial \phi}{\partial y} = 0 \tag{4-18}$$

The second fundamental law of fluids is the conservation of momentum. The momentum of a fluid is defined by the product of flow and velocity:

$$F_x(t,x,y) = f(t,x,y)u(t,x,y) = \rho(t,x,y)u^2(t,x,y) \tag{4-19}$$

$$F_y(t,x,y) = f(t,x,y)v(t,x,y) = \rho(t,x,y)v^2(t,x,y) \tag{4-20}$$

Consider a generic infinitesimal 2D section of the fluid shown in Figure 4-2.

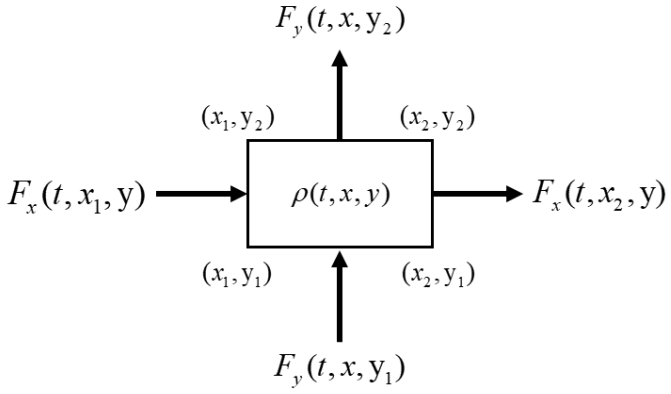

Figure 4-2. Conservation of momentum

According to Newton's law, the change in the linear momentum in any direction is equal to the force in that direction. Similar to the mass conservation, we can derive the equations for the momentum conservation in the x and y directions, as shown in

$$\frac{\partial}{\partial t}\rho u + \frac{\partial}{\partial x}(\rho u^2 + p) + \frac{\partial}{\partial x}\rho uv = 0 \tag{4-21}$$

$$\frac{\partial}{\partial t}\rho v + \frac{\partial}{\partial x}\rho uv + \frac{\partial}{\partial x}(\rho v^2 + p) = 0 \tag{4-22}$$

where p is the force applied on the fluid section.

4.1.1. Well-Known Crowd Dynamics Models

A few mesoscopic models have been developed to simulate crowd motions using laws of fluid dynamics. The Lighthill-Whitham-Richards (LWR) model [147–149] uses the mass conservation law to describe the flow of pedestrians:

$$\frac{\partial \rho}{\partial t} + \frac{\partial}{\partial x}\rho V cos\theta + \frac{\partial}{\partial y}\rho V sin\theta = 0 \tag{4-23}$$

where V is the speed of the fluid calculated using a speed-density equation.

The Payne-Whitham (PW) model [150,151] uses the mass and momentum conservation laws to provide a viscous description for the flow of pedestrians:

$$\frac{\partial \rho}{\partial t} + \frac{\partial}{\partial x}\rho u + \frac{\partial}{\partial y}\rho v = 0$$

$$\frac{\partial u}{\partial t} + u\frac{\partial u}{\partial x} + u\frac{\partial u}{\partial y} = \frac{V_x - u}{\tau} - \frac{A_x(\rho)}{\rho} + \frac{\mu}{\rho}\left(\frac{\partial^2 u}{\partial x^2} + \frac{\partial^2 u}{\partial y^2}\right)$$

$$\frac{\partial v}{\partial t} + v\frac{\partial v}{\partial x} + v\frac{\partial v}{\partial y} = \frac{V_y - v}{\tau} - \frac{A_y(\rho)}{\rho} + \frac{\mu}{\rho}\left(\frac{\partial^2 v}{\partial x^2} + \frac{\partial^2 v}{\partial y^2}\right) \tag{4-24}$$

where V_x and V_y are the components of the speed in x and y directions, τ is the relaxation time, $A(\rho)$ is the anticipation function, and μ is the viscosity term.

The Aw-Rascle model [152,153], similar to the PW model, uses the mass and momentum conservation laws:

$$\frac{\partial \rho}{\partial t} + \frac{\partial}{\partial x}\rho u + \frac{\partial}{\partial y}\rho v = 0$$

$$\frac{\partial}{\partial t}(u + p(\rho)) + u\frac{\partial}{\partial x}(u + p(\rho)) + v\frac{\partial}{\partial y}(u + p(\rho)) = 0$$

$$\frac{\partial}{\partial t}(v + p(\rho)) + u\frac{\partial}{\partial x}(v + p(\rho)) + v\frac{\partial}{\partial y}(v + p(\rho)) = 0 \quad (4\text{-}25)$$

in which $p(\rho)$ is the pressure term.

The Zhang model [154,155] uses the mass and momentum conservation laws to describe pedestrian flows based on microscopic car-following models. The Zhang model is given in Equation (4-26).

$$\frac{\partial \rho}{\partial t} + \frac{\partial}{\partial x}\rho u + \frac{\partial}{\partial y}\rho v = 0$$

$$\frac{\partial u}{\partial t} + (u + \rho V_x')\frac{\partial u}{\partial x} + (u + \rho V_x')\frac{\partial u}{\partial x} = \frac{V_x - u}{\tau}$$

$$\frac{\partial v}{\partial t} + \left(v + \rho V_y'\right)\frac{\partial v}{\partial x} + (v + \rho V_v')\frac{\partial v}{\partial x} = \frac{V_y - v}{\tau} \quad (4\text{-}26)$$

where $V' = \frac{\partial V}{\partial \rho}$.

Significant modeling efforts have been conducted to study crowd behaviors using these FDMs. In the next section, we will review the literature and learn about these efforts.

4.2. Literature Review

In the past twenty years, a number of studies have used fluid dynamics models to describe crowd behaviors through numerical simulation. In these studies, different crowd behaviors such as lane formation, oscillations at bottlenecks, and congestions due to high densities are investigated.

Hughes [156] modeled the crowd flow on the Jamarat Bridge near Mecca, where every year hundreds of thousands of Muslims cross the bridge during the Holy Hajj pilgrimage. Expanding the previous study by Selim and Al-Rabeh [143], Hughes studied the effect of the bridge pillars on the flow of pilgrims using the original first order equation developed by himself, as shown in Equation (4-18). Huang et al. [157] modeled crowd flow on a railway platform using Hughes' first order model. The railway platform is a 100-m by 50-m rectangular environment with a large obstruction in the middle and two exit doors. This study shows that the route choice method proposed by Hughes satisfies the reactive dynamic user equilibrium principle. A few other solutions have also been developed for the reactive dynamic user equilibrium model (e.g. [158,159]). Piccolo and Tosin [160] used the Hughes' model and applied their previously proposed discrete-time Eulerian model for the solution of the potential field on a few test cases, including narrow passages, rooms with multiple obstacles, lane formation, and crossing flows. Jiang et al. [161] formulated a 2D model based on the PW model. The model's ability to explain flow instability is presented by linear stability analysis. Numerical experiments are conducted on a 100-m by 50-m long corridor with a circular column in the middle to investigate the effect of obstacles on the flow of crowds. In another study [162], the behaviors of different first order (i.e. based on mass conservation) and second order (i.e. based on mass and momentum conservation) models are compared on two test cases: a corridor with two exits and a room with one exit and an obstacle close to exit door. The results show that first order models cannot produce behaviors such as the formation of stop-and-go waves and clogging at bottlenecks.

The literature on mesoscopic FDMs shows that these models can produce observed crowd dynamics in high densities, while the second order models, such as the PW model, which is based on both the conservation of mass and momentum show better capabilities. A

limitation of the FDMs is that they do not show promising behaviors for low density crowds [156,163,164]. Another limitation of FDMs that is not discussed in the literature is high-dense crowds of individuals with diverse mobility characteristics (e.g. large crowds of patients). FDMs use the aggregate measures of the population (speed and density) to reformulate the micro-scale model of agents and decision rules by a meso-scale model of population densities and PDEs. This implies that the heterogenous characteristics of the individuals are aggregated into homogenous characteristics of the population. Although as discussed before, studies have shown that in large crowds, the crowd behavior converges to the average behavior of the population, in cases such as hospital evacuation, the diversities in the groups of evacuees are more significant, such that a homogeneous macro-scale behavior may not be observed. To address the diversity limitation of FDMs, the PW model is extended by introducing multiple waves to represent different types of evacuees (patients).

4.3. The Fluid Dynamics Model

In this section, the PW model is further extended, and the addition of multiple waves and an inter-wave interaction mechanism is explained.

4.3.1. The PW Model

As introduced before in Section 4.1., the Payne-Whitham (PW) model [150,151] uses the mass and momentum conservation laws to provide a viscous description for the flow of pedestrians. The model as a system of PDEs is shown in Equations (4-27) to (4-29). In these equations, the parameters of waves are calculated at each time step t and location (x, y); i.e. $\rho = \rho(t, x, y), u = u(t, x, y), v = v(t, x, y)$.

$$\frac{\partial \rho}{\partial t} + \frac{\partial}{\partial x}\rho u + \frac{\partial}{\partial y}\rho v = 0 \tag{4-27}$$

$$\frac{\partial u}{\partial t} + u\frac{\partial u}{\partial x} + u\frac{\partial u}{\partial y} = \frac{V_x - u}{\tau} - \frac{A_x(\rho)}{\rho} + \frac{\mu}{\rho}\left(\frac{\partial^2 u}{\partial x^2} + \frac{\partial^2 u}{\partial y^2}\right) \tag{4-28}$$

$$\frac{\partial v}{\partial t} + v\frac{\partial v}{\partial x} + v\frac{\partial v}{\partial y} = \frac{V_y - v}{\tau} - \frac{A_y(\rho)}{\rho} + \frac{\mu}{\rho}\left(\frac{\partial^2 v}{\partial x^2} + \frac{\partial^2 v}{\partial y^2}\right) \tag{4-29}$$

where ρ is density, u and v are the x and y components of speed, V_x and V_y are the components of the equilibrium speed in the x and y directions, τ is the relaxation time, $A(\rho)$ is the anticipation function, and μ is the viscosity parameter.

Equation (4-27) is the mass conservation law, and Equations (4-28) and (4-29) are momentum conservation laws in the x and y directions, respectively. The anticipation function $A(\rho)$ corresponds to the sonic speed in fluid dynamics and can be expressed as:

$$A(\rho) = a_0\left(\frac{\rho}{\rho_m}\right)^{\beta} \tag{4-30}$$

in which a_0 is the full density sonic speed which corresponds to the free walking speed of pedestrians (e.g. $a_0 = 1.25\ m/s$ for non-disabled pedestrians) and $\beta = 1$ [161].

Regarding viscosity, according to the crowd modeling studies, due to strongly nonlinear behavior of the viscosity forces, especially near zero velocities, the numerical simulation of viscous dynamics equations is cumbersome [165]. Furthermore, the friction forces between pedestrians are small and have a negligible effect on the flow [156]. Hence, the effect of viscosity can be neglected, and the crowd flows can be considered inviscid $(\mu = 0)$ [161].

As discussed before, the route choice method proposed by Hughes [146] can be used to find the desired direction of motion based on the reactive dynamic user equilibrium principle. According to Hughes, the velocity components can be obtained as follows:

$$u = V(\rho)\hat{\phi}_x \ , \quad v = V(\rho)\hat{\phi}_y, \tag{4-31}$$

where $f(\rho)$ is the speed as a function of density, and $\hat{\phi}_x$ and $\hat{\phi}_y$ are the direction cosines of the trajectory. Among the proposed models for the speed-density relationship, the modified Drake's model, shown in Equation (4-32), is used most commonly in the literature. Furthermore, the speed-density relationship obtained from the ABM in Chapter 3 agrees with this model. Therefore, the modified Drake's model provides a good basis to compare the results from the PW model with those of ABM for the benchmark test cases.

$$V(\rho) = v_f exp\left(-7.5\left(\frac{\rho}{\rho_m}\right)^2\right) \tag{4-32}$$

The direction cosines of the trajectory can be found using the potential field method. In this method, the potential at each time step t and location (x, y) depends on the distance from the destination, presence of boundaries, and local density. The direction of motion of pedestrians is perpendicular to the potential field, i.e.:

$$\hat{\phi}_x = \frac{-\frac{\partial \phi}{\partial x}}{\sqrt{\left(\frac{\partial \phi}{\partial x}\right)^2 + \left(\frac{\partial \phi}{\partial y}\right)^2}} \ , \quad \hat{\phi}_y = \frac{-\frac{\partial \phi}{\partial y}}{\sqrt{\left(\frac{\partial \phi}{\partial x}\right)^2 + \left(\frac{\partial \phi}{\partial y}\right)^2}}, \tag{4-33}$$

in which $\phi(x, y)$ is the potential field at (x, y). Equation (4-33) is an alternative format for the Eikonal-type equations, $|\nabla\phi(x, y)| = f(x, y)$, which is a minimization problem for the instantaneous cost of walking from origin to destination. Different methods have been proposed for the solution of the Eikonal equation [158,166–168].

To incorporate the effect of local density into the calculations for the direction of motion, the distance between potential levels must be proportional to pedestrian density, as shown in Equation (4-34).

$$\frac{1}{\sqrt{\left(\frac{\partial \phi}{\partial x}\right)^2 + \left(\frac{\partial \phi}{\partial y}\right)^2}} = g(\rho)\sqrt{u^2 + v^2} \tag{4-34}$$

where $g(\rho)$ is the discomfort factor for pedestrians. There have not been any experimental studies on the format and parameters of the discomfort factor. According to Jiang et al. [161], the discomfort cost distribution should be an increasing function of density:

$$g(\rho) = g_0 \left(\frac{\rho}{\rho_m}\right)^{\alpha} \tag{4-35}$$

where $g_0 = 0.02\ s/m$ and $\alpha = 2$.

The numerical schemes to solve the PW model are complicated. The first order schemes, such as the Upwind, Lax-Friedrichs, and the Lax-Wendroff schemes are rather simpler but may fail to completely produce behaviors associated with turbulence and spurious oscillations. Higher-order schemes such as the Godunov's method are more capable but expensive to implement. The reader is referred to the references of numerical methods for fluid dynamics and hyperbolic PDEs (e.g. [61,62,169]) for further information about numerical solutions.

4.3.2. Addition of Multiple Waves to the PW Model

As discussed before, one limitation of FDMs for strongly heterogenous crowds is that the diverse characteristics of the individuals are aggregated into homogenous characteristics of the population. To address the population diversity in FDMs, the PW model is extended by introducing multiple waves to represent different types of evacuees (patients).

Extension to pedestrians of multiple types has been proposed and implemented in a limited number of studies [156,170,171]. The Hughes' hypotheses for crowd flows are still valid when considering multiple types of pedestrians [156]:

- Hypothesis 1: the walking speed of each type of pedestrian follows similar speed-density models introduced before; however, the density in these models refers to the total population density considering all types of pedestrians moving in the environment.
- Hypothesis 2: each type of pedestrian can have their own potential field based on which they follow their paths.
- Hypothesis 3: each type of pedestrians tries to minimize their path based on their potential field while this behavior can be tempered to avoid high density locations.

Therefore, for each type of pedestrian i, we have:

$$\frac{\partial \rho_i}{\partial t} + \frac{\partial}{\partial x}\rho_i u_i + \frac{\partial}{\partial y}\rho_i v_i = 0 \tag{4-36}$$

$$\frac{\partial u_i}{\partial t} + u_i\frac{\partial u_i}{\partial x} + u_i\frac{\partial u_i}{\partial y} = \frac{V_{ix} - u_i}{\tau} - \frac{A_x(\rho_i)}{\rho_i} + \frac{\mu}{\rho_i}\left(\frac{\partial^2 u_i}{\partial x^2} + \frac{\partial^2 u_i}{\partial y^2}\right) \tag{4-37}$$

$$\frac{\partial v_i}{\partial t} + v_i\frac{\partial v_i}{\partial x} + v_i\frac{\partial v_i}{\partial y} = \frac{V_{iy} - v_i}{\tau} - \frac{A_y(\rho_i)}{\rho_i} + \frac{\mu}{\rho_i}\left(\frac{\partial^2 v_i}{\partial x^2} + \frac{\partial^2 v_i}{\partial y^2}\right) \tag{4-38}$$

The velocity components can be obtained as follows:

$$u_i = V(\rho)\hat{\phi}_{ix} \ , \quad v_i = V(\rho)\hat{\phi}_{iy} \tag{4-39}$$

The equilibrium speed $V(\rho)$ can be calculated using the modified Drake's model as follows:

$$V_i(\rho) = v_{if} exp\left(-7.5\left(\frac{\rho}{\rho_m}\right)^2\right) \tag{4-40}$$

in which v_{if} is the free walking speed of pedestrian type i and ρ is total density, i.e. $\rho = \sum_{i=1}^{N}\rho_i$. Similarly, the anticipation and the discomfort terms can be calculated using total density.

The direction of motion of pedestrians in each group is perpendicular to their corresponding potential field, i.e.:

$$\hat{\phi}_{ix} = \frac{-\frac{\partial \phi_i}{\partial x}}{\sqrt{\left(\frac{\partial \phi_i}{\partial x}\right)^2 + \left(\frac{\partial \phi_i}{\partial y}\right)^2}} \quad , \quad \hat{\phi}_{iy} = \frac{-\frac{\partial \phi_i}{\partial y}}{\sqrt{\left(\frac{\partial \phi_i}{\partial x}\right)^2 + \left(\frac{\partial \phi_i}{\partial y}\right)^2}}, \tag{4-41}$$

where $\phi_i(x, y)$ is the potential field for pedestrian type i.

4.3.3. Wave Interactions

Certain types of social behaviors, such as grouping, herding, rescuing, and information sharing, were implemented in the microscopic ABM explained in Chapter 3. In this section, a mesoscopic implementation of the herding and rescuing behaviors is developed.

Meso-scale herding can be implemented using the potential field of the evacuees. Similar to the micro-scale herding behavior explained in Section 3.3.4., on meso-scale, for the flow of evacuees representing the unfamiliar patients, the potential field of other types of patients will be used.

The rescuing behavior introduces the altruism probability into the model. For each type of evacuees that can offer help to other evacuees (based on the patient classification framework in Section 3.3.1.) an altruism probability is assigned (P_i^{alt}) which follows a normal distribution for patient agents, $P^{alt} \sim N(0.8, 0.05)$ and is set to 1 for staff agents. In what follows, the mesoscopic mechanics of altruism is explained with an example. Let's denote the density of a certain evacuee type which can offer help by ρ_1 and the densities of two evacuee types that need help with ρ_2 and ρ_3. For simplicity, assume no preference between ρ_2 and ρ_3 for assistance. This implies that the ratio of evacuee types 2 and 3 which are receiving assistance depends on their relative densities, i.e.

$$P_{12}^{alt} = P^{alt}\frac{\rho_2}{\rho_2+\rho_3}\ , \quad P_{13}^{alt} = P^{alt}\frac{\rho_3}{\rho_2+\rho_3} \tag{4-42}$$

where P_{12}^{alt} and P_{13}^{alt} are the probabilities that type 1 evacuees will help type 2 and type 3 evacuees, respectively. The free walking speed of each of the evacuee types is then updated based on weighted average speeds according to Equations (4-43)-(4-45),

$$v_{1f}^{updated} = \frac{\rho_{12}v_{2f}^{assist} + \rho_{13}v_{3f}^{assist} + (\rho_1 - \rho_{12} - \rho_{13})v_{1f}}{\rho_1} \tag{4-43}$$

$$v_{2f}^{updated} = \frac{\rho_{12}v_{2f}^{assist} + (\rho_2 - \rho_{12})v_{2f}}{\rho_2} \tag{4-44}$$

$$v_{3f}^{updated} = \frac{\rho_{13}v_{3f}^{assist} + (\rho_3 - \rho_{13})v_{3f}}{\rho_3} \tag{4-45}$$

$$\rho_{12} = \min(P_{12}^{alt}\rho_1, \rho_2) \tag{4-46}$$

$$\rho_{13} = \min(P_{13}^{alt}\rho_1, \rho_3) \tag{4-47}$$

where ρ_{12} and ρ_{13} are the densities of type 1 evacuees that are assisting type 2 and type 3 evacuees, respectively, and v_{2f}^{assist} and v_{3f}^{assist} are the assisted free walking speed of type 2 and type 3 evacuees, respectively, according to Table 3-3. In Equations (4-43)-(4-47), it is assumed that each type 1 evacuee can only assist 1 evacuee. Consequently, the density of type 1 evacuees that are assisting type 2 evacuees is equal to the density of type 2 evacuees being assisted by type 1 evacuees ($\rho_{12} = \rho_{21}$).

4.4. PW++ vs ABM on Benchmark Test Cases

In this section, we will evaluate if the PW++ model can produce evacuation outputs close to what the ABM predicts, and how its results compare with those from the PW model.

4.4.1. Single Room Test Case

In Chapter 3, the single room test case and the outputs from the ABM were presented. To remind readers, the room setup is shown again in Figure 4-3: a rectangular 4-m by 8-m room with a 1-m wide door, 20 occupants with size (body diameter) of 0.5m and free walking speed of 1.25 m/s.

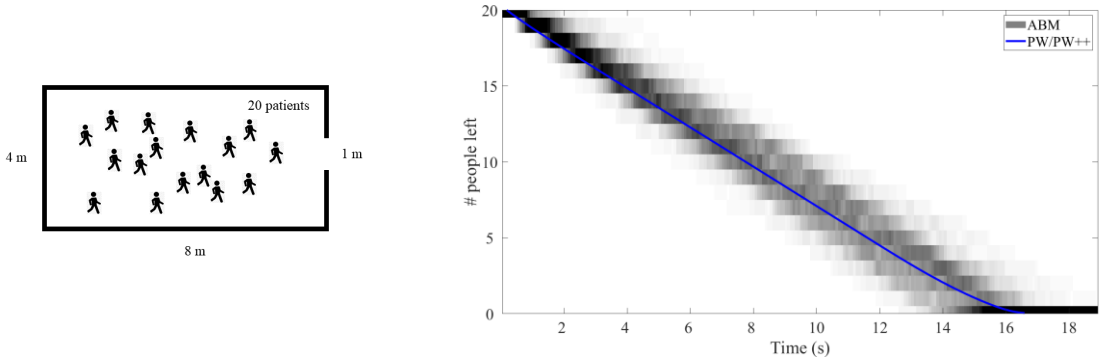

Figure 4-3. Single room test case. Left: room setup; right: results of the PW++ and the ABM.

As discussed in Chapter 3, the ABM predicts a final evacuation time ranging from 12 seconds to 18 seconds with a linear dominant exit pattern resulting in an average final evacuation time of 15.3 s. The PW++ produces a similar exit dynamic and converges to the average of results from the ABM with the final evacuation time of 16.6 s which is 8% higher than the average final evacuation time from the ABM. As shown in Table 4-1, the PW++ estimation of the total evacuation time agrees with the ABM's average time (with only 8% difference), and also the evacuation times at different percentile measures largely agrees. This implies that as expected, for simple cases with a homogeneous population the PW++ converges to the average behavior of the ABM. As there is only one type of evacuees in this test case, there is no difference between the PW model and the PW++.

Table 4-1. Evacuation time at specific percentile measures for the single room test case (ABM vs. PW++)

Percentile	ABM (average) [s]	PW++ [s]	Relative difference
25%	4.0	3.9	-3%
50%	7.9	7.8	-1%
75%	11.6	11.6	0%
90%	13.9	14.1	1%
100%	15.3	16.6	8%

Figure 4-4 shows the initial potential field calculated using the fast sweeping method for the single room test case. The potential is defined as the distance to the exit door considering local population density as a discomfort factor, as explained in Section 4.1.

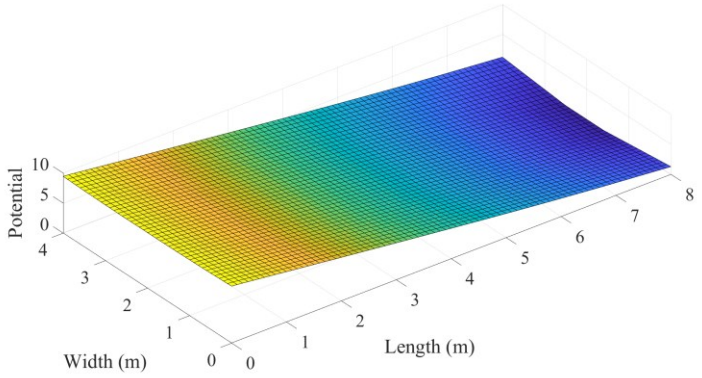

Figure 4-4. Initial potential field for the single room test case

To better analyze the results of the PW++, the population density and desired direction of motion (based on the potential field) are shown at $t = 0\,s, 5\,s, 10\,s, 15\,s$ in Figure 4-5. Initially, when the occupants are uniformly distributed over the room, the potential field only depends on the distance from the exit door as there is no variations in the density. This is indicated by the monocentric equidistant contour lines of the potential field at $t = 0$.

As time passes, the flow of evacuees moves towards the exit door and creates a congestion condition close to the far-left boundary. The local congestion changes the discomfort factor over the room such that the evacuees prefer to avoid the congestion if possible. This is indicated by the distortion in the potential field contour lines close to the exit door where the distance between contour lines is smaller at $t = 5\ s, 10\ s$.

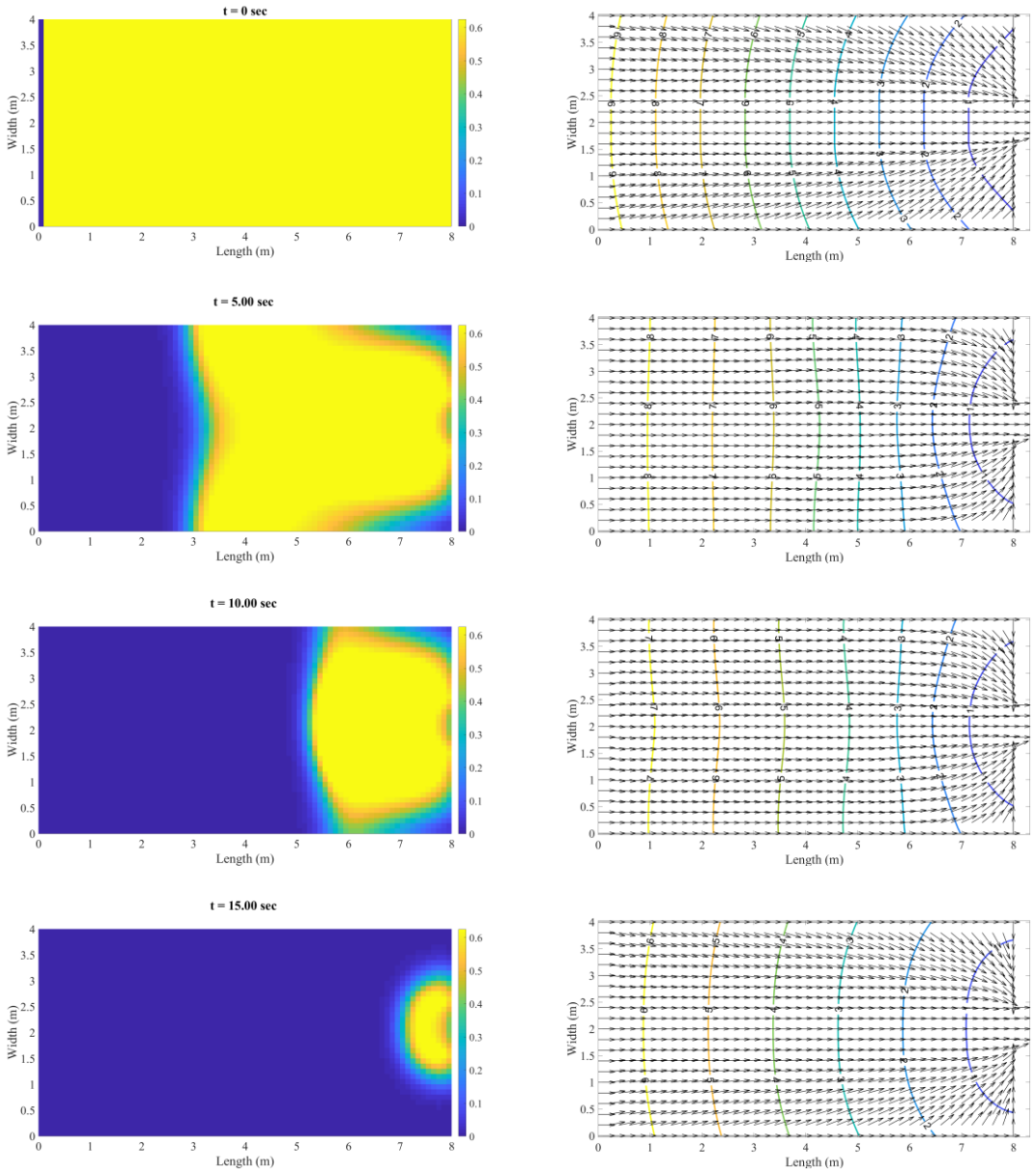

Figure 4-5. Spatial population density and desired direction of motion at different times for the single room test case

4.4.2. Two-Room Test Case

The two-room test case is shown again in Figure 4-6: a rectangular 4-m by 6-m back room (Room 1) with a 1.5-m wide door, 40 occupants from which 30 has mobility impairment, and a 6-m by 6-m front room (Room 2) with a 1.5-m wide door, 20 occupants from which 5 has mobility impairment. The body size of all the occupants is 0.5 m, and the free walking speed for non-disabled and mobility impaired occupants is 1.25 and 0.5 m/s, respectively.

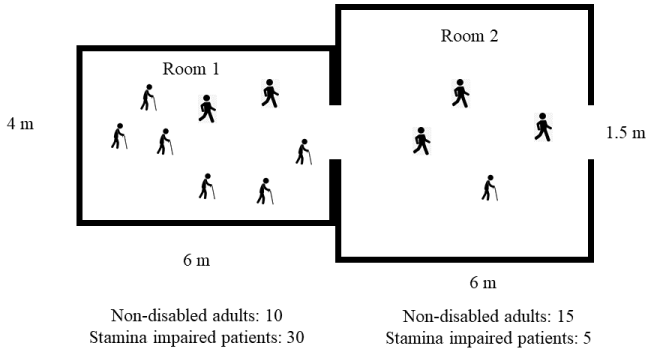

Figure 4-6. The two-room test case

The results of the evacuation of the two-room test case modeled with the ABM, PW, and PW++ are shown in Figure 4-7 and Figure 4-8. According to the ABM, Room 1 has a simple linear exit pattern with an average evacuation time of 31.4 seconds. The PW model, in which all the evacuees are modeled as a homogenous population density, overestimates the exit rates and predicts a linear exit pattern for Room 1 with a 40% underestimated evacuation time of 18.8 seconds, which does not agree with the results from the ABM. The PW++ provides better results for Room 1, to compare with the PW model, with a liner exit pattern and a 14% underestimated evacuation time of 27.1 seconds. For Room 1, the PW++ produced exit rates which resulted in 10-40% differences in the partial evacuation times, while the range of differences for the PW model is 40-50%, when compared with the ABM. Looking at the

results for Room 2, the evacuation time according to the PW model is 27.6 seconds. Compared with the results from the ABM, similar to Room 1, the PW model underestimates the evacuation time. The PW++ estimates the evacuation time to be 40.2 seconds which is an improvement when compared with the PW model. Furthermore, the PW++ is more successful in converging to the results of the ABM as it is clear from Figure 4-7. The exit dynamics obtained by the PW++ is within 15% of that from the ABM at partial evacuation percentiles, while the range of differences for the PW model is 20-35%, when compared with the ABM.

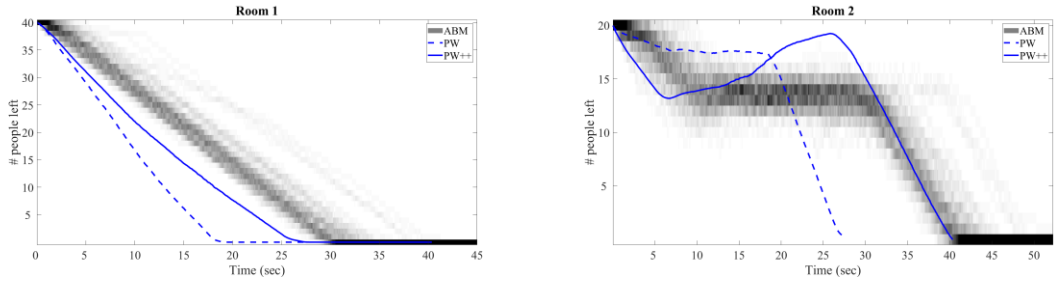

Figure 4-7. Results of the PW++ and the ABM for the two-room test case: Left: Room 1; Right: Room 2.

As it can be seen in Figure 4-8, the overall evacuation pattern of the two-room test case obtained from PW++ agrees with that of the ABM to some extent. Initially, the exit rates are overestimated for the first 5 seconds. However, for the next 15 seconds, PW++ underestimates the exit rates such that at $t = 20\ s$, PW++ meets the ABM, after which the third linear section of the PW++ strongly agrees with the dominant exit pattern of the ABM. The PW model shows a simple linear exit rate with an underestimated total evacuation time of 27.7 seconds.

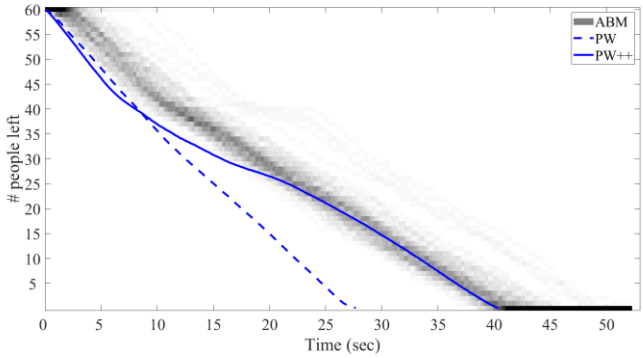

Figure 4-8. Results of the PW++ and the ABM for total evacuation of the two-room test case

According to Table 4-2, PW++ initially diverges from the average of the ABM, but for the second 50% of the evacuation process, PW++ underestimates times by only less than 4% when compared with the ABM. On the other hand, the PW model does not agree with the ABM and underestimates the partial evacuation times by 34% to 53%.

Table 4-2. Evacuation time at specific percentile measures for the two-room test case

Percentile	**ABM_{avg} [s]**	**PW**		**PW++**	
		Time [s]	**Relative Difference**	**Time [s]**	**Relative Difference**
25%	9.0	4.5	-50%	5.4	-40%
50%	19.3	9.0	-53%	15.8	-18%
75%	30.1	14.4	-52%	29.8	-1%
90%	36.8	17.4	-53%	36.0	-2%
100%	41.9	27.7	-34%	40.4	-4%

Figure 4-9 shows the initial potential field calculated using the fast sweeping method for the two-room test case. The potential is defined as the distance to the exit door considering local population density as a discomfort factor and walls as obstacles.

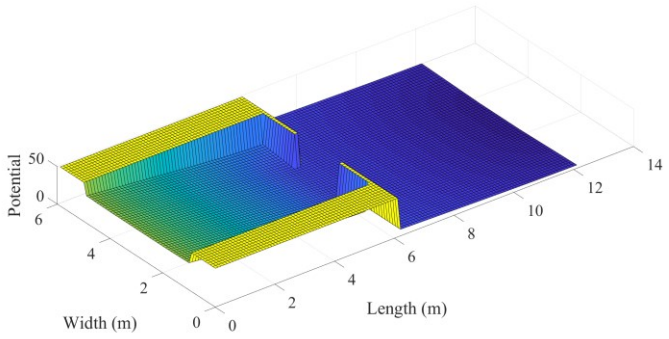

Figure 4-9. Initial potential field for the two-room test case

To better analyze the results of the PW++, the population density and desired direction of motion (based on the potential field) are shown at $t = 0\ s, 10\ s, 20\ s, 30\ s$ in Figure 4-10. Similar to the single room test case, at first when the occupants are uniformly distributed over the room, the potential field only depends on the distance from the exit door as there is no variations in the density. This is indicated by the monocentric equidistant contour lines of the potential field at $t = 0$. As time passes, the flow of evacuees moves towards the exit doors and makes local congestion conditions at the bottlenecks. The local congestions change the discomfort factor over the environment such that the evacuees prefer to avoid the congestion if possible. This is indicated by the distortion in the potential field contour lines close to the exit doors where the distance between contour lines is smaller at $t = 10\ s, 20\ s$.

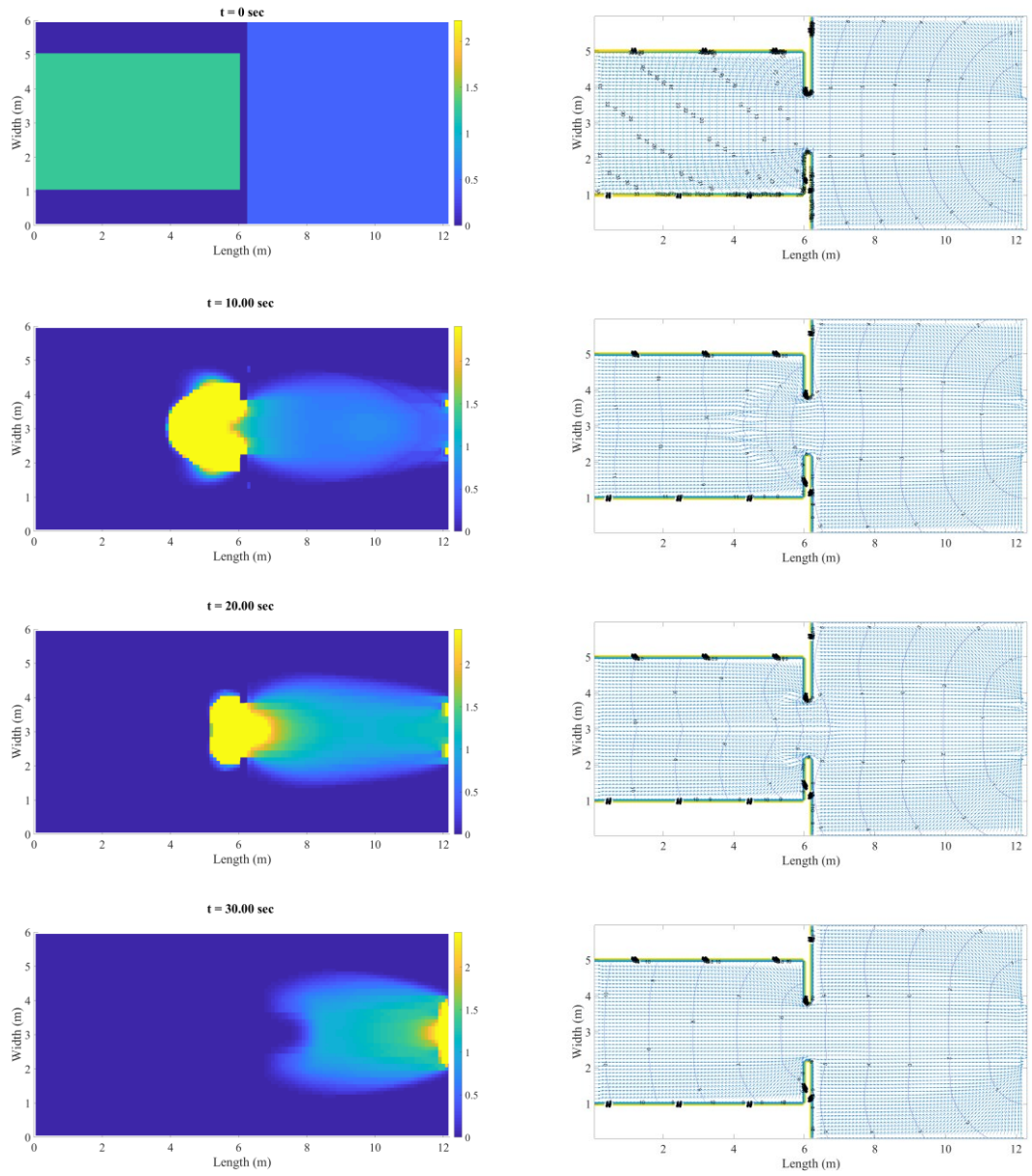

Figure 4-10. Spatial population density and desired direction of motion at different times for the two-room test case

As mentioned above, the improvement that the PW++ shows over the PW model is because of the introduction of multiple densities to represent different types of evacuees. In Figure 4-11, the multiple waves formed for the stamina impaired and non-disabled patients are illustrated.

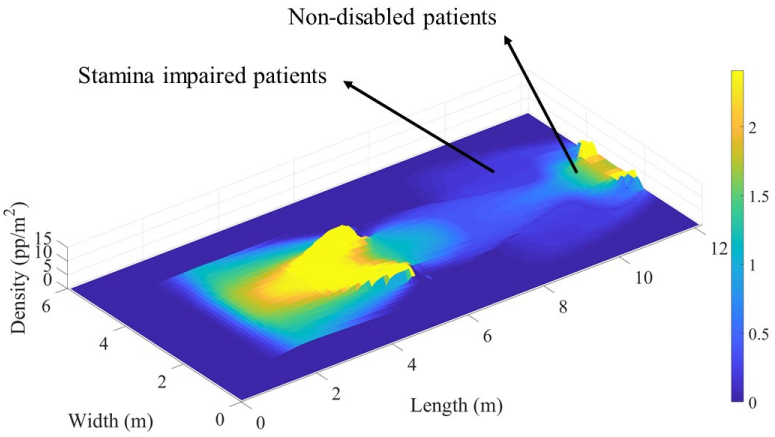

Figure 4-11. Formation of separate waves for different types of evacuees

Having different waves of evacuees in PW++ enables us to specifically investigate the exit dynamics for each type of patients. As shown in Figure 4-12, PW++ overestimates the exit rate of stamina impaired patients in the first 20 seconds; however, the total evacuation time is estimated to be 40.2 s which is only 1% more than the average time from the ABM ($T = 39.7\ s$). In general, the exit dynamics obtained by PW++ is within 18% of that of the ABM. In case of non-disabled patients, PW++ fails to estimate the initial delay of 2-3 seconds in the evacuations of the patients; however, the resulting exit pattern in the first 10 seconds lies within the ABM margin. PW++ does not perfectly capture the following decrease in the exit rates for the non-disabled patients after $t = 10\ s$, which leads to an underestimated evacuation time of 26.5 s. The difference between PW++ and the average results of the ABM at the specified partial evacuation percentiles are 33-55%.

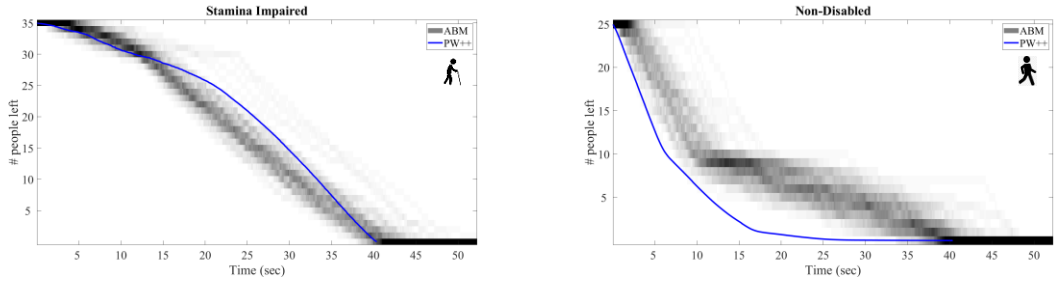

Figure 4-12. Two-room test case: evacuation results from the ABM and PW++ for stamina impaired and non-disabled patients

4.4.3. Two-Room-Corridor Test Case

The two-room-corridor test case is shown again in Figure 4-13: two 4-m by 4-m rooms, each with a 1.2-m wide door, with 5 wheelchair users in Room 1 and 10 visitors in Room 2, where both rooms open to a 14-m by 3-m corridor with a 1.2-m wide exit door. The body size of wheelchair users is 0.8 m and their free moving speed is 0.69 m/s. For visitors, body size is 0.5 m and free walking speed is 1.4 m /s.

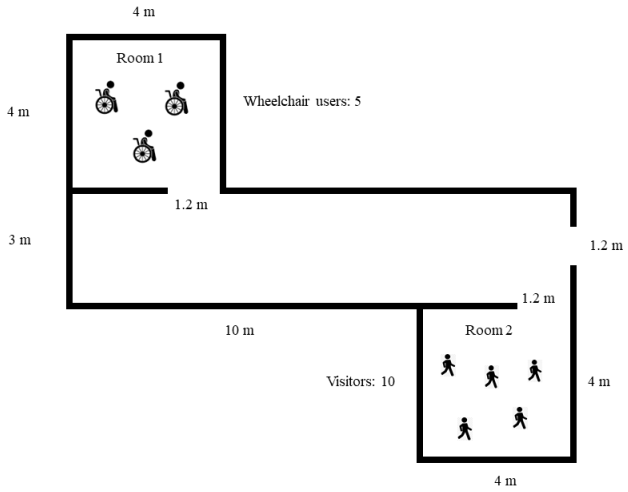

Figure 4-13. The two-room-corridor test case

The results of the evacuation of the two-room-corridor test case modeled with ABM, PW, and PW++ are shown in Figure 4-14 and Figure 4-15 and Table 4-3. According to ABM, Room 1 has a simple linear evacuation pattern with an average evacuation time of 13.3 seconds. The PW model, in which all the evacuees are modeled as a homogenous population density, overestimates the exit rates and results in a nonlinear exit pattern for Room 1 with an underestimated evacuation time of 8.8 seconds, which does not agree with the results from the ABM. PW++ provides better results for Room 1, when compared with the PW model, with a nonlinear evacuation pattern and an evacuation time of 12.3 seconds. Looking at the results for Room 2, the evacuation time according to the PW and PW++ is 9.3 seconds and 6.8 seconds, respectively. Compared with the estimated average time from ABM, the differences are -3% and -29% for PW and PW++, respectively. As discussed before, the fluid dynamics models do not provide accurate results and overestimate the flow for low densities. In the PW model, there is only one type of crowd wave with an averaged flow speed (1 m/s), while in PW++, there are two waves with their specific flow speeds (0.69 and 1.4 m/s). As a result, the flow in Room 2 moves slower in the PW to compare with PW++, and this inaccurate slow flow balances the inaccurate overestimation of the flow in the PW model.

For the corridor, the evacuation time according to PW and PW++ are 21.4 and 31.4 seconds, respectively, which comparing with the average evacuation time from the ABM (31.3 s), shows the improvement of PW++over the PW model. In addition, the exit pattern from PW++ lies within 13% of the average exit pattern from the ABM. The specific exit pattern in the corridor provides an interesting basis to compare the behavior of PW++ and the PW model. Initially, the number of evacuees in the corridor increases linearly due to the linear inflow from the rooms. After 5 to 10 seconds, as evacuees enter the corridor, those from Room 2 (which is closer to the corridor's exit door) start to exit the corridor, which makes the

number of evacuees in the corridor fluctuate. Following the fluctuation, the number of evacuees stays constant at 5, which denotes the delay time between the last visitor and the first wheelchair user exiting the corridor. The last part is the evacuation of wheelchair users with a linear dynamic. This specific exit pattern is reproduced by PW++.

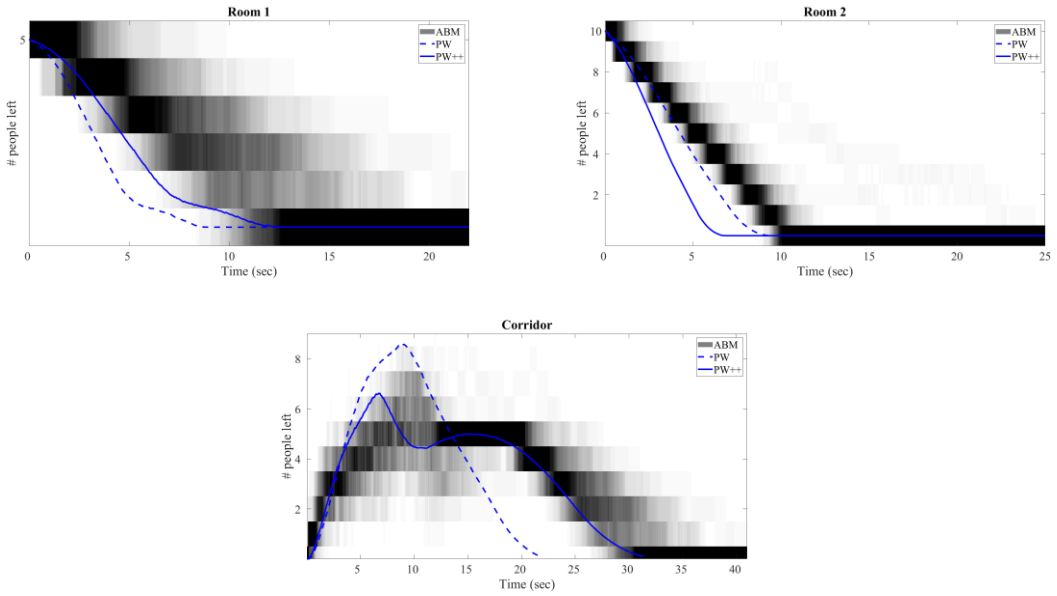

Figure 4-14. Results of PW++ and ABM for the two-room-corridor test case.

Looking at the total evacuation results shown in Figure 4-15, the advantage of PW++ over the PW model is evident. PW++ reproduced the delay in the arrival of the evacuees and converges to the exit pattern obtained from the ABM, while the PW model fails to do so.

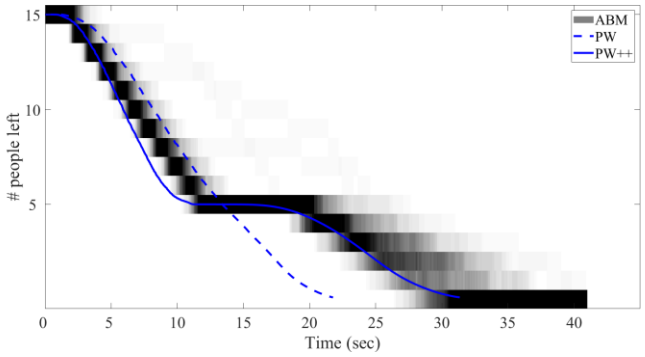

Figure 4-15. Results of PW++ and ABM for total evacuation of the two-room-corridor test case

According to Table 4-3, the results of the PW model differ from the average of the ABM by 20% to 30%, and it underestimates the total evacuation time by 30%. On the other hand, PW++ strongly agrees with the ABM with differences below 13% at the specified evacuation percentile measures.

Table 4-3. Evacuation time at specific percentile measures for the two-room-corridor test case

Percentile	**ABM_{avg} [s]**	**PW**		**PW++**	
		Time [s]	**Relative Difference**	**Time [s]**	**Relative Difference**
25%	5.7	7.1	25%	5.1	-11%
50%	8.8	10.7	22%	7.7	-13%
75%	20.8	15.1	-27%	21.4	3%
90%	26.5	18.2	-31%	26.2	-1%
100%	31.3	21.8	-30%	31.4	0%

Figure 4-16 shows the initial potential field calculated using the fast sweeping method for the two-room test case. The potential is defined as the distance to the exit door considering local population density as a discomfort factor and walls as obstacles.

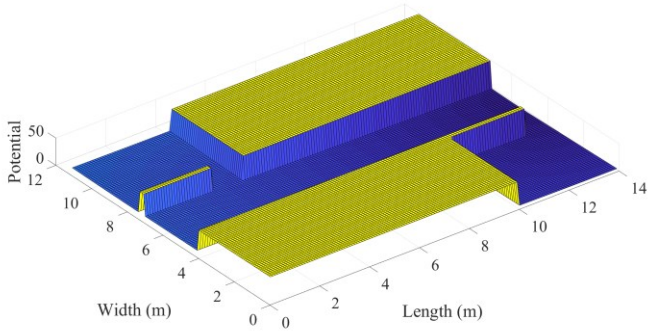

Figure 4-16. Initial potential field for the two-room-corridor test case

To better analyze the results of PW++, the population density and desired direction of motion (based on the potential field) are shown at $t = 0\ s, 5\ s, 15\ s, 25\ s$ in Figure 4-17. Similar to the single-room and the two-room test cases, at first when the occupants are uniformly distributed over the rooms, the potential field only depends on the distance from the exit door as there is no variations in the densities in each room. This is indicated by the monocentric equidistant contour lines of the potential field at $t = 0$. As time passes, the flow of evacuees moves towards the exit doors and makes local congestion conditions at the bottlenecks. The local congestions change the discomfort factor over the environment such that the evacuees prefer to avoid the congestion if possible. This is indicated by the distortion in the potential field contour lines at $t = 5\ s, 15\ s$.

Having different waves of evacuees in PW++ enables us to specifically investigate the exit dynamics of each type of patients. As shown in Figure 4-18, the results of FDM agrees with those of the ABM. PW++ have successfully estimated the time it takes for the wheelchair

users and the visitors to reach the corridor's exit door. PW++ estimates the evacuation time for the wheelchair users and the visitors to be 31.4 and 11.6 seconds, respectively, which agrees with the average evacuation times from the ABM (31.3 and 12.1 seconds).

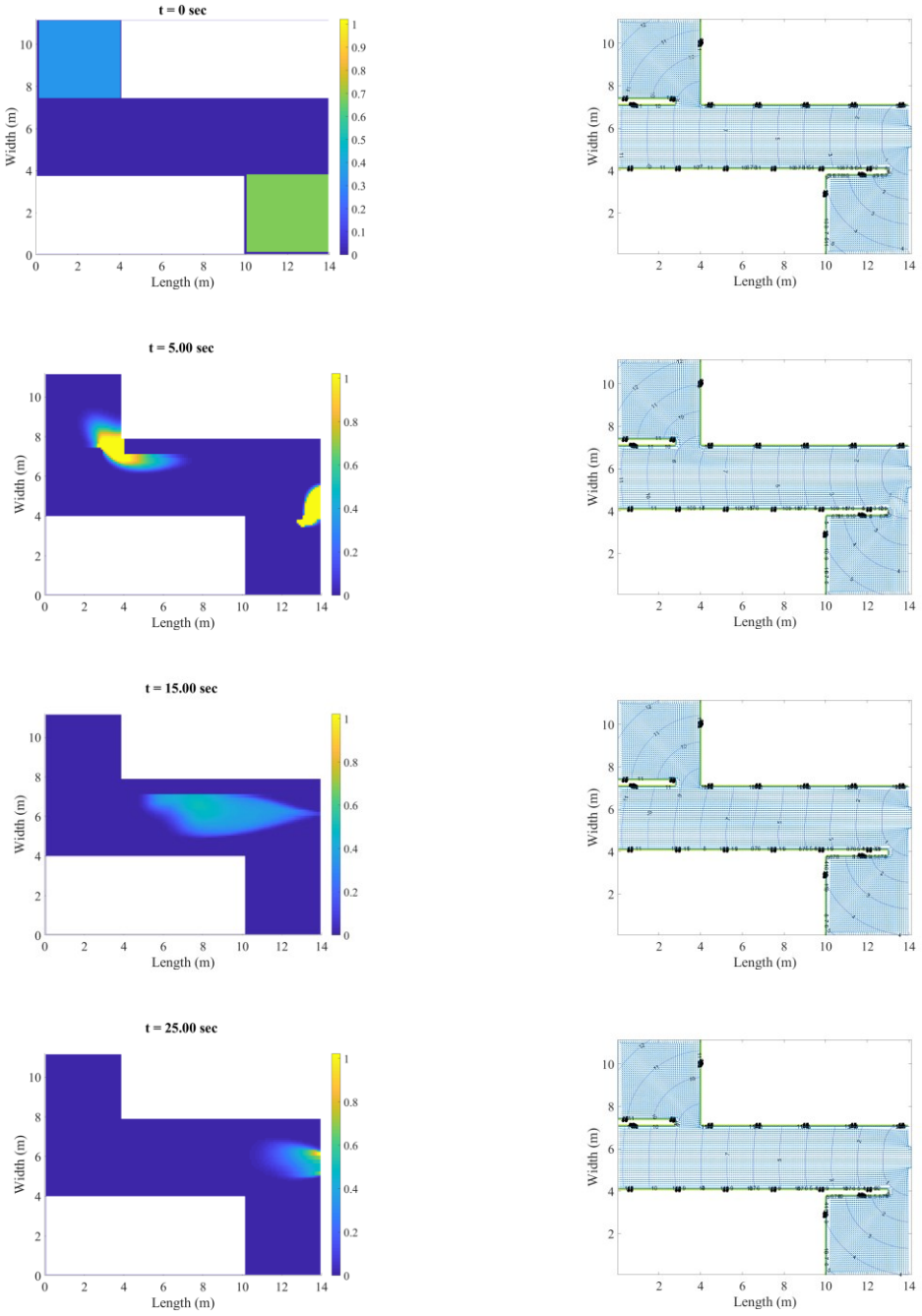

Figure 4-17. Spatial population density and desired direction of motion at different times

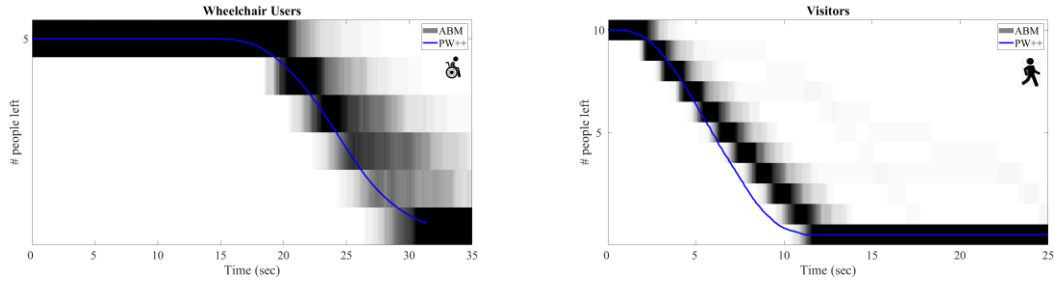

Figure 4-18. Two-room-corridor test case: evacuation results from the ABM and FDM for wheelchair users and visitors.

4.5. Discussion

Fluid dynamics models have shown to be useful tools to study the dynamics of crowds, specifically for highly dense crowds. The basis of these models is that in large crowds, the diverse characteristics of individuals do not significantly affect the collective crowd behavior. This may not hold true for crowds with strongly heterogenous mobility characteristics, such as large groups of patients. The introduction of multiple waves for different types of pedestrians can address this shortcoming in fluid dynamics models.

For cases of homogenous crowds with relatively medium densities like the single room test case, as expected, PW++ (and the PW model) converges to the average behavior of the ABM. However, in the two-room and the two-rom-corridor test cases where there are two types of evacuees with different mobility characteristics (walking speed), the agreement between PW++ and the average behavior of the ABM is more than that of the PW model. This implies that adding different types of evacuees to the PW model improves its capabilities in estimation of evacuation rates. However, PW++ does not completely reproduce the specific exit patterns observed in the ABM and mainly underestimates the evacuation times. In other words, if an emergency management team wants to estimate the partial evacuation of a small

section of a hospital with only two rooms and two groups of patients, PW++ can be used to obtain an estimation for the final evacuation time, it provides more reliable results than the PW model, but it cannot provide the emergency planners with reliable information about the intermediate exit rates and how the evacuation process would proceed from the beginning to the end. From an operational management perspective, emergency planners prefer to have overestimation rather than underestimation. Therefore, aside from discrepancies in the resulted exit patterns, the underestimations of PW++ is another drawback compared to the ABM.

The drawback of fluid dynamics models in the simulation of low-density crowds is clearer in the two-room-corridor test case, however, the addition of the specific waves for each type of evacuees has improved the behavior of the PW model. The relative superiority of PW++ over the PW model is negated in the evacuation of Room 2. The discrepancies at defined percentile measures are between 11-22% for the PW model and 21-43% for PW++ when compared with the average of the ABM. As explained before in Section 4.3.3, the fluid dynamics models do not provide accurate results and overestimate the flow for low densities. In the PW model, there is only one type of crowd wave with an averaged flow speed (1 m/s), while in PW++, there are two waves with their specific flow speeds (0.69 and 1.4 m/s). As a result, the flow in Room 2 moves slower in the PW model to compare with PW++, and this inaccurate slow flow balances the inaccurate overestimation of the flow in the PW model.

As mentioned above, although PW++ shows improvement over the PW model for heterogenous populations, from a decision-making perspective, PW++ cannot provide adequate informative results. There are considerable discrepancies between the results of PW++ and those from the ABM. For a complete evacuation of a hospital with hundreds of patients with different mobility characteristics, the limitations of PW++ can be accumulated,

hence providing results which are not useful or even misinform the hospital emergency planners regarding total evacuation time and intermediate exit rates.

4.6. Conclusions

With the increasing urban growth rates, the study of pedestrian and crowd dynamics has become important, specifically for safety and security management of human traffic. There have been significant improvements on the simulation of crowds using microscopic modeling techniques such as Cellular Automata or Agent-Based Modeling (ABM). From a theoretical perspective, the microscopic models cannot provide mathematical explanations for different crowd dynamics. Another modeling technique that can address this limitation is mesoscopic models which are based on fluid dynamics rules. Fluid dynamics models (FDMs) consider crowds as a whole (i.e. a wave) and use partial differential equations (PDEs) to mathematically formulate crowd dynamics.

The FDMs have shown to be useful tools to study the behaviors of large crowds; however, they come with two major limitations: less accurate results for (1) low density populations, and (2) high-dense crowds of individuals with strongly diverse mobility characteristics (e.g. in case of hospital evacuation). This study tries to address the second limitation by extending current FDMs with the introduction of multiple waves to represent different types of evacuees. The extent of improvements in the application of FDMs for heterogenous crowds is investigated by comparing the results of the original and improved FDMs with those from the ABM developed in Chapter 3 over the benchmark test cases. The results of this study shows that the addition of multiple types of pedestrians into the FDMs improve the behavior of these models for simulation of heterogenous crowds, however, from an decision-making perspective, the FDMs may not be the best candidates to support

emergency planners with adequate information. The improved FDM cannot produce crowd motions and exit rates which are obtained from the ABM and fails to provide an acceptable estimation for the overall evacuation time for different types of evacuees. The results of this study agree with the literature on the main applicability of fluid dynamics models. These models are developed specifically to study the dynamics of dangerously high-density crowds, for relatively homogenous populations, where pressure waves can occur.

Considering the relative advantages and disadvantages of FDMs and ABMs in the context of hospital evacuation simulation, FDMs can be considered as a complementary tool by which the dynamics of specific crowds can be studied. However, for simulation as a tool to support emergency decision making, there is much room left to improve on FDMs, while ABMs possess better capabilities to study the evacuation behaviors of patients with different mobility characteristics and needs.

Chapter 5

Hospital Evacuation: Macroscopic System Dynamics Modeling

5.1. Introduction

Recent advances in macro models, such as regression and machine learning, have made models more capable of predicting possible outcomes of complex systems when there is lack of solid knowledge. However, these so-called black-box models cannot describe the mechanics of complex systems such as socio-physical systems. From a Systems Engineering perspective, we desire to understand the underlaying mechanics and interactions between the components of a system so that we can develop models to explain the dynamics of the system. System dynamics modeling, originally developed in the 1950s by Jay W. Forrester [172] to understand industrial processes, is one of the modeling methods that is used to break down, understand, and describe complex systems.

System dynamics is a top-down modeling approach that enables researchers and decision makers across academia, industry, and government to study the behaviors of complex systems. The first step in developing System Dynamics Models (SDMs) is to identify the internal components of the system and external systems or subsystems that can have impacts on the behavior of the system. This is an interdisciplinary process where experts try to identify

and find causal linkages between these components. The result of this effort is illustrated using Causal Loop Diagrams (CLDs).

5.1.1. The Predator-Prey Model

For demonstration purposes, we will develop a simple CLD for the famous Predator-Prey Model [173]. This model explains the dynamics of a predator-prey ecosystem. In such a system, species evolve, compete, and disperse with the purpose of seeking resources to live. Considering species as the components of an ecosystem, the model describes the win-loss interactions between the components. One can see that this model has applications outside of ecology, where the components of a system have to compete over a limited amount of resources. We can use SDMs to study different behaviors of these systems and understand how they can become stable or unstable. The system is stable if it maintains itself over time with fluctuations in populations of species and is unstable if it leads to the extinction of one or more species.

A simple variation of the predator-prey model consists of a predator (e.g. wolf) and a prey (e.g. sheep); therefore, wolves and sheep are the components of an ecosystem. The next step is to identify the interactions between wolves and sheep. In this model, wolves and sheep roam randomly around the landscape, while the wolves look for sheep to prey on. As wolves wander around, they lose energy and must eat sheep to regain their energy. This implies the more wolves there are, the more sheep will be eaten by wolves, hence the less sheep there will be (negative effect). On the other hand, the more sheep there are, the more food is available for wolves to feed on, survive, and reproduce (positive effect). We also need to identify other factors affecting the population of wolves and sheep. The birth rates of wolves and sheep have a positive effect, and the death rate has a negative effect on the population. In this variation,

the grass is considered to be infinite, so the sheep always have enough food to survive. We can show this wolf-sheep ecosystem with a CLD shown in Figure 5-1.

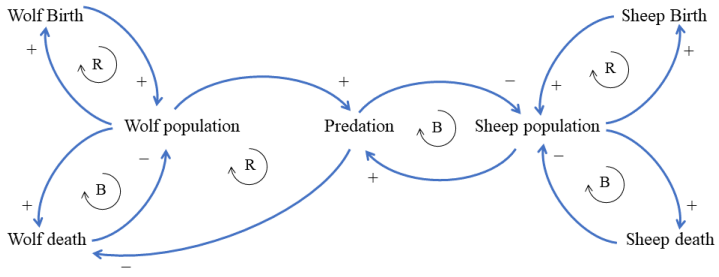

Figure 5-1. Causal loop diagram for the predator-prey model

In CLDs, the components and parameters of the system are depicted as nodes, and causal links are shown with arrows. The arrows are unidirectional pointing from the influencer component to the influenced component. The signs on the arrows show the direction of influence. A positive influence implies that the direction of change is the same in the cause and effect. For example, an increase (decrease) in population of wolves will lead to an increase (decrease) in the volume of predation. A negative influence means the directional of change in the cause and effect are reversed. For example, an increase (decrease) in the predation volume will result in a decrease (increase) in the population of sheep. Furthermore, CLDs can help us identify feedback loops. There are two types of feedback loops: reinforcing (R) and balancing (B). A reinforcing feedback loop implies a magnifying effect on parameters in the loop, i.e. an initial change in one of the parameters in the loop will be reinvested to magnify that change in the future. A balancing feedback loop implies equilibrium, i.e. an initial change in one of the parameters in the loop will be countered to balance that change back in the future.

The next step is to convert the CLD into an SDM. In SDMs, components of the system are shown as stocks, and the causal links are modeled as flows between stocks. Figure 5-2 shows the stock-and-flow diagram developed based on the CLD in Figure 5-1.

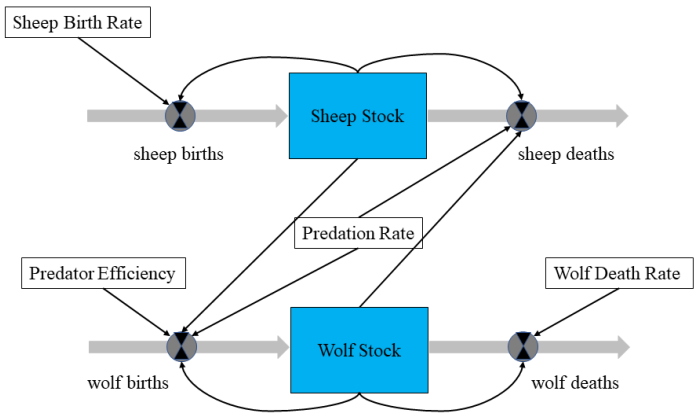

Figure 5-2. System dynamics model for the predator-prey system represented by a stock-and-flow diagram

SDMs are mathematically expressed with ordinary differential equations (ODEs). The stocks are considered as the variables, and the flows are expressed as rates of change or derivatives. The predator-prey model has evolved significantly in the last century [173]. The variation described above is the Lotka-Volterra model, also known as the *logistic model* [174,175]. According to this model, the rate of change in population is proportional to the product of species' biomass densities. The Lotka-Volterra model expressed in ODEs are shown in Equations 5-1)-(5-2):

$$\frac{ds(t)}{dt} = s(t)[b - pw(t)] \quad (5\text{-}1)$$

$$\frac{dw(t)}{dt} = w(t)[rs(t) - d] \quad (5\text{-}2)$$

in which $s(t)$ is the population of the sheep at time t, $\frac{ds(t)}{dt}$ is the rate of change in the population of the sheep at time t, $w(t)$ is the population of the wolves at time t, $\frac{dw(t)}{dt}$ is the rate of change in the population of the wolves at time t, b is the birth rate of sheep in the absence of interaction with wolves, p is the impact of predation on the rate of change of the population of sheep, r is the impact of predation on the rate of change of the population of wolves, and d is the death rate of wolves in the absence of interaction with sheep. Figure 5-3 shows the results from the Lotka-Volterra model if we set b, d, p, and r to 0.04, 0.15, 0.0003, and 0.0003, respectively, and 30 wolves and 100 sheep as the initial conditions.

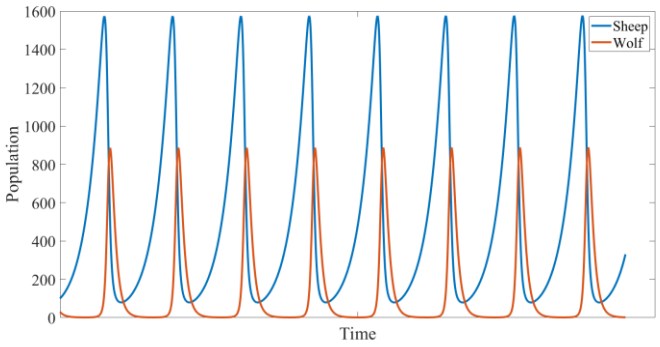

Figure 5-3. The Lotka-Volterra model

To better study the behavior of SDMs for different initial conditions, we can use a phase portrait. A phase portrait is a graphical representation of possible trajectories of a dynamical system. The phase portrait for the Lotka-Volterra model for different initial conditions is shown in Figure 5-4.

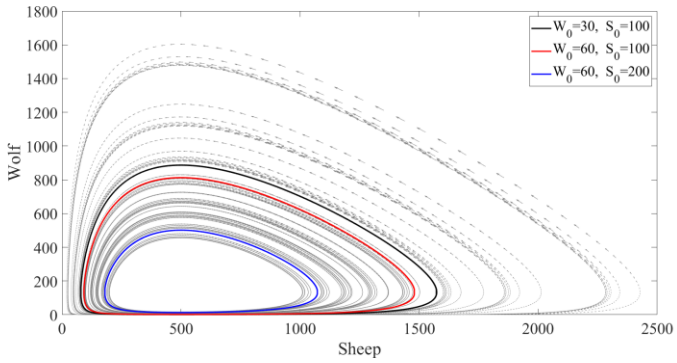

Figure 5-4. Phase portrait for the Lotka-Volterra model

Now that we have introduced dynamical systems, we can study evacuation from a system dynamics perspective. As discussed before in Chapter 1, evacuation is a socio-physical process in which humans interact with each other and with the built environment under extreme conditions. In the next section, we will review the literature on the application of system dynamics in modeling crowd dynamics.

5.2. Literature Review

System dynamics has been used in a vast variety of applications in engineering and social sciences, specifically as a supporting tool for decision making. In the context of evacuation, system dynamics is used to evaluate emergency management and regulatory structures when there is a need to order mass evacuations [176,177].

Simonovic and Ahmad [133] developed an SDM to study evacuation decision making during flood emergencies on a community level. In this model, the decision-making process is broken down to four psychological phases of concern, recognition, acceptance, and decision based on the work of Laska [178]. Furthermore, the parameters of the model are divided into four categories: initial conditions (e.g. risk awareness or knowledge of safety zones), social factors (e.g. income or age), external factors (e.g. inundation condition or information sharing),

and psychological factors (mentioned above). The time it takes for evacuees to reach the destination is estimated on the community level as a function of total population in the evacuation process, knowledge of safety zones, a route factor, and a random delay variable. Voyer et al. [179] developed an SDM to study the process of patient relocation during evacuations. The model focuses on the operational aspects of patient transfer such as means of transportation and acceptance procedure at receiving hospitals. Anjomshoae et al. [180] used system dynamics to analyze evacuation planning and flood preparedness policies. The SD model consists of an evacuation sub-model and a medical service supply sub-model. In the evacuation sub-model, evacuation rate at each time step is estimated based on flood risk level on the community level.

All these studies are dedicated to operational aspects or decision making processes of emergencies and disasters; however, the objective of this study is to apply the system dynamics approach to model the flow of patients (or in general evacuees) between rooms and corridors and eventually out of the hospital (or in general a building). In this regard, the literature is limited to one study. In this study, Shen [181] developed an SDM to simulate the evacuation of a building in a fire emergency. In this model, each section of the building (e.g. room or corridor) is considered as a stock, and the flows are the flows of evacuees between rooms and corridors. The model is based on the classical hand calculation methods for the evacuation of buildings and ships. In these methods, evacuation flow rate is calculated using the density and characteristics of the rooms and corridors (i.e. length and width). Density refers to *occupant density* which is defined as number of occupants in a room divided by the area of the room. Walking speed is calculated based on Nelson and Mowrer [182] as in Equation (5-3):

$$S = \begin{cases} 1.19 & \rho < 0.54\ pp/m^2 \\ 1.4(1 - 0.266\rho) & 0.54 \leq \rho < 3.8\ pp/m^2 \\ 0.01 & \rho \geq 3.8\ pp/m^2 \end{cases} \quad (5\text{-}3)$$

in which ρ is occupant density.

The flow rate between rooms and corridors is then calculated as follows:

$$S_{adj} = S \times F_{mob} \quad (5\text{-}4)$$

$$R_u = \rho \times S_{adj} \quad (5\text{-}5)$$

$$R_w = w \times R_u \quad (5\text{-}6)$$

$$R = R_w \times F_{fam} \times F_{com} \times F_{aff} \times F_{vis} \quad (5\text{-}7)$$

$$T_t = \frac{d}{S_{adj}} \quad (5\text{-}8)$$

in which F_{mob} is the occupant mobility factor, S_{adj} is the adjusted speed, R_u is the unit flow rate, w is width, R_w is the width flow rate, F_{fam} is the occupant familiarity factor, F_{com} is the space complexity factor, F_{aff} is the occupant affiliation factor, F_{vis} is the space visibility factor, R is flow rate, d is distance between two rooms, and T_t is travel time to the next room . In this study, the mobility, familiarity, complexity, affiliation, and visibility factors are set to one, and no metrics are presented or recommended for the calibration of these factors.

Reviewing the literature on the application of system dynamics on evacuation modeling, there seems to be a great potential for further advances. Although the work of Shen [181] is unique in taking into account the aggregated characteristics of the evacuees, it does not explain how different parameters such as walking abilities or mobility needs should be interpreted and used in the model. Considering the wide application of system dynamics in modeling socio-physical processes and to further improve the capabilities of macroscopic hospital evacuation models, an SDM is developed to model the evacuation of patients with

different mobility characteristics. In the following sections, the underlying concepts and key variables in the evacuation process, and the methodology that was taken to develop and evaluate the model are explained.

5.3. The System-Dynamics Model

5.3.1. A Stock-and-Flow Representation of Evacuation

In what follows, the development of an SDM to determine patient flows in hospital evacuations is described. In this model, the mobility characteristics and needs of patients are considered on an aggregate level to estimate the flow of patients between rooms and corridors.

As explained in Chapter 3, there are three main factors that have a major impact on the flow of evacuees in the ABM: (1) agents' behaviors: the path planning algorithm, the collision avoidance algorithm, and the information sharing algorithm; (2) primary agents' attributes: population, free flow walking speed, and size (diameter) of the agents; and (3) characteristics of the space: type of pathways, dimension of rooms and corridors, and width of doors.

In Chapter 3, it was illustrated that how different behavioral algorithms can change the flow of evacuees in the ABM. This implies that if we change the collision avoidance algorithm in the ABM, the behavior of the agents changes, hence we expect a change in the behavior of the SDM. However, all agent-based evacuation models or software packages are developed using specific path planning and collision avoidance algorithms. This implies that the SDM will ideally converge to the specific ABM which is used as the basis. As the objective of this work is to develop an SDM that can produce results which are within the margin of results from the ABM and can capture the specific emerging patterns in the flow of patients from the ABM, the behavioral algorithms and their parameters are not included as variables

in the SDM. In other words, the SDM can be interpreted as the mathematical representation of an agent-based evacuation model that uses the Dijkstra's algorithm for path planning and the Karamouzas' algorithm [183] for collision avoidance.

Although all the agents' parameters affect the flow of agents, these parameters mainly lead to a change in the walking speed or the size of the agents. For example, parameters such as health status, age, or gender affects walking speed. If a patient needs specific equipment such as a wheelchair, this need can be considered as a factor affecting the size and the walking speed of the patient. There is a large body of work dedicated to the mobility characteristics of different groups of evacuees characterized by parameters such age, gender, health status, type of mobility impairment, etc. (e.g. Hurley et al. 2015; Shi et al. 2009) These studies provide a useful basis for reducing all individual-level parameters into 2 key mobility parameters, free flow walking speed and physical size, which in turn can be aggregated to be used in the SDM.

The characteristics of the physical space affect the way evacuees interact with the space which in turn affects the evacuation flow. The most critical aspect of the space that has a major effect on the evacuation is bottlenecks, i.e. doors or entrance and exit gates. Another critical factor is the type of the pathways. Evacuees, specifically those with mobility impairments, interact differently with ramps and stairs. Different types of pathways affect the walking speed of evacuees, but this effect is local, i.e. it does not affect the intrinsic walking capability of the evacuees, rather it only affects evacuees' walking speed on ramps and stairs.

In the context of building evacuation (vertical evacuation), each section of a building (e.g. rooms or corridors) can be considered as a component (stock) of the building system, and the flow of evacuees moving through these components can be expressed as the inflow/outflow between stocks. Figure 5-5 shows a system dynamics representation for the evacuation of a two-room building.

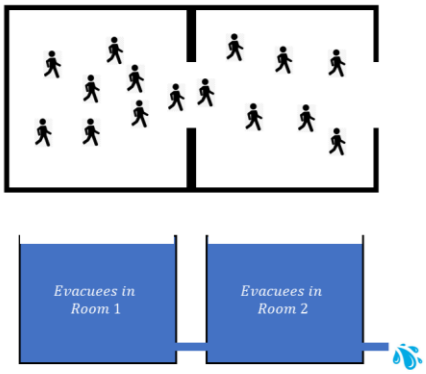

Figure 5-5. A system dynamics representation of building evacuation process

The mathematical representation of the system dynamics model shown in Figure 5-5 for a two-room building is as follows:

$$\frac{dp_1(t)}{dt} = -r_1(t) \tag{5-9}$$

$$\frac{dp_2(t)}{dt} = r_1(t) - r_2(t) \tag{5-10}$$

in which $p_1(t)$ is the number of evacuees in Room 1 at time t, $p_2(t)$ is the number of evacuees in Room 2 at time t, $r_1(t)$ is the outflow from Room 1 at time t, and $r_2(t)$ is the outflow from Room 2 at time t.

The core component of the SDM is the rate function r(t). As explained above, this rate function should consider the key evacuees' parameters (population, free flow walking speed, and physical size) and the main characteristics of the physical space (type of pathway, dimensions of pathway, and width of exit door). Furthermore, this rate function should be derived from the ABM. In other words, the rate function is a reduced model for the underlying behavioral model in the ABM, hence the SDM is a reduced model for the ABM (Figure 5-6). It is important to note that the SDM is not a reduced model of the ABM for a specific building

or evacuation scenario, rather, it can be considered as a macro level substitute for the underlying behavioral model in the ABM which can be used to simulate the evacuation of any building with any evacuee demographics.

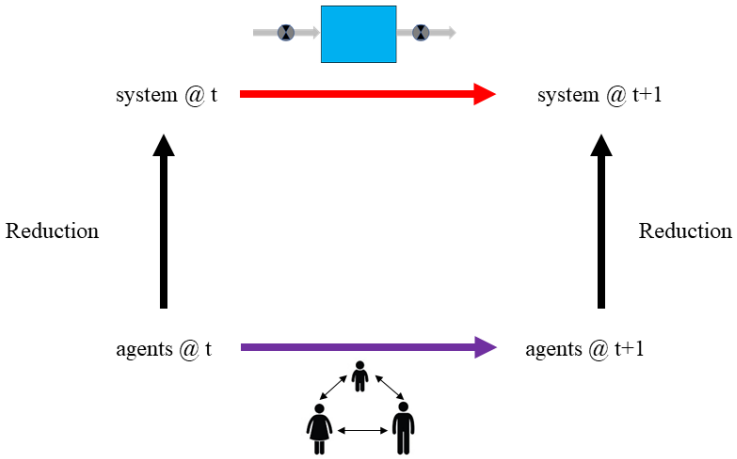

Figure 5-6. Reducing an agent-based model to a system dynamics model

The model reduction approach used in this study is to approximate the micro level decision processes of agents by statistical parameters and regression models. This technique has wide applications in model reduction for ABMs of complex systems and processes [184–186].

5.3.2. Model Reduction

The first step in model reduction is to identify the input and output parameters. The input parameters are the key parameters of the evacuation process explained before, which are: population, free flow walking speed, physical size of evacuees, dimension of rooms/corridors, width of doors, and type of pathways. The output parameter is the exit rate as a function of input parameters. As the population size changes through time, exit rate changes as time passes, as well. Since the SDM is intended to be a macro level substitute for

the underlying behavioral model in the ABM, it should be developed based on the ABM and considering reasonable ranges of the input parameters. For this purpose, the ABM is used to obtain the overall exit rate for each possible combination of input parameters. To account for randomness in the initial position of evacuees, the room evacuation simulation for each combination is repeated 100 times. In each simulation, the agents are randomly scattered in the room with their parameters set to specific values selected from a reasonable range. Figure 5-7 illustrates the general scheme of the model reduction framework for the development of the SDM from the ABM.

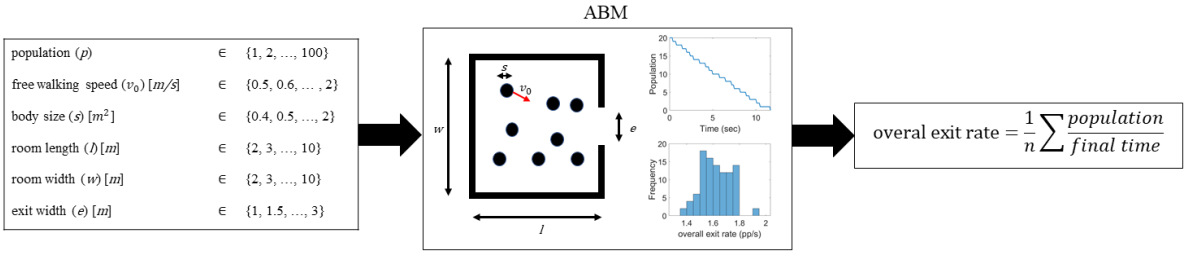

Figure 5-7. Model reduction framework

The next step in model reduction is to find the best mathematical equation that can describe the outputs from the ABM. In other words, we need to find a mathematical formula which best describe how exit rate changes as a function of the key input parameters. Figure 5-8 shows the visualization of the outputs from the ABM. Figure 5-8a shows how exit rate changes as a function of population. As it is clear, exit rate increases as population increases, but it reaches to a saturation condition at specific population sizes. This implies exit rate follows a sigmoid-like function as represented in Equation (5-11).

$$r(p) = \beta \frac{1 - e^{-\alpha p}}{1 + e^{-\alpha p}} \tag{5-11}$$

To better understand these saturation conditions and find the sigmoid function parameters (α and β), we have to study how other key parameters affect the exit rate. Figure 5-8b shows the effect of free flow walking speed of evacuees on overall exit rate for a specific room dimension and body size. As walking speed increases, the initial slope and the saturated exit rate change accordingly. Figure 5-8c and 5-8d show the effect of body size and exit width on exit rate, respectively. It can be seen that these parameters (i.e. speed, size, and exit width) do not affect the form of the function, but the shape of the sigmoid function, i.e. α and β. Figure 5-8e and 5-8f show how room length and room width affect the exit rate, respectively, for a specific room dimension, walking speed, and body size. As one can see, the absolute dimensions of the room do not have a significant effect on the shape of the sigmoid function; however, the effect is not too small to be negligible, especially for low population sizes. This implies that a higher-level parameter of the physical space might be sufficient. Figure 5-8g and 5-8h are similar to Figure 5-8e and 8f except that instead of population, population density is used as the independent variable. By comparing these two sets of figures, we can conclude that population density can reasonably describe the effect of population and room dimensions on exit rate.

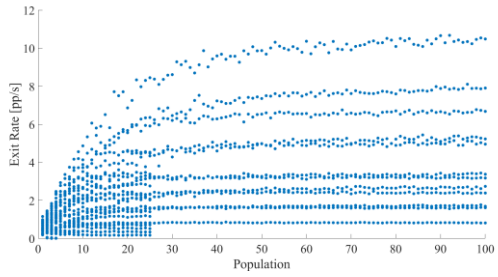

(a) All data

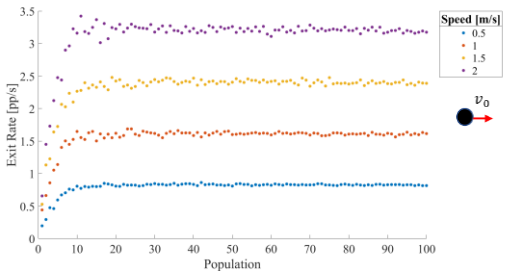

(b) $l = 4\ m, w = 4\ m, e = 1\ m, s = 0.4\ m$

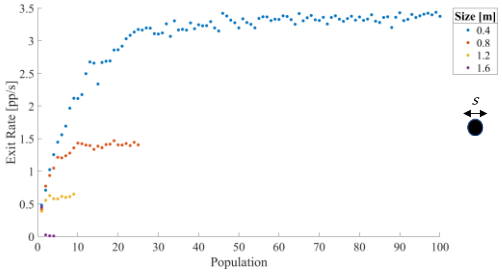

(c) $l = 4\ m, w = 4\ m, e = 2\ m, v = 1\frac{m}{s}$

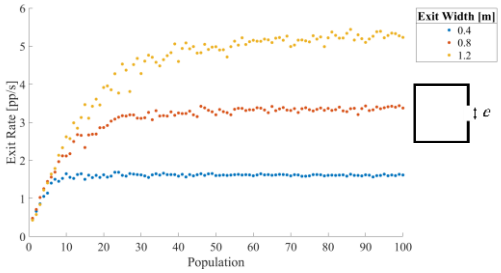

(d) $l = 4\ m, w = 4\ m, s = 0.4\ m, v = 1\frac{m}{s}$

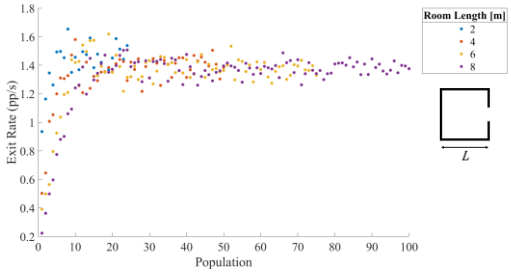

(e) $e = 1\ m, v = 1\frac{m}{s}, s = 0.4\ m$

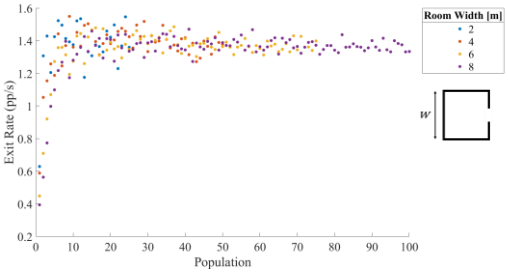

(f) $e = 1\ m, v = 1\frac{m}{s}, s = 0.4\ m$

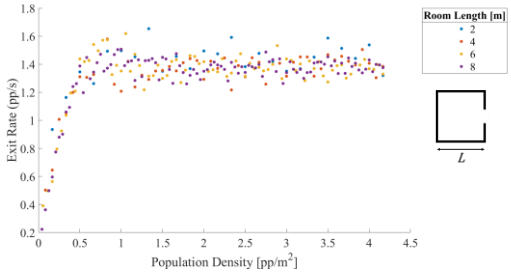

(g) $e = 1\ m, v = 1\frac{m}{s}, s = 0.4\ m$

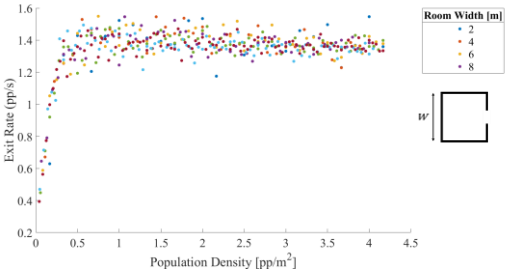

(h) $e = 1\ m, v = 1\frac{m}{s}, s = 0.4\ m$

Figure 5-8. Visualization of outputs from the ABM showing the effect of key parameters on the exit rate: (a) all the data; (b) free flow speed; (c) physical size; (d) exit width; (e) room length and population; (f) room width and population; (g) room length and population density; (h) room width and population density.

Furthermore, we need to consider how the key input parameters affect α and β. It has been shown that many real-world phenomena, such as traffic congestions, stock market crashes, or urban growth, follow power-law distributions, and ABMs have been able to reproduce these patterns from emerging behaviors of agents [185,187–192]. To ensure that the best model is found to describe exit rate, we will try to fit 3 variations of a sigmoid function with linear functions, quadratic functions, and power laws for α and β, as shown in Equations (5-12) to 5-15).

$$r(\rho) = \beta \frac{1 - e^{-\alpha\rho}}{1 + e^{-\alpha\rho}} \tag{5-12}$$

Variation 1: $\alpha = \alpha_0 + \alpha_1 s + \alpha_2 v + \alpha_3 e\,, \qquad \beta = \beta_0 + \beta_1 s + \beta_2 v + \beta_3 e$ (5-13)

Variation 2:
$$\alpha = \alpha_0 + \alpha_1 s^2 + \alpha_2 v^2 + \alpha_3 e^2 + \alpha_4 sv + \alpha_5 se + \alpha_6 ve + \alpha_7 s + \alpha_8 v + \alpha_9 e$$
$$\beta = \beta_0 + \beta_1 s^2 + \beta_2 v^2 + \beta_3 e^2 + \beta_4 sv + \beta_5 se + \beta_6 ve + \beta_7 s + \beta_8 v + \beta_9 e \tag{5-14}$$

Variation 3: $\alpha = \exp(\alpha_0)\, s^{\alpha_1} v^{\alpha_2} e^{\alpha_3}\,, \qquad \beta = \exp(\beta_0)\, s^{\beta_1} v^{\beta_2} e^{\beta_3}$ 5-15)

A common first step in evaluation of a regression model is to calculate R^2 (R-squared). The R^2 values for the sigmoid regression models with linear, quadratic, and power-law functions for α and β are -4.40, 0.96, and 0.99, respectively. The sigmoid-linear model has a negative R^2 value. The sigmoid-quadratic and sigmoid-power models are successful in explaining the variations in exit rate based on variations in the key parameters of the model. In Figure 5-9, a set of examples of how the regression models can estimate exit rate for different population densities are shown. The sigmoid-linear model clearly is not a good candidate. Although in some cases such as one shown in Figure 5-9b, it is successful in estimating the exit rate close to what the ABM produces, in most cases, it fails to do so such that for some cases the sigmoid-linear model gives a negative value for the exit rate.

Considering the R^2 of the sigmoid-quadratic model and the sigmoid-power model, and comparing their outputs with the data from ABM over a wide range of variations in the key parameters (e.g. Figure 5-9c to 5-9f), the later shows the be the best model that can estimate exit rate as a function of population density (ρ), exit width (e), occupants' average physical size (s), and occupants' average free walking speed (v).

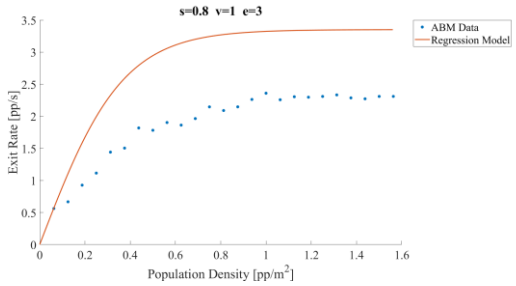

(a) Sigmoid-linear: $e = 3\ m, v = 1\ m/s, s = 0.8\ m$

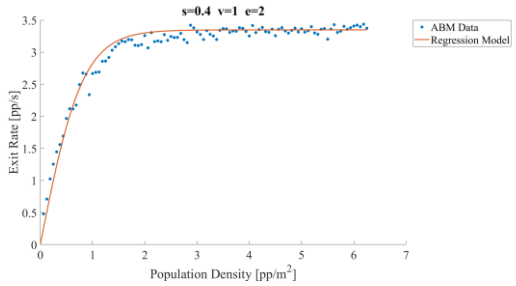

(b) Sigmoid-linear: $e = 2\ m, v = 1\ m/s, s = 0.4\ m$

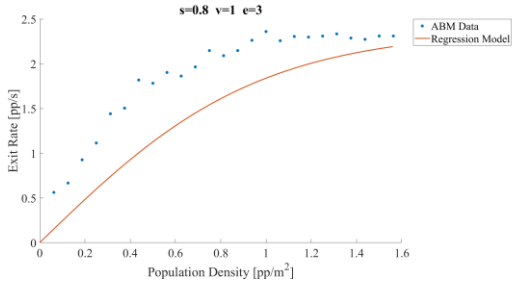

(c) Sigmoid-quadratic: $e = 3\ m, v = 1\ m/s, s = 0.8\ m$

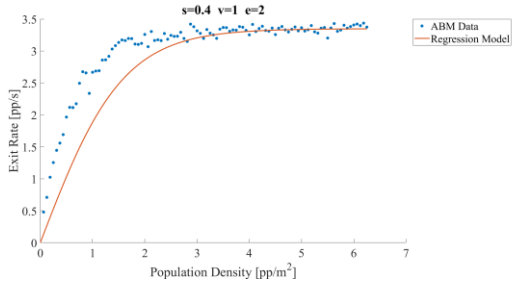

(d) Sigmoid-quadratic: $e = 2\ m, v = 1\ m/s, s = 0.4\ m$

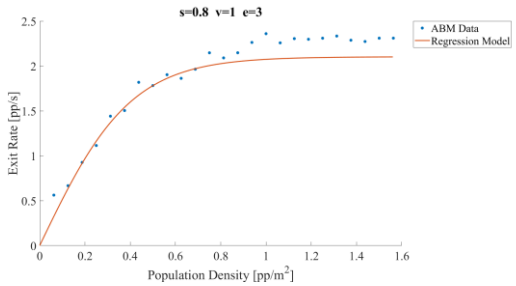

(e) Sigmoid-power: $e = 3\ m, v = 1\ m/s, s = 0.8\ m$

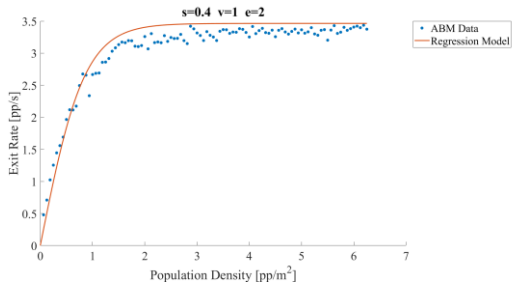

(f) Sigmoid-power: $e = 2\ m, v = 1\ m/s, s = 0.4\ m$

Figure 5-9. Examples of how the regression models can estimate exit rate for different population densities

Equation (5-16) represents the reduced model, based on the sigmoid-power regression variation, for the underlying behavioral model in the ABM, which can be used in the SDM.

$$r(\rho) = \beta \frac{1 - e^{-\alpha\rho}}{1 + e^{-\alpha\rho}} \tag{5-16}$$

$$\alpha = 38.58\, s^{1.94} e^{-1.47}$$

$$\beta = 0.42\, s^{-1.41} v^{0.99} e^{1.18}$$

5.3.3. Further Improvements

As discussed before, reduction or aggregation implies loss of information, and the extent of the loss increases as the model becomes more complex. To better understand the extent of information loss in reducing the agent-based evacuation simulation model to an SDM, we should take a step back and think about evacuation as a dynamical process. Evacuation is a spatio-temporal process, i.e. it evolves in time and space through space-time dependencies. In general, understanding and modeling complex and non-deterministic spatio-temporal dynamics is challenging. One of the common modeling techniques for these types of processes is to derive partial differential equations (PDEs) that can describe the behavior of the observed phenomena (as discussed in Chapter 4). However, as SDMs are based on ODEs, the spatial component of the processes is lost. This implies the distribution of evacuees over the evacuation area, which is a critical factor in how the evacuation process evolves, is not considered in the SDM. To better understand the effect of spatial distribution of evacuees on the evacuation rate, let's consider a simple example illustrated in Figure 5-10. Consider a 4-m by 4-m room with 5 occupants and a 1-m wide door. All the occupants have a diameter of 0.5 m and a free walking speed of 1 m/s.

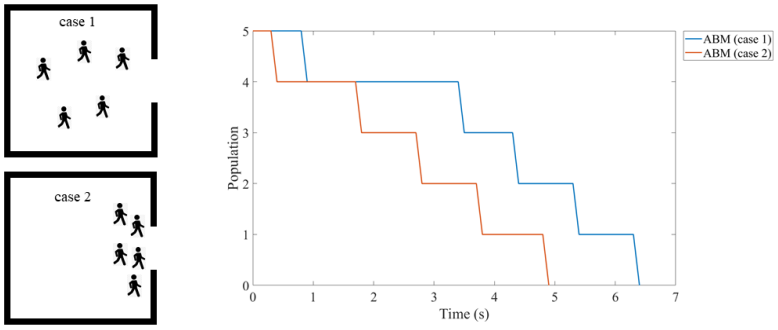

Figure 5-10. Effect of spatial distribution of evacuees on the evacuation rate

As it is clear from Figure 5-10, the distribution of evacuees affects the evacuation rate, specifically for low population densities.

As discussed above, evacuation is a spatio-temporal process. The distribution of evacuees is constantly changing as the evacuation continues; however, the spatial information of evacuees is not considered in the SDM. This implies the need to include an aggregate measure of evacuees' distribution as a variable in the SDM. This variable can be the average distance of evacuees from the exit door. It can also be interpreted as the equivalent mass center of the occupants (Figure 5-11).

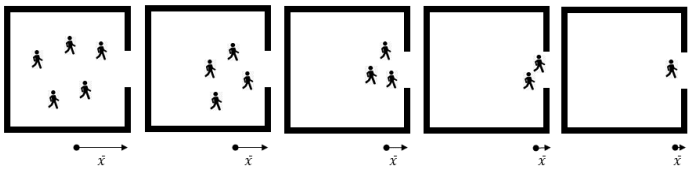

Figure 5-11. Average distance of evacuees from the exit door

The model reduction method described in Section 5.3.1 is repeated with the x variable added as another key input parameter into the model. x is obtained by normalizing the average

distance of agents from the exit door in the ABM to the length of the room (i.e. $x \in [0,1]$). Equation (5-17) represents the improved exit rate formula to be used in the SDM.

$$r(\rho) = \beta \frac{1 - e^{-\alpha\rho}}{1 + e^{-\alpha\rho}} \tag{5-17}$$

$$\alpha = 125.64\, s^{2.62} e^{-2.33} x^{-0.68}$$

$$\beta = 0.31\, s^{-1.47} v^{0.99} e^{1.16} x^{-0.11}$$

Introducing the mass center parameter into the model implies that the flow of patients from one room to a second room will go through a delay period to consider the distance from entering door to the mass center of occupants in the second room. This delay variable is illustrated schematically in Figure 5-12. During this delay period the new groups of evacuees will be in transit to join the current evacuees in the room.

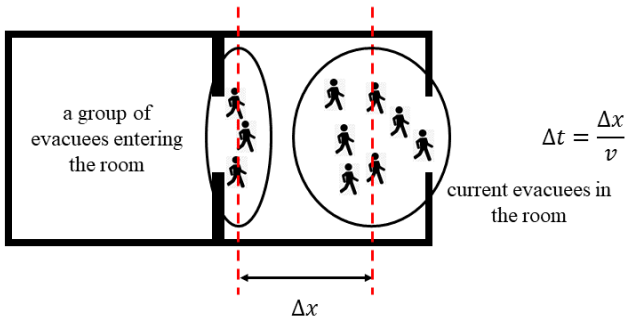

Figure 5-12. The delay variable to consider when a new group of evacuees enter a room

The delay variable should be calculated at each time step for the volume of evacuees entering the second room as follows:

$$\Delta t^i = \frac{1 - x_2^i}{v_2^i} \tag{5-18}$$

$$v_2^i = v_2^{free} e^{-7.5\left(\frac{\rho_2^i}{\rho_{max}}\right)^2} \tag{5-19}$$

$$\rho_2^i = \frac{p_2^i + p_2^{t,i}}{A_2} \tag{5-20}$$

in which Δt^i is the delay time for the evacuees that entered the second room at time i, x_2^i is the mass center of occupants in the second room at time i, v_2^i is the current flow speed of occupants in the second room at time i calculated using Equation (5-19), v_2^{free} is the free walking speed of occupants in the second room, ρ_2^i is the population density in the second room at time i calculated by Equation (5-20), ρ_{max} is the maximum possible population density, p_2^i is the number of evacuees in the second room at time i, $p_2^{t,i}$ is the number of evacuees in the transition phase in the second room at time i, and A_2 is the floor area of the second room.

To better evaluate the effect of adding the x variable to the model, the outputs of the primary model (SDM) and the improved model (SDM++) are compared with those from the ABM for the two cases shown in Figure 5-10.

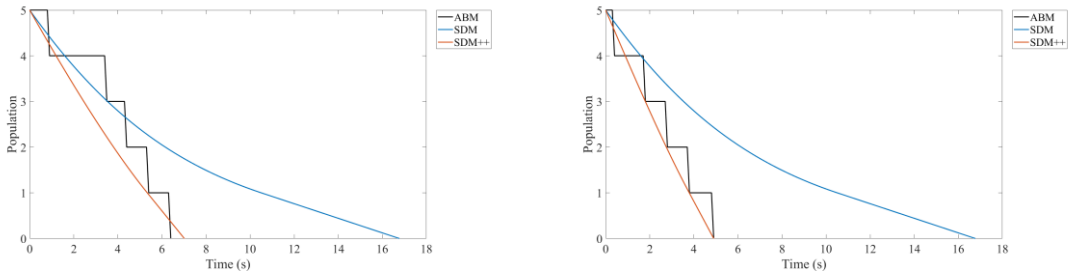

Figure 5-13. Improvement in the SDM by including an aggregate measure of evacuees' spatial distribution. Left: case 1; Right: case 2.

As it is shown in Figure 5-13, the primary SDM cannot explain the effect of the distribution of evacuees on the evacuation process, while the improved model (SDM++) does.

5.3.4. Residual Analysis

For each independent variable x_i, the residual is the difference between the actual dependent variable y_i and the predicted value using the regression model $\hat{y}_i$:

$$r_i = y_i - \hat{y}_i \tag{5-21}$$

It is common to use standardized residuals in analyses. The standardized residual is defined as the residual divided by its standard deviation. Residuals are used in regression analyses to evaluate the validity of the model assumptions, verify homoscedasticity, normality, and independence of errors, and presence of outliers. The residual plot for estimated exit rates is shown in Figure 5-14. In this figure, the red dashed lines denote the $\pm 3\sigma$ (plus or minus 3 standard deviation). From all the data points, 97% lies within the $\pm 3\sigma$ margin, which implies that 3% of the exit rates estimated by the regression model are significantly lower or higher than those obtained from the ABM. Moreover, it is clear that for low exit rates, the regression model underestimates the values, but for higher exit rates, it mostly overestimates the exit rates when compared with the data from the ABM. This implies the heteroscedasticity of the variances in the regression model. The regression model fails the Bartlett's and Levene homoscedasticity tests with p-values of 0.000 for a significance level of 0.05.

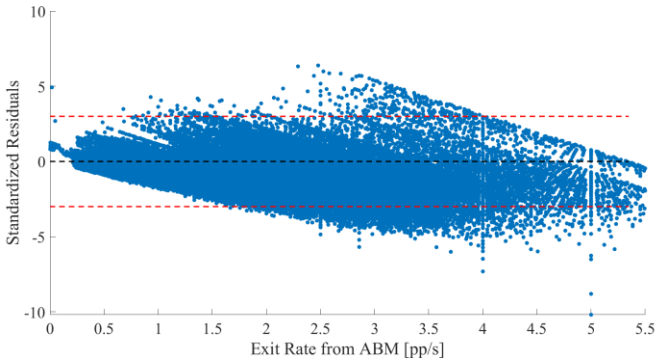

Figure 5-14. standardized residual plot

To further analyze the residuals of the regression model, the histogram of standardized residuals and the normal probability plot are shown in Figure 5-15.

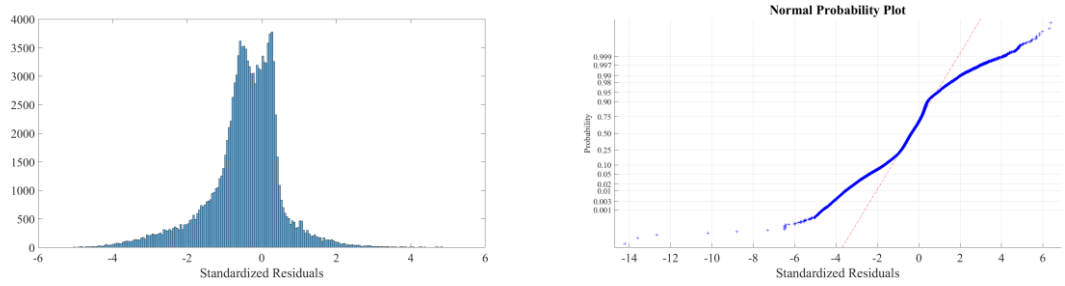

Figure 5-15. Left: histogram of standardized residuals. Right: normal probability plot

From Figure 5-15, the residuals are not normally distributed, which is also implied by the rejection of the Lilliefors test with a p-value of 0.000 at the 5% significance level. Furthermore, the S shaped curve of the normal probability plot indicates that the tails of the distribution are shorter than the tails of a normal distribution.

The non-normality and heteroscedasticity of the residuals imply that there are other parameters that affect the exit rate which are not included in the regression model. This is expected, as explained before in Chapters 1, 3, and earlier in this chapter, evacuation is a

complex spatio-temporal process which is controlled by many individual-related and space-related factors. However, it is helpful to understand the residuals of the regression model and identify conditions under which the regression model (i.e. the SDM++) will specifically overestimate or underestimate exit rates. Further investigations of the residuals are shown in Figure 5-16. The heteroscedasticity of the variances is clear when residuals are visualized by the parameters of the model. Figure 5-16a and b show that the SDM++ underestimates exit rates for rooms with wider exit doors, specifically when evacuees are very close to the door and are small in population. Figure 5-16c and d show that the underestimation of exit rates is more significant for evacuees with smaller body size. Figure 5-16e verifies the interpretation drawn from Figure 5-16a and b about the underestimation of exit rates for the cases with small populations who are close to the exit door. Therefore, we can summaries the residual analysis for the SDM++ as follows:

- In general, the exit rates estimated by the SDM++ show more discrepancies with those of the ABM as the width of exit door gets wider, size of the evacuees gets smaller, and the evacuees get closer to the exit door.
- In general, the SDM++ tends to underestimate the exit rate.
- To compare with the ABM, the SDM++ significantly underestimates exit rates for cases with less than 5 evacuees (low population densities) who are within the 10% distance (with respect to the length of the room) from the exit door, the size of an average person (size < 0.5 m), and evacuating through a 2-m or wider door.
- To compare with the ABM, the SDM++ significantly overestimates exit rates for cases with wide exit doors (3 m), with evacuees of an average person who are within the 10-20% distance (with respect to the length of the room) from the exit door. The number of evacuees has an adverse effect on the overestimation of the exit rate.

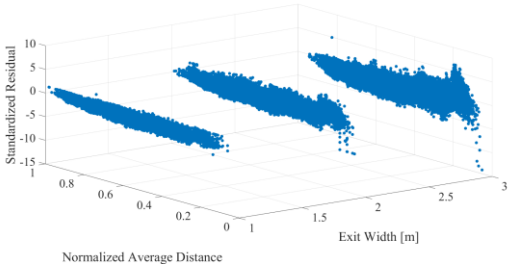

(a) $e \in \{1, 2, 3\}\ m$

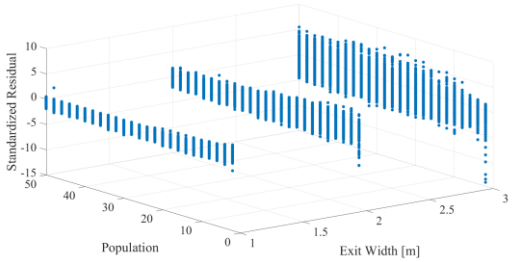

(b) $e \in \{1, 2, 3\}\ m$

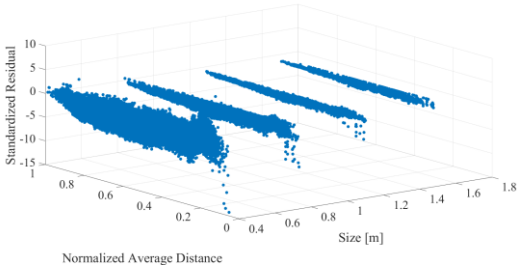

(c) $s \in \{0.4, 0.8, 1.2, 1.6\}\ m$

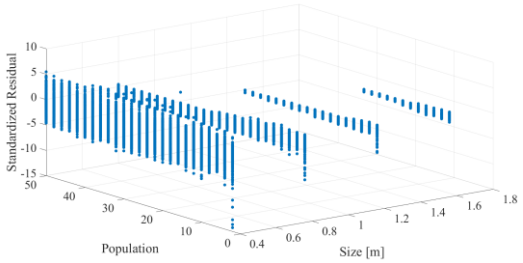

(d) $s \in \{0.4, 0.8, 1.2, 1.6\}\ m$

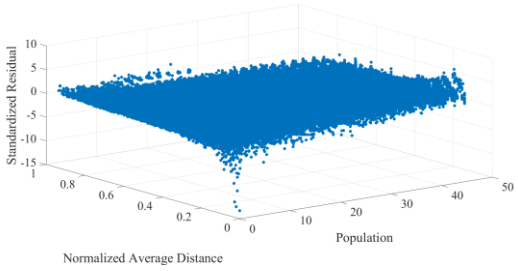

(e) $p \in \{1{:}\,50\}$

Figure 5-16. Multivariable standardized residual plots

5.4. SDM vs. ABM on Benchmark Test Cases

In this section, we will evaluate if the system dynamics model can produce exit dynamics close to what the ABM predicts. Similar to Chapter 4, we will compare the outputs of the SDM developed in this study (denoting the primary model SDM and the improved one

SDM++) with the SD model developed by Shen [181] and the ABM based on which the SDM and SDM++ is developed.

5.4.1. Single Room Test Case

In Chapter 3, we discussed about the single room test case and what the outputs from the ABM implies. To remind readers, the room setup is shown again in Figure 5-17: a rectangular 4-m by 8-m room with a 1-m wide door, 20 occupants with size (body diameter) of 0.5m and free walking speed of 1.25 m/s.

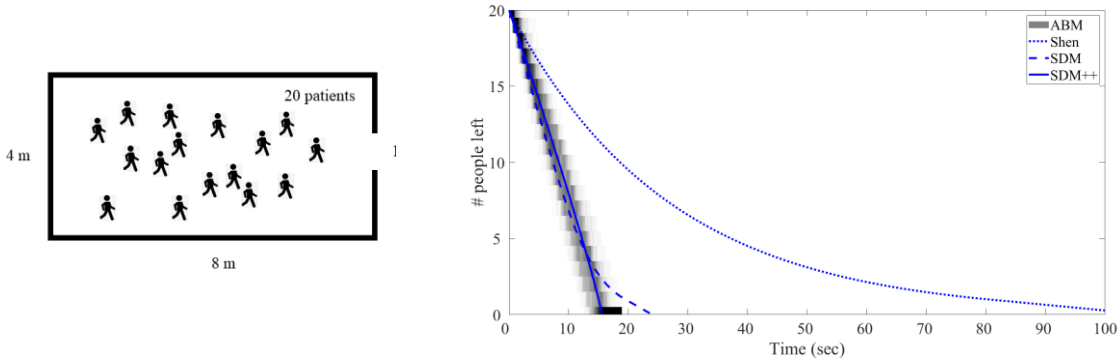

Figure 5-17. Single room test case. Left: room setup; right: results of the SDM and the ABM.

As discussed before in Chapter 3, the ABM predicts a final evacuation time ranging from 12 seconds to 18 seconds, over 100 simulation, with a linear dominant exit pattern resulting in an average final evacuation time of 15.3 s. The SDM and SDM++ are successful in converging to the dominant behavior from the ABM resulting a final evacuation time of 23.6 seconds and 23.6 seconds, respectively. The SDM predicts a drop in the exit rate for the last few evacuees which is not in accordance with the ABM. The results imply that for simple cases with a homogeneous population where the crowd dynamics is limited to one room and one exit door, the SDM++ is a valid substitute as a reduced model for the ABM. However, the results from Shen's model show that the model fails to estimate exit rates ($T = 104.7\ s$)

and overestimates final evacuation time by a factor of 6.8 with respect to the average of the ABM, and the resulted exponentially decreasing exit rate does not agree with the linear pattern from the ABM. The results at the specified percentile measures for the three models are compared in Table 5-1, which shows the better performance of the SDM++ over the SDM and Shen's model.

Table 5-1. Evacuation time at specific percentile measures for the single room test case

Percentile	ABM_{avg} [s]	Shen		SDM		SDM++	
		Time [s]	Relative Difference	Time [s]	Relative Difference	Time [s]	Relative Difference
25%	4.0	7.7	93%	3.6	-10%	4.3	8%
50%	7.9	18.6	135%	7.4	-6%	8.4	6%
75%	11.6	37.2	221%	11.8	2%	12.2	5%
90%	13.9	61.8	345%	16.3	17%	14.4	4%
100%	15.3	104.7	584%	23.6	54%	15.6	2%

5.4.2. Two-Room Test Case

The two-room test case is shown again in Figure 5-18: a rectangular 4-m by 6-m back room (Room 1) with a 1.5-m wide door, 40 occupants from which 30 has mobility impairment, and a 6-m by 6-m front room (Room 2) with a 1.5-m wide door, 20 occupants from which 5 has mobility impairment. The body size of all the occupants is 0.5 m, and the free walking speed for non-disabled and mobility impaired occupants is 1.25 and 0.5 m/s, respectively.

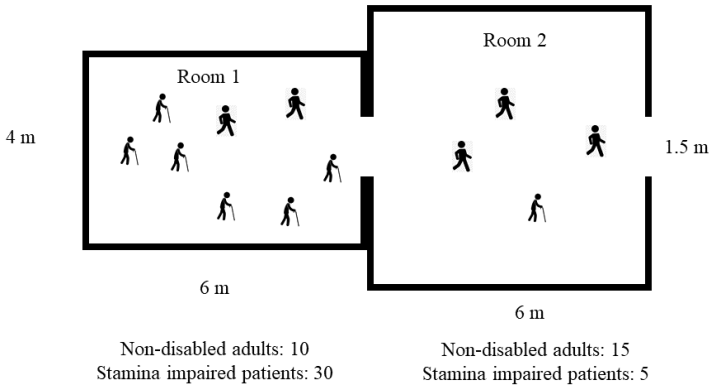

Figure 5-18. The two-room test case

The results of the evacuation of the two-room test case modeled with the ABM, SDM, SDM++, and Shen's model are shown in Figure 5-19 and Figure 5-20. According to the ABM, Room 1 has a simple linear evacuation which is captured by the SDM++, in which total evacuation time is estimated to be 30.5 s to compare with the average of the ABM which is 31.4 s. The SDM, as highlighted before, underestimates the exit rate at low population sizes ($T = 44.6\ s$). Shen's model, as in the case of the single-room case, shows an exponential change in the exit rate, overestimates the exit rate in the first 10 seconds, and gives very low exit rates afterwards which leads to overestimating the total time ($T = 61.4\ s$). Looking at Room 2, the SDM++ can capture the evacuation pattern resulted from the ABM and gives an estimate for the final evacuation time ($T = 42.0\ s$) which corresponds to the average of the results from the ABM ($T = 41.9\ s$). Regarding SDM, as for the most part it overestimates the exit rate from Room 1, and since it does not have the delay parameter and underestimates exit rate for low populations, the number of evacuees in Room 2 is overestimated over the entire time. Shen's model fails to either give an acceptable estimate for the final evacuation time or capture the evacuation dynamics.

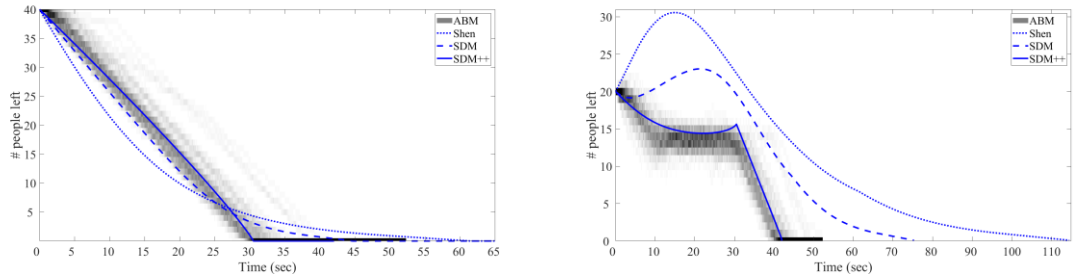

Figure 5-19. Results of the SDM and the ABM for the two-room test case: Left: Room 1; Right: Room 2.

The linear evacuation pattern of the two-room test case obtained from SDM++ lies within the ABM margin and deviates from the average of the ABM by less than 3%.; however, the SDM and the Shel's model produced nonlinear curves with overestimated total evacuation times of 75.3 and 114.5 seconds, respectively.

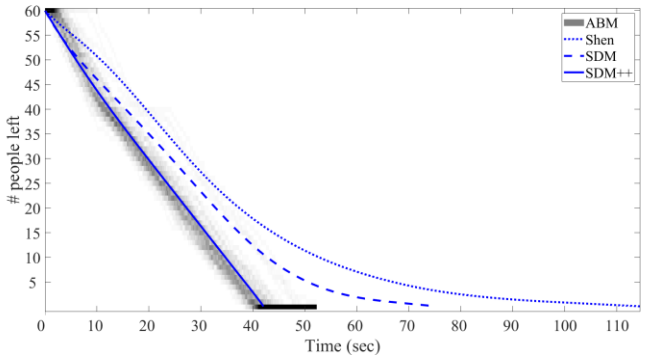

Figure 5-20. Results of the SDM and the ABM for total evacuation of the two-room test case

The results at the specified percentile measures for the three models are compared in Table 5-2, which shows the better performance of the SDM++ over the SDM and Shen's model.

Table 5-2. Evacuation time at specific percentile measures for the two-room test case

Percentile	ABM_{avg} [s]	Shen		SDM		SDM++	
		Time [s]	Relative Difference	Time [s]	Relative Difference	Time [s]	Relative Difference
25%	9.0	15.3	70%	11.0	22%	9.2	2%
50%	19.3	27.6	43%	24.3	26%	19.8	3%
75%	30.1	43.9	46%	37.4	24%	31.0	3%
90%	36.8	63.4	72%	48.7	32%	37.7	2%
100%	41.9	114.5	173%	75.3	80%	42.0	0%

5.4.3. Two-Room-Corridor Test Case

The two-room-corridor test case is shown again in Figure 4-13: two 4-m by 4-m rooms, each with a 1.2-m wide door, with 5 wheelchair users in Room 1 and 10 visitors in Room 2, where both rooms open to a 14-m by 3-m corridor with a 1.2-m wide exit door. The body size of wheelchair users is 0.8 m and their free moving speed is 0.69 m/s. For visitors, body size is 0.5 m and free walking speed is 1.4 m /s.

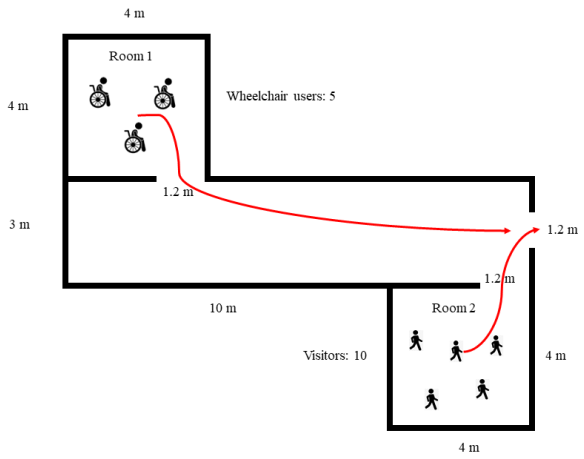

Figure 5-21. The two-room-corridor test case

The results of the evacuation of the two-room test case modeled with the ABM, SDM, SDM++, and Shen's model are shown in Figure 5-22 and Figure 5-23. According to the ABM, Room 1 has a simple linear evacuation which is perfectly captured by the SDM++, in which total evacuation time is estimated to be 12.9 seconds to compare with the average of the ABM which is 13.3 seconds. The SDM, as highlighted before, underestimates the exit rate at low population sizes (T = 14.5 s). Shen's model, as in the case of the single-room and two-room cases, shows an exponential change in the exit rate, underestimates the exit rates after 5 seconds leading to overestimating the total time (T = 29.3 s).Looking at results for Room 2, the ABM and SDM++ give linear exit patterns but with different evacuation times of 10.5 and 6.6 seconds, respectively. The SDM produces a piecewise linear exit pattern with lower rates for the last 3 evacuees, resulting in an evacuation time of 9.9 seconds. As in other cases, Shen's model gives exponentially decreasing exit rates resulting in a heavily overestimated evacuation time of 37.0 seconds. The specific evacuation pattern obtained by the ABM for the corridor is best captured by the SDM++ with a final evacuation time of 29.0 seconds. The evacuation pattern resulted from the SDM is similar to the ABM in shape but not in values. The SDM significantly underestimates the exit rates from the corridor.

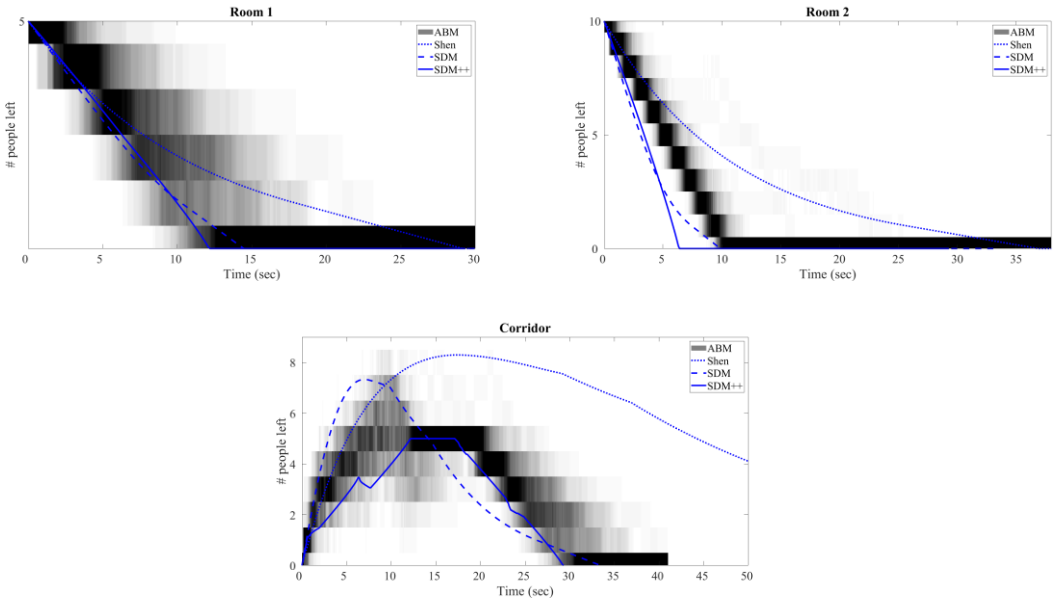

Figure 5-22. Results of the SDM and ABM for the two-room-corridor test case

The piecewise linear evacuation pattern of the two-room-corridor test case obtained from the ABM is captured almost perfectly by the SDM++, however, the SDM and the Shen's model do not reproduce the delay in the arrival of the evacuees.

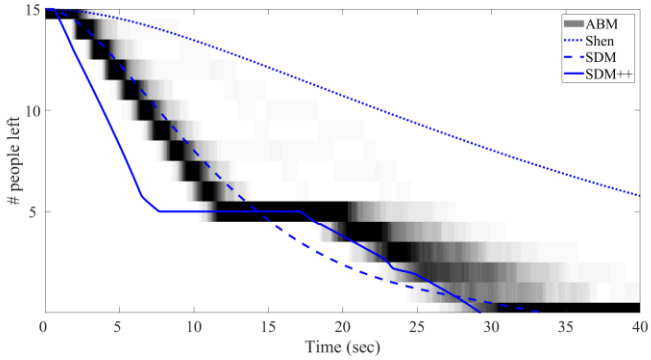

Figure 5-23. Results of SDM++, SDM, Shen's model, and ABM for total evacuation of the two-room-corridor test case

The results at the specified percentile measures for the three models are compared in Table 5-3. The SDM provides better results for the first part of the evacuation which

corresponds to Room 2, when compared to SDM++, however, the SDM fails to reproduce the delay in the arrival of the evacuees, while the SDM++ reproduces the delay and the linear exit of Room 1's evacuees.

Table 5-3. Evacuation time at specific percentile measures for the two-room-corridor test case

Percentile	ABM_{avg} [s]	Shen		SDM		SDM++	
		Time [s]	Relative Difference	Time [s]	Relative Difference	Time [s]	Relative Difference
25%	5.7	18.1	218%	6.2	9%	3.1	-46%
50%	8.8	32.2	266%	10.7	22%	5.5	-38%
75%	20.8	52.7	153%	16.6	-20%	20.1	-3%
90%	26.5	79.6	200%	23.3	-12%	25.9	-2%
100%	31.3	120.6	285%	33.4	7%	29.3	-6%

5.5. Discussion

System dynamics has seen significant applications in engineering and social sciences, helping researchers and decision-makers break down and understand complex socio-physical systems and processes. One drawback of SDMs is their deficiency in providing micro-level results. This can be a significant limitation when studying complex systems with heterogeneous components. In the context of evacuation, emergency planners can use SD models to evaluate evacuation plans under different emergency scenarios; however, in case of hospital evacuation where there are different types of patients with diverse mobility characteristics and need, the aggregate results of SDMs cannot provide emergency planners with required insight about the evacuation process.

The SDM developed in this study has addressed the limitation of SD models mentioned above by considering mobility characteristics of the evacuees and the physical environment. Compared with the current SD models (Shell's model) from the literature, the SDM shows a major improvement by incorporating the average speed and average size of the evacuees into the estimation of the exit rates. However, the SDM does not give exit rates which are close to what the ABM does, although the SDM is developed by reducing the ABM. As discussed in Section 5.3.3, this is due to loss of spatial information when reducing the micro-level data of the ABM to the macro-level aggregate data of the SDM. This shows the complexity of spatio-temporal processes such as evacuation in which the state of the process (or the system) changes over space and time. Interestingly, considering a spatial parameter of the crowd, the average distance of evacuees in a room from the exit door, can significantly improve the behavior of the SDM such that the SDM++ converges to the average behavior of the ABM. For simple cases with a homogeneous population such as the single-test case, the results of the SDM++ are within a 10% margin from the average ABM, and the times for the final 10% of the evacuation are only overestimated by less than 4%, while the SDM significantly overestimates the final evacuation time by 54%.

Although the SDM++ is relatively successful in reproducing the average behavior of the ABM, it fails to show the variabilities and uncertainties in the evacuation process of patients with different mobility characteristics.

5.6. Conclusions

When it comes to modeling of complex systems, the first question which needs to be addressed is whether we want a complex model that can describe the underlying mechanics of the system and predict emergent behaviors, or a simple model that is easy to understand,

implement, and use for decision making. In other words, we need to consider the tradeoff between simplicity/efficiency and complexity/capability. From a science perspective, it is interesting to decompose a complex system into its elements, study the interactions between the elements, and develop a model that can predict how the system behaves under different circumstances. Microscopic modeling is a common approach for this purpose, but these models are difficult to formulate, expensive to develop, and need a lot of data for validation of each component of the model. From a practical perspective, decision makers tend toward simple models such as system dynamic models (SDMs). These models are less challenging to formulate, easier to develop, and need aggregate level data, but they are potentially not as capable of microscopic models in giving an accurate explanation of the dynamics of the system under scrutiny. This gap between macro and micro models should be approached from two perspectives. From the science perspective, we need to improve macro models so that they can provide a better explanation of complex systems while their simplicity is not compromised. From a practical perspective, we, as modelers, need to provide decision makers with guidelines and information on why modeling and simulation can be useful and how they can use models to make more informed decisions or devise more effective interventions.

In this study, we tried to tighten the gap between the capabilities of macro and micro models for hospital evacuation simulation from a science perspective as mentioned above. A methodology is introduced to reduce a complex agent-based evacuation simulation models (ABM) to an SDM. For doing so, key parameters of the ABM are identified. Hundreds of thousands of simulations are conducted with the ABM to collect data on how exit rate changes as the key parameters vary. Subsequently, the data are aggregated, and an equation is obtained using regression analysis, which best describes the data. In the SDM, each component of the hospital (e.g. rooms, corridors, or staircases) is modeled as a stock. The exit rate equation

estimates the flow of patients between stocks based on the average body size, the average free walking speed, the average distance of patients from the exit door, dimensions of the room/corridor/staircase, and number of patients, at each time step. To evaluate the SDM, the evacuation process for 3 simple test cases with one, two, and three rooms and two types of patients is modeled. The results show that the SDM is capable of capturing the dominant evacuation behavior resulted from the ABM, hence it is a competent substitute for the ABM as a reduced macro model.

The SDM developed in this study can be used by hospital emergency planners and responders as a simple and easy-to-use evacuation simulation app. As discussed before, to support decision makers, it is important to provide information on the differences between the ABM and the SDM in terms of input and output parameters and the interpretation of the outputs. In the next chapter, we will simulate the evacuation of the emergency department of the Johns Hopkins Hospital using the agent-based model, the fluid dynamics model, and the system dynamics model developed in this study to provide a better understanding of the features and quirks of these models and how they can be useful for hospital decision makers. Furthermore, there is much left to improve on macroscopic, especially system dynamics, hospital evacuation simulation and modeling. Patient mobility and patient transfer is a complex subject with a lot of parameters to consider, specifically when considering ICU patients — an important group of patients that are excluded in this study.

Chapter 6

Multi-Scale Hospital Evacuation Simulation Tools to Support Decision Making

6.1. Simulation and Decision Making

In disaster studies, simulation is widely used to explore how natural hazards might evolve in the future, and how societies might respond to these events. In many disasters, evacuation of buildings or urban areas is an important step towards ensuring public safety. Public and healthcare officials should decide whether to evacuate patients or shelter in place. Evacuation is costly, disruptive, and risky for fragile patients, and on the other hand, sheltering in place may expose patients and hospital staff to major safety risks as the event (e.g. a hurricane) intensifies. To make this complicated decision and perform an efficient evacuation (mass or single facility evacuation), emergency teams and decision makers need to evaluate current policies and available resources. To evaluate the efficiency of emergency policies and plans, emergency teams need training and drills, however, training and drill programs can be costly and disruptive.

A mass evacuation drill requires the cooperation and coordination of the residents, police, firefighters, and all involved parties for a significant time. It may disrupt the daily routine of the commercial sector and be a financial burden on the public and private sector. Hospital evacuation drills are also costly and disruptive [63–65]. They interrupt the complex healthcare schedules and requires the participation of the core personnel of the hospital. Due

to the limitations of evacuation drills, they cannot be conducted frequently to simulate different emergency scenarios. Other limitations of hospital evacuation drills are short shelf life, lack of design focus, danger, and poor reliability [65]. This is where modeling and simulation come to support emergency planning. Evacuation simulation is a helpful tool that can support emergency planers and decision makers by providing an estimation of intermediate and final evacuation times. Emergency planners and decision makers use these estimations to develop emergency plans or evaluate the efficiency of current plans in terms of available resources and level of utilization. These tools can be used to run what-if scenarios to further evaluate the response performance under different likely or unlikely conditions.

As described in this dissertation, evacuation simulation can be classified into three families of macroscopic, mesoscopic, and microscopic models. Macroscopic models, such as system dynamics models, consider a macro-scale model of homogenous population stocks with a time-dependent exit rate, mesoscopic models, such as fluid dynamics models, consider population as a whole by a meso-scale model of homogenous population densities propagating in time and space, while microscopic models, such as agent-based models, consider a micro-scale model of heterogenous evacuees making decisions and moving toward the safe zones. Each of these modeling approaches has specific advantages and disadvantages which have been discussed in Chapters 3 to 5 based on a few simple test cases. In general, macroscopic and mesoscopic models fail to incorporate social behaviors of individuals in decision-making processes while microscopic models possess the advantage of having the capability of implementing unique behaviors and interactions of heterogeneous individuals by which diverse and unexpected macroscopic responses can be observed, but they are difficult to implement due to complexities in defining exhaustive rules for human behaviors and decision-making processes and required individual level data.

In this chapter, to demonstrate the applicability of the evacuation models developed in Chapters 3, 4, and 5, the evacuation of the Emergency Department of the Johns Hopkins Hospital (JHH) is simulated. The agent-based, fluid dynamics, and system dynamics models are evaluated and compared in terms of modeling complexity, required input data, provided output data, and performance.

6.2. Application: Emergency Department, Johns Hopkins Hospital

The Johns Hopkins Hospital, located in Baltimore, Maryland, was founded in 1873 (and opened in 1889) by the Baltimorean businessman, Johns Hopkins, who left his fortune of $7 million (equivalent to about $150 million in 2020) to establish the hospital and the university. Today, the Johns Hopkins health system (comprised of more than a dozen sister hospitals across Maryland) is an $8.5 billion integrated global health enterprise and one of the leading health care systems in the United States. The Johns Hopkins Hospital, a 1000-bed (1162 beds) academic Level 1 trauma institution, is ranked third in the nation for patients of all ages based on U.S. News and World Report's 2019–20 rankings. The facility includes separate emergency departments for children and adults which see more than 100,000 patients annually. The adult emergency department (ED) consists of a total of 72 private examination rooms for patients and their families (see Figure 6-1): 25 in the main ED unit, 8 in the psychiatry unit, 6 trauma care rooms, a 17-room emergency acute care unit (EACU), and 16 in the rapid assessment process (RAP) unit. The adult ED also is equipped with an on-site diagnostic radiology suite with computed tomography scan, ultrasound, and MRI capabilities.

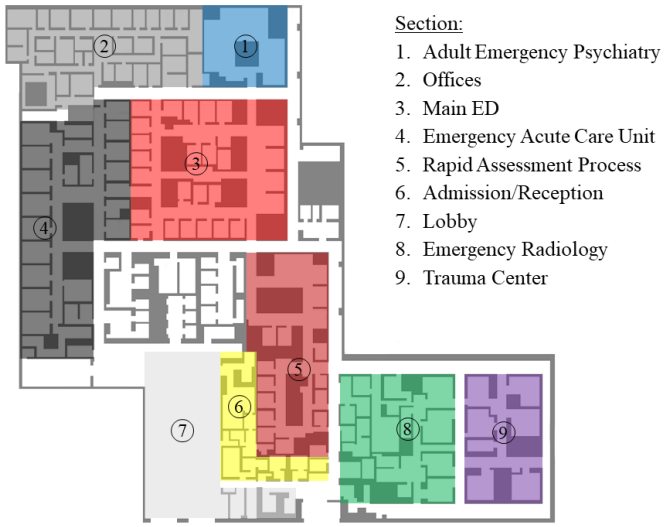

Figure 6-1. Adult emergency department floor plan

6.2.1. Evacuation Scenarios

To develop a scenario for the simulation of emergency department evacuation, two main variables are considered: number of patients in each section of the ED and the nurse-to-patient ratio. The number of patients at any time a day can be estimated from the patient service area (PSA) utilization data. For the Johns Hopkins Hospital, the PSA utilization rate for an average day is shown in Figure 6-2. In addition, the nurse-to-patient ratio is 1:4 or 1:5, depending on the area assigned to the nurse.

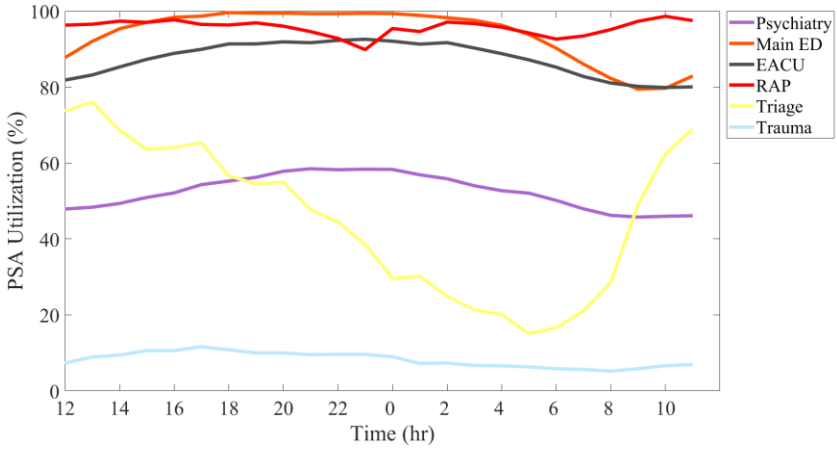

Figure 6-2. PSA utilization for different sections of the ED

To better demonstrate the ability of the models in simulating the evacuation process, a midnight scenario is considered where according to the PSA utilization, most of the sections of the ED are occupied at their highest volume during an average day, with two different nurse-to-patient ratios to evaluate the effect of nursing team on the speed of evacuation. In scenario A, an average ratio of 1:5 is considered for all the units. In Scenario B, the proposed ratios by the National Nurses United Organization (https://www.nationalnursesunited.org/ratios) is used: 1:4 for psychiatric, 1:3 for ED, RAP, and triage, 1:2 for EACU, and 1:1 for the trauma unit. It is noteworthy to mention that currently California is the only state that has legally established required minimum nurse-to-patient ratios to be maintained at all times by unit [193]. The details of the scenarios are listed in Table 6-1.

Table 6-1. ED evacuation scenarios

Scenario		Psychiatry	Main ED	EACU	RAP	Triage	Trauma	Total
A	Patients	5	25	16	15	18	1	80
	Nurses	2	5	4	4	3	2	20
B	Patients	5	25	16	15	18	1	80
	Nurses	2	9	9	6	5	6	37

The class of patients in each unit of ED is randomly selected as follows according to the patients classification system developed in Chapter 3: psychiatric patients consist of mentally impaired and non-disabled; main ED patients consist of wheelchair users, stamina impaired, bed bound, and non-disabled; EACU patients consist of wheelchair users and bed bound; RAP patients consist of wheelchair users, stamina impaired, bed bound, and non-disabled; triage patients consist of wheelchair users, stamina impaired, and non-disabled; and trauma patients consist of only bed bound patients. Those bed bound patients in the EACU and the trauma unit need two nurses for preparation and evacuation. Other bed bound patients and wheelchair users need one nurse.

The pre-evacuation time is an important factor in evacuation simulation. It denotes the time it takes for the patients and staff to start to evacuate after the alarm is raised. This delay is mainly due to two factors: event perception and patient preparation. There have been a few studies on the reaction time and preparation time during hospital evacuations for patients with different mobility needs [65,194–197]. Table 6-2 lists the pre-evacuation time ranges for different classes of patients and the nurses. The preparation times for bed bound patients and wheelchair users include the time it takes to bring the equipment and prepare the patients to start moving.

Table 6-2. Pre-evacuation time

Evacuee Type	Pre-evacuation time range [sec]
Staff	16 – 45
Ambulatory patients	30 – 63
Wheelchair users and Bed bound patients in main ED, RAP, and triage	30 – 100
Bed bound patients in EACU and trauma unit	180 – 900

6.2.2. Modeling

The main components of the ABM, PW++, and SDM++ are described completely in prior chapters. Here, the specific details for modeling the ED of the Johns Hopkins Hospital are presented.

6.2.2.1. ABM

The agent-based model is developed in NetLogo, a multi-agent programmable modeling environment developed by Uri Wilensky in 1999 [81]. It can easily read GIS shapefiles and convert them to patches, which makes NetLogo a good choice for agent-based evacuation simulation. The GIS shapefiles of the floor plan of the ED are developed based on available online information on Johns Hopkins Hospital website [198,199]. The shapefile of the floor plan with the network of nodes and connecting routes, developed in ArcMap, is shown in Figure 6-3. Using the node-route network, the node connectivity matrix is obtained which is used to calculate the shortest paths for all pairs of nodes using the Floyd-Warshall algorithm as explained in Chapter 3.

Figure 6-3. GIS shapefile of the ED floor plan with the node network

For each unit of the ED, the patients are created and positioned in the examination rooms and over the waiting area, the nurses are positioned randomly in their assigned unit area, and their attributes are set as explained in Sections 3.3 and 6.2.1. The class of each patient is randomly assigned using a randomly generated disability ratio (between 0 and 1) which indicates the proportion of patients that have any type of disability. The bed bound patients are modeled with two agents attached to each other, as explained in Table 3-3. One of the agents is a dummy agent that does not show any behavior but is observed by other agents, except for the attached agent, for collision avoidance.

At the beginning of the simulation, each nurse approaches one of the bed bound patients or wheelchair users. The priorities for nurses are first, patients in their assigned unit, and second, patients in other units.

6.2.2.2. FDM (PW++)

The fluid dynamics model is developed in MATLAB. The environment used in the PW++ is the same used in the ABM. The shapefile of the ED floor plan is imported into MATLAB and used to obtain the potential fields. The initial potential field for the ED is shown in Figure 6-4. For each unit in the ED, the initial wave density is set by dividing the number of patients by the net unit area. The properties of densities are set to the average values from the ABM (Table 6-3).

To consider how nurses help patients to evacuate, the average waiting time of patients to receive help from the nursing team is added to the preparation time. To calculate the average waiting time, let us consider an example: suppose there are 10 patients in the main ED unit with two nurses. This implies each nurse is responsible for 5 patients, assuming the response time of patients are the same, so the patients will be evacuated in two groups simultaneously.

In each group, the first patient does not need to wait to receive help, the second patient has to wait the time it takes to prepare and evacuate one patient, the third patient has to wait the time it takes to prepare and evacuate two patients, and so on, i.e. the n^{th} patient has to wait the time it takes to prepare and evacuate (n-1) patients. Then, the average waiting time for each patient is $\frac{0+1+2+3+4}{5} = 2$ times the average preparation and evacuation of one patient. For preparation, the average preparation time from Table 6-3 is used. As for evacuation, the average distance of each unit from the exit door is known, however the average moving speed is not known as it depends on the characteristics of the route and population density through the evacuation route which changes with time.

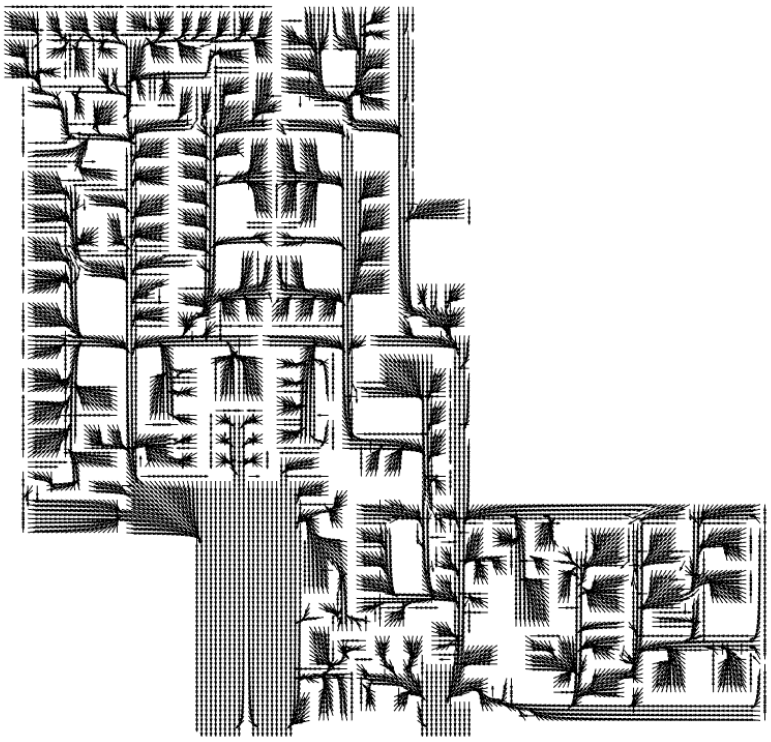

Figure 6-4. Initial potential field

The time it takes to take the first patient out is longer than that for the last patient as for the first patient, there are a significant number of patients trying to leave the ED, while for the last patient, most of the patients are already evacuated and the corridors are not congested. Therefore, the average moving speed of patients is considered to be 50% of their free moving speed. Hence, the average waiting time in each ED unit can be calculated as follows:

$$T_i^w = \beta_i \frac{g_i - 1}{2} \left(T_i^p + \frac{8 d_i}{v_{fi} + 1.4} \right) \quad 6\text{-}1)$$

where for each ED unit i, $g_i = \left\lceil \frac{p_i}{n_i} \right\rceil$ is number of groups, in which p_i is number of patients waiting for help and n_i is number of nurses, T_i^p is average preparation time, d_i is average distance to exit door, v_{fi} is average free moving speed, and β_i is the disability ratio, which is 0 for the psychiatric unit, 0.5 for the main ED, RAP, and triage, and 1 for EACU and the

trauma unit. Consequently, the overall evacuation delay time (waiting time + preparation time) can be calculated as:

$$T_i^d = T_i^w + T_i^p. \quad (6\text{-}2)$$

Table 6-3. Parameters of patient densities

ED Unit	v_f $[m/s]$	S [m]	ρ_{max} $[pp/m^2]$	Preparation Time $[sec]$
Psychiatry	1.175	0.5	4	47
Main ED	1.03	0.79	1.60	56
EACU	0.95	1.78	0.31	540
RAP	1.09	0.58	2.97	56
Triage	1.09	0.58	2.97	56
Trauma	0.89	1.4	0.5	540

6.2.2.3. SDM++

The system dynamics model is implemented in MATLAB. The main challenge in developing the SDM++ to model the evacuation of the ED is modeling the ED units. If each partition or examination room is modeled as a stock (in the stock and flow model), the model will be significantly large with hundreds of stocks, but most importantly, it does not agree with a macro-scale modeling perspective. A macroscopic model should consist of only macro-scale information of the system or process. For ED units, the macro-scale information includes the overall dimensions and the capacity of each unit. However, if we neglect the partitions and internal geometry of the environment, the SDM++ will fail to provide a reasonable estimate of evacuation rate. For example, the main ED unit is a 30 m by 30 m environment with 25

examination rooms, as shown in Figure 6-5a. The equivalent overall room is also shown in Figure 6-5b.

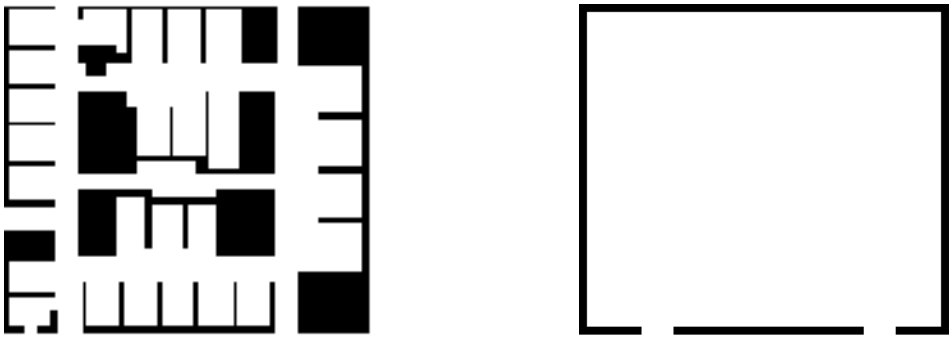

(a) (b)

Figure 6-5. Floor plan of the main ED unit: (a) actual, (b) simplified.

According to the ABM, it takes 37 seconds for 25 non-disabled patients to leave the unit if no preparation or pre evacuation time is considered. SDM++ estimates this time to be 310 seconds. This is due to the significant underestimation of exit rates by SDM++ for very low population densities (0.03 pp/m^2 in this case) as explained in Section 5.3.4 on residual analysis of SDM++. Therefore, we need to consider a better macro-scale geometry of the environment for the ED units. The proposed method to model ED units with only macro-scale information is shown in Figure 6-6. First, the average room per patient is calculated by dividing total unit area by the capacity of the unit. For the main ED, this gives an average 6 m by 6 m room for each patient. Each patient leaves their average room to enter into a corridor that leads them outside of the unit. The length of this corridor is half the length of the unit and its width is equal to the sum of main exit corridors of the unit.

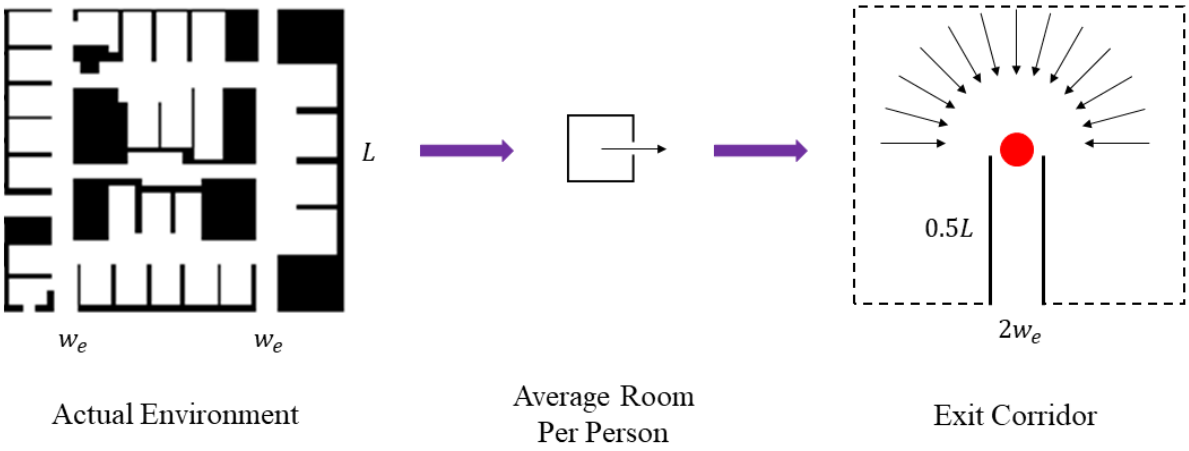

Figure 6-6. Proposed method for modeling complex shaped environment for SDM++

Similar to PW++, the parameters of population stocks are set to the average values from the ABM as listed in Table 6-3. The stock and flow representation of the SDM++ is shown in Figure 6-7.

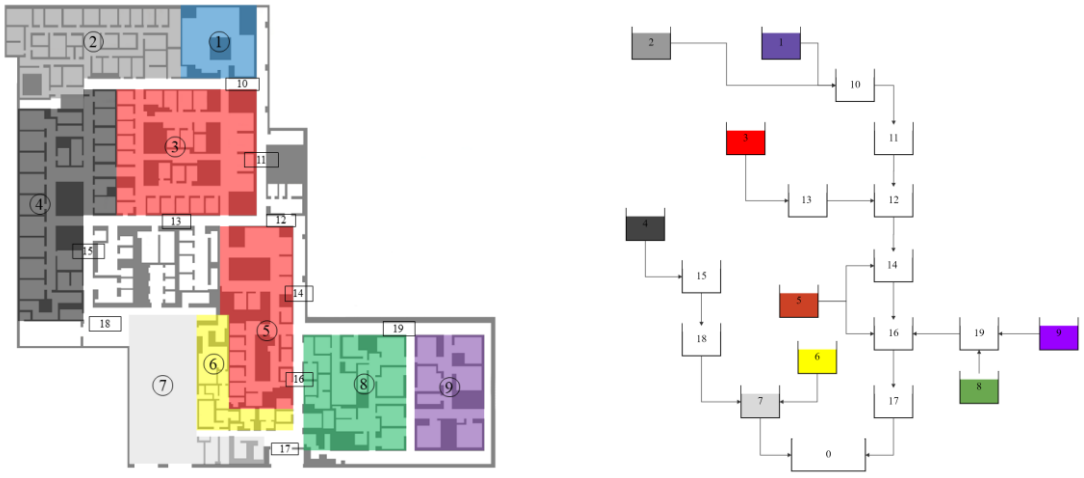

Figure 6-7. Stock and flow representation of the system dynamics model for the ED

6.2.3. Results

6.2.3.1. Scenario A

The results of the evacuation of the emergency department from the models for Scenario A are shown in Figure 6-8. According to the ABM, the total evacuation time can range from 18.8 to 33.5 minutes with an average of 26.0 minutes over 100 simulations. PW++ and SDM ++ estimate this average time to be 26.2 minutes and 27.4 minutes, respectively.

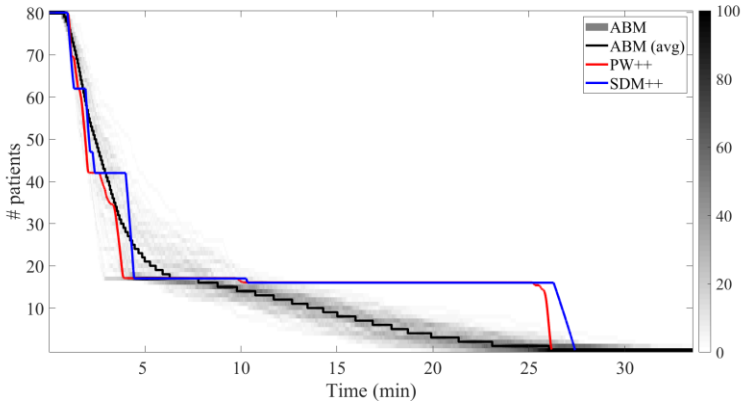

Figure 6-8. Total evacuation curves for Scenario A

While the estimated final evacuation time from all three models (average ABM, PW++, and SDM++) differ by less 5%, the models estimate different intermediate patient arrival times. Looking at the results of the ABM, two distinctive patterns can be observed. For simulations with low disability ratios where most of the patients in the psychiatry, main ED, RAP, and triage are ambulatory, the initial slope of the evacuation curve is between 20 to 30 patients per minute. In these cases, most of these ambulatory patients exit the building within the first 5 minutes, and the other bed bound patients (mostly EACU and trauma patients) are gradually evacuated with a significantly lower rate than the initial exit rate. As the disability ratio increases, the initial slope of the evacuation curve decreases to as low as 12 patients per minute, and the overall exit pattern takes a convex shape with longer final

evacuation times to compare with the piecewise pattern and shorter evacuation times for low disability ratio cases (see Figure 6-9).

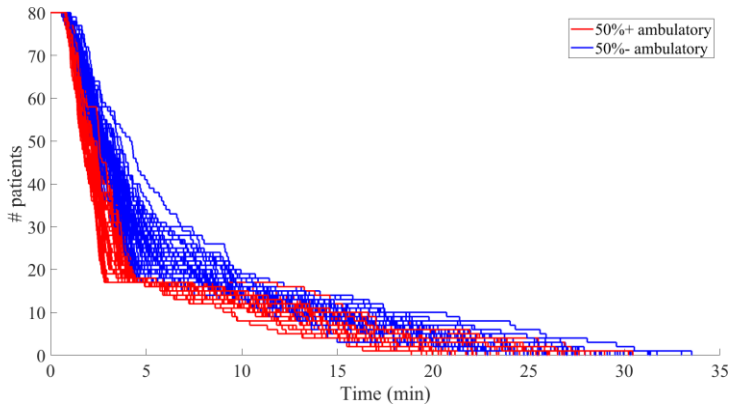

Figure 6-9. Effect of ambulatory patients on the evacuation pattern

To better analyze the variations in the outputs of the ABM, the statistics for the partial evacuation times at different evacuation percentiles are obtained (Figure 6-10). Table 6-4 lists the statistical measures at 25%, 50%, 75%, 90%, and 100% of the evacuation process. The values of standard deviation show that as the evacuation process continues in time, the variability increases. The values of skewness and kurtosis show that the variability over 100 evacuation simulations is slightly right-skewed with a shorter tail and a broader peak than a normal distribution, which implies that more of the variance is the result of frequent modestly sized deviations.

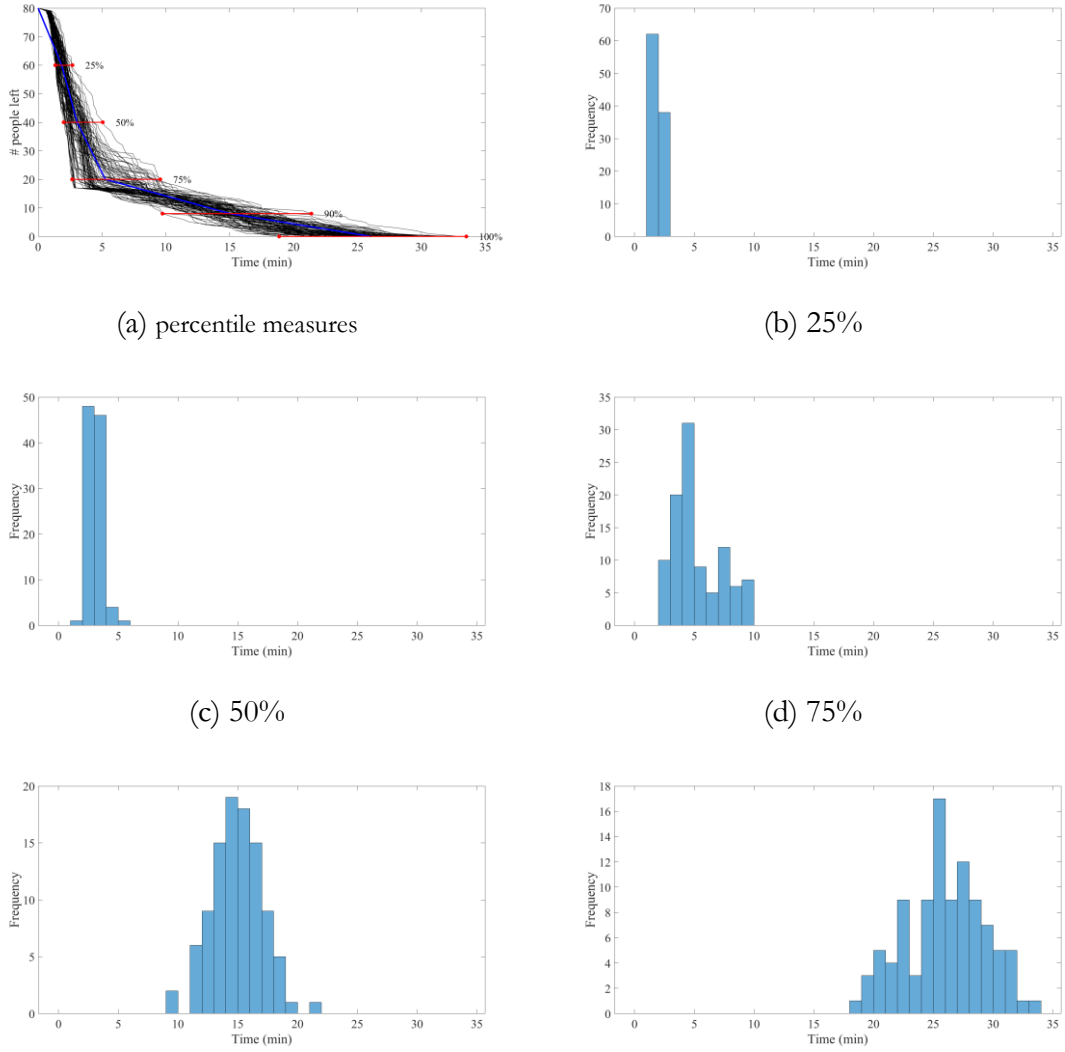

(a) percentile measures

(b) 25%

(c) 50%

(d) 75%

(e) 90%

(f) 100%

Figure 6-10. JHH evacuation: partial evacuation times at different evacuation percentiles (Scenario A)

Table 6-4. JHH: statistical measures at different evacuation percentiles (Scenario A)

Evacuation Percentile	Mean [min]	Standard Deviation [min]	Skewness	Kurtosis
25%	1.8	0.3	0.3	2.2
50%	3.1	0.6	0.3	2.4
75%	5.3	2.0	0.7	2.3
90%	15.0	2.1	0.1	3.2
100%	26.0	3.3	-0.1	2.4

The statistics for the partial evacuation times at different evacuation percentiles are obtained for the patients in the main ER, EACU, RAP, and triage units (see Figure 6-11 to Figure 6-14). Correspondingly, The statistical measures at 25%, 50%, 75%, 90%, and 100% of the evacuation process are listed in Table 6-5 to Table 6-8. The statistics for the final evacuation time of the psychiatric patients (only 5 patients) are: an average of 3.7 minutes, standard deviation of 0.5 minute, skewness of -0.1, and kurtosis of 3.1. For the one patient in the trauma unit, the statistics are 11.9 minutes, 3.6 minutes, 0.2, and 2.6, respectively. The values of standard deviation show that as the evacuation process continues in time, the variability increases. However, the values of skewness and kurtosis for different groups of patients show how the variabilities in their evacuation times are of different shape. The variabilities in evacuation time for patients in the EACU, psychiatry, and trauma units are symmetric and approximately follows a normal distribution. For patients in the main ER, the evacuation times are slightly right-skewed with broader peaks and shorter tails than a normal distribution. For triage patients, the evacuation times are highly right-skewed with stronger peaks than a normal distribution. For the patients in the RAP unit, the situation is more complicated: in the first half of the patients, the evacuation times are slightly right-skewed with

broader peaks than a normal distribution, but for the second half, the evacuation times are highly right-skewed with stronger peaks than a normal distribution. These statistics imply that for triage patients and second half of RAP patients, more of the variance is the result of infrequent extreme deviations, while for other patients, the variance in evacuation time is due to frequent modestly sized deviations.

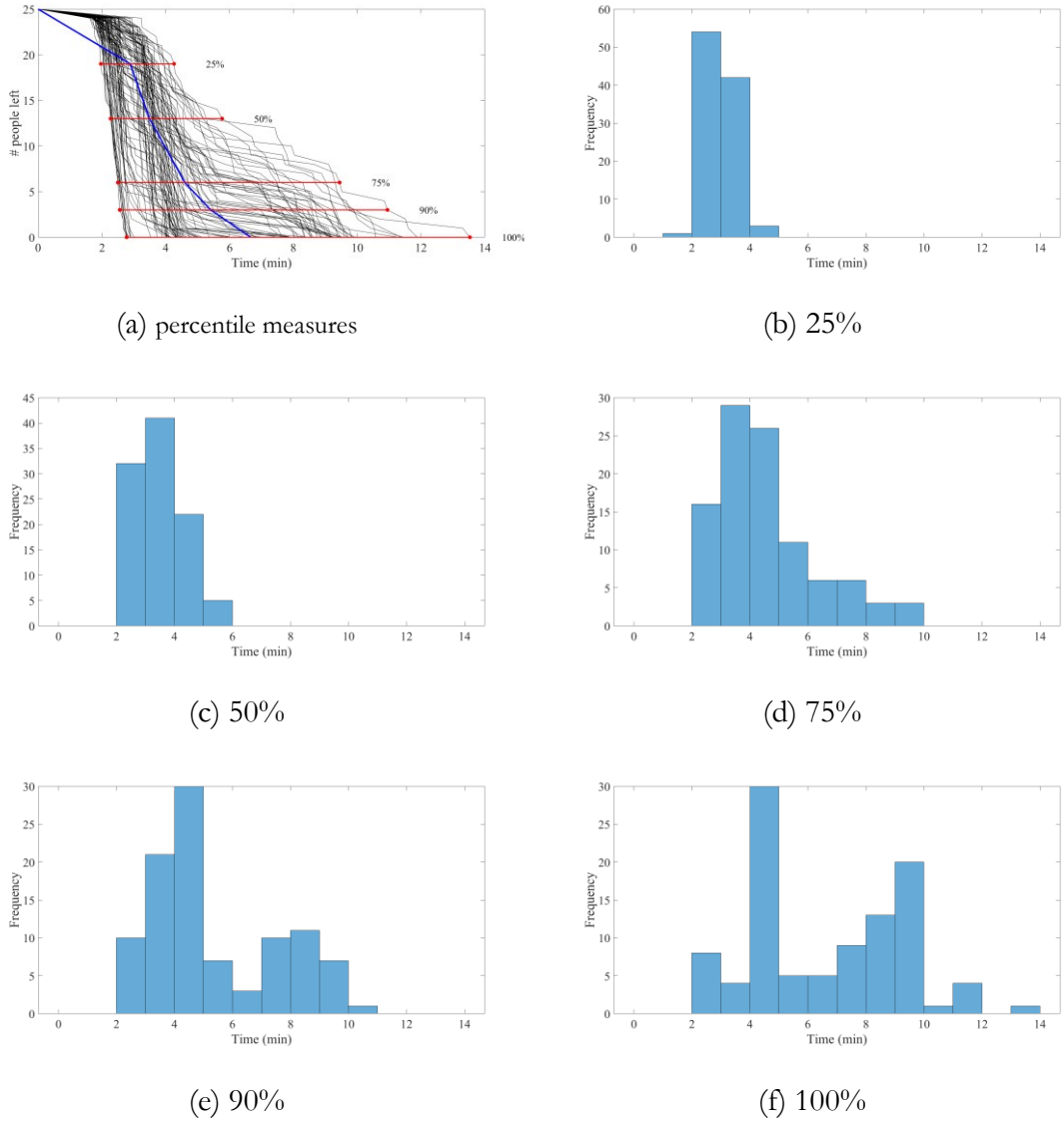

(a) percentile measures

(b) 25%

(c) 50%

(d) 75%

(e) 90%

(f) 100%

Figure 6-11. JHH evacuation: partial evacuation times at different evacuation percentiles for patients in the main ER (Scenario A)

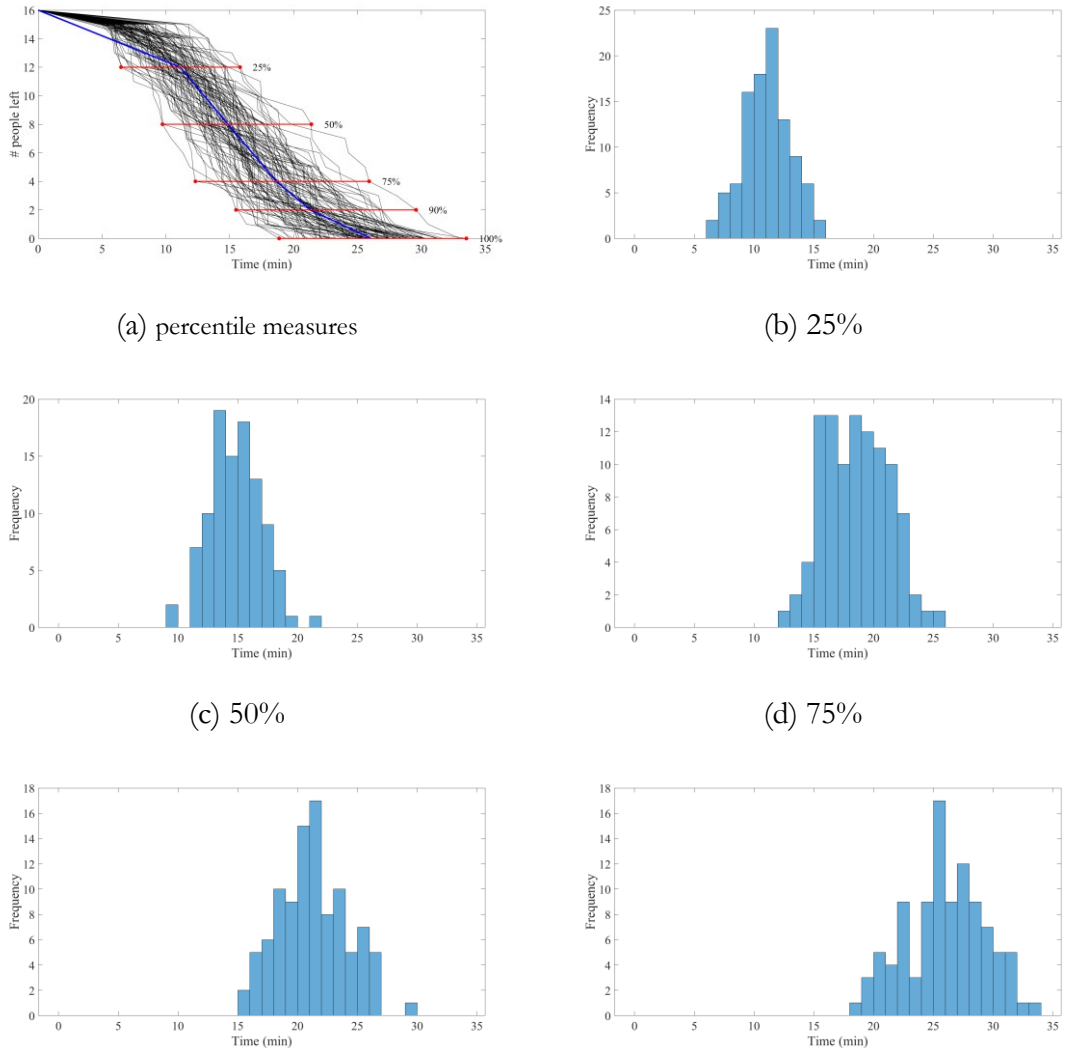

(a) percentile measures

(b) 25%

(c) 50%

(d) 75%

(e) 90%

(f) 100%

Figure 6-12. JHH evacuation: partial evacuation times at different evacuation percentiles for patients in the EACU (Scenario A)

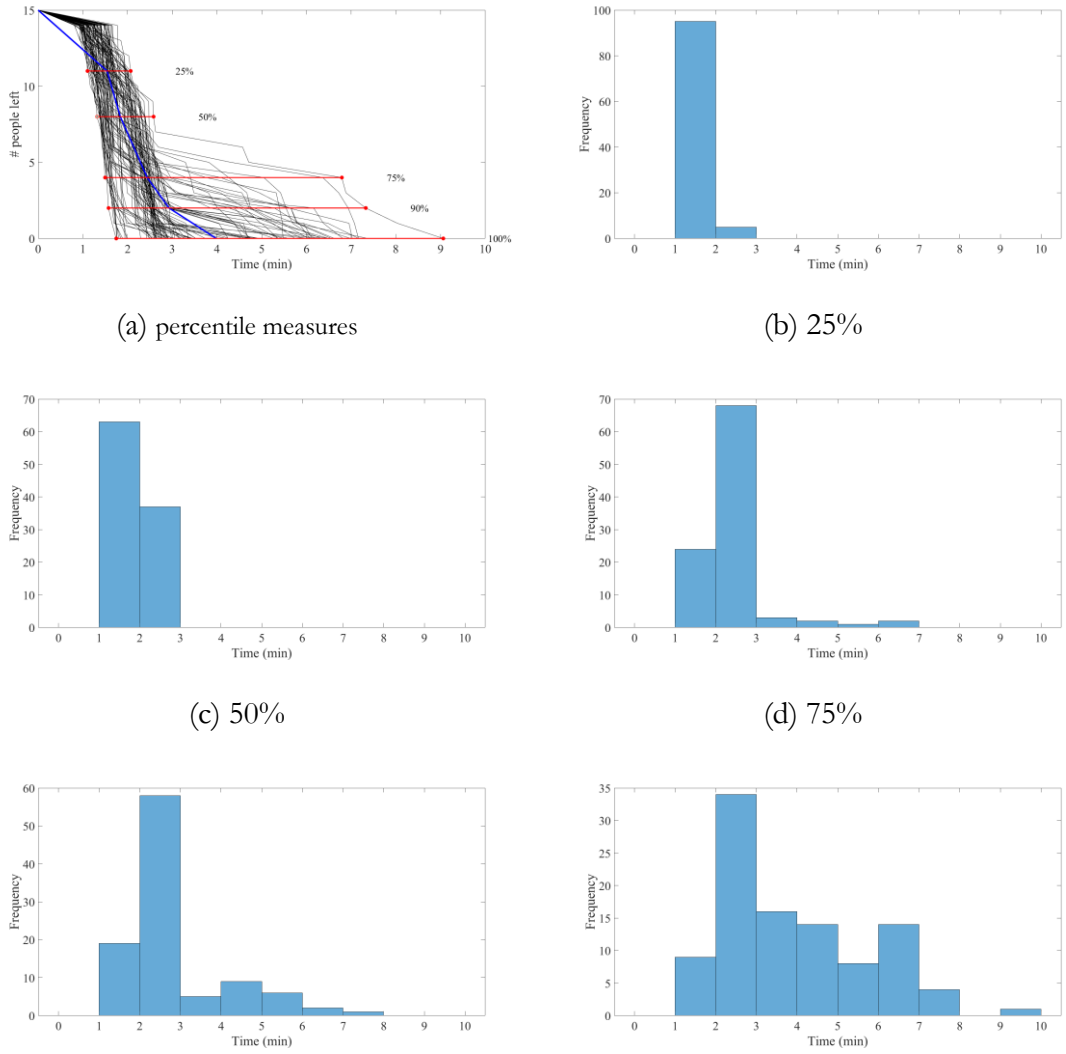

(a) percentile measures

(b) 25%

(c) 50%

(d) 75%

(e) 90%

(f) 100%

Figure 6-13. JHH evacuation: partial evacuation times at different evacuation percentiles for patients in the RAP unit (Scenario A)

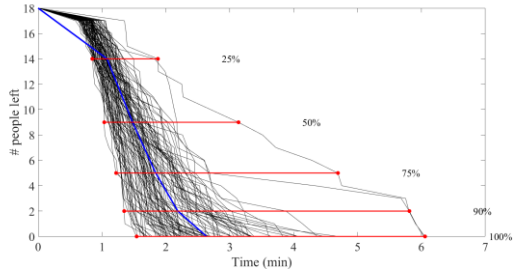

(a) percentile measures

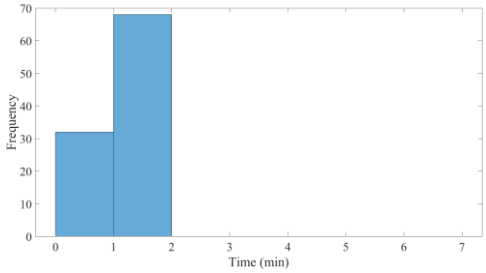

(b) 25%

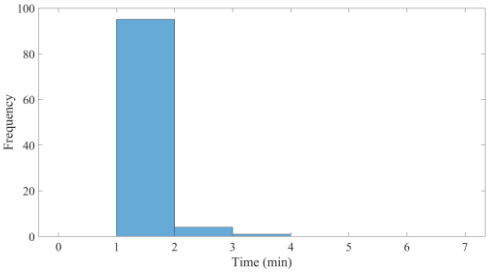

(c) 50%

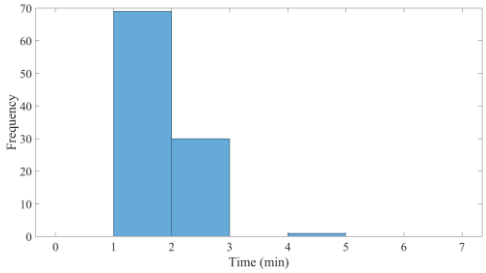

(d) 75%

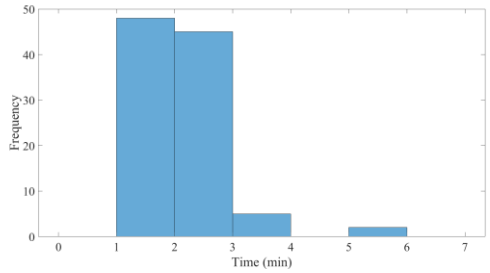

(e) 90%

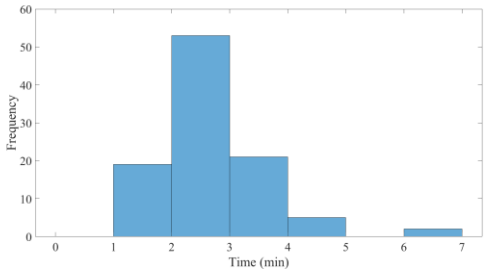

(f) 100%

Figure 6-14. JHH evacuation: partial evacuation times at different evacuation percentiles for patients in the triage unit (Scenario A)

Table 6-5. JHH evacuation: statistical measures at different evacuation percentiles for patients in the main ER (Scenario A)

Evacuation Percentile	Mean [min]	Standard Deviation [min]	Skewness	Kurtosis
25%	2.9	0.6	0.3	2.0
50%	3.5	0.8	0.4	2.6
75%	4.6	1.7	1.1	3.6
90%	5.4	2.2	0.7	2.2
100%	6.7	2.7	0.2	1.9

Table 6-6. JHH evacuation: statistical measures at different evacuation percentiles for patients in the EACU (Scenario A)

Evacuation Percentile	Mean [min]	Standard Deviation [min]	Skewness	Kurtosis
25%	11.1	2.0	0.0	2.8
50%	14.9	2.1	0.2	3.1
75%	18.6	2.7	0.1	2.6
90%	21.3	2.9	0.2	2.7
100%	26.0	3.3	-0.1	2.4

Table 6-7. JHH evacuation: statistical measures at different evacuation percentiles for patients in the RAP unit (Scenario A)

Evacuation Percentile	Mean [min]	Standard Deviation [min]	Skewness	Kurtosis
25%	1.5	0.3	0.3	2.1
50%	1.8	0.3	0.2	1.8
75%	2.4	0.8	3.0	14.8
90%	2.9	1.2	1.7	5.2
100%	4.0	1.7	0.7	2.5

Table 6-8. JHH evacuation: statistical measures at different evacuation percentiles for patients in the triage unit (Scenario A)

Evacuation Percentile	Mean [min]	Standard Deviation [min]	Skewness	Kurtosis
25%	1.1	0.2	1.9	9.2
50%	1.5	0.3	1.9	10.4
75%	1.8	0.5	2.6	16.8
90%	2.2	0.7	2.8	14.2
100%	2.6	0.8	1.6	6.8

The results of PW++ and SDM++ are similar mainly because the same average delay times calculated for each groups of patients using Equation 6-1) are considered in both models. However, as multiple population densities are considered in the PW++, the results of

the evacuation for each group of patients can be studied separately. Figure 6-15 shows the evacuation curves for different groups of patients obtained from the ABM and PW++.

From Figure 6-15, the evacuation curves resulting from PW++ do not agree with the average curves from the ABM. As explained in Chapters 4 and 5, meso- and macro-scale models lose significant information, and for evacuation as a spatiotemporal process, this loss of spatial information and ignoring the heterogeneity of the evacuees lead to significant discrepancies between outputs from microscopic models and those from meso and macro models. Certainly, the averaging of delay and preparation times has significantly affected the evacuation results. In the ABM, the patient-nurse interactions and heterogeneous characteristics of the agents result in more realistic and gradual patient arrival times, while in PW++ (and also SDM++), all the patients from each unit start the evacuation simultaneously based on the average delay times, which results in a step-like evacuation curve.

Another factor that contributes to the discrepancies between the results of PW++ and ABM is the calculated average waiting times. The calculated times using Equation 6-1) and those obtained from the ABM are listed in Table 6-9. As it is clear, Equation 6-1) mainly overestimates the average waiting time, specifically for EACU patients. This difference is due to the fact that the nurses from those units which are completely evacuated earlier (psychiatry, main ED, RAP, triage) join the nursing teams in other units, which will significantly decrease the patient waiting time in the EACU as the slowest unit. Certainly, Equation 6-1) can be improved to account for this behavior; however, the current approach to calculate average waiting time per unit can show how aggregation can lead to neglecting micro-scale behaviors that can affect the estimation of evacuation time.

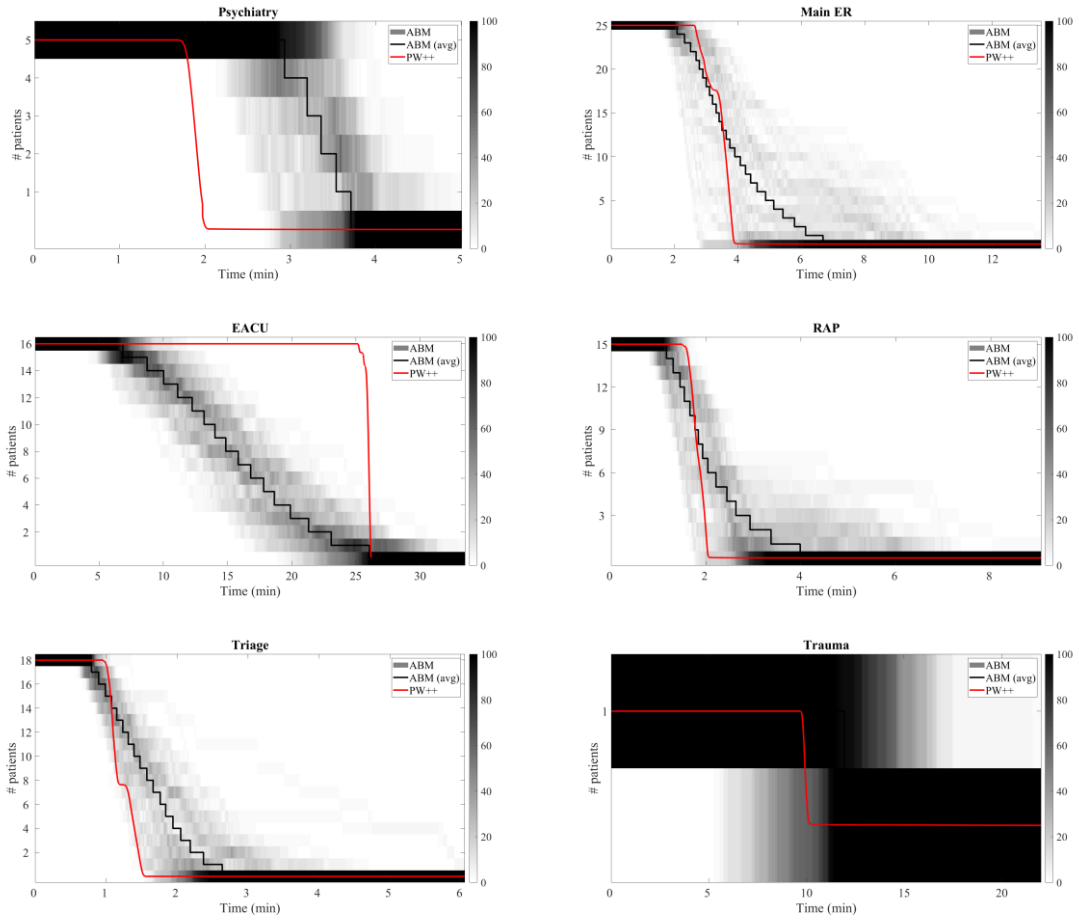

Figure 6-15. Evacuation curves for different groups of patients from the ABM and PW++ (Scenario A)

Table 6-9. Comparison of calculated average waiting times with those obtained from the ABM for scenario A

Unit	Calculated average waiting time [sec]	Average waiting time from ABM [sec]
Psychiatry	0	0
Main ED	97	47
EACU	963	313
RAP	26	21
Triage	27	19
Trauma	47	48

Last but certainly not least, as shown in test cases in Chapter 4, PW++ tends to overestimate evacuation speed for low density populations. This particularly can be observed in the results for the psychiatry and trauma units.

6.2.3.2. Scenario B

Figure 6-16 shows the results for Scenario B. According to the ABM, the total evacuation time can range from 14.6 to 27.5 minutes, over 100 simulation, with an average of 18.7 minutes. PW++ and SDM++ estimate this time to be 15.5 minutes and 16.6 minutes, respectively. The graphical outputs from the three models at $t = 2\ min, t = 10\ min,$ and $t = 15\ min$ are shown in Figure 6-17 to Figure 6-19.

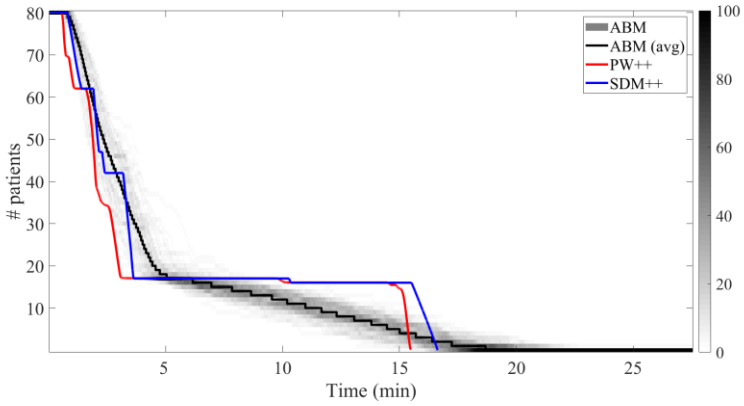

Figure 6-16. Total evacuation curves for Scenario B

In Scenario B, with the increase in the nurse-to-patient ratio, the effect of the disability ratio (non-ambulatory ratio) is less than in Scenario A as the patient waiting time decreases. The patient waiting times for the two scenarios are compared in Table 6-10 and Figure 6-20. An important issue observed in the waiting times is that their distributions are highly right-skewed with possible extreme outliers. These outliers, e.g. in Figure 6-20c for EACU patients, represent those high-acuity patients in need of longer preparation times that were last in line to be evacuated. Moreover, increasing the number of nurses leads to 28% decrease in total evacuation time according to the ABM. This decrease is estimated to be 40% as per PW++ and SDM++.

Table 6-10. Average waiting times from the ABM

Unit	Scenario A [sec]	Scenario B [sec]
Main ED	47	20
EACU	313	113
RAP	21	12
Trauma	48	48

Figure 6-17. Graphical outputs of the ABM, PW++, and SDM++ at t = 2 min (Scenario B)

Figure 6-18. Graphical outputs of the ABM, PW++, and SDM++ at t = 10 min (Scenario B)

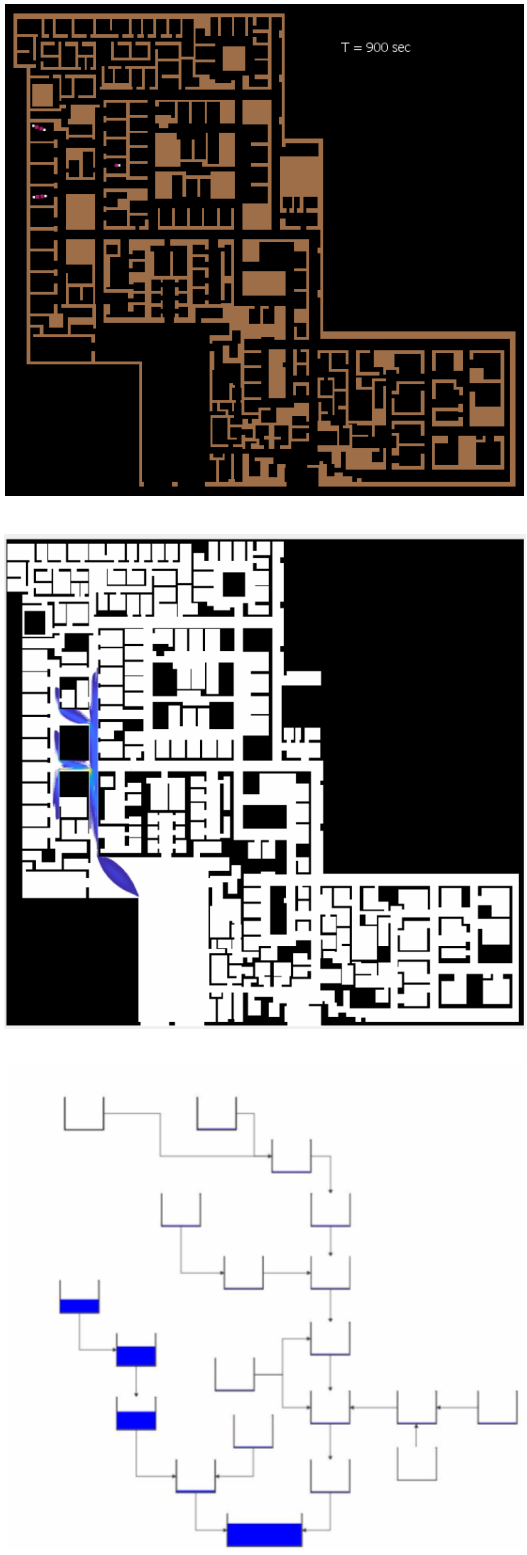

Figure 6-19. Graphical outputs of the ABM, PW++, and SDM++ at t = 15 min (Scenario B)

Figure 6-21 shows the evacuation curves for different groups of patients obtained from the ABM and PW++. As explained for Scenario A, the discrepancies between the results of the ABM and PW++ are due to using an average waiting time and preparation time for each unit, inter-unit cooperation of nurses, and the weakness of the PW++ in low density populations.

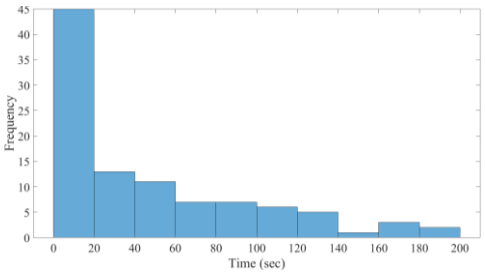

(a) main ER (Scenario A)

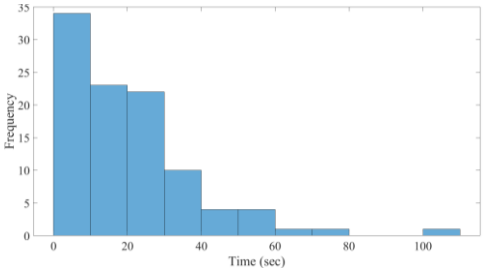

(b) main ER (Scenario B)

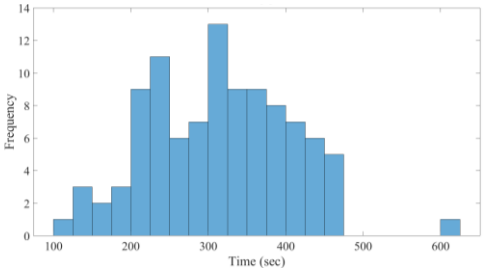

(c) EACU (Scenario A)

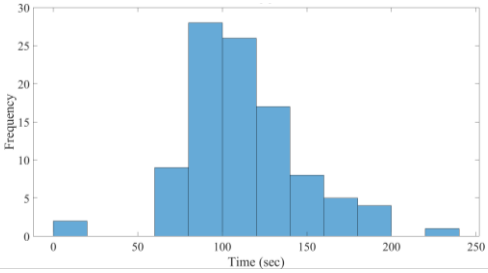

(d) EACU (Scenario B)

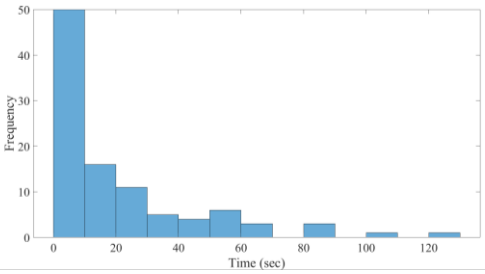

(e) RAP (Scenario A)

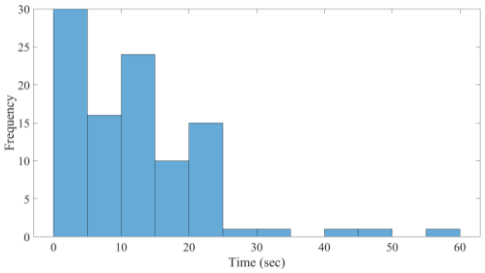

(f) RAP (Scenario B)

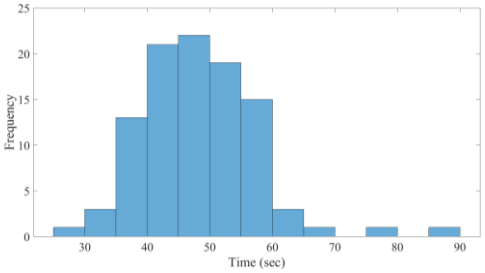

(g) Trauma (Scenario A)

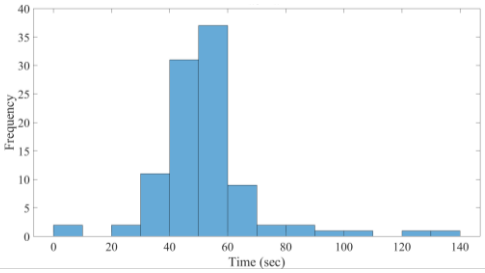

(h) Trauma (Scenario B)

Figure 6-20. Histograms of waiting time from the ABM

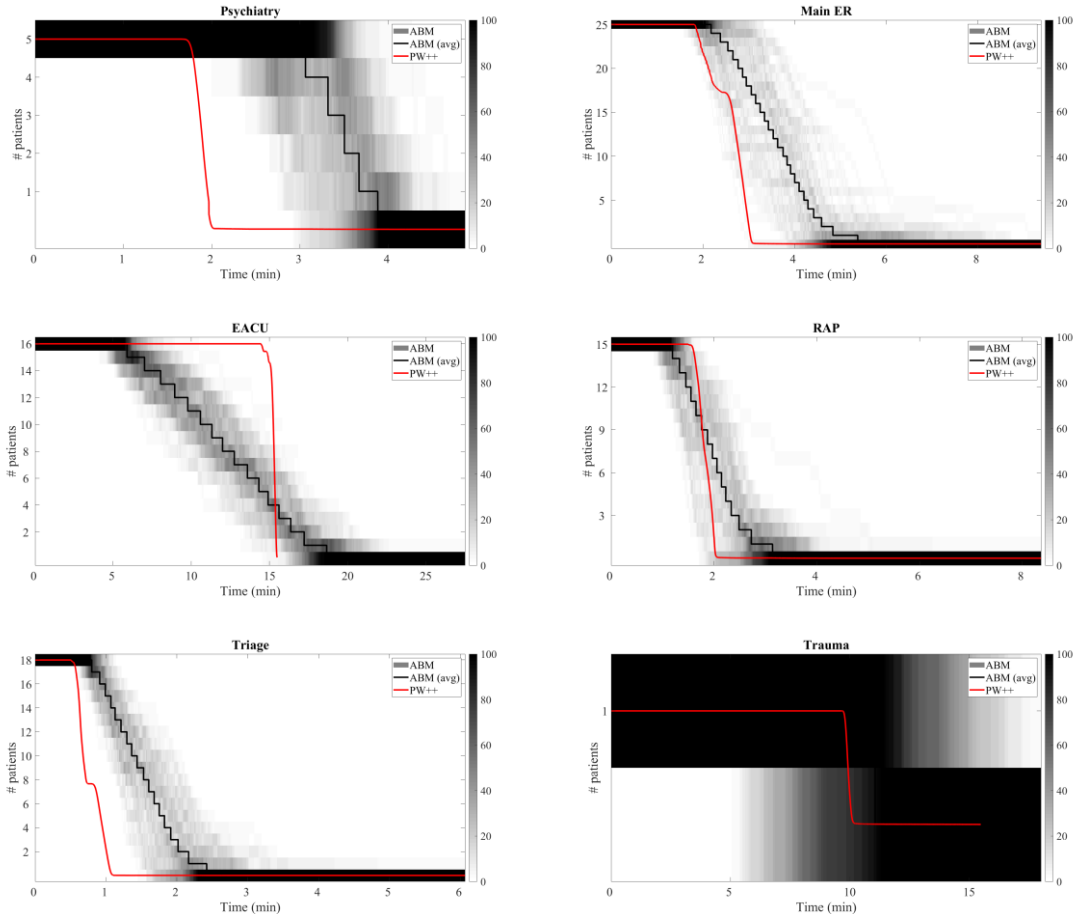

Figure 6-21. Evacuation curves for different groups of patients from the ABM and PW++ (Scenario B)

6.2.4. Recommendations for Decision Makers

The three models developed in this dissertation and used in this chapter to simulate the evacuation of the emergency department at the Johns Hopkins Hospital have relative advantages and disadvantages. The challenges in developing these models and their features are explained throughout the dissertation. A summary of these models in terms of development challenges, required input data, providing output data, and performance is presented in what follows.

The ABM requires expertise in agent-based modeling, programming, and implementing the path planning, collision avoidance, and social behavior modules. One of the challenges of agent-based modeling is verifying the model to ensure the agents behave properly in different conditions. Particularly, in evacuation simulation where agents constantly interact with each other and with the environment (walls and obstacles), the modeler has to perform comprehensive tests to find any anomalies in the behavior of agents. The PW++ model is also challenging to develop. In general, fluid dynamics models require significant efforts for setting up the boundary conditions; however, the most challenging task is the numerical solution. The numerical solutions to hyperbolic PDEs of fluid dynamics models are complicated to learn and implement and needs prior experience. On the other hand, the SDM++ model is less challenging when it comes to implementation. With the macro-level exit rate formula provided in Chapter 5, setting up the stock-and flow model and calculating the parameters such as the average waiting time is straight forward and relatively fast.

Regarding input and output data, as it is clear, the microscopic agent-based model requires and provides patient-level data, while the mesoscopic fluid dynamics model and the macroscopic system dynamics model only require and can provide aggregated data. For the agent-based model, the patient classification framework is an essential component of the model as the patient-level data should be categorized according the patient classes. Moreover, the detailed floor plan of the hospital is also required. Although PW++ also requires the detailed floor plan, but it only requires average data for patients in each unit of the hospital. As expected, SDM++ requires fewer input data — only the general plan of the hospital to know how units and corridors are connected, overall dimensions of each unit, and average characteristics of patients in each unit. Correspondingly, the outputs of the ABM are more comprehensive and detailed accounting for randomness, while PW++ provides deterministic

results, which as explained in Section 6.2.3, do not provide reliable patient arrival times, however, the total arrival times are acceptable when compared with the results of the ABM. SDM++ can only provide total patient arrival times which are very similar to those from PW++, but it does not provide any information about different patient groups.

The performance of the models in terms of computation speed can also be an important criterion if there is a need for rapid assessment in an imminent emergency scenario. The simulation time for 100 simulations with the ABM and single simulations with PW++ and SDM++ are 3 hours, 10 hours, and 5 seconds, respectively. it noteworthy to highlight that the ABM is developed in NetLogo, PW++ and SDM++ are developed in MATLAB, and the simulations are run using a computer with an Intel Xeon E3-1505M v5 @ 2.8 GHz processor and 32GB memory. The summary of the challenges in the implementation of the evacuation simulation models developed in this study and their characteristics are listed in Table 6-11.

Table 6-11. Implementation challenges and characteristics of the evacuation simulation models

Criteria	ABM	PW++	SDM++
Implementation	Defining exhaustive agent-level behaviors; Model verification	Implementation of the numerical solution	Setting up the stock-and-flow model for units and corridors
Input data	Detailed floor plan; Patient-level data	Detailed (or simplified) floor plan; Aggregated unit-level data	Schematic floor plan with overall dimensions; Aggregated unit-level data
Output data	Probabilistic patient-level data	Deterministic and less reliable unit-level data	Deterministic overall data
Performance	3 hours (100 simulations)	10 hours	5 seconds

6.3. Conclusions

Simulation is a potentially useful tool for decision makers to evaluate the efficiency of current operations or policies and find alternative solutions. One of the challenges that hospitals face is emergency evacuations. To evaluate the efficiency of emergency policies and plans, emergency teams need training and drills, however, hospital evacuation drills are costly and disruptive, therefore, modeling and simulation can support emergency planning by providing an estimation of intermediate and final evacuation times.

In Chapters 3 to 5, three evacuation models were developed: a microscopic agent-based model (ABM), a mesoscopic fluid dynamics model (PW++), and a macroscopic system dynamics model (SDM++). Each of these modeling approaches has specific advantages and disadvantages which have been discussed before based on a few simple test cases. In this chapter, to demonstrate the applicability of these evacuation models, the evacuation of the Emergency Department of the Johns Hopkins Hospital was simulated. These multi-scale models were evaluated and compared in terms of modeling complexity, required input data, provided output data, and performance. Although the ABM requires specific modeling expertise and patient-level data for implementation, the patient-level statistical outputs make the model the most competent approach. Furthermore, as hospitals typically have records of daily operations, and considering the recent advances in high performance computations, the challenge of developing microscopic evacuation models can be reduced to recruiting an advance modeling team of scientists. Consequently, a microscopic hospital evacuation model can be regarded as the recommended tool for the hospital emergency teams to use to evaluate different scenarios and evacuation plans. On the other hand, PW++ does not provide any competency when compared with the ABM and SDM++. Having an average computation speed of three time the ABM while not providing useful results as the ABM does makes

PW++ the least useful technique. Finally, SDM++ presents a very interesting advantage. Although it does not provide patient- or unit-level results, the results that it provides for the overall evacuation times have shown to be acceptable when compared with the ABM, while its simplicity can make it the best choice for a mobile app to be used by emergency teams in case of a need for rapid situation assessment and rapid decision making.

Without a doubt, there is much room left for improvement in hospital evacuation simulation. Aside from further model improvements which was discussed in Chapters 3 to 5, to improve the applicability of these models, specifically the ABM for in-depth decision makings and SDM++ for rapid evaluations, there is a significant need to acquire feedback from hospital emergency teams. Emergency officials can best scrutinize the applicability of these evacuation simulation tools by evaluating the outputs of these models for different scenarios based on their knowledge and past experiences. This calls for more collaborations between the modeling and simulation society and the hospital operational professionals.

Chapter 7

Conclusions and Future Work

7.1. Major Contributions

This dissertation is devoted to modeling evacuation on different scales. The large-scale evacuation if urban areas and the evacuation of hospitals with mobility impaired patients are studied and modeled using agent-based modeling, fluid dynamics models, and system dynamics modeling. In what follows, the major contributions are summarized.

The application of bug navigation algorithms is proposed for more efficient large-scale agent-based city evacuation models. To evaluate the suitability of bug algorithms and compare their relative performances, a performance evaluation framework is developed. The framework consists of a set of bug navigation algorithms, a set of proposed benchmark obstacles, and a performance metrics with four performance measures: convergence, optimality, precision, and efficiency. Based on the analyses, the DB1 algorithm is proposed as a candidate algorithm for the navigation of the evacuees.

To demonstrate applicability, a large-scale agent-based city evacuation model is developed, with the DB1 algorithm, to simulate the evacuation of the city of Iquique in Chile. The results of the comparison with drill data and a competing more sophisticated agent-based model shows that the proposed model can perform relatively acceptable in terms of accuracy, while the computation time is reduced significantly by 2 orders of magnitude.

For microscopic hospital evacuation simulation, a patient classification system is proposed considering mobility characteristics and needs of patients. Accordingly, patients are classified into 9 groups: visually impaired, hearing impaired, wheelchair users, motorized wheelchair users, stamina impaired, bed bound, mentally impaired, non-disabled elderly or children, and non-disabled adults. The mobility characteristics (free flow walking speed on floors, ramps, and stair, and their occupied area) and needs (preparation time and number of needed nurses) of these 9 groups of patients are consolidated from the literature, as well.

The development of an agent-based hospital evacuation model elaborated with the most commonly acceptable path planning and collision avoidance (recalibrated for emergency evacuation) algorithms and a social behavior model.

Three simple test cases with predictable outcomes are proposed as benchmark for the evaluation and comparison of multi-scale evacuation models.

For mesoscopic hospital evacuation simulation, the PW fluid dynamics model is modified by the addition of multiple densities. This allows to model heterogenous groups of people as multiple densities that simultaneously and interactively propagate in time and space.

For macroscopic hospital evacuation simulation, a system dynamics model is developed by reducing the agent-based model. In this model, the mobility characteristics and needs of patients are considered on an aggregate level to estimate the flow of patients between rooms and corridors based on a regression model.

To demonstrate the applicability of the agent-based model, the fluid dynamic model, and the system dynamics model in simulating hospital evacuations, the evacuation of the emergency department at Johns Hopkins University is simulated using the models, and their outputs and performance are compared in terms of implementation complexity, required input data, provided output data, and computation time.

It is concluded that the microscopic agent-based model is recommended to hospital emergency planners for long-term use such as evaluating different emergency scenarios and effectiveness of different evacuation plans. On the other hand, the macroscopic system dynamics model is best to be used as a simple tool (like an app) for rapid situation assessment and decision making in case of imminent events.

7.2. Limitations

Although it is critically important in any research study to minimize the scope of limitations of the work, like any other research study, this dissertation comes with certain shortcomings. The limitations of this study and their impacts on the findings are explained below.

To find the candidate bug algorithm for the large-scale agent-based evacuation model in Chapter 2, only 5 bug algorithms and their variations are evaluated. There are about 10 more bug algorithms that needed to be evaluated to find a better candidate.

The performance evaluation metrics developed in Chapter 2 for bug algorithms provides a normalized index score with regard to the evaluated algorithms. This implied that the performance indices can change when more algorithms are evaluated. Although this does not affect the current findings, but to provide a more informative performance index for each algorithm, this limitation should be addressed. This can be done by defining benchmark values for optimality and efficiency.

The patient classification system proposed in Chapter 3 does not include all types of patients, particularly ICU patients are excluded. This limits the application of the agent-based model to evacuation of non-ICU units.

The patient classification system and consequently the agent-based model does not consider specific equipment, such as oxygen tanks and ventilators, that patients may need during the evacuation. The availability of these equipment can affect the evacuation process by introducing extra delay times. This is very critical as mainly patients in more critical conditions are in need of such equipment, and extra delay in the evacuation of these critically ill patients can impose serious risks to their lives if the complete evacuation of all patients is required in a short time.

Although the system dynamics model is a macroscopic model which requires macro-level input data, there are certain meso- or micro-level input data that can be aggregated to improve the behavior of the system dynamics models. In this regard, a major shortcoming is the architectural characteristics of hospital units. This has been addressed with the equivalent unit approach, however, for hospitals with more irregular floor plans, the architectural characteristics of internal spaces can significantly affect patient flow rate.

Regarding the full-scale emergency department evacuation simulation, certain important details are not considered in the scenarios, e.g. the dynamic evolution of the emergency and its impact on the evacuation process. In case of fire evacuations, certain parts of the building may be inaccessible. In addition, fire smoke or heat affects the behavior and capabilities of evacuees.

7.3. Future work

Evacuation simulation, particularly for hospitals with mobility impaired patients, has seen a specific attention within cross-disciplinary studies on transportation networks, healthcare resilience, and disaster response. In what follows, the future paths based on the work conducted in this study are briefly explained.

To improve our knowledge of the capabilities of large-scale agent-based evacuation models, it is necessary to study how other types of agent-based evacuation models (e.g. models based on social forces or potential field theory) perform. The first step towards this goal is to develop a comprehensive performance evaluation framework for microscopic evacuation models, consisting of metrics for accuracy, optimality, implementation cost, and efficiency. The results of such studies can provide decision makers with information on the capabilities and requirements of different large-scale microscopic models for cost-benefit analyses for adopting the best modeling tool based on expectancies, available budget, and available expertise.

For microscopic hospital evacuation models, the essential component is a comprehensive knowledge on mobility characteristics and needs of different classes of patients, including ICU, CCU, and other inpatient classes. Although there has been a few studies trying to identify what different patients need for an emergency exit, there is much opportunity left for empirical studies and theoretical works to clearly identify what patients need in terms of equipment and medical attention for safe emergency evacuations.

For microscopic hospital evacuation models, the evacuation of ICU and CCU patients poses different challenges to compare with non-ICU patients. Comprehensive qualitative studies on the evacuation needs of these patients followed by quantitative studies to collect data is a promising research path.

Hospitals as critical infrastructure are critical nodes in the functionality of societies and their operations is interdependent to the operations of other infrastructure systems. Consequently, hospitals' behaviors, such as evacuations, during disasters should be incorporated into larger frameworks, as well. In regional disasters, the evacuation of a hospital is considered as completed when all patients have moved to safe regions (i.e. shelters or other

hospitals). Hence, hospital evacuation models can be integrated into a network model to consider the inter-hospital patient transfer process, as well. This also includes transportation modeling. Such larger models can help local and regional responders and decision makers understand better the impact of disasters on societies, which in turn leads to better policy and response measures to ensure the resilience of communities in facing disruptive events.

Appendix A

Details of Meetings with Health Professionals

In this section, the highlights of the meetings are presented. Each meeting was conducted uniquely due to the unique expertise of these experts, however, the following questions were expected to be answered as a result of these meetings:

1. Is there any specific plan or guideline for hospital evacuation or patient transfer at the Johns Hopkins Health System?
2. Does the hospital emergency plan consider evacuation? To what extent?
3. What are the differences between the designed hospital evacuation procedure and the actual procedure in practice?
4. What are the minimum requirements for capital, reusable, and consumable resources set forth in the hospital's emergency plan?
5. How patients are classified in Johns Hopkins Hospital's databases?
6. How patients are prioritized for transfer? And what are the transfer procedures for ICU and non-ICU patients?
7. How resources (e.g. wheelchairs and ambulances) are distributed among different types of patients or different hospital units (e.g. ICU and ER)?
8. How to manage staff distribution among different units during an evacuation?
9. How to ask for external support (resources, equipment, staff, etc.)?
10. How to find receiving hospitals and ICU beds?

11. What equipment patients need for transfer? How to get information about specific transfer needs for different types of patients?
12. How to find ambulances or other means of transportation?
13. How receiving hospitals admit transferred patients?
14. How receiving hospitals manage public patient surge and transferred patients together?
15. What are the specific challenges and stories from prior evacuation experiences that we need to consider?
16. Whose expertise and feedback are required for a hospital evacuation simulation study?
17. What do you expect from a helpful hospital evacuation simulation tool in terms of input data, output data, and specific features or capabilities?

Meeting #1

Date: October 2, 2018

Location: Johns Hopkins Center for Health Security

Expert: Dr. Eric Toner, Senior Scholar at Johns Hopkins Center for Health Security, Senior Scientist at Johns Hopkins Bloomberg School of Public Health

Notes: I was referred to Dr. Toner by Dr. Tom Inglesby, Director of the Center for Health Security

Highlights:

- Evacuation prioritization depends on the nature of each event, e.g. what timing or imminence of the event implies? Is the main issue the loss of infrastructure or is it patient safety?
- Patient transfer: Hospitals keep patients within their networks for different reasons such as financial interests, insurance limitations, pre-determined agreements, etc.
- Special needs of ICU patients are different on a case-by-case basis. Maybe it is not the best approach to focus on ICU patients based on categories such as NICU, PICU, etc.
- Patients' evacuation needs depend on many factors: nature of health issue, acuity level, length of evacuation, means of evacuation, etc.
- During mass evacuations, the receiving hospital sets up a separate triage for transferred non-ICU patients.
- There is a need for fast and reliable models to be used in real-time decision-making processes.
- There are many other complications based on prior experiences, e.g. sometimes there is a need for mental health units due to special situation of mental health patients. As

another example, in hurricane Sandy, a hospital was faced with many issues to evacuate patients under the criminal justice system. The situation was exacerbated as none of the patients could speak English.

Meeting #2

Date: October 5, 2018

Location: Johns Hopkins Hsopital

Expert: Mr. Robert Maloney, Director of the Johns Hopkins Hospital Office of Emergency Management

Notes: I was also referred to Mr. Maloney by Dr. Gabor Kelen, Director of the Department of Emergency Medicine, and Director of the Johns Hopkins Office of Critical Event Preparedness and Response (CEPAR)

Highlights:

- The discussion was conducted while walking around the hospital and Mr. Maloney showing me different sections of the hospital, specifically the patient tracking facility.
- The evacuation procedure completely depends on the scenario; evacuation due to a heatwave is completely different than a fire scenario.
- In some states, the procedure for finding ICU beds is centralized on a state level, however, hospitals still make their own phone calls to speed up the process of evacuating ICU patients. As Dr. Toner also pointed out, this is due to many reasons, such as pre-determined agreements, financial interests, or insurance issues.
- Patient prioritization for evacuation takes place on the spot by the physician in charge of an ICU based on his/her assessments over the statuses of patients.
- There is no specific framework for pre-prioritization of ICU patients for evacuation.
- Focusing on specific patients (e.g. transplant patients) can be more practical and useful and will lead to something that actually hospitals and emergency managers (including himself) are willing to use.

- He is willing to work directly with us to develop a helpful tool. He emphasized that although a lot of studies are being done and many models and tools are developed, hospitals and emergency teams do not use these products. There is a need for a more practical approach.

Meeting #3

Date: October 18, 2018

Location: Department of Civil Engineering (now Civil and Systems Engineering)

Expert: Dr. Takeru Igusa, Professor, Department of Civil Engineering, joint appointment at Department of International Health and Department of Mental Health, Johns Hopkins University

Notes: Marietta Squire, a PhD student in Dr. Igusa's group also joined the meeting as she had experience in hospital-related research studies.

Highlights:

- As for ICU patients, the problem is too broad, so a case-by-case approach is preferred. We need to focus on one specific patient because the evacuation and transfer process for each patient are different and depending on the scenario and how ill the patient is, the process would vary. The problem is too broad, and it needs to be broken down. Modeling all patients together would not be the best and most practical approach. According to Dr. Igusa, this is one of those problems that should be approached from bottom.
- Marietta pointed out, from her knowledge and experience of working with patients and physicians, that hospitals would be interested in a model for one specific type of patient and for a specific scenario.
- To decide on how much we may want to go deep into the problem of ICU patients (e.g. focus on transplant patients or on heart transplant patients), we need the physicians' opinions.

– It is very important to set a specific scenario as evacuation procedures differ drastically in different scenarios.

Meeting #4

Date: November 13, 2018

Location: Office of the Provost, Johns Hopkins University

Expert: Dr. Jonathan Links, Vice Provost and Chief Risk and Compliance Officer

Highlights:

- Why agent-based modeling when we can discretize evacuation processes of different patients and model the indirect interactions between patients and staff due to mutual needs for equipment as a prioritization issue.
- Agent interaction exists among ambulatory patients and between ambulatory patients and hospital staff when they voluntarily help those having trouble walking. Moreover, agent-based modeling helps us track the patients and find main reasons for evacuation delays. As these are the main advantages of using agent-based modeling for hospital evacuation, we should have a specific focus on altruism, staff support, and agent tracking.
- I need to have a section in the dissertation dedicated to a discussion on what agent-based modeling brings for us that other modeling approaches do not.

Meeting #5

Date: November 15, 2018

Location: USU National Center for Disaster Medicine and Public Health

Expert: Dr. Thomas Kirsch, Director and Professor, National Center for Disaster Medicine and Public Health, Uniformed Services University of the Health Sciences, formerly Professor of Emergency Medicine and Public Health at Johns Hopkins University

Highlights:

- The criticality of hospital evacuation and its complications are acknowledged by all healthcare professionals.
- There are different Levels of Care identified for ICU patients. This idea can be the criteria for classification of ICU patients and/or required equipment.
- There is almost no available data on hospital evacuation. Certain hospitals and health systems (specifically in southern states) that have prior evacuation experiences possess data on their evacuation procedures, however, these data are completely inaccessible to research societies.
- ASPR (Assistant Secretary for Preparedness and Response) has initiated the Hospital Preparedness Program (HPP) to enhance the ability of hospitals and healthcare systems to prepare for and respond to bioterrorism and other public health emergencies.
- Southeast Texas Regional Advisory Council (SETRAC) is probably the best source of data for hospital evacuation but the database is not available to any public or private entity.

- Evacuation time per se is not interesting, instead required resources as a function of available time for safe evacuation is a more interesting idea.
- Vertical evacuation of hospital buildings is not interesting, but patient distribution to other hospitals is a major challenge.
- Dr. Kirsch is working on a review of current models (beyond those available publicly) for hospital evacuation for ASPR aiming at developing a grand model for hospital evacuation.
- Equipment can be classified as physiological needs (e.g. ventilators and ECMO), patient-care needs (e.g. monitors) and regular needs (e.g. wheelchairs); or from a simpler perspective clinical vs. non-clinical needs (specifically for ICU patients).
- There are a few state-level ICU bed database and patient transfer systems (NY, MD, and TX); however, these databases are not much practical, that is why hospitals still make phone calls to find ICU beds during evacuations.
- For classification of ICU patients, it may not be a good and practical approach to go deeper than ICU, NICU, PICU, etc. The problem will be too complex and with no data, there is in fact absolutely no advantage from a practical point of view.

Informal Meetings

There have been many informal conversations and discussions with many students, professors, and hospital staff on the challenges of hospital evacuation and evacuation modeling. Although these conversations are not recorded, they have had a major impact on my understanding of the subject matter. Particularly, I learned a lot in a conversation with two nurses from the MedStar Union Memorial Hospital (whom I interrupted during their lunch time in a local restaurant) about how hospitals may have their own policies on limiting mobility of specific patients. As an example, new mothers that have given birth within the last 24 hours may not be allowed to leave their rooms without the hospitals staff permission, whether they have their babies in room or not.

Bibliography

[1] D. Mileti, Disasters by design: A reassessment of natural hazards in the United States. Joseph Henry Press., 1999.

[2] C. Bach, S. Bouchon, A. Fekete, J. Birkmann, D. Serre, Adding value to critical infrastructure research and disaster risk management: the resilience concept., SAPI EN. S. Surv. Perspect. Integr. Environ. Soc. 6 (2013).

[3] F. Haghpanah, Multilevel alignment of critical infrastructure protection and resilience (CIP-R) programmes: a systematic analysis of international good. MS Thesis. Politecnico di Milano, Milan, Italy. practices, 2015.

[4] S. Bouchon, The vulnerability of interdependent critical infrastructures systems: Epistemological and conceptual state of the art. Institute for the Protection and Security of the Citizen, Joint Research Centre, European Commission, 99., 2006.

[5] UN, Living with risk: A global review of disaster reduction initiatives (Vol. 1). United Nations Publications., 2004. https://www.undrr.org/publication/living-risk-global-review-disaster-reduction-initiatives.

[6] C. Pursiainen, The challenges for European critical infrastructure protection, Eur. Integr. 31 (2009) 721–739.

[7] M. De Bruijne, M. Van Eeten, Systems that should have failed: critical infrastructure protection in an institutionally fragmented environment, J. Contingencies Cris. Manag. 15 (2007) 18–29.

[8] S. Menoni, C. Margottini, (Eds.), Inside risk: a strategy for sustainable risk mitigation.

Springer Science & Business Media., 2011.

[9] J. Covington, D.M. Simpson, An overview of disaster preparedness literature: Building blocks for an applied Bay Area template. Center for Hazards Research and Policy Development. Working Paper, 2006.

[10] ODPM, Assessing the Impacts of Spatial Interventions: Regeneration, Renewal and Regional Development, The 3Rs guidance., 2004.

[11] A. Boin, E. Stern, B. Sundelius, The politics of crisis management: Public leadership under pressure. Cambridge University Press., 2016.

[12] S.K. Schneider, Flirting with disaster: Public management in crisis situations. ME Sharpe., 1995.

[13] A. Schadschneider, W. Klingsch, H. Klüpfel, T. Kretz, C. Rogsch, A. Seyfried, Evacuation Dynamics: Empirical Results, Modeling and Applications, Extrem. Environ. Events. (2011) 517–550. https://doi.org/10.1007/978-1-4419-7695-6_29.

[14] R.W. Perry, The social psychology of civil defense. Lexington Books., 1982.

[15] P. Bolton, Managing pedestrians during evacuations of metropolitan areas (No. FHWA-HOP-07-066). United States. Federal Highway Administration., 2007.

[16] K. Elder, S. Xirasagar, N. Miller, S.A. Bowen, S. Glover, C. Piper, African Americans' decisions not to evacuate New Orleans before Hurricane Katrina: A qualitative study., Am. J. Public Health. 97 (2007) S124–S129.

[17] D. Helbing, L. Buzna, A. Johansson, T. Werner, A. Johansson, T. Werner, Self-Organized Pedestrian Crowd Dynamics : Experiments , Simulations , and Design Solutions, Transp. Sci. 39 (2005) 1–24. https://doi.org/10.1287/trsc.1040.0108.

[18] C. Arnold, Design guide for improving school safety in earthquakes, floods, and high winds: providing protection to people and buildings. US Department of Homeland

Security, Federal Emergency Management Agency., 2004.

[19] H. Fischer, Über die Leistungsfähigkeit von Türen, Gängen und Treppen bei ruhigem, dichtem Verkehr (Doctoral dissertation, Druck von Richard Holle)., 1933.

[20] D. Dieckmann, Die feuersicherheit in theatern. K. Techn.-hochschule, Hannover. (in German), 1906.

[21] M. Ahrens, High-rise building fires. NFPA (National Fire Protection Association): Quincy, MA, USA., 2016.

[22] E. Ronchi, D. Nilsson, Fire evacuation in high-rise buildings: a review of human behaviour and modelling research, Fire Sci. Rev. 2 (2013) 7. https://doi.org/10.1186/2193-0414-2-7.

[23] ADA, Am. With Disabil. Act 1990. (1990). https://www.ada.gov/ta-pubs-pg2.htm.

[24] WHO, International classification of functioning, disability and health: ICF. World Health Organization., 2001.

[25] American Medical Response, U.S. Department of Health and Human Services, Guidelines for Evacuation of Individuals with Disabilities During Disasters, 2013. https://www.amr.net/solutions/federal-disaster-response-team/references-and-resources/guidelines-for-evacuation-of-individuals-with-disa.pdf.

[26] Harvard School of Public Health, MDPH Hospital Evacuation Toolkit, 2014. https://www.mass.gov/lists/hospital-evacuation-toolkit.

[27] J. Bagaria, C. Heggie, J. Abrahams, V. Murray, Evacuation and sheltering of hospitals in emergencies: a review of international experience., Prehosp. Disaster Med. 24 (2009) 461–467.

[28] N. Squillace, Hospital evacuations: Historical precedence and modern preparedness. Master's Thesis. Wright State University Boonshoft School of, 2010.

[29] H. Tanaka, A. Iwai, J. Oda, Y. Kuwagata, T. Matsuoka, T. Shimazu, T. Yoshioka, Overview of evacuation and transport of patients following the 1995 Hanshin-Awaji earthquake, J. Emerg. Med. 16 (1998) 439–444.

[30] K.H. Sexton, L.M. Alperin, J.D. Stobo, Lessons from Hurricane Rita: the University of Texas Medical Branch Hospital's evacuation., Acad. Med. 82 (2007) 792–796.

[31] I.L. Taylor, Hurricane Katrina's impact on Tulane's teaching hospitals, Trans. Am. Clin. Climatol. Assoc. 118 (2007).

[32] et al. Fuzak, Julia K., Mass transfer of pediatric tertiary care hospital inpatients to a new location in under 12 hours: lessons learned and implications for disaster preparedness, J. Pediatr. 157 (2010) 138–143.

[33] S. Orlando, M.L. Bernard, P. Mathews, Neonatal nursing care issues following a natural disaster: lessons learned from the Katrina experience, J. Perinat. Neonatal Nurs. 22 (2008) 147–153.

[34] M. Blau, Irma forces at least 35 hospitals to evacuate patients. Here's a rundown, STAT News. (2017). https://www.statnews.com/2017/09/09/irma-hospital-evacuations-rundown/.

[35] TRACIE, EVACUATING A REGION: How a Healthcare Coalition Helped Evacuate 1504 Patients from 45 Facilities after Hurricane Harvey, HHS. (2017). https://files.asprtracie.hhs.gov/documents/aspr-tracie-evacuating-a-region-post-hurricane-harvey-508.pdf.

[36] E. Sternberg, G.C. Lee, D. Huard, Counting crises: US hospital evacuations, 1971-1999, Prehosp Disaster Med. 19 (2004) 150–157.

[37] A. Sharma, S. Mace, Reviewing Disasters: Hospital Evacuations in the United States from 2000 to 2017., Prehosp. Disaster Med. 34 (2019) s22.

[38] et al. Espiritu, Michael, Evacuation of a neonatal intensive care unit in a disaster: lessons from Hurricane Sandy, Pediatrics. 134 (2014) e1662–e1669.

[39] P. Manion, I.J. Golden, Vertical evacuation drill of an intensive care unit: design, implementation, and evaluation, Disaster Manag. Response. 2 (2004) 14–19.

[40] J.R. Gildea, S. Etengoff, Vertical evacuation simulation of critically ill patients in a hospital, Prehosp. Disaster Med. 20 (2005) 243–248.

[41] M. Femino, S. Young, V.C. Smith, Hospital-based emergency preparedness: evacuation of the neonatal intensive care unit—the smallest and most vulnerable population., Pediatr. Emerg. Care. 29 (2013) 107–113.

[42] FEMA, Framework for Healthcare Emergency Management, FEMA. (n.d.). https://cdp.dhs.gov/find-training/course/AWR-900.

[43] JCAHO, hospitals - The Joint Commission, JCAHO. (n.d.). file:///C:/Users/Fardad/Downloads/SEA_WPV_TJC_requirements1.pdf.

[44] J.M. Epstein, Agent-based computational models and generative social science, Complexity. 4 (1999) 41–60.

[45] R.M. Axelrod, The complexity of cooperation: Agent-based models of competition and collaboration. Princeton University Press., 1997.

[46] C. Adami, J. Schossau, A. Hintze, Evolutionary game theory using agent-based methods, Phys. Life Rev. 19 (2016) 1–26.

[47] J. Groeneveld, B. Müller, C.M. Buchmann, G. Dressler, C. Guo, N. Hase, F. Hoffmann, F. John, C. Klassert, T. Lauf, V. Liebelt, Theoretical foundations of human decision-making in agent-based land use models–A review, Environ. Model. Softwar. 87 (2017) 39–48.

[48] J.M. Epstein, Generative social science: Studies in agent-based computational

modeling. Princeton University Press, 2006.

[49] L. Tesfatsion, K.L. (Eds. . Judd, Handbook of computational economics: agent-based computational economics. Elsevier, 2006.

[50] L. Hamill, G.N. Gilbert, Agent-based modelling in economics. Chichester: John Wiley & Sons., 2016.

[51] Q. Huang, D.C. Parker, T. Filatova, S. Sun, A review of urban residential choice models using agent-based modeling, Environ. Plan. B Plan. Des. 41 (2014) 661–689.

[52] D.G. Brown, D.T. Robinson, Effects of heterogeneity in residential preferences on an agent-based model of urban sprawl, Ecol. Soc. 11 (2006).

[53] A.H. Auchincloss, A. V. Diez Roux, A new tool for epidemiology: the usefulness of dynamic-agent models in understanding place effects on health, Am. J. Epidemiol. 168 (2008) 1–8.

[54] M. Tracy, M. Cerdá, K.M. Keyes, Agent-based modeling in public health: current applications and future directions, Annu. Rev. Public Health. 39 (2018) 77–94.

[55] D. Vlachos, P. Georgiadis, E. Iakovou, A system dynamics model for dynamic capacity planning of remanufacturing in closed-loop supply chains, Comput. Oper. Res. 34 (2007) 367–394.

[56] W.A.N.G. Jifeng, L.U. Huapu, P.E.N.G. Hu, System dynamics model of urban transportation system and its application, J. Transp. Syst. Eng. Inf. Technol. 8 (2008) 83–89.

[57] et al. Links, Jonathan M., COPEWELL: a conceptual framework and system dynamics model for predicting community functioning and resilience after disasters, Disaster Med. Public Health Prep. 12 (2018) 127–137.

[58] N.R. Draper, H. Smith, Applied regression analysis (Vol. 326). John Wiley & Sons.,

1998.

[59] J.H. Harding, Mesoscopic modelling, Curr. Opin. Solid State Mater. Sci. 2 (1997) 728–732.

[60] A.M. Stoneham, J.H. Harding, Not too big, not too small: the appropriate scale., Nat. Mater. 2 (2003) 77–83.

[61] P. Kachroo, Pedestrian dynamics: Mathematical theory and evacuation control. CRC Press., 2018.

[62] E.F. Toro, Riemann solvers and numerical methods for fluid dynamics: a practical introduction. Springer Science & Business Media., 2013.

[63] et al. Farra, Sharon L., Comparative Cost of Virtual Reality Training and Live Exercises for Training Hospital Workers for Evacuation, CIN Comput. Informatics, Nurs. 37 (2019) 446–454.

[64] C. Verni, A hospital system's response to a hurricane offers lessons, including the need for mandatory interfacility drills., Health Aff. 31 (2012) 1814–1821.

[65] C.W. Johnson, Using Computer Simulations to Support A Risk-Based Approach For Hospital Evacuation, A Dep. Comput. Sci. Briefing. Univ. Glas. (2006) 1–24.

[66] X. Zheng, T. Zhong, M. Liu, Modeling crowd evacuation of a building based on seven methodological approaches, Build. Environ. 44 (2009) 437–445.

[67] Z. Liu, C.C. Jacques, S. Szyniszewski, J.K. Guest, B.W. Schafer, T. Igusa, J. Mitrani-Reiser, Agent-based simulation of building evacuation after an earthquake: coupling human behavior with structural response, Nat. Hazards Rev. 17 (2015) 4015019.

[68] G.K. Still, Crowd dynamics [Ph. D. thesis], Univ. Warwick, Coventry, UK. (2000).

[69] D. Helbing, I. Farkas, T. Vicsek, Simulating dynamical features of escape panic, Nature, v. 407, pp 487-490, (2000).

[70] X. Pan, C.S. Han, K. Dauber, K.H. Law, A multi-agent based framework for the simulation of human and social behaviors during emergency evacuations, Ai Soc. 22 (2007) 113–132.

[71] J. Shi, A. Ren, C. Chen, Agent-based evacuation model of large public buildings under fire conditions, Autom. Constr. 18 (2009) 338–347.

[72] Y. Lin, I. Fedchenia, B. LaBarre, R. Tomastik, Agent-based simulation of evacuation: An office building case study, in: Pedestr. Evacuation Dyn. 2008, Springer, 2010: pp. 347–357.

[73] E. Mas, A. Suppasri, F. Imamura, S. Koshimura, Agent-based simulation of the 2011 great east japan earthquake/tsunami evacuation: An integrated model of tsunami inundation and evacuation, J. Nat. Disaster Sci. 34 (2012) 41–57.

[74] B. Anguelov, Video game pathfinding and improvements to discrete search on grid-based maps, University of Pretoria, 2012.

[75] I. Karamouzas, P. Heil, P. van Beek, M.H. Overmars, A Predictive Collision Avoidance Model for Pedestrian Simulation., MIG. 9 (2009) 41–52.

[76] A.S. Mordvintsev, V. V Krzhizhanovskaya, M.H. Lees, P.M.A. Sloot, Simulation of city evacuation coupled to flood dynamics, in: Pedestr. Evacuation Dyn. 2012, Springer, 2014: pp. 485–499.

[77] J. Van Den Berg, S. Guy, M. Lin, D. Manocha, Reciprocal n-body collision avoidance, Robot. Res. (2011) 3–19.

[78] M. Di Mauro, M. Lees, K. Megawati, Z. Huang, Pedestrian-vehicles interaction during evacuation: agent-based hybrid evacuation modelling of Southeast Asian cities, in: Pedestr. Evacuation Dyn. 2012, Springer, 2014: pp. 435–443.

[79] B.R. Werberich, C.O. Pretto, H.B.B. Cybis, Simulation Model for Vehicle and

Pedestrian Interaction Considering Road Crossing Activities, in: Pedestr. Evacuation Dyn. 2012, Springer, 2014: pp. 917–924.

[80] J. Poulos, A., Tocornal, F., de la Llera, J.C. and Mitrani-Reiser, Validation of an agent-based building evacuation model with a school drill, Transp. Res. Part C Emerg. Technol. 97 (2018) 82–95.

[81] U. Wilensky, I. Evanston, NetLogo: Center for connected learning and computer-based modeling, Northwest. Univ. Evanston,. 4952 (1999).

[82] G. Filomeno, I.I. Romero, R.L. Vasquez, D.H. Biedermann, M. Bügler, Construction site pedestrian simulation with moving obstacles, in: 28 Forum Bauinfomatik, Leibniz Univ. Hann., 2016.

[83] K.N. McGuire, G.C.H.E. de Croon, K. Tuyls, A comparative study of bug algorithms for robot navigation, Rob. Auton. Syst. 121 (2019) 103261. https://doi.org/10.1016/j.robot.2019.103261.

[84] V. Lumelsky, A. Stepanov, Dynamic path planning for a mobile automaton with limited information on the environment, IEEE Trans. Automat. Contr. 31 (1986) 1058–1063.

[85] J. Ng, T. Bräunl, Performance comparison of bug navigation algorithms, J. Intell. Robot. Syst. 50 (2007) 73–84.

[86] P.G. Gipps, B. Marksjö, A micro-simulation model for pedestrian flows, Math. Comput. Simul. 27 (1985) 95–105.

[87] E. Papadimitriou, G. Yannis, J. Golias, A critical assessment of pedestrian behaviour models, Transp. Res. Part F Traffic Psychol. Behav. 12 (2009) 242–255.

[88] I. Kamon, E. Rivlin, Sensory-based motion planning with global proofs, IEEE Trans. Robot. Autom. 13 (1997) 814–822.

[89] R.A. Langer, L.S. Coelho, G.H.C. Oliveira, K-Bug, a new bug approach for mobile

robot's path planning, in: Control Appl. 2007. CCA 2007. IEEE Int. Conf., 2007: pp. 403–408.

[90] I. Kamon, E. Rimon, E. Rivlin, Tangentbug: A range-sensor-based navigation algorithm, Int. J. Rob. Res. 17 (1998) 934–953.

[91] N. Buniyamin, W.A.J. Wan Ngah, N. Sariff, Z. Mohamad, A simple local path planning algorithm for autonomous mobile robots, Int. J. Syst. Appl. Eng. Dev. 5 (2011) 151–159.

[92] J.S. Ng, An analysis of mobile robot navigation algorithms in unknown environments, University of Western Australia, 2010.

[93] J.-M. Walker Rousseau, Informe Técnico de Evaluación: Simulacro Macrozona de Terremoto y Tsunami, Evacuación del Borde Costero. National Office of Emergency of the Ministry of Interior and Security, Santiago, Chile, 2013.

[94] P.A. Catalán, R. Aránguiz, G. González, T. Tomita, R. Cienfuegos, J. González, M.N. Shrivastava, K. Kumagai, C. Mokrani, P. Cortés, A. Gubler, The 1 April 2014 Pisagua tsunami: Observations and modeling, Geophys. Res. Lett. 42 (2015) 2918–2925. https://doi.org/10.1002/2015GL063333.

[95] ONEMI, RISK MODEL OF HUMAN EVACUATION UNDER EARTHQUAKE LOADS, Protocolo ONEMISHOA para evento de tsunami en las costas de Chile (ONEMI-SHOA protocol for tsunami event on the coasts of Chile), 2011. http://www.elmostrador.cl/media/%0A2012/05/Protocolo_SHOA_para_respuesta_Usuarios.pdf (accessed October 3, 2019).

[96] S. Castro, A. Poulos, J.C. Herrera, J.C. de la Llera, Modeling the impact of earthquake-induced debris on tsunami evacuation times of coastal cities, Earthq. Spectra. 55 (2019) 137–158. https://doi.org/10.1193/101917EQS218M.

[97] P. Aguirre, J. Vásquez, J.C. de la Llera, J. González, G. González, Earthquake damage assessment for deterministic scenarios in Iquique, Chile, Nat. Hazards. 92 (2018) 1433–1461. https://doi.org/10.1007/s11069-018-3258-3.

[98] S. Hoogendoorn, W. Daamen, Microscopic calibration and validation of pedestrian models: Cross-comparison of models using experimental data, Traffic Granul. Flow'05. (2007) 329–340.

[99] W. Tobler, Three Presentations on Geographical Analysis and Modeling: Non-Isotropic Geographic Modeling; Speculations on the Geometry of Geography; and Global Spatial Analysis, Santa Barbara CA, 1993. https://escholarship.org/content/qt05r820mz/qt05r820mz.pdf (accessed October 7, 2019).

[100] N. Gilbert, Agent-based models, Sage Publications, 2008.

[101] T.C. Schelling, Dynamics Model of Segregation, J. Math. Sociol. 1 (1971) 143–186.

[102] Thomas C. Schelling Facts, Noble Prize. (2005). https://www.nobelprize.org/prizes/economic-sciences/2005/schelling/facts/ (accessed February 17, 2020).

[103] E. Hatna, I. Benenson, The Schelling model of ethnic residential dynamics: Beyond the integrated-segregated dichotomy of patterns, J. Artif. Soc. Soc. Simul. 15 (2012).

[104] V.A. Oven, N. Cakici, Modelling the evacuation of a high-rise office building in Istanbul, Fire Saf. J. 44 (2009) 1–15.

[105] N. Zarboutis, N. Marmaras, Searching efficient plans for emergency rescue through simulation: the case of a metro fire, Cogn. Technol. Work. 6 (2004) 117–126.

[106] K. Christensen, Y. Sasaki, Agent-Based emergency evacuation simulation with individuals with disabilities in the population, J. Artif. Soc. Soc. Simul. 11 (2008) 1–13.

[107] M. Manley, Y.S. Kim, K. Christensen, A. Chen, Modeling emergency evacuation of individuals with disabilities in a densely populated airport, Transp. Res. Rec. 2206 (2011) 32–38.

[108] M. Manley, Y.S. Kim, Exitus: Agent-based evacuation simulation for individuals with disabilities in a densely populated sports arena, Int. J. Intell. Inf. Technol. 8 (2012) 1–13.

[109] J. Koo, Y.S. Kim, B.I. Kim, Estimating the impact of residents with disabilities on the evacuation in a high-rise building: A simulation study, Simul. Model. Pract. Theory. 24 (2012) 71–83.

[110] M.J. Hurley, D.T. Gottuk, J.R. Hall Jr, K. Harada, E.D. Kuligowski, M. Puchovsky, J.M. Watts Jr, C.J. eds. Wieczorek, SFPE handbook of fire protection engineering. Springer, 2015.

[111] L. Shi, Q. Xie, X. Cheng, L. Chen, Y. Zhou, R. Zhang, Developing a database for emergency evacuation model, Build. Environ. 44 (2009) 1724–1729. https://doi.org/10.1016/j.buildenv.2008.11.008.

[112] D.R. Bish, H. Tarhini, R. Amara, R. Zoraster, N. Bosson, M. Gausche-Hill, Modeling to Optimize Hospital Evacuation Planning in EMS Systems, Prehospital Emerg. Care. 21 (2017) 503–510. https://doi.org/10.1080/10903127.2017.1302531.

[113] E.D. Kuligowski, R.D. Peacock, A review of building evacuation models. Gaithersburg, MD: US Department of Commerce, National Institute of Standards and Technology, 2005.

[114] E.W. Dijkstra, A note on two problems in connexion with graphs, Numer. Math. 1 (1959) 269–271.

[115] R.W. Floyd, Algorithm 97: shortest path, Commun. ACM. 5 (1962) 345.

[116] S. Warshall, A theorem on boolean matrices, J. ACM. 9 (1962) 11–12.

[117] R. Bellman, On a routing problem, Q. Appl. Math. 16 (1958) 87–90.

[118] L.R. Ford Jr, Network flow theory (No. P-923), RAND CORP St. MONICA CA. (1956).

[119] P.E. Hart, N.J. Nilsson, B. Raphael, A formal basis for the heuristic determination of minimum cost paths, IEEE Trans. Syst. Sci. Cybern. 4 (1968) 100–107.

[120] N. Bellomo, D. Clarke, L. Gibelli, P. Townsend, B.J. Vreugdenhil, Human behaviours in evacuation crowd dynamics : From modelling to " big data " toward crisis management, Phys. Life Rev. 18 (2016) 1–21. https://doi.org/10.1016/j.plrev.2016.05.014.

[121] F. Lamarche, S. Donikian, Crowd of virtual humans: a new approach for real time navigation in complex and structured environments, Comput. Graph. Forum. 23 (2004) 509–518.

[122] D. Helbing, P. Molnar, Social force model for pedestrian dynamics, Phys. Rev. E. 51 (1995) 4282–4286.

[123] J. Van Den Burg, S.J. Guy, M. Lin, D. Manocha, Reciprocal n -body Collision Avoidance, Robot. Res. Springer, Berlin, Heidelb. (2011) 1–16.

[124] X. Pan, Computational modeling of human and social behaviors for emergency egress analysis., Stanford Univ., Stanford, CA., 2006.

[125] M.L. Chu, P. Parigi, K. Law, J.-C. Latombe, Modeling social behaviors in an evacuation simulator, Comput. Anim. Virtual Worlds. 25 (2014) 373–382.

[126] S. Horiuchi, Y. Murozaki, A. Hokugo, A case study of fire and evacuation in a multi-purpose office building, Osaka, Japan, Fire Saf. Sci. 1 (1986) 523–532.

[127] R.D. Peacock, J.D. Averill, E.D. Kuligowski, Egress from the World Trade Center

towers on September 11, 2001, Fire Technol. 49 (2013) 7–35.

[128] C.W. Johnson, Lessons from the evacuation of the world trade centre, 9/11 2001 for the development of computer-based simulations, Cogn. Technol. Work. 7 (2005) 214–240.

[129] R. Nagai, M. Fukamachi, T. Nagatani, Evacuation of crawlers and walkers from corridor through an exit, Phys. A Stat. Mech. Its Appl. 367 (2006) 449–460. https://doi.org/10.1016/j.physa.2005.11.031.

[130] A. Seyfried, O. Passon, B. Steffen, M. Boltes, T. Rupprecht, W. Klingsch, New insights into pedestrian flow through bottlenecks, Transp. Sci. 43 (2009) 395–406. https://doi.org/10.1287/trsc.1090.0263.

[131] T. Rinne, K. Tillander, Peter Grönberg, Data collection and analysis of evacuation situations, 2010.

[132] S.C. Wong, W.L. Leung, S.H. Chan, W.H.K. Lam, N.H.C. Yung, C.Y. Liu, P. Zhang, Bidirectional pedestrian stream model with oblique intersecting angle, J. Transp. Eng. 136 (2010) 234–242.

[133] S.P. Simonovic, S. Ahmad, Computer-based model for flood evacuation emergency planning, Nat. Hazards. 34 (2005) 25–51. https://doi.org/10.1007/s11069-004-0785-x.

[134] B. Zou, C. Lu, Y. Li, Simulation of a hospital evacuation including wheelchairs based on modified cellular automata, Simul. Model. Pract. Theory. 99 (2020) 1–18. https://doi.org/10.1016/j.simpat.2019.102018.

[135] B.D. Greenshields, W. Channing, H. Miller, A study of traffic capacity, Highw. Res. Board Proceedings. Natl. Res. Counc. (USA), Highw. Res. Board. 1935 (1935).

[136] J.L. Drake, J.L. Schofer, A statistical analysis of speed-density hypotheses, Highw. Res.

Rec. 154 (1966).

[137] R.T. Underwood, Speed, volume, and density relationship: Quality and theory of traffic flow, Yale Bur. Highw. Traffic. (1961) 141–188.

[138] M.R. Wigan, Why should we worry about pedestrians?, in: Conf. Aust. Institutes Transp. Res. (CAITR), 15th, 1993, Park. Victoria, Aust., 1993.

[139] R.A. Smith, J.F. Dickie, (Eds.), Engineering for Crowd Safety.Elsevier, Amsterdam., 1993.

[140] A. Toshiyuki, Prediction systems of passenger flow, in: Eng. Crowd Saf., 1993: pp. 249–258.

[141] R.A. Smith, Volume flow rates of densely packed crowds, in: Eng. Crowd Saf., 1993: pp. 313–319.

[142] G.E. Bradley, A proposed mathematical model for computer prediction of crowd movements and their associated risks, in: Proc. Int. Conf. Eng. Crowd Saf., 1993: pp. 303–313.

[143] S.Z. Selim, A.H. Al-Rabeh, On the modeling of pedestrian flow on the Jamarat bridge, Transp. Sci. 25 (1991) 257–263.

[144] T. Tanaka, A study for performance based design of means of escape in fire, Fire Saf. Sci. 3 (1991) 729–738.

[145] C. McPhail, The myth of the madding crowd. Routledge., 1991.

[146] R.L. Hughes, The flow of human crowds, Annu. Rev. Fluid Mech. 35 (2003) 169–182. https://doi.org/10.1146/annurev.fluid.35.101101.161136.

[147] M.J. Lighthill, G.B. Whitham, On kinematic waves I. Flood movement in long rivers, in: Proc. R. Soc. London. Ser. A. Math. Phys. Sci., 1955: pp. 281–316.

[148] M.J. Lighthill, G.B. Whitham, On kinematic waves II. A theory of traffic flow on long

crowded roads, in: Proc. R. Soc. London. Ser. A. Math. Phys. Sci., 1955: pp. 317–345.

[149] P.I. Richards, Shock waves on the highway, Oper. Res. 4 (1956) 42–51.

[150] H.J. Payne, Model of freeway traffic and control, Math. Model Public Syst. (1971) 51–61.

[151] G.B. Whitham, Linear and nonlinear waves (Vol. 42). John Wiley & Sons., 1975.

[152] M. Rascle, An improved macroscopic model of traffic flow: derivation and links with the Lighthill-Whitham model, Math. Comput. Model. 35 (2002) 581–590.

[153] A.A.T.M. Aw, M. Rascle, Resurrection of "second order" models of traffic flow, SIAM J. Appl. Math. 60 (2000) 916–938.

[154] H.M. Zhang, A theory of nonequilibrium traffic flow, Transp. Res. Part B Methodol. 32 (1998) 485–498.

[155] H.M. Zhang, A non-equilibrium traffic model devoid of gas-like behavior, Transp. Res. Part B Methodol. 36 (2002) 275–290.

[156] R.L. Hughes, A continuum theory for the flow of pedestrians, Transp. Res. Part B Methodol. 36 (2002) 507–535. https://doi.org/10.1016/S0191-2615(01)00015-7.

[157] L. Huang, S.C. Wong, M. Zhang, C.W. Shu, W.H.K. Lam, Revisiting Hughes' dynamic continuum model for pedestrian flow and the development of an efficient solution algorithm, Transp. Res. Part B Methodol. 43 (2009) 127–141. https://doi.org/10.1016/j.trb.2008.06.003.

[158] Y. Xia, S.C. Wong, M. Zhang, C.W. Shu, W.H. Lam, An efficient discontinuous Galerkin method on triangular meshes for a pedestrian flow model, Int. J. Numer. Methods Eng. 76 (2008) 337–350.

[159] Y. Xia, S.C. Wong, C.W. Shu, Dynamic continuum pedestrian flow model with memory effect, Phys. Rev. E. 79 (2009).

[160] B. Piccoli, A. Tosin, Pedestrian flows in bounded domains with obstacles, Contin. Mech. Thermodyn. 21 (2009) 85–107.

[161] Y.Q. Jiang, P. Zhang, S.C. Wong, R.X. Liu, A higher-order macroscopic model for pedestrian flows, Phys. A Stat. Mech. Its Appl. 389 (2010) 4623–4635. https://doi.org/10.1016/j.physa.2010.05.003.

[162] M. Twarogowska, P. Goatin, R. Duvigneau, Comparative study of macroscopic pedestrian models, Transp. Res. Procedia. 2 (2014) 477–485. https://doi.org/10.1016/j.trpro.2014.09.063.

[163] D. Helbing, A Fluid-Dynamic Model for the Movement of Pedestrians, Complex Syst. 6 (1992) 391–415.

[164] A. Kormanová, A Review on Macroscopic Pedestrian Flow Modelling, Acta Inform. Pragensia. 2 (2013) 39–50. https://doi.org/10.18267/j.aip.22.

[165] M.A. Hassan, R.J. Rogers, Friction modelling of preloaded tube contact dynamics, Nucl. Eng. Des. 235 (2005) 2349–2357.

[166] J. Qian, Y.T. Zhang, H.K. Zhao, Fast sweeping methods for eikonal equations on triangular meshes, SIAM J. Numer. Anal. 45 (2007) 83–107.

[167] H. Zhao, Parallel implementations of the fast sweeping method, J. Comput. Math. 25 (2007) 421–429.

[168] H.K. Zhao, A fast sweeping method for eikonal equations, Math. Comput. 74 (2005) 603–627. https://doi.org/10.1137/060670298.

[169] W. Jin, H.M. Zhang, Solving the Payne-Whitham traffic flow model as a hyperbolic system of conservation laws with relaxation, Transp. Sci. (2001).

[170] K. Ando, H. Ota, T. Oki, Forecasting the flow of people, Railw. Res. Rev. 45 (1988) 8–14.

[171] S.A. AlGadhi, H.S. Mahmassani, Simulation of crowd behavior and movement: Fundamental relations and application, Transp. Res. Rec. 1320 (1991).

[172] J.W. Forrester, The beginning of system dynamics, McKinsey Q. (1995) 4–17.

[173] A.A. Berryman, The Orgins and Evolution of Predator-Prey Theory, Ecology. 73 (1992) 1530–1535.

[174] A.J. Lotka, Elements of physical biology. Williams and Wilkins, Baltimore, MD, USA, A Metacommunity Herbiv. (1925).

[175] V. Volterra, Variazioni e fluttuazioni del numero d'individui in specie animali conviventi, Mem. Della Regia Accad. Naz. Del Lincei Ser. 62 (1926) 31–113.

[176] R.G. Little, E.A. Weaver, Protection from extreme events: Using a socio-technological approach to evaluate policy options, Int. J. Emerg. Manag. 2 (2005) 263–274. https://doi.org/10.1504/IJEM.2005.008739.

[177] B.P. Thompson, L.C. Bank, Use of system dynamics as a decision-making tool in building design and operation, Build. Environ. 45 (2010) 1006–1015. https://doi.org/10.1016/j.buildenv.2009.10.008.

[178] S.B. Laska, Homeowner adaptation to flooding An application of the general hazards coping theory, Environ. Behav. 22 (1990) 320–357.

[179] J. Voyer, M.D. Dean, C.B. Pickles, Hospital evacuation in disasters: uncovering the systemic leverage using system dynamics, Int. J. Emerg. Manag. 12 (2016) 152–167.

[180] A. Anjomshoae, A. Hassan, C. Samuel, W.K. Yew, Effect of information sharing and capacity adjustment on healthcare service supply Chain: The case of flood disaster, J. Appl. Environ. Biol. Sci. 7 (2017) 57–64.

[181] T.S. Shen, ESM: A building evacuation simulation model, Build. Environ. 40 (2005) 671–680. https://doi.org/10.1016/j.buildenv.2004.08.029.

[182] H.E. Nelson, F.W. Mowrer, SFPE Handbook of Fire Protection Engineering. National Fire Protection Association, Quincy, MA, 1995.

[183] I. Karamouzas, P. Heil, P. Van Beek, M.H. Overmars, A predictive collision avoidance model for pedestrian simulation, in: Int. Work. Motion Games. Springer, Berlin, Heidelberg, 2009, 2009: pp. 41–52.

[184] Y. Zou, V.A. Fonoberov, M. Fonoberova, I. Mezic, I.G. Kevrekidis, Model reduction for agent-based social simulation: Coarse-graining a civil violence model, Phys. Rev. E - Stat. Nonlinear, Soft Matter Phys. 85 (2012) 1–13. https://doi.org/10.1103/PhysRevE.85.066106.

[185] S.E. Page, Aggregation in agent-based models of economies, Knowl. Eng. Rev. 27 (2012) 151–162. https://doi.org/10.1017/S0269888912000112.

[186] D. Heard, G. V. Bobashev, R.J. Morris, Reducing the complexity of an agent-based local heroin market model, PLoS One. 9 (2014) 1–10. https://doi.org/10.1371/journal.pone.0102263.

[187] H.A. Simon, On a class of skew distribution functions, Biometrika. 42 (1955) 425–440.

[188] P. Bak, How Nature Works: The Science of Self Organized Criticality. Springer Verlag. New York, 1996.

[189] R. Axtell, The emergence of firms in a population of agents: local increasing returns, unstable Nash equilibria, and power law size distributions. Brookings Institution Discussion paper: Center on Social and Economic Dynamics, 1999.

[190] R. Axtell, Zipf distribution of U.S. firm sizes, Science (80-.). 293 (2001) 1818–1820.

[191] A.L. Barabási, Linked: how everything is connected to everything else and what it means for business." Science, and Everyday Life. Plume Books, 2003.

[192] L.M.A. Bettencourt, J. Lobo, D. Helbing, C. Kuehnert, G.B. West, Growth, innovation,

scaling, and the pace of life in cities, in: Proc. Natl. Acad. Sci., 2007: pp. 7301–7306.

[193] J.A. Seago, The California experiment: alternatives for minimum nurse-to-patient ratios, JONA J. Nurs. Adm. 32 (2002) 48–58. https://doi.org/10.5822/978-1-61091-005-7_8.

[194] R. Machado Tavares, S. Gwynne, E. Galea, Collection and analysis of pre-evacuation time data collected from evacuation trials conducted in library facilities in Brazil, J. Appl. Fire Sci. 15 (2007) 23–40.

[195] S. Gwynne, E.R. Galea, J. Parke, J. Hickson, The collection of pre-evacuation times from evacuation trials involving a Hospital Outpatient area and a University Library facility, Fire Saf. Sci. 7 (2003) 877–888.

[196] A. Rahouti, R. Lovreglio, P. Jackson, S. Datoussaïd, Evacuation Data from a Hospital Outpatient Drill The Case Study of North Shore Hospital, Collect. Dyn. 5 (2020) 142–149.

[197] A.L.E. Hunt, Simulating Hospital Evacuation. Doctoral Dissertation, University of Greenwich, University of Greenwich, 2016.

[198] Johns Hopkins Hospital, No Title, (n.d.). https://www.hopkinsmedicine.org/the_johns_hopkins_hospital/about/enhanced_facilities/floor_maps/ground_level.html.

[199] SIMUL8, Johns Hopkins Health System optimizes emergency department patient flow using simulation, (n.d.). https://www.simul8.com/case-studies/optimizing-ed-patient-flow-johns-hopkins.

Biographical Statement

Fardad Haghpanah was born on April 6, 1987 in Tehran, Iran. He attended Sharif University of Technology where he obtained his bachelor's degree in Civil Engineering in 2010. Fardad worked as a research engineer at Sharif University and as a retrofit engineer in the construction industry for 2 years. In 2012, he moved to Italy and started his master's studies in Risk Mitigation at Politecnico di Milano. During his master's, he did numerous projects on risk assessment for hydrogeological and seismic hazards, and for his thesis, he joined the Miracle Project, an international European project on critical infrastructure resilience strategies and initiatives, in which he developed a framework that is used to evaluate the alignment of public, private, and public-private resilience programs on different regional, national, and international levels. In 2015, he graduated summa cum laude from POLIMI and moved to Baltimore to start his PhD in the Department of Civil Engineering (now Civil and Systems Engineering) at Johns Hopkins University. His PhD research was focused on developing models in support of disaster studies. He contributed to performance-based earthquake engineering and seismic resiliency of repetitively framed mid-rise cold-formed steel buildings by developing probabilistic fragility functions for cold-formed steel framed shear walls. For his dissertation, he developed multi-scale evacuation models to support city and hospital officials in their decision-making during emergencies and disasters.